FACULTY OF ENGINEERING
AND ARCHITECTURE

Data-Driven Adaptive Operational Strategies for Wind Energy Conversion Systems Incorporating Frequency Containment Reserve

Nezmin Kayedpour

Doctoral dissertation submitted to obtain the academic degree of
Doctor of Electromechanical Engineering

Supervisors

Prof. Guillaume Crevecoeur, PhD - Prof. Jeroen De Kooning, PhD

Department of Electromechanical, Systems and Metal Engineering
Faculty of Engineering and Architecture, Ghent University

December 2023

GHENT
UNIVERSITY

FACULTY OF ENGINEERING
AND ARCHITECTURE

Data-Driven Adaptive Operational Strategies for Wind Energy Conversion Systems Incorporating Frequency Containment Reserve

Nezmin Kayedpour

Doctoral dissertation submitted to obtain the academic degree of
Doctor of Electromechanical Engineering

Supervisors
Prof. Guillaume Crevecoeur, PhD - Prof. Jeroen De Kooning, PhD
Department of Electromechanical, Systems and Metal Engineering
Faculty of Engineering and Architecture, Ghent University

December 2023

GHENT
UNIVERSITY

ISBN 978-94-6355-781-8
NUR 959, 961
Wettelijk depot: D/2023/10.500/113

Members of the Examination Board

Chair

Prof. Sabine Wittevrongel, PhD, Ghent University

Other members entitled to vote

Annelies Coene, PhD, Ghent University
Prof. Mia Loccufier, PhD, Ghent University
Prof. François Vallée, PhD, Université de Mons
Prof. Xiaowei Zhao, PhD, University of Warwick, United Kingdom

Supervisors

Prof. Guillaume Crevecoeur, PhD, Ghent University
Prof. Jeroen De Kooning, PhD, Ghent University

Contents

Summary

Renewable energy sources, especially wind energy, are recognized as vital components of the global energy transition. Wind energy conversion systems can help to mitigate climate change. The remarkable clean and abundant nature of wind energy presents substantial opportunities for electricity generation, significantly reducing greenhouse gas emissions compared to fossil fuel-based energy sources. However, the intermittent and variable characteristics inherent in wind energy create substantial challenges to ensuring the reliable and efficient operation of large-scale wind energy conversion systems. These challenges include integrating fluctuating wind resources into the grid, maintaining grid stability, optimizing power generation, and effectively managing the complex dynamics of wind turbines and wind farms.

To address these challenges and unlock the full potential of wind power, there is a pressing need to develop advanced control strategies and monitoring techniques to optimize the performance, reliability, and grid integration of wind energy conversion systems. To do so, we focus on adaptive strategies that can optimally operate wind energy conversion systems. We particularly use data-driven approaches and known control and monitoring approaches to make the adaptation and the corresponding optimizations. With this research, we hope to provide tangible solutions to policymakers as well as the industry involved with Belgian offshore wind, like wind turbine manufacturers and operators, as well as wind farm owners and teams responsible for the maintenance and operation of their wind parks. This research covers both wind farm and wind turbine operations.

Wind energy conversion systems can provide ancillary services to maintain the reliability of electricity systems. They are particularly well suited to provide frequency containment reserve (FCR): they can act on that specific time scale to help stabilize the grid. The optimization of wind power systems providing such services requires innovative approaches that go beyond conventional control and monitoring methods to address the unique characteristics and complexities associated with wind energy and grid frequency. The research conducted in this thesis explores and develops methodologies that leverage state-of-the-art data-driven technologies such as machine learning, advanced data analytics, and predictive modeling. Using these techniques that possess the capability to learn from data, novel control strategies, and monitoring techniques are devised to enhance the adaptive performance of wind energy conversion systems and, more specifically, optimize energy production and provide FCR. These techniques are helpful in overcoming the inherent challenges posed by wind variability, intermittency, and uncertainty.

The presented research encompasses three primary areas: wind farm supervisory control, wind turbine local control, and wind turbine health monitoring. Each area addresses specific challenges and contributes to the overall objective of improving the operation and performance of wind energy conversion systems that deliver FCR.

Chapter 2 covers the wind farm supervisory control domain. A novel operation strategy to optimize wind farms' contribution to reserve and energy markets is proposed. It also optimally allocates the decided Frequency Containment Reserve (FCR), the primary frequency control of ancillary services, among wind turbines while effectively managing wake formation. The research introduces a two-stage stochastic programming approach that considers possible scenarios to account for uncertainties associated with intermittent wind speed, wind direction, grid frequency variability, and the complex aerodynamics of wake formation. Additionally, a data-driven surrogate model of wake formation is integrated using an adaptive network-based fuzzy inference system (ANFIS) trained on the Gauss-Curl-Hybrid wake model. This integration significantly reduces computational complexity and enables rapid estimation of optimal wake control parameters, such as yaw angles and axial induction factors. The proposed algorithm's effectiveness is evaluated through an existing wind farm case study, showcasing its potential to improve overall wind farm performance under various operational conditions. Notably, it demonstrates the algorithm's ability to enhance FCR provision and optimize wake control.

Building upon the insights gained from wind farm supervisory control, the research shifts its focus to wind turbine local control, explicitly supporting the activation of FCR at individual wind turbines based on predetermined optimal setpoints established at the wind farm supervisory control level. The research aims to extend and improve the existing understanding of wind turbine local control systems to facilitate FCR activation. To achieve this, the research focuses on the development of advanced control algorithms that deal with various limitations, such as wind turbine nonlinearities, stochasticity of wind speed, and grid frequency. Employing computationally efficient algorithms ensures that the wind turbines operate within specified setpoints, considering physical constraints and restrictions projected by Transmission System Operators (TSO).

In this context, Chapter 3 proposes a neural network-based Model Predictive Control (MPC) approach developed to support FCR provision in full load

conditions, utilizing the advantages of a fast pitch control system. The research utilizes a closed-loop Hammerstein structure to approximate the nonlinear behavior of wind turbines equipped with a Permanent Magnet Synchronous Generator (PMSG). The proposed MPC structure can accurately predict the turbine's aerodynamic behavior by combining multilayer perceptron neural networks that reflect the steady-state nonlinear part and linear AutoRegressive with Exogenous input (ARX) model that estimates the linear dynamic part of the system. It provides optimal control actions in response to grid frequency variations. A comparison with baseline proportional-integral (PI) controllers demonstrates the superior performance of the MPC approach in terms of improved power reference tracking and reduced mechanical loads on turbine blades and the tower. The MPC system ensures a fast and stable response to grid frequency variations while optimizing pitch and torque cooperation for maximum power generation and grid stability.

Continuing the local control level investigation, Chapter 4 introduces an adaptive operational strategy for providing FCR in both full and partial-load operating regions. This strategy employs a generator torque control system instead of a blade pitch control system to enable the wind turbine to provide FCR in the suboptimal region of maximum power point tracking mode for the entire operation without imposing aggressive structural loads on the pitch control mechanism. This operational strategy also considers the unpredictable behavior of grid frequency and wind speed. The research contributes an adaptive reserve margin estimation method based on short-term grid frequency predictions, which dynamically adjusts control setpoints in a supplementary FCR control loop, enhancing stability and reliability. Additionally, gain scheduled fuzzy-PI control is integrated to improve FCR provision in turbulent wind conditions. This chapter demonstrates stable control performance in all operating regions and reserve modes, ensuring reliable operation and power regulation even in the presence of turbulent wind speeds without causing excessive structural loads on blade roots and tower fore-aft bending moments.

To address the challenge of wind turbine health monitoring, Chapter 5 presents a novel physics-informed deep learning framework. This framework accurately approximates the time-varying correlation between wind turbine control sequences and system response, enabling precise detection of anomalies and degradations in wind turbine operation. Notably, the research considers the curtailment mode, where wind turbines operate at reduced capacity. The framework utilizes a hybrid structure and support vector machine for classification in both the time and frequency domains, accounting for uncertainties such as wind stochasticity and power curve variations. An iterative learning framework enables dynamic updating of the classifier, enhancing its ability to learn from new anomalies during active operations. The chapter's significance lies in its potential to improve the

accuracy and efficiency of wind turbine health monitoring, leading to more efficient assessments of turbine conditions and reduced downtime.

In conclusion, this thesis presents a comprehensive approach to optimizing the operation of wind power systems by addressing key challenges in wind farm supervisory control, wind turbine local control, and wind turbine health monitoring, considering maximizing energy production and delivering FCR. The research contributes novel strategies and techniques to enhance the performance, reliability, and grid integration of wind power systems. By optimizing FCR provision, controlling wake formation, improving control strategies, and enhancing health monitoring techniques, this research paves the way for a more sustainable and resilient future powered by wind energy. The outcomes of this research are crucial for the efficient and reliable integration of wind power into the global energy landscape, promoting sustainability and reducing greenhouse gas emissions.

Samenvatting

Hernieuwbare energiebronnen, vooral windenergie, worden erkend als essentiële onderdelen van de wereldwijde energietransitie. Windenergiesystemen kunnen helpen om klimaatverandering tegen te gaan. De opmerkelijk schone en overvloedige aard van windenergie biedt aanzienlijke kansen voor elektriciteitsopwekking, waarbij de uitstoot van broeikasgassen aanzienlijk wordt verminderd in vergelijking met op fossiele brandstoffen gebaseerde energiebronnen. De echter, de wisselende en variabele kenmerken die inherent zijn aan windenergie, creëren aanzienlijke uitdagingen om de betrouwbare en efficiënte werking van grootschalige windenergie-conversiesystemen te waarborgen. Deze uitdagingen omvatten het integreren van fluctuerende windbronnen in het elektriciteitsnet, het handhaven van de netstabiliteit, het optimaliseren van de energieopwekking en het effectief beheren van de complexe dynamiek van windturbines en windparken.

Om deze uitdagingen aan te pakken en het volledige potentieel van windenergie te ontsluiten, is er een dringende behoefte aan de ontwikkeling van geavanceerde controlestrategieën en bewakingstechnieken om de prestaties, betrouwbaarheid en integratie in het elektriciteitsnet van windenergie-conversiesystemen te optimaliseren. Om dit te doen, richten we ons op adaptieve strategieën die windenergie-conversiesystemen optimaal kunnen laten werken. We maken met name gebruik van op gegevens gebaseerde benaderingen en bekende besturings- en bewakingsbenaderingen om de aanpassing en de bijbehorende optimalisaties uit te voeren. We hopen met dit onderzoek concrete oplossingen te bieden aan beleidsmakers, evenals aan de industrie die betrokken is bij Belgische offshore wind, zoals fabrikanten en exploitanten van windturbines, evenals windmolenparkbeheerders en teams die verantwoordelijk zijn voor het onderhoud en de werking van hun windparken. Dit onderzoek omvat zowel de werking van windmolenparken als individuele windturbines.

windenergie-conversiesystemen kunnen ondersteunende diensten bieden om de betrouwbaarheid van elektriciteitssystemen te handhaven. Naast energieproductie kunnen ze ondersteunende diensten leveren. Ze zijn bijzonder geschikt om primaire frequentieregeling (FCR) te bieden: ze kunnen op die

specifieke tijdschaal acteren om het net te stabiliseren. De optimalisatie van windenergiesystemen die dergelijke diensten leveren, vereist innovatieve benaderingen die verder gaan dan conventionele besturings- en bewakingsmethoden om de unieke kenmerken en complexiteiten van windenergie en netfrequentie aan te pakken. Het onderzoek dat in deze thesis wordt uitgevoerd, verkent en ontwikkelt methodologieën die gebruikmaken van state-of-the-art op data gebaseerde technologieën zoals machine learning, geavanceerde gegevensanalyse en voorspellende modellering. Met behulp van deze technieken, die de mogelijkheid hebben om te leren van gegevens, worden nieuwe besturingsstrategieën en bewakingstechnieken bedacht om de adaptieve prestaties van windenergie-conversiesystemen en, meer specifiek, de optimalisatie van energieproductie en het bieden van FCR te verbeteren. Deze technieken zijn nuttig om de inherente uitdagingen van windvariatie, intermittentie en onzekerheid te overwinnen.

Het gepresenteerde onderzoek omvat drie primaire gebieden: superviserende regeling van windmolenparken, lokale regeling van windturbines en monitoring van de gezondheid van windturbines. Elk gebied adresseert specifieke uitdagingen en draagt bij aan het algehele doel van het verbeteren van de werking en prestaties van windenergie-conversiesystemen die FCR leveren.

Hoofdstuk 2 behandelt het domein van de superviserende regeling van windmolenparken. Een nieuwe operationele strategie wordt voorgesteld om de bijdrage van windmolenparken aan reserve- en energiemarkten te optimaliseren. Het verdeelt ook de besloten Frequency Containment Reserve (FCR), de primaire frequentiebesturing van ondersteunende diensten, optimaal onder windturbines, terwijl het de vorming van de wake effectief beheert. Het onderzoek introduceert een tweestaps stochastische programmeringsbenadering die mogelijke scenario's overweegt om rekening te houden met onzekerheden die gepaard gaan met wisselende windsnelheid, windrichting, variabiliteit van de netfrequentie en de complexe aerodynamica van wakevorming. Bovendien wordt een op gegevens gebaseerd surrogaatmodel van wakevorming geïntegreerd met behulp van een adaptief op netwerk gebaseerd fuzzy-inferentiesysteem (ANFIS) dat is getraind op het Gauss-Curl-Hybrid wake-model. Deze integratie vermindert aanzienlijk de rekencomplexiteit en maakt snelle schatting van optimale wakebesturingsparameters mogelijk, zoals kruihoeken en axiale inductiefactoren. De effectiviteit van het voorgestelde algoritme wordt geëvalueerd aan de hand van een bestaande casestudy van een windmolenpark, waarbij het potentieel wordt gedemonstreerd om de algehele prestaties van het windmolenpark te verbeteren onder verschillende operationele omstandigheden. Met name toont het de mogelijkheid van het algoritme om FCR-voorziening te verbeteren en wakebesturing te optimaliseren aan.

Op basis van de inzichten uit de superviserende regeling van windmolenparken, verschuift het onderzoek de focus naar de lokale regeling van windturbines, waarbij expliciet ondersteuning wordt geboden voor de activering van FCR bij individuele windturbines op basis van vooraf bepaalde optimale setpoints die zijn vastgesteld op het niveau

van de superviserende regeling van het windmolenpark. Het onderzoek heeft tot doel het bestaande begrip van lokale regelingssystemen van windturbines uit te breiden en te verbeteren om FCR-activering te vergemakkelijken. Om dit te bereiken, richt het onderzoek zich op de ontwikkeling van geavanceerde regelalgoritmen die omgaan met verschillende beperkingen, zoals de niet-lineariteiten van windturbines, de stochasticiteit van windsnelheid en de netfrequentie. Het gebruik van rekenkundig efficiënte algoritmen zorgt ervoor dat de windturbines binnen gespecificeerde setpoints werken, rekening houdend met fysieke beperkingen en beperkingen die zijn geprojecteerd door de transmissienetbeheerders (TSO).

In dit verband stelt hoofdstuk 3 een op kunstmatige neurale netwerken gebaseerde Model Predictive Control (MPC) benadering voor die is ontwikkeld om FCR te ondersteunen voor windsnelheden boven de nominale waarbij gebruik wordt gemaakt van de voordelen van een snel pitch-regelsysteem. Het onderzoek gebruikt een gesloten Hammerstein-structuur om het niet-lineaire gedrag van windturbines met een Permanent Magnet Synchronous Generator (PMSG) bij benadering vast te leggen. De voorgestelde MPC-structuur kan het aerodynamische gedrag van de turbine nauwkeurig voorspellen door multilayer perceptron neurale netwerken te combineren die het stationaire niet-lineaire deel weerspiegelen en een lineair AutoRegressive with Exogenous input (ARX) model dat het lineaire dynamische deel van het systeem schat. Het biedt optimale regelacties als reactie op variaties in de netfrequentie. Een vergelijking met basale proportioneel-integrale (PI) regelaars toont de superieure prestaties van de MPC-benadering aan in termen van verbeterde vermogensreferentie-tracking en verminderde mechanische belastingen op de turbinebladen en de toren. Het MPC-systeem zorgt voor een snelle en stabiele respons op variaties in de netfrequentie en optimaliseert krui- en koppelregeling voor maximale energieopwekking en netstabiliteit.

Verdergaand met het onderzoek op het niveau van lokale regeling, introduceert hoofdstuk 4 een adaptieve operationele strategie voor het leveren van FCR in zowel volledige als gedeeltelijke belastingsregio's. Deze strategie maakt gebruik van een regelsysteem voor generator-koppel in plaats van een pitch-regelsysteem om de windturbine in staat te stellen FCR te leveren in het suboptimale gebied van de modus voor het volgen van het maximale vermogenspunt gedurende de hele werking, zonder agressieve structurele belastingen op het pitch-regelmechanisme op te leggen. Deze operationele strategie houdt ook rekening met het onvoorspelbare gedrag van de netfrequentie en de windsnelheid. Het onderzoek draagt bij aan een adaptieve schatting van de reserve-marge op basis van korte-termijn voorspellingen van de netfrequentie, die de controle setpoints dynamisch aanpast in een aanvullende FCR-regelkring, wat de stabiliteit en betrouwbaarheid verbetert. Bovendien wordt gain scheduled fuzzy-PI-regeling geïntegreerd om FCR-levering te verbeteren in turbulente windomstandigheden. Dit hoofdstuk toont stabiele controleprestaties in alle werkingsgebieden, wat zorgt voor betrouwbare werking en vermogensregeling, zelfs in aanwezigheid van turbulente windsnelheden zonder overmatige structurele belastingen op de wortels van de bladen en buigmomenten van de toren.

Om de uitdaging van het monitoren van de gezondheid van windturbines aan te pakken, presenteert hoofdstuk 5 een nieuwe fysica-geïnformeerde deep learning methode. Deze methode benadert nauwkeurig de tijdvariërende correlatie tussen de regeling van windturbines en de systeemrespons, wat zorgt voor een precieze detectie van afwijkingen en degradaties in de werking van windturbines. Met name houdt het onderzoek rekening met ’curtailment’, waarbij windturbines op verminderde capaciteit werken. Het systeem maakt gebruik van een hybride structuur en een ’support vector machine’ voor classificatie in zowel de tijd- als frequentiedomeinen, rekening houdend met onzekerheden zoals de stochastiek van de wind en variaties in de vermogenscurve. Een iteratief leerframework maakt dynamische bijwerking van de classifier mogelijk, wat de mogelijkheid verbetert om te leren van nieuwe afwijkingen tijdens actieve operaties. De meerwaarde van dit hoofdstuk ligt in het potentieel om de nauwkeurigheid en efficiëntie van de gezondheidsmonitoring van windturbines te verbeteren, wat leidt tot efficiëntere beoordelingen van de toestand van de turbine en verminderde stilstand.

Tot slot presenteert deze scriptie een allesomvattende benadering om de werking van windenergiesystemen te optimaliseren door de belangrijkste uitdagingen aan te pakken in de superviserende regeling van windmolenparken, de lokale regeling van windturbines en de monitoring van de gezondheid van windturbines, met als doel de energieproductie te maximaliseren en FCR te leveren. Het onderzoek draagt nieuwe strategieën en technieken bij om de prestaties, betrouwbaarheid en integratie in het elektriciteitsnet van windenergie-conversiesystemen te verbeteren. Door FCR-levering te optimaliseren, wakevorming te regelen, regelstrategieën te verbeteren en monitoringsmethoden te verbeteren, legt dit onderzoek de weg vrij voor een meer duurzame en veerkrachtige toekomst aangedreven door windenergie. De resultaten van dit onderzoek zijn cruciaal voor de efficiënte en betrouwbare integratie van windenergie in het wereldwijde energielandschap, ter bevordering van duurzaamheid en vermindering van de uitstoot van broeikasgassen.

List of Figures

List of Tables

Chapter 1

Introduction

1.1 Introduction to offshore wind farms

1.1.1 Wind Energy: potential and impact

The global transition to renewable energy is a fundamental power generation and consumption shift. It is driven by the urgent need to address climate change and environmental degradation. By reducing our dependence on fossil fuels, renewable energy provides a cleaner, greener, and more sustainable pathway [1]. This transition restrains greenhouse gas emissions, stabilizes global temperatures, and fosters environmental preservation. This green transition furthermore helps to foster economic growth, improve public health, enhance energy security, and promote sustainable development [2].

In recent years, wind energy has experienced a remarkable surge in popularity as a clean and renewable alternative to traditional fossil fuel sources. Unlike fossil fuels, which are finite resources, wind power relies on an abundant and virtually limitless wind source. Wind energy is a sustainable and long-term solution that can help, together with other power generation solutions, to address our energy needs. Recent studies have highlighted its advantages, showcasing its potential as a sustainable energy solution [3, 4].

One of the key advantages of wind energy is its cost-effectiveness. With its relatively low operating expenditures (OPEX), it is an economically viable power generation solution [5]. This cost-effectiveness contributes to the overall competitiveness of wind energy in the market. Actually, after a reasonable investment payback period, the revenues exceed the costs associated with the designing (with Capital Expenditures, CAPEX) and operating (OPEX) them [6, 7].

Wind energy also offers the advantage of prompt market entry. Wind farms can be deployed relatively fast compared to large-scale traditional power plants. This allows for a rapid expansion of renewable energy capacity and a faster transition away from fossil fuels. Regarding environmental impact, wind energy is highly regarded for its friendliness to the ecosystem [8]. Additionally, wind turbines are known for their relatively smaller physical footprint compared to many conventional power plants, which can contribute to mitigating habitat disruption and reducing potential land use conflicts [9]. Wind energy is a suitable complementary solution to solar energy that relies on sunlight, and hydroelectric power plants rely on available water sources [10].

Wind farms enable the efficient use of wind resources, optimizing land/sea use and generating electricity at a larger scale. They facilitate supporting infrastructure development, streamline operations and maintenance, and enhance grid integration. They furthermore contribute to job creation, local investment, and reliable electricity supply [11].

The growth of wind energy has been remarkable in recent years. 2022 marked the third most successful year in new capacity, as the global addition reached 78 GW [12]. The overall installed capacity worldwide reached 906 GW, showing a Year-on-Year expansion of 9%. Anticipated for 2023 is a significant milestone: the first instance of global new capacity exceeding 100 GW [12]. Global Wind Energy Council (GWEC) Market Intelligence predicts a 15% year-on-year growth [12]. Looking ahead to the five years of 2023-2027, GWEC Market Intelligence forecasts a cumulative new capacity of 680 GW, averaging 136 GW annually. This positive trajectory extends to 2030 with an additional 143 GW [12]. The earlier forecast of 1078 GW between 2022 and 2030 has been revised to 1221 GW, representing the new capacity extention to be added to Horizon 2030 [12].

There is a consistent trend towards higher-rated power capacities in wind turbine designs. This pursuit reduces the levelized energy cost (LCOE) and enhances the annual energy yield (AEY). A significant trend in wind energy conversion systems is the development of offshore wind turbines in sea areas. Figure 1.1 illustrates the Compound Annual Growth Rate (CAGR) of offshore wind installations, with Europe (green) being a key player until 2030. Offshore renewable energy sources have become economically mature, and many regions have achieved cost competitiveness compared to fossil fuels. The levelized cost of electricity (LCOE) - the rate of the total energy output of wind turbines to build and operate it over its lifetime to the average total cost of the wind turbines over that lifetime [13] - and enhancing Annual Energy Production (AEP) [14, 15]. The development and maintenance of offshore wind is currently one of the most important parts of the Blue Economy. The objectives outlined in the Paris Agreement, which aim to limit global temperature rise to below 1.5 °C, are driving efforts to surpass 380 GW of cumulative installed offshore wind capacity worldwide by 2030, with a projected capacity of over 2,000 GW by 2050 [15].

Offshore wind farms provide distinct advantages compared to onshore wind

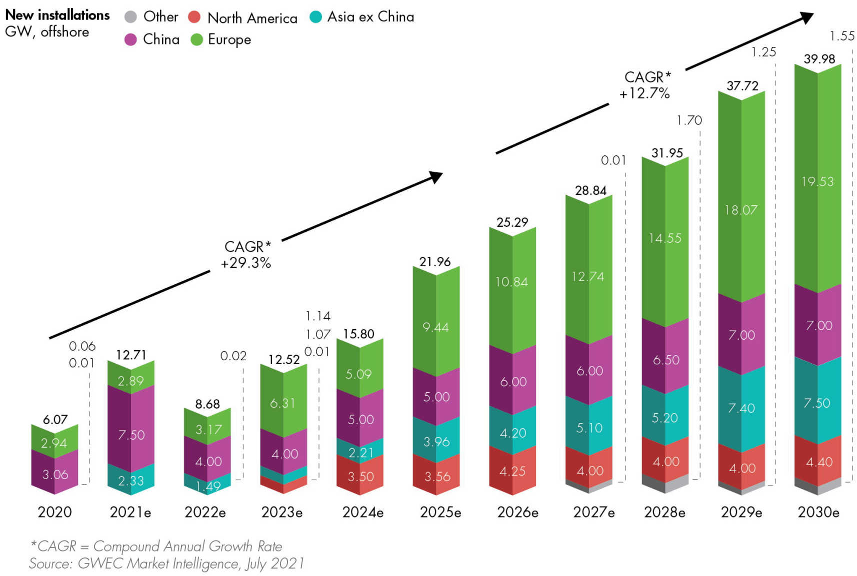

Figure 1.1: Evolution of offshore wind installations on different continents from 2020 until 2030. Numbers show the total amount of projected GW installations together with the Compound Annual Growth Rate (CAGR) [12].

farms. They benefit from more robust and consistent winds, resulting in higher AEP and reliability. Offshore placement reduces visual and noise impact on coastal communities and conserves valuable land resources [16]. Europe's investment in offshore wind has been substantial, with countries like Belgium capitalizing on their significant offshore wind potential. Belgium, situated in the North Sea with favorable wind conditions, is actively using this valuable renewable resource [17]. The country has emerged as a leader in offshore energy installations, demonstrating a solid commitment to renewable energy. In 2020 alone, Belgium added 0.7 GW of new offshore wind capacity, further solidifying its position in renewable energy endeavors. Currently, Norther is the largest offshore wind farm in Belgium and has a capacity of 370 MW. The Thorntonbank wind farm, with C-Power operating the wind farm, is the second largest offshore wind farm in Belgium having a total capacity of 325 MW, equal to the annual average electricity consumption of 300k families. Figure 1.2 shows the Belgian offshore wind farms with e.g. the Norther and C-Power. With a clear vision for expansion, the federal government of Belgium decided in 2021 to further amplify offshore wind energy capacity. The objective is to achieve an additional production capacity ranging from a minimum of 3.15 GW to a maximum of 3.5 GW in the Princess Elisabeth Zone (PEZ) that is indicated in Fig.

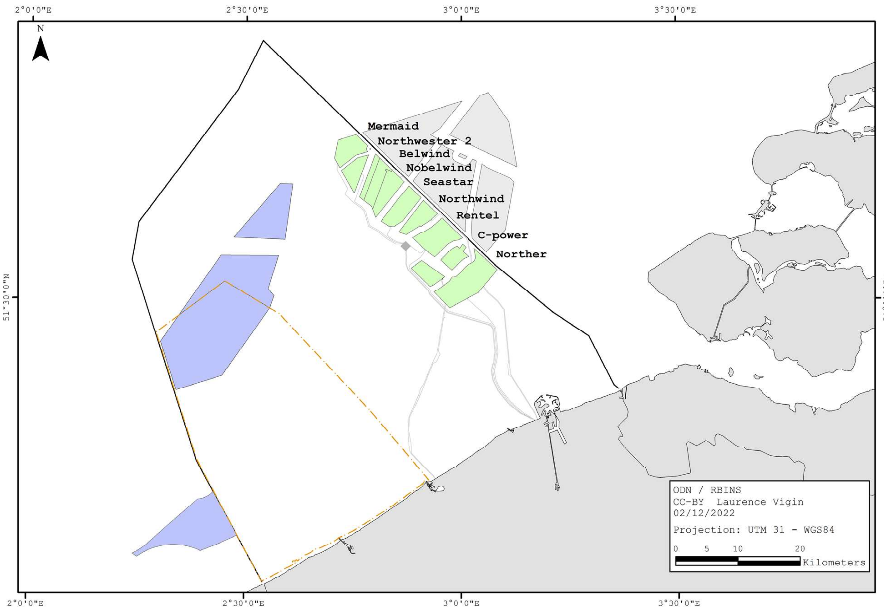

Figure 1.2: Belgian offshore wind farms. The blue areas inside the dashed area represent the Princess Elisabeth zone [20].

1.2 The Belgian government has set targets to increase offshore wind capacity, aiming to reach 4 GW installed capacity by 2026. Moreover, future expansion plans envision a remarkable 6.75 GW by 2030 [17]. These targets underscore Belgium's steadfast dedication to renewable energy and position the country as a significant player in the offshore wind sector.

The offshore wind energy development in Belgium contributes to reducing carbon emissions; e.g., the Thornton Bank wind reduces CO2 emissions equivalent to 415 kilotonnes per year compared to a gas-fired power plant. It furthermore aligns with the blue economy's principles. Offshore wind projects in Belgium create employment opportunities and stimulate the growth of the renewable energy industry, driving the transition towards a more sustainable and resilient blue economy [18, 19]. Belgium's substantial progress in offshore wind installations, ambitious expansion plans, and favorable wind conditions highlight the country's potential for further growth in the offshore wind sector.

1.1.2 Key components and infrastructure requirements

Offshore wind farms require various key components and a vast infrastructure to convert wind energy to electrical power and transmit it to the electrical grid. Fig. 1.3 illustrates these key components. Offshore wind turbines are specif-

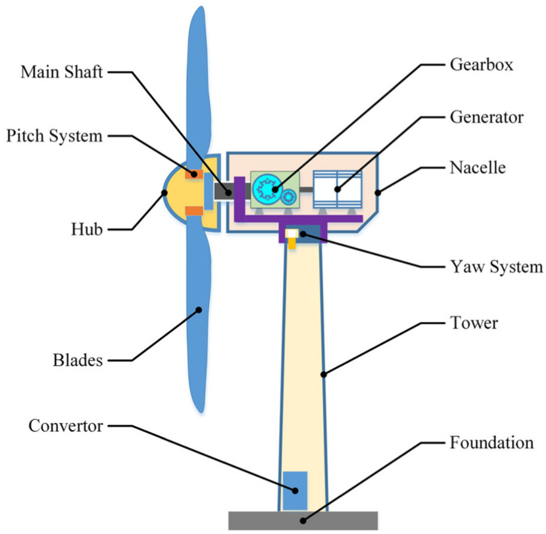

Figure 1.3: The main structure of a wind turbine with its main components [21].

ically designed to withstand the harsh marine environment and operate efficiently in varying wind conditions. In the text below, we provide details on the tower, nacelle, rotor, pitch control system, yaw control system, generator, and the foundations of wind turbines [21].

The tower provides structural support for the turbine and is typically made of steel or concrete. The higher the tower above sea level, the higher, on average, the wind speeds and, hence, the ability to capture higher wind energy. The tower ranges in height depending on the specific offshore site's water depth and wind conditions. Advanced tower designs, such as multi-section or hybrid towers, are being developed to support more giant turbines and enable installation in deeper waters [22].

The nacelle houses the critical components of the turbine, including the generator, gearbox, and control systems. It is mounted on top of the tower and is responsible for converting the mechanical energy from the rotor into electrical energy. Traditionally, wind turbines have utilized geared drive-trains, where the rotor speed is increased through a gearbox before being transferred to the generator. Direct-drive wind turbines consist of a generator, particularly Permanent Magnet Synchronous Generators (PMSG), that is directly connected to the rotor. They have gained more popularity over the past years, and their design offers several advantages that can be attributed to the fact that the drive-train is not geared with higher efficiency, reduced maintenance requirements, and improved reliability [23]. A contemporary trend in large turbines has emerged, exemplified by models like the Vestas V164. In these instances, a PMSG is integrated yet paired with a gearbox. This strategic choice arises due to the monumental scale of these turbines, where the nominal rotor speed becomes excessively low for economically viable direct drive implementation [24].

The rotor is the part of the turbine that captures the wind's kinetic energy. It consists of multiple blades, usually lightweight and durable materials such as fiberglass or carbon fiber-reinforced composites. The number of blades can vary, with three being the most common configuration. The length and shape of the blades are carefully designed to maximize energy capture by utilizing aerodynamic principles. Most recent turbine designs incorporate variable pitch blades that can adjust their angle to optimize performance in different wind conditions [25].

As mentioned, wind turbines are also equipped with pitch, yaw, and generator torque control systems. As readily mentioned, the pitch control system is responsible for adjusting the pitch angle of the rotor blades [26]. The pitch angle refers to the angle of the blades with respect to the incoming wind. Pitch control primarily aims to regulate the aerodynamic forces acting on the blades. By adjusting the pitch angle, the pitch control system can control the rotational speed of the rotor and manage the turbine's power output. During high wind speeds, the pitch control system can feather or change the pitch angle of the blades to reduce their angle of attack, thus limiting the amount of power generated and protecting the turbine from potential damage. Conversely, the pitch angle can be adjusted during low wind speeds to maximize power production. The pitch control system comprises blade pitch actuators, sensors, and a controller. The sensors measure parameters such as wind speed, rotor speed, and power output, while the controller adjusts the pitch angle based on the desired performance and operational conditions [26, 27].

The yaw control system is responsible for adjusting the orientation or yaw angle of the wind turbine rotor with respect to the wind direction. The primary purpose of yaw control is to ensure that the rotor blades face directly into the incoming wind, maximizing wind energy capture. It involves the rotation of the entire nacelle and rotor assembly to align with the wind direction. The yaw control system typically consists of sensors, a yaw drive mechanism, and a controller. Sensors measure the wind direction, and the controller sends signals to the yaw drive mechanism to adjust the yaw angle accordingly. By maintaining proper alignment with the wind, the yaw control system helps to optimize the turbine's performance and energy production [28].

The generator converts the rotational mechanical power from the drive train into electrical power. To do so, a generator torque control system is needed. In a PMSG, the generator type we consider throughout this dissertation, Direct Torque Control (DTC), is a control system that continuously fine-tunes the torque output of the PMSG to match the instantaneous wind conditions. It ensures the generator operates within its maximum power capture range with the

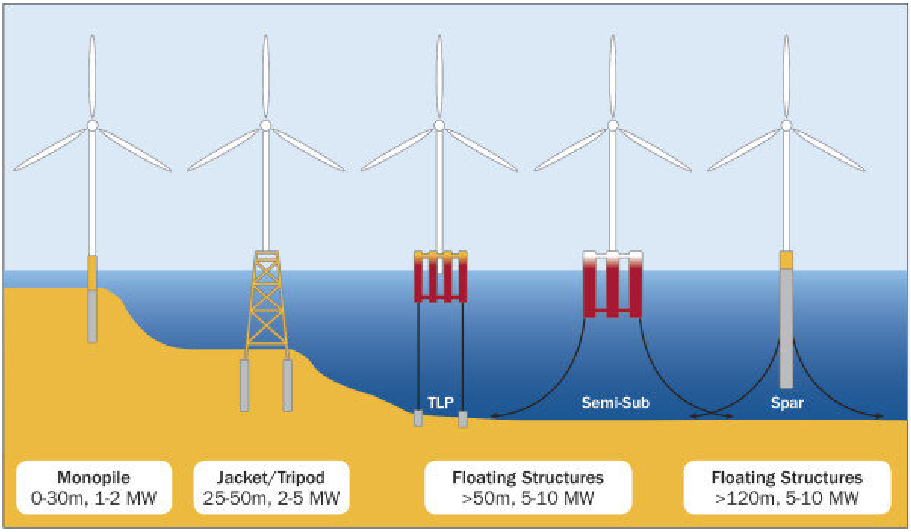

Figure 1.4: Types of offshore wind turbine foundations [30].

highest conversion efficiency. Through the intricate interplay of torque commands, stator voltage, and flux adjustments, the control system maximizes the conversion of kinetic wind energy into electrical power, enhancing energy production while maintaining stability and reliability [29].

In addition to the turbines, various types of foundations are employed in offshore wind farms, depending on the water depth and seabed conditions and the height or rated power of the wind turbines. Figure 1.4 shows different types of wind turbine foundations. Monopile foundations are the most common and cost-effective solution for shallow waters with a firm seabed [30]. These cylindrical steel structures are driven into the seabed using specialized installation equipment. Jacket structures, consisting of lattice-like steel frames, are used in deeper waters and more challenging soil conditions. They provide increased load-bearing capacity and stability. Floating platforms, such as floating wind turbines or tension leg platforms, are utilized in even deeper waters where fixed foundations are not feasible. These platforms are tethered to the seabed and use mooring systems to maintain stability [31].

The subsea cables in offshore wind farms are essential in transmitting the generated electricity to the onshore grid. Export cables transmit the power from the wind farm to the onshore substation, which is connected to the main electrical grid. Inter-array cables connect individual turbines within the wind farm, forming a network for power collection and distribution. Both cables are specially designed to withstand the marine environment, with appropriate insulation and protection against mechanical stress and corrosion. Advanced cable technologies, such as dynamic cables, are being developed to address challenges associated with floating wind farms and increased power transmission capacity. These cutting-edge cables exhibit a remarkable capability to accommodate the dynamic movements intrinsic to floating installations, solidifying their role as a linchpin in ensuring reliable, adaptable, and efficient energy transmission [32, 33].

Offshore platforms serve as hubs for the wind farm, providing the necessary infrastructure for operation and maintenance activities. They are typically equipped with control rooms, accommodation facilities, spare parts, and equipment storage areas. These platforms also house systems for monitoring and controlling the wind turbines remotely, allowing for efficient operation and maintenance activities. In some cases, offshore wind farms may require the use of High-Voltage Alternating Current (HVAC) or High-Voltage Direct Current (HVDC) platforms [34]. HVAC platforms are typically used for shorter-distance transmission, while HVDC platforms are employed for offshore wind farms due to their superior efficiency over long distances, reduced cable costs, improved voltage control, and the ability to interconnect remote sites. They enhance grid integration, especially for deep-sea installations, provide stable power transmission, and offer environmental benefits through fewer cables. HVDC systems also facilitate energy trading between countries and can accommodate future wind farm expansion. These platforms play an important role in efficiently transmitting renewable energy from offshore wind farms to onshore grids, supporting the growth of sustainable energy sources [35].

1.1.3 Wind turbine aerodynamics

Wind turbine aerodynamics is a complex field of study due to the intricate flow phenomena and the aerodynamic forces' nonlinear behavior. This involves complex flow interactions between the rotating blades and the incoming wind. As the wind encounters the rotating blades, it creates unsteady and turbulent flows characterized by vortices, wake interactions, and flow separation. Studying these complex flow patterns helps to understand their effect on wind turbine and wind farm performance [36].

Wind turbine nonlinearity

Wind turbines exhibit nonlinear behavior regarding the relationship between their inputs, i.e., wind conditions, control parameters; and outputs such as power production and structural loads. The relationship between wind speed and power output is nonlinear. The power output is minimal at low wind speeds as the turbine requires a certain threshold wind speed, called the cut-in speed, to start producing power. As the wind speed increases, power production grows rapidly until it reaches its rated power output. Beyond the rated wind speed, the power curve saturates, and the increase in power becomes less steep [37].

Another nonlinear behavior is the relationship between blade pitch angle and power output is nonlinear. Adjusting the blade pitch alters the angle of attack and, hence, the aerodynamic forces acting on the blades, affecting power production. Furthermore, wind turbines need to face the incoming wind for optimal power production. If the turbine experiences yaw misalignment, the power output decreases nonlinearly due to increased aerodynamic losses and changes in wind loading on the blades [37].

One of the nonlinear characteristics is dynamic stall. Dynamic stall occurs when the blade's angle of attack changes rapidly due to its rotation, leading to unsteady flow separation. This phenomenon significantly influences the lift and drag forces on the blades and can lead to fluctuations in power production and increased structural loads. Another element of the system's complexities is varying wind conditions and the cyclic loading that wind turbine blades experience due to the periodic changes in wind speed and direction. These dynamic effects introduce nonlinearities in the system's response, affecting fatigue life and structural integrity [38].

Modern wind turbine blades are also quite flexible, which introduces additional nonlinear behavior. The blade's elastic deformation can affect the aerodynamic performance and alter the blade's shape during operation, further complicating the aerodynamics [39].

Researchers and engineers use computational fluid dynamics (CFD) simulations and experimental testing to model wind turbine aerodynamics accurately. CFD simulations allow the capture of the complexities of the flow and provide valuable insights into the nonlinear aerodynamic behavior. However, these simulations require sophisticated turbulence models and high computational resources to represent wind turbine aerodynamics' turbulent and unsteady nature adequately. Experimental testing in wind tunnels and on operational wind turbines also plays a vital role in validating and refining these models, ensuring a better understanding of the aerodynamic behavior of wind turbines [40, 41].

The Fatigue, Aerodynamics, Structures, and Turbulence (FAST) simulator, developed by the National Renewable Energy Laboratory (NREL), is widely recognized as a reliable and accurate simulation tool for wind turbine systems. NREL has made significant efforts in developing and refining FAST over the years, making it a widely used software in the wind energy industry and research community [42].

FAST is specifically designed to simulate the dynamic behavior of wind turbines, including the interactions between aerodynamics, structures, controls, and environmental conditions. It enables researchers and engineers to analyze various aspects of wind turbine performance, such as structural integrity, fatigue life, and power production. It can also be used for design optimization, control and monitoring developments, and wind turbine certification purposes [42].

NREL has extensively validated FAST by comparing its results with experimental data, field measurements, and other simulation tools. Although no simulation tool is entirely exempt from uncertainties and limitations, FAST has consistently demonstrated its ability to provide reliable and accurate results when used appropriately, considering the necessary inputs and assumptions [42–44].

Wake interactions in wind farms

The arrangement of wind turbines in offshore farms is carefully designed to extract the maximum amount of wind energy available at the site. However, multiple turbines at close distances create complex aerodynamic interactions that can significantly affect the wind farm's overall performance and power output, i.e., LCOE and AEP. One of the challenges in offshore wind farm design is managing the wakes generated by upstream turbines. When a wind turbine extracts energy from the wind, it creates a wake of slower-moving air behind it. When downstream turbines are exposed to these wakes, their performance is adversely affected. This phenomenon is known as wake interference or wake effects [45, 46].

Wake redirection control is a method used to mitigate the adverse effects of wakes on downstream turbines. It involves adjusting the yaw angles of the turbines to redirect the wakes away from downstream turbines. By changing the yaw angles, the wake can be deflected and spread out, reducing its impact on the performance of downstream turbines. This control strategy aims to optimize the power output and efficiency of the entire wind farm. On the other hand, axial induction control involves adjusting the rotational speed of the turbines to control the amount of energy extracted from the wind. By decreasing the turbine's rotational speed, the extraction of energy is reduced, leading to a decrease in wake intensity. This approach helps to manage the wakes and improve the overall performance of the wind farm [47–49].

Specialized tools and software can be employed to analyze and model the complex wake interactions in offshore wind farms. One such tool is FLORIS (FLOw Redirection and Induction in Steady State) [50, 51]. In addition to FLORIS, several other wake modeling tools are available that help analyze and predict the wake effects in offshore wind farms. Tools like WindPRO, OpenFAST, and Fuga offer a range of wake modeling capabilities, including different wake models, CFD techniques, and optimization features. These tools provide valuable insights into wake behavior, allowing for better wind farm design, layout optimization, and supporting turbine placement decisions [52–54].

Nevertheless, FLORIS offers a simplified yet practical modeling approach.

It utilizes simplified mathematical models and algorithms to simulate the flow and wake behavior within wind farms. This simplicity allows for faster simulations and efficient computations, making it suitable for large-scale wind farm analysis. FLORIS also incorporates wake models that capture the essential characteristics of wake effects, such as the spread and intensity of wakes. These models consider parameters like turbine characteristics, wind direction, and atmospheric conditions to accurately predict wake behavior. By accurately modeling the wake effects, FLORIS enables a better assessment of power losses and performance impacts within the wind farm.

Moreover, FLORIS provides optimization features that allow users to explore different layout configurations, turbine positions, and control strategies within the wind farm. This optimization capability helps to maximize the overall AEP and LCOE. Using FLORIS, designers and engineers can assess various scenarios and find the most optimal wind farm configuration [50, 51].

1.1.4 Offshore wind energy and challenges of intermittency

Despite the vast potential of renewable energy sources, including offshore wind, these sources face challenges related to intermittency, which refers to the variability in their power output due to fluctuations in weather conditions. This intermittency poses difficulties in maintaining a balanced and reliable supply of electricity. The intermittent nature of renewable energy sources can impact grid stability, as rapid changes in generation can create imbalances in the grid, affecting voltage and frequency. Conversely, offshore wind can also help to address challenges by providing grid balancing services [55].

To overcome the challenges of renewable energy intermittency, grid operators and energy systems require effective grid balancing services. This involves maintaining a stable and balanced electricity supply to meet the varying demands of consumers. Offshore wind can contribute to these grid-balancing services in several ways. Firstly, offshore wind generation tends to be more predictable than onshore wind due to higher wind speeds and less turbulence at sea. Advanced weather forecasting models enable better anticipation of offshore wind power output, allowing grid operators to plan and manage grid resources more effectively [56].

Furthermore, offshore wind farms can be developed at larger scales than onshore wind, offering higher capacity and more consistent power generation. This scalability enhances the potential contribution of offshore wind to grid balancing services. Moreover, offshore wind farms can be located across a wide geographical area, tapping into different wind patterns and reducing the likelihood of simultaneous low generation. This geographical diversity helps to mitigate the impact of localized weather conditions on power generation, and thus enhancing grid stability [56].

1.2 Wind energy and the provision of ancillary services

1.2.1 Offshore wind farms providing ancillary services

Offshore wind farms have the potential to provide valuable grid balancing services and, as such, support power systems. They can help to maintain grid stability and balance the supply and demand of electricity [57]. One significant grid balancing service that offshore wind farms can offer is frequency regulation. The grid's frequency can deviate from its optimal level as the electricity demand fluctuates throughout the day. Offshore wind farms can actively participate in frequency regulation by adjusting their power output in response to changes in grid frequency, which should be maintained at 50 Hz with ±20 mHz allowed deviation [58].

Another grid balancing service that offshore wind farms can contribute to is voltage control. Fluctuations in power generation can affect voltage levels in the grid. Offshore wind farms equipped with modern control system designs can actively manage their output to regulate voltage with a deviation allowance of around ±5% from the nominal voltage, helping to maintain voltage stability of the electrical grid within acceptable limits. This ensures that electrical appliances and equipment connected to the grid receive the appropriate voltage, safeguarding their functionality and longevity [59].

Furthermore, offshore wind farms can play a role in providing reactive power support. Reactive power is essential for maintaining voltage levels in alternating current (AC) transmission systems. Offshore wind farms can supply or absorb reactive power as needed, helping to regulate voltage and enhance the grid's stability. For instance, an offshore wind farm with a total rated capacity of 500 megawatts (MW) can supply or absorb reactive power in the range of 50 to 200 megavolt-amperes (MVA). By providing reactive power support, offshore wind farms assist in maintaining optimal operating conditions for the entire electrical network [60].

Moreover, offshore wind farms can be integrated with energy storage systems, such as batteries or pumped hydro storage. Excess electricity generated during periods of high wind can be stored in these systems for later use during periods of low wind or increased demand. This integration enables offshore wind farms to act as a dispatchable energy source, providing power when needed, thus enhancing grid flexibility and stability [61].

1.2.2 Ancillary services in Europe

Ancillary services provision in European power systems refers to the suite of services that support the reliable and efficient operation of the electricity grid beyond the energy supply [62]. In European power systems, several ancillary services are commonly provided. They are detailed here below, and their activation time, i.e., in what time frame are they active, is shown in Fig. 1.5:

Inertial Response (IR) with wind turbines: Traditional synchronous generators, like those in thermal power plants, have rotating masses that inherently provide inertia to the system, and their power reacts to the derivative of the grid frequency. In the context of wind turbines, a similar inertial response can be realized through synthetic or virtual inertia. Wind turbines, being asynchronous generators, lack this rotating mass and, therefore, do not have the same natural inertial response. Modern wind turbines are required to emulate or mimic the inertial response of traditional generators. These turbines need to respond to frequency deviations by temporarily reducing or increasing their power output. The timescale of this response depends on the control strategies and the technology used. Generally, the inertial response can range from seconds to tens of seconds for wind turbines with synthetic inertia capabilities. This is faster than the natural inertial response of traditional generators but slower than the fast frequency response provided by batteries and other resources.

Fast Frequency Response (FFR): This frequency service refers to the ability of power system resources to rapidly respond to changes in system frequency to maintain grid stability. Unlike inertial response, FFR involves non-rotating resources like battery energy storage systems (BESS), demand response, and other flexible resources that can rapidly adjust their power output or consumption to help stabilize the system frequency. FFR operates on a much faster timescale, often in fractions of a few seconds [62].

Frequency Containment Reserve (FCR): This ancillary service refers to the reserve capacity that power system operators maintain to respond quickly to changes in frequency and maintain grid stability. FCR is an essential ancillary service in wind energy integration that facilitates frequency regulation to help support the grid's frequency within an acceptable range. Grid frequency is a critical parameter that must be kept stable at a specific level, i.e., 50 Hz is the most common frequency utilized in most electrical grid systems for the proper functioning of electrical equipment. Wind turbines with improved control systems and fast response capabilities can participate in FCR. When a sudden frequency deviation occurs due to power supply and demand imbalances, these wind energy systems can adjust their power output rapidly to help bring the frequency back to its nominal value. This response can happen in seconds and provides valuable support in stabilizing the grid during transient disturbances. Wind turbines need control algorithms to quickly detect frequency deviations, estimate the required power adjustment, and implement the necessary changes to their power output to participate in the FCR market. The responsiveness of wind turbines in FCR can mitigate the initial impact of disturbances and reduce the need for traditional synchronous generators to provide all the frequency support [62].

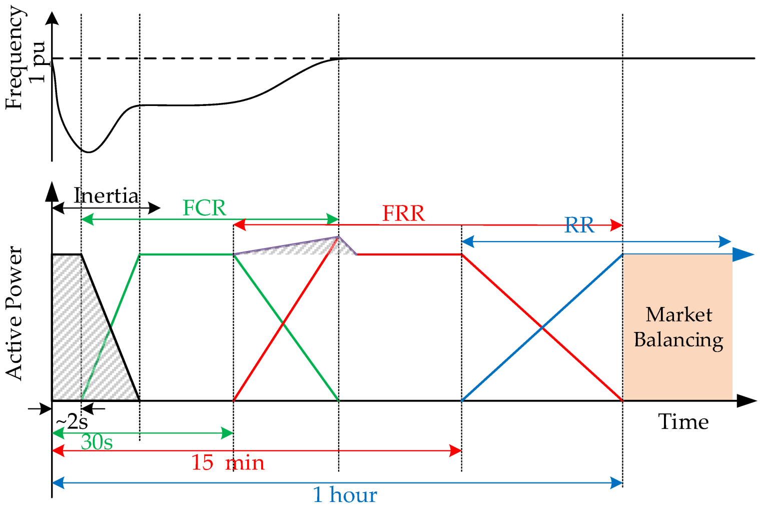

Figure 1.5: Ancillary services activation time [62].

Frequency Restoration Reserve (FRR) capacity: This ancillary product refers to the additional power generation capacity kept in reserve to be activated when needed. It is a backup to ensure sufficient supply to meet unexpected changes in demand or supply disruptions. Both conventional power plants and flexible resources such as energy storage systems or demand response can provide reserve capacity. In addition to traditional reserve capacity, Manual Frequency Restoration Reserve (mFRR) and Automatic Frequency Restoration Reserve (aFRR) are specialized reserves used for frequency restoration after a large-scale disturbance or blackout. These reserves can be activated to restore the grid's frequency and stability [62].

Replacement Reserve (RR): This capability represents the active power reserve that can be utilized to replenish and maintain the necessary level of FRR and remain ready to address additional system imbalances, such as generation reserve requirements. The activation of FRR is initiated manually in response to system optimization by the system operator.

The diagram presented in Figure 1.5 illustrates the order in which the mentioned frequency control services are engaged by the Belgian Transmission System Operator (Elia) in response to a system imbalance. Inertia support takes immediate action, while FCR respond within a few seconds, achieving full activation within 30 seconds to address any disparities between power generation and load, with the primary goal of mitigating frequency deviations. Frequency Restoration Reserves FRR are initiated after 30 seconds to restore the system frequency to its nominal value following the imbalance. RR are committed within 15 minutes to reload FRR for potential future system imbalances.

Voltage Control: Ancillary services related to voltage control help maintain the grid's voltage levels within predefined limits. Voltage is essential for the proper operation of electrical devices and equipment. Voltage control services involve adjusting reactive power flows, voltage regulation equipment, and coordination between generators and voltage control devices to maintain voltage stability and optimize the grid's performance [63, 64].

Black Start Capability: Black start capability is the ability of power plants or other resources to restore the power grid after a complete blackout or system-wide failure. Power plants with black start capability can restart their operations without an external power supply and initiate the gradual restoration of power to the rest of the grid. This service is critical for grid resilience and ensuring rapid recovery from severe disruptions [65].

System Restoration: System restoration services involve the coordinated and sequential process of bringing the entire power system back online after a significant disruption or blackout. It includes prioritizing power restoration to critical infrastructure, synchronizing power plants, and gradually restoring power to different areas and customers. System restoration services aim to minimize downtime and restore electricity supply safely and efficiently [66].

The services discussed in this section can be efficiently provided at both the wind turbine and wind farm control levels. System Restoration and Black Start Capability, vital for grid recovery during blackouts and system-wide failures, are uniquely feasible for offshore wind farms to execute. Their location and scale make offshore wind farms well-suited for supporting the grid's restoration in such critical situations. Wind farms can contribute to system restoration by injecting power and aiding grid stabilization during blackout recovery, while their gradual power ramp-up can ensure smooth integration. Some wind turbines, designed with black start capability, can participate in restarting the power system independently after a total blackout, contingent on features like islanding, synchronization, and communication. Integration of wind turbines into these processes demands careful planning and coordination with grid infrastructure [67].

1.2.3 Market mechanisms for the provision of ancillary services

Market mechanisms refer to the institutional frameworks and processes established to facilitate the buying and selling of electricity and ancillary services in a regulated market environment [68, 69]. These mechanisms play a critical role in ensuring the efficient provision of ancillary services and the reliable operation of electricity systems. In Europe, market mechanisms consist of various types of markets, including day-ahead and intraday markets, and energy and reserve markets.

Day-ahead markets serve as a primary platform for market participants, such as generators, retailers, and traders, to submit their bids and offers for energy supply and demand for the following day. These markets enable participants, including offshore wind farms, to adjust their production schedules based on market outcomes, facilitating efficient resource allocation and price discovery. Offshore wind farms can participate in day-ahead markets by submitting their expected energy production and offering ancillary services such as reserve capacity to enhance grid stability.

The intraday market provides a more flexible and dynamic trading platform closer to real-time operations as a complementing program to the day-ahead market. Market participants, including offshore wind farms, can adjust their positions and trade energy in shorter time intervals, allowing them to respond to unexpected changes in supply and demand. Offshore wind farms participating in the intraday market can optimize their generation schedules in real-time, contributing to grid balancing and reducing the need for corrective measures.

Energy markets form the backbone of electricity trading, enabling the buying and selling of electricity across different timeframes, including the day-ahead and intraday periods. Offshore wind farms can participate in energy markets by offering their generated electricity for sale. Reserve markets focus on ensuring the availability of reserves to address sudden changes in supply or demand, and maintain system stability. Offshore wind farms can participate in reserve markets by offering their capabilities to provide reserves, such FCR or aFRR. Offering their resources as reserves, offshore wind farms can contribute to the reliable operation of the grid and help mitigate potential imbalances [68, 69].

Belgium, as an example, has established a well-defined market mechanism for providing ancillary services, including those related to offshore wind. The Belgian ancillary service market enables offshore wind farms to participate and provide various services to support the grid. Next to offering reserve capacity, they can also participate in an imbalance settlement mechanism, which allows them to adjust their energy production based on real-time grid conditions and market signals [70, 71].

The participation of offshore wind in market mechanisms, including day-ahead or intraday for energy and reserve markets, enhances the flexibility and efficiency of the electricity system. It allows offshore wind farms to monetize their energy production and ancillary services, incentivizing their participation and contribution to grid stability. Moreover, integrating offshore wind in market mechanisms supports the overall decarbonization efforts and the transition to a more sustainable energy system [68, 69].

1.2.4 Benefits and challenges of integrating wind energy into ancillary services markets

To provide ancillary services holds certain challenges so that offshore wind farm resources can effectively participate and optimize in ancillary services markets. We first list below the benefits of integrating wind energy conversion systems into these markets, followed by the challenges.

Benefits:

- Enhanced Grid Stability: Wind farms can respond quickly to changes in wind conditions can provide valuable ancillary services for grid stability. By participating in frequency regulation, wind farms can adjust their power output in real-time to help balance the supply and demand of electricity. This contributes to maintaining grid frequency within acceptable limits, reducing the need for conventional power plants to provide frequency regulation services.

- Increased Renewable Energy Integration: Integrating wind farms into ancillary services markets facilitates growing wind energy. Wind farms can offer reserve capacity and voltage control services essential for reliable grid operation. This helps to address the intermittency and variability associated with wind power generation, supporting the reliable integration of a higher share of renewable energy sources.

- Cost Reduction: Participation in ancillary services markets can provide additional revenue streams for wind farm operators. By monetizing their ability to provide ancillary services, wind farms can offset operational costs and potentially reduce the overall cost of renewable energy generation. This can make wind energy more economically competitive with conventional sources, accelerating the transition to a cleaner energy mix.

Challenges:

- Technical Challenges: Integrating wind farms into ancillary services markets requires addressing technical challenges associated with wind power's intermittent and variable nature. Wind farms must be equipped with optimal control strategies and forecasting techniques to accurately predict their power output and respond to real-time grid signals. This necessitates the development of sophisticated models and algorithms for efficient scheduling and dispatch of wind farm resources. Additionally, advancements in control systems are needed. This includes the development of desired control algorithms that can handle the complexity of multiple wind turbines operating in coordination to provide grid support services.

- Forecasting and Scheduling Challenges: Accurate forecasting of wind power generation is a fundamental key for effective participation in ancillary services markets. Wind farms need to provide accurate forecasts of their power output to ensure proper planning and coordination with other resources. Additionally, wind farms may face challenges aligning their operational schedules with market requirements to effectively deliver the contracted ancillary services.

- Market Design and Regulations: Integrating wind farms into ancillary services markets requires appropriate market design and regulations. Clear rules and mechanisms should be established to enable wind farms to participate effectively, ensuring fair competition with other market players. Additionally, the regulatory framework should incentivize the provision of ancillary services by wind farms and promote their integration into the broader energy system.

- Grid Infrastructure and Interconnection: The successful integration of wind farms into ancillary services markets depends on the availability and adequacy of grid infrastructure and interconnection. The grid must be capable of accommodating the additional power flows and fluctuations resulting from wind farm participation. Upgrading and expanding the grid infrastructure, including transmission and distribution networks, may be necessary to accommodate the integration of wind farms and ensure smooth operation and reliable delivery of ancillary services.

- Market Access and Participation: Wind farm operators need to have fair and non-discriminatory access to ancillary services markets. This requires transparent and efficient market platforms that enable easy participation and provide accurate price signals. Ensuring equal market access for both conventional and renewable energy resources promotes competition, fosters innovation, and encourages the efficient utilization of wind farm assets.

- System Coordination and Planning: Coordinating the operation and planning of wind farms participating in ancillary services markets with other grid assets is essential. The integration of wind farms should be aligned with system-level planning and coordination to ensure the reliable and secure operation of the overall energy system. This includes considering the impact of wind farm participation on system reserves, stability, and congestion management.

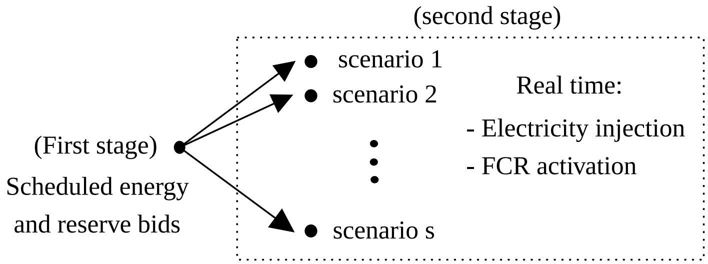

Figure 1.6: Two-stage stochastic programming framework for optimal contribution in ancillary services market.

1.2.5 Optimal contribution in ancillary services market

Decision-makers need to plan strategically based on the available information and future uncertainties. To maximize the contribution of wind farms in ancillary markets while effectively considering the inherent uncertainty associated with wind scenarios, an optimization problem is needed. To find the decisions that need to be made, a two-stage approach that looks at the day-ahead market (first stage) and the real-time (second stage, within the day) operation is typically needed. Figure 1.6 illustrates these two stages. The mathematical tool that can be specifically used to make the optimization is a two-stage stochastic programming approach [72–74].

In the first stage, decisions are made before the uncertain parameters of wind power generation are realized. This stage aligns with the day-ahead market, where wind farm operators must determine their optimal bids or offers for ancillary services based on available information at that time. This includes forecasts of wind power generation, market prices, and system requirements [75]. Subsequently, in the second stage, decisions are made based on the realized values of the uncertain parameters. This stage corresponds to the real-time operation of the ancillary market, where wind farm operators need to adjust their actual generation and ancillary service provision based on the actual wind power generation and system conditions. The decisions made in the first stage may need to be revised or updated to respond to the real-time variability of wind power [75].

The primary goal of two-stage stochastic programming is to find the optimal decisions in the first stage that maximize the expected profit or minimize the expected cost, considering the uncertainties in wind power generation. This is achieved by considering various scenarios of wind power generation and their corresponding probabilities. The optimization problem seeks to find the best dispatch of wind farms and their participation in ancillary services that minimize the expected costs or maximize the expected revenues, accounting for the probabilistic nature of wind power forecasts [73].

Applying the above mentioned two-stage planning enables wind farm operators to effectively manage the uncertainties associated with wind power generation and make informed decisions in the ancillary market's day-ahead and real-time stages. This approach allows them to optimize their participation and contribution to the market while considering the probabilistic nature of wind power forecasts. By doing so, wind farms can improve their overall efficiency and reliability in providing FCR and other ancillary services to the electricity grid [73].

1.3 Curtailing wind energy to provide FCR

FCR, with its immediate response capabilities and grid frequency regulation, plays a critical role in maintaining a steady power supply and preventing frequency deviations. Understanding FCR and other ancillary services is crucial as the energy sector undergoes an energy transition, necessitating effective integration of renewable energy sources and enhanced grid resilience. The optimization of ancillary services deployment enables compliance with regulatory requirements, techno-economic efficiency, and the utilization of advanced technologies for grid stability.

Nevertheless, it is worth mentioning that if an optimal control design and framework of an energy system can support FCR provision, it possesses the necessary features to respond swiftly to grid frequency deviations and adjust power generation accordingly. Such capabilities can be exploited to contribute to other ancillary services that demand similar fast or slower response times and real-time adjustments. As mentioned in Section 1.2.4, there are technical challenges associated to integrating wind farms into ancillary services that can be mainly attributed to the intermittent and variable nature of wind. This is no different to consistently and reliable provide FCR. The limited controllability of wind turbines compared to conventional power plants also hampers their ability to meet the fast response times required for FCR provision.

Curtailment is one potential solution to address this challange. It is however generally seen as a measure of last resort due to its impact on wind farms' overall efficiency and revenue generation. To illustrate this, Fig. 1.7 shows the cost of curtailment in the UK per MWh of wind energy produced. Curtailment involves intentionally reducing or restricting wind power generation when the grid cannot absorb or accommodate the available wind power. By curbing the power output, wind energy conversion systems can prevent grid overloading, maintain grid stability, and address operational constraints [76].

While curtailment can help manage grid constraints and ensure reliability, it is not an ideal solution [78]. Curtailing wind power generation means lost potential energy production and reduced revenue for wind farm operators. Maximizing the utilization of renewable energy resources and minimizing curtailment is preferable to achieve the highest possible renewable energy penetration and cost-effectiveness. To minimize the need for curtailment, several strategies are being followed:

- Grid Expansion and Transmission Upgrades: Enhancing the grid infrastructure, including expanding transmission capacity and improving interconnections, allows for better integration of wind energy and reduces the need for curtailment.
- Enhanced Forecasting and Grid Management: Accurate wind power forecasting and efficient grid management systems help optimize the utilization of available wind resources, reducing the likelihood of curtailment.
- Flexible Grid Operation: Implementing flexible grid operation strategies, such as demand response programs, load shifting, and energy storage integration, enables better-balancing wind power generation with grid demand, minimizing curtailment.
- Market Reforms and Incentives: Adapting market mechanisms, pricing structures, and incentive schemes to value the flexibility and services provided by wind energy encourages efficient utilization of wind power and reduces the need for curtailment.

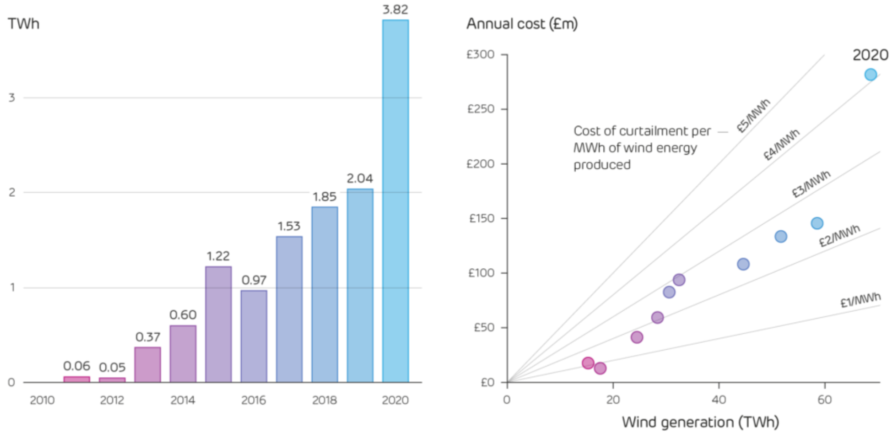

Figure 1.7: Over the past ten years, the yearly reduction of wind energy generation in UK [on the left] and the associated cost of curtailment per produced MWh of wind energy [on the right] [77].

1.3.1 Providing Frequency Containment Reserve with wind turbine controllers

To support FCR by using curtailment methods, wind turbines employ various control strategies and techniques [79, 80]. These strategies aim to adjust the power output of wind turbines in response to grid frequency deviations. One such control strategy is the deloading of wind turbines.

Wind turbines require a deloading mechanism and a power reserve margin to adapt their active power output according to grid frequency changes. Particularly, during wind speeds below the rated threshold, the reserve should be factored in to ensure the wind turbine operates optimally relative to the Maximum Power Point Tracking (MPPT) system. The deloading control mechanism involves intentionally reducing the power generation from the wind turbine below its maximum capacity. By operating the wind turbine below its rated power level, it retains the ability to quickly ramp up its power output when necessary, effectively serving as a power reserve for the grid. This reserve capability is crucial to support grid stability and meet sudden increases in power demand. The deloading process does not compromise the turbine's long-term performance or health; instead, it enhances its flexibility to respond to grid requirements efficiently. During low wind speeds or other situations where curtailment is necessary, the wind turbine can seamlessly adjust its output, preventing any adverse impact on the grid. The power reserve margin acts as a safety buffer, ensuring the turbine can respond swiftly to frequency deviations and maintain grid frequency within acceptable limits. This dynamic adaptation allows wind turbines to actively participate in grid frequency regulation actively, enhancing the grid's stability and reliability [79, 80]. Here are some commonly employed control strategies and techniques:

- Feathering the Blades: One of the primary deloading methods is feathering the blades of wind turbines. Feathering refers to changing the angle of the turbine blades to reduce their aerodynamic efficiency. Wind turbines can reduce their power output by increasing the blade angle and decreasing the electricity injected into the grid. Feathering is typically achieved through pitch control mechanisms, introduced in Section 1.1.2 that adjust the angle of the blades based on frequency signals received from the grid [81].

- Generator Control: Wind turbines can employ generator control techniques to deload power output. Generator control involves adjusting the generator settings, such as rotor speed and mechanical power, to regulate the electrical power output of individual turbines or the entire wind farm. By modifying these control parameters, wind turbines can deload their power generation and support FCR provision [80].

- Deloading by Substation Control: In some cases, deloading can be implemented at the substation level rather than at the individual turbine level. Substation control systems enable centralized curtailment of power output from multiple turbines within the wind farm. By adjusting the substation control settings, wind farms can collectively curtail their power generation in response to grid frequency deviations [82].

- Communication and Control Systems: Innovative communication and control systems can be employed in coordinating the deloading of wind turbines for FCR provision. These systems enable the exchange of frequency signals between grid operators and wind farm control centers. Real-time data on grid frequency deviations is used to trigger deloading actions and adjust the power reserve of wind turbines accordingly. These systems ensure timely response and coordination between wind turbines and the grid.

These control strategies and techniques are typically employed as part of a broader control system that considers factors such as wind farm operational constraints, grid requirements, and market signals. High-tech monitoring, communication, and control technologies facilitate the effective implementation of these control strategies, enabling wind turbines to provide FCR services through deloading methods while ensuring the reliable and efficient operation of the electricity grid.

1.3.2 Providing Frequency Containment Reserve with wind farms

To provide FCR on a wind farm level demands the consideration of the wake effect. As mentioned in Section 1.1.3, the wake interactions in wind farms are a complex behavior that is difficult to fully simulate. Sophisticated control systems are needed to ensure effective activation while coping with optimized power reserves. To support FCR using deloading methods in wind farms, a combination of optimization techniques and an adaptive control strategy needs to be employed, considering both the wake effect and optimal power reserve activation.

One critical aspect is the implementation of wake modeling and prediction techniques. These methods estimate the wake effects on downstream turbines by analyzing wind speed, direction, and turbulence data. By incorporating wake models into the control systems, wind farms can predict the spatial and temporal characteristics of the wake, enabling optimized curtailment strategies.

Wake-aware curtailment techniques are employed to account for the wake effect. The control systems prioritize the deloaded turbines based on their location in wake-affected areas to minimize the overall power loss while maintaining efficient FCR provision. By dynamically adjusting power reserve levels based on real-time wake conditions, wind farms can balance power generation and mitigating the wake impact [83].

Additionally, wind farms may adopt various wake mitigation techniques. These measures aim to reduce the wake effect and enhance power generation efficiency. Strategies include optimizing turbine spacing, adjusting operating parameters, and utilizing optimal wake control technologies. By mitigating the wake effect, wind farms can potentially minimize the need for curtailment and maximize the overall power output [84].

Furthermore, wind farm layout design is the primary element in addressing the wake effect. Wind farms can reduce wake interactions through careful placement and optimization of turbine positions. Innovative algorithms and simulation tools assist in determining the optimal layout configuration that reduces wake effects, maximizing power generation and minimizing curtailment requirements [73].

Combining improved control systems, wake modeling and prediction, wake-aware curtailment techniques, wake mitigation strategies, and layout optimization allows wind farms to effectively support FCR provision while accounting for the complex nature of wake effects. These strategies ensure efficient utilization of wind resources, optimal power generation, and grid stability while minimizing power losses in wind farms due to curtailment. By continuously refining these techniques, wind farms can contribute to the reliable and responsive operation of the electricity grid while exploiting the full potential of wind energy.

Wind farms can seamlessly integrate with the grid and actively contribute to grid stability by providing FCR. To improve control and adapt to the complex environment, variable wind, markets, etc., demands data-driven techniques. These techniques, with, amongst others, deep learning, have impacted various fields and can help wind farms adapt to their environment while executing their task to the best of their abilities: maximize power generation and provide ancillary services. Deep learning techniques have, for instance, been used for forecasting as they have the ability to analyze historical data and apprehend complex patterns. Next to forecasting, they can be used to identify anomaly detection methods when systems deviate from nominal operation. This enhances the decisions to perform maintenance interventions. Finally, such methodologies can analyze real-time sensor data and related features to optimize, for instance, power generation and curtailment decisions. Overall, data-driven approaches can be due to their ability to find patterns in data and handle the uncertain nature of the environment in wind farms.

1.4 Data-driven approaches supporting wind energy integration

Traditional models that apprehend the behavior of wind energy conversion systems often rely on simplified assumptions and theoretical equations, which may not capture the complexities of turbine behavior. In contrast, data-driven models can process and learn from data to find input-output relationships. The data or features can be turbine sensor measurements, historical performance data, and even meteorological conditions. Supervised learning - a subfield in machine learning - is used to train a model that is often a neural network, i.e., a deep learning model, that approximates the input-output relationship. These data-driven models enable to close the reality gap that traditional models face and facilitate the development of more effective control strategies [85].

Adaptive control strategies can benefit from data-driven methodologies by learning from historic and real-time sensor data. These algorithms learn from the operational data and identify patterns that correlate with optimal turbine behavior. By adapting control strategies to changing operating conditions, such as wind speed and grid requirements, data-driven-based control systems can enhance turbine efficiency, reduce wear and tear on components, and extend the turbine's lifespan [86].

Moreover, data-driven techniques have the potential to transform wind farm modeling and control approaches by exploring and exploiting vast amounts of data to create more accurate and sophisticated wind farm models. These models can capture interactions between turbines, terrain, and atmospheric conditions, leading to more precise predictions of power generation and overall wind farm performance. Additionally, deep learning algorithms can optimize wind turbine control strategies and wake steering techniques, maximizing energy capture and mitigating wake effects. This, in turn, enables wind farms to be smoothly integrated into the power grid, allowing grid operators to manage power generation and demand more effectively [87].

Section 1.4.1 handles the data collection and preprocessing related to wind energy. In the subsequent sections, we provide an overview of data-driven methodologies that can help to model and predict (Section 1.4.2), control (Section 1.4.3), and monitor (Section 1.4.4) wind energy conversion systems.

1.4.1 Data collection and preprocessing

Data preprocessing is a crucial initial step to build up data-driven models of wind turbines [88]. It encompasses several key techniques that enhance data quality and suitability for further analysis. One fundamental aspect of data preprocessing is data cleaning. This involves the identification and removal of outliers in the dataset. Outliers can significantly skew the training process of machine learning models, potentially leading to less accurate results. Addressing missing data is also essential, as missing values can introduce biases. In practice, techniques like interpolation or data imputation are employed to handle these missing values effectively. Another essential preprocessing technique is feature scaling, which aims to standardize the range of features within the dataset. Normalizing or standardizing the data ensures that all features contribute equally to the learning process, preventing any variable from dominating the model's training.

Feature engineering is another aspect of data preprocessing. This step involves selecting relevant features, creating new features, or transforming existing ones to enhance the predictive power of the data. Domain knowledge is vital in determining the most informative features, especially in specialized fields like wind turbine control. Temporal aggregation techniques are commonly employed for time series data from wind turbines, which are often collected at high frequencies. These techniques, i.e., averaging or resampling, reduce data dimensionality while providing meaningful representations of underlying patterns, simplifying subsequent analysis. Eventually, efficient data storage and accessibility are required when implementing machine learning algorithms, especially in wind turbine control systems. Properly managed data storage solutions, such as balanced database systems, cloud-based solutions, or data lakes, ensure that collected and preprocessed data is readily available for model training and inference, facilitating the overall success of machine learning applications in this domain.

By addressing these considerations, wind turbine operators can ensure the availability of high-quality data for training machine learning models. This, in turn, enables accurate prediction, fault detection, condition monitoring, and optimization of wind turbine operations. Continued research and development in data collection techniques, preprocessing methodologies, and data management systems are required to improve further the potential of machine learning algorithms in wind energy applications.

1.4.2 Data-driven time series prediction methods

Time series predictions involve data-driven techniques that can forecast wind and grid frequency, enabling effective planning and management of wind energy integration into the power grid [89, 90]. Time series prediction models can provide valuable insights into future wind conditions and grid frequency behavior by analyzing historical data patterns. This information aids in optimizing energy generation, grid stability, and resource allocation. An overview of statistical models and machine learning methods that are widely used in time series prediction, modeling, and control approaches in the field of wind energy:

- Autoregressive Integrated Moving Average (ARIMA): ARIMA models are widely used for time series prediction, including wind and grid frequency forecasting [91]. ARIMA models capture the data's underlying trend, seasonality, and noise to make future predictions. They are particularly suitable for stationary time series, where the statistical properties remain constant.

- Seasonal ARIMA (SARIMA): SARIMA models extend the capabilities of ARIMA by incorporating seasonality patterns. This is especially relevant for wind and grid frequency data exhibiting regular seasonal variations. By capturing both short-term fluctuations and long-term seasonal patterns, SARIMA models can provide accurate forecasts for different time horizons [92].

- Recurrent Neural Networks (RNNs): RNNs are designed to handle sequential data and are widely used for time-series prediction. Unlike feedforward networks, RNNs have feedback connections, allowing information to flow in cycles within the network. This enables the network to retain memory of past inputs and consider temporal dependencies when making predictions. The recurrent nature of RNNs makes them suitable for modeling, pattern recognition, and time-series prediction tasks. Long Short-Term Memory (LSTM) and Gated Recurrent Unit (GRU) are popular variants of RNNs that address the vanishing gradient problem and improve the ability to capture long-term dependencies [93].

- Convolutional Neural Networks (CNNs): CNNs are primarily known for their success in image recognition tasks, but they can also be applied to time-series prediction. CNNs are designed to extract spatial features from 2D inputs, but time-series data can be treated as a 1D signal and processed with CNNs. Using 1D convolutions and pooling operations, CNNs can effectively capture local patterns and hierarchically learn representations in time-series data. CNNs are particularly useful when spatial or localized patterns exist in the time series, such as in wind speed prediction [94].

- Adaptive Neuro-Fuzzy Inference Systems (ANFIS) is a hybrid modeling approach that combines the capabilities of neural networks and fuzzy logic. ANFIS models have been widely used for time-series prediction and other data-driven tasks. ANFIS provides a flexible framework for modeling complex relationships between input variables and output predictions while incorporating human-like fuzzy logic reasoning. This mathematical framework allows for approximate reasoning and handling of uncertainty. It is beneficial when dealing with data exhibiting a high level of stochasticity. Fuzzy logic enables representing vague or imprecise relationships between variables through linguistic rules and membership functions [95].

- Group Method of Data Handling (GMDH) is a data-driven modeling and regression technique used for modeling complex systems and making predictions. GMDH is known for its ability to automatically select relevant input variables and construct mathematical models based on the available data. GMDH models have been successfully applied to various domains, including time-series prediction, pattern recognition, and data analysis. GMDH is based on the principle of self-organization, where a complex system is modeled by iteratively selecting and combining input variables to optimize the model's predictive performance. GMDH aims to find an optimal mathematical model that can accurately represent the relationship between the input and output variable [96].

- Hybrid Models: Hybrid models combine the strengths of different machine learning architectures to improve time-series prediction. For example, combining CNNs and RNNs in a hybrid model, such as a Convolutional Recurrent Neural Network (CRNN), allows the network to capture spatial and temporal patterns. This fusion of architectures takes advantage of the power of CNNs in feature extraction and RNNs in modeling sequential dependencies, resulting in improved prediction accuracy [97, 98].

The choice of data-driven based methods for time series prediction depends on the system's specific characteristics, data availability, seasonality, trend, and noise. Furthermore, the models should be regularly updated with new data to ensure accurate, up-to-date, and dynamic prediction. The continuous advancement of machine learning techniques presents exciting opportunities for further improving time series prediction in wind and grid frequency forecasting and understanding the nonlinear complexity of wind turbines, enabling more reliable and efficient integration of wind energy into the power grid.

1.4.3 Recently developed control approaches

Conventional control approaches, such as Proportional-Integral (PI) control systems, have been widely employed to regulate various aspects of wind turbine operation. The pitch control system adjusts the blade angles to regulate the aerodynamic force and maintain a constant rotational speed, optimizing power output and preventing damage in varying wind conditions. Meanwhile, the torque control system manages the generator's torque, controlling the electrical power generated by the turbine. Both systems are required for efficient

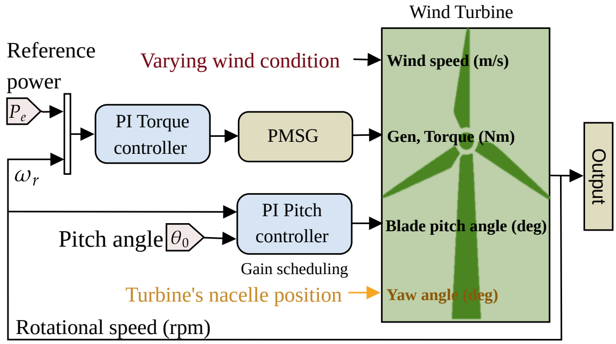

Figure 1.8: Classical control systems in wind turbines with pitch and generator torque control systems.

and safe operation, capturing maximum wind energy while safeguarding the turbine from potential harm caused by extreme forces. Figure 1.8 shows classical pitch and torque controllers in wind turbines. To adapt the operation of wind turbines and farms in the face of uncertain environmental conditions, data-driven control methodologies can be devised, ranging from adapting the gains in PI controllers to data-driven-based model predictive controllers (MPC) to full-blown black box Reinforcement Learning (RL). All these controllers start from a certain state of the system, which can be based directly on sensor data or extracted from data, to take actions, e.g., pitch angle and generator torque.

Adaptive gain scheduling PI

By continuously adjusting the control gains of PI controllers, the controller can adapt to changing wind speeds, turbulence, and environmental conditions. Such adaptive control has the potential to adapt the turbine to capture maximum energy and manage loads within safe limits, mitigate turbulence effects, improve grid integration, enhance overall reliability, and reduce maintenance costs, ensuring efficient and sustainable wind power generation. In that respect, adaptive gain scheduling fuzzy PI control is a promising approach for optimizing wind turbine operation. This method combines the benefits of fuzzy logic and adaptive control to enhance the performance and robustness of wind turbines [99]. Using linguistic rules and membership functions, the control system can make decisions based on fuzzy inputs and continuously adjust its parameters to optimize turbine performance. The adaptive gain scheduling aspect further improves the control system's adaptability, dynamically adjusting the gains of the PI controller based on real-time data and system conditions. This allows wind turbines to operate closer to their optimal performance, leading to increased energy production and reduced wear and tear on the system [100].

Data-driven approaches and machine learning tools present new opportunities for adaptive and intelligent control of wind turbines and offer promising solutions to address the challenges that conventional control systems face.

Data-driven tools enable the creation of accurate models for wind turbines and wind farms, considering the complex dynamics, non-linearities, uncertainties, and even wake interaction inherent in wind energy systems [101, 102]. Neural networks, for example, can be trained using historical data to learn the relationships between inputs (e.g., wind conditions, turbine locations) and outputs (e.g., power output, turbine performance) while accounting for wake effects [101]. These models can then be used for control system optimization, layout design, and other tasks related to wind farm management.

To address wake interaction, machine learning methods can be applied to develop sophisticated models that capture the complex flow patterns and interactions within wind farms. These models can consider factors such as wind direction, wind speed, turbine spacing, and the layout of turbines to predict the wake effects and optimize the overall performance of the wind farm [101,103]. The accurate modeling can enhance control strategies in wind turbine and wind farm systems, specifically for addressing wake interaction and optimal reserve allocation considering the Wind farm's contribution in energy and reserve markets [73].

Data-driven MPC

Classically, model predictive control uses a physics-based model of the system that needs to be controlled. The corresponding optimal actions can be found by solving an optimization problem that maximizes (or minimizes) a certain reward (or cost) function, e.g., maximum power. By using the model's predictive capabilities, it is possible to foresee what the optimal control actions can be in the future.

Since physics-based models face a reality gap, i.e., they are subject to uncertainties, which is typically the case for wind turbines, the actions can become suboptimal. By using a data-driven model that is trained on historical and/or real-time data, a predictive model that better aligns with the real-world system can eventually be obtained. By optimizing a cost function with an underlying data-driven model, corresponding optimal control actions can be found.

Data-driven model predictive control (MPC) strategies can be implemented to anticipate changes in wind speed and direction, proactively adjusting the turbine's parameters to maximize energy capture and minimize fatigue loads. Moreover, these methods can learn from historical data and real-time measurements, allowing turbines to continuously improve their control strategies and adapt to complex and dynamic wind patterns [104–106]. Additionally, coordinated control of wind farms through creative optimization algorithms

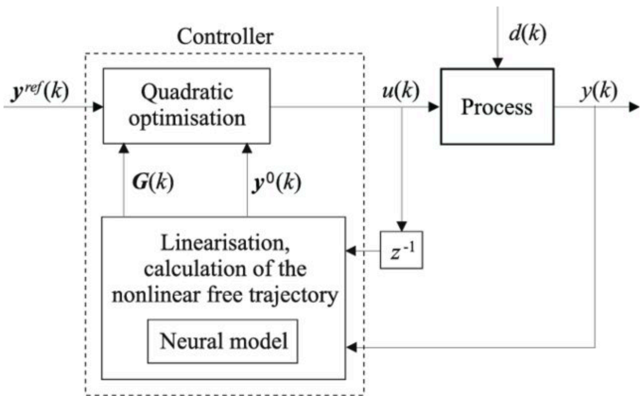

Figure 1.9: Schematic of a data-driven MPC methodology consisting of a neural network model that is being updated based on measurement data $y(k)$ and control inputs $u(k)$, with delay z^{-1}. The data-driven model is nonlinear and can be linearized G(k) at each time instant to predict the behavior of the wind turbine (Process). The predictive behavior of the model is used to find the control actions u(k) by optimizing a cost function. This cost function can for instance be the tracking of a reference power value $y^{ref}(k)$ to what the model predicts and the current power value $y^0(k)$ [110].

enables efficient power and reserve distribution and enhanced grid integration [107, 108].

Adaptivity can be realized in a classical MPC approach by adapting the model parameters. A similar strategy can be followed in data-driven MPC where the model is continuously updated with adjusted control actions based on real-time data [104, 109]. Figure 1.9 consists of a nonlinear data-driven model, here a neural network model, that is linearized and where a quadratic optimization is done of the cost function. The underlying model can be updated based on sensor data. The loop is in feedback to have stability and robustness to unmeasured disturbances, which need to be analyzed each time. On the wind farm supervisory level, by incorporating information about wake interaction into the model, data-driven MPC can generate control strategies that account for the wake effects and optimize the wind farm's power output [73].

Reinforcement learning

Machine learning with supervised learning can be used to train a neural network model like in Fig. 1.9. Another strategy is using Reinforcement Learning (RL), a subfield different from supervised learning in machine learning. Re-

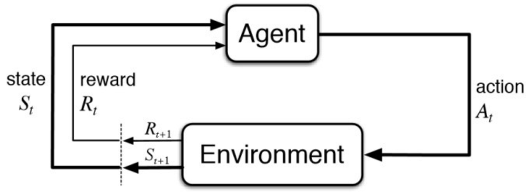

Figure 1.10: Reinforcement learning framework:A_t is the action taken by the agent at time t, S_t is the state of the environment at time t, and R_{t+1} stands for the reward at time $t + 1$ [114].

inforcement learning is an agent that, based on the state of the system, e.g., measurement data related to the wind speed, rotor speed, and power output, optimizes short-term and long-term rewards, e.g., maximum power output. It does so by adjusting the control actions like rotor pitch and/or generator torque.

A simulation model approximating system dynamics can be employed to train RL agents, which typically require many interactions with the environment to learn a control policy. In the case of less complex systems/operations, running RL methods in real time can be facilitated by applying adaptive methods such as dynamic programming approaches. Nevertheless, developing accurate simulation models that faithfully represent system dynamics in wind turbines and wind farms also smoothes the transition from simulated training to real-world applications and minimizes the reality gap that demands real-world interactions. The state of the environment can involve parameters such as wind speed, rotor speed, and power output, and the agent's actions, such as adjusting rotor pitch or turbine yaw angles [111]. As shown in Fig. 1.10, a reward function is designed to provide feedback to the agent, guiding it toward optimal control actions. RL algorithms, such as deep Q-network (DQN) and deep deterministic policy gradient (DDPG), are used to train the agent by iteratively interacting with the environment, learning from experience, and updating control policies [112, 113].

Comparing data-driven MPC with RL

The above mentioned data-driven methodologies have the ability to address the following challenges:

- Handling Complexity and Non-Linearity: Wind turbine and wind farm control systems involve complex dynamics and non-linearities that can be challenging to model accurately using traditional control methods. Data-driven MPC and RL have the ability to learn from historical data and adapt to the system's non-linear behavior, allowing them to capture complex relationships and make better control decisions.

- Adaptability and Flexibility: Data-driven MPC and RL excel in adaptive control. Wind conditions in a wind farm are dynamic and can change rapidly. Data-driven MPC continuously updates system models based on real-time data, while RL agents learn optimal control policies through interactions with the environment. This adaptability allows these strategies to adjust to changing conditions and uncertainties, optimizing control actions in real-time.

- Handling Uncertainties: Wind energy systems, like wind farms, are subject to various sources of uncertainties, such as fluctuating wind speeds and directions. Data-driven MPC and RL can account for these uncertainties and optimize control actions while considering possible variations in the system behavior. This robustness to uncertainties is crucial for achieving stable and efficient operation.

- Enhanced Performance through Learning: Both data-driven MPC and RL can potentially improve the performance of control systems beyond what traditional control methods can achieve. They can learn from past experiences and adjust their control strategies to achieve better power output, minimize wake losses, and optimize overall system performance.

- Handling High-Dimensional State Spaces: In wind turbine and wind farm control, the state space can be high-dimensional, involving multiple variables and parameters to be controlled. Data-driven MPC and RL are well-suited to handle such high-dimensional state spaces, making them applicable to complex control tasks.

- Combining Physics-Based Models with Data: Data-driven MPC and RL can be integrated with physics-based models in a hybrid approach, exploiting the benefits of both approaches. This hybrid modeling can lead to more accurate and efficient control strategies, especially when data is scarce or when there is a need to exploit the knowledge from physics-based models.

- Autonomy and Minimal Human Intervention: Once data-driven MPC and RL models are trained and deployed, they can operate autonomously, requiring minimal human intervention. This autonomy is advantageous in wind farm management, where control actions need to be continuously adjusted based on real-time data and conditions.

On the other hand, model-based Reinforcement Learning (RL) holds promise in addressing some of the challenges associated with model-free RL approaches. One key advantage of model-based RL is its potential for sample efficiency. By using an internal model of the environment, the agent can simulate trajectories and learn from these simulated experiences, reducing the need for extensive real-world interactions. This is particularly advantageous in scenarios where collecting data is resource-intensive, costly, or time-consuming. The internal model in model-based RL can take various forms, ranging from simple parametric models to more complex non-parametric models, such as neural networks. The choice of the model architecture depends on the characteristics of the environment and the computational resources available. Advanced model-based RL methods often involve refining the internal model through a combination of real-world interactions and simulated learning, striking a balance between exploration and exploitation.

The selection between RL and data-driven MPC depends on various factors, including data availability, computational resources, system complexity, and the desired level of interpretability. Model-free RL algorithms may require a higher sample complexity as they explore the system dynamics through trial and error. At the same time, data-driven MPC is more sample-efficient as it uses existing data. Model-free RL algorithms often operate as black-box models, making them less interpretable, while model-based RL and data-driven MPC provide more transparency and interpretability.

Although both approaches have their limitations and challenges, Data-driven MPC heavily relies on the quality of data and accuracy of system models. It may not generalize well to different systems or operating conditions, and solving the optimization problem in real time can be computationally intensive for large-scale wind farms. Model-free RL requires a large number of interactions with the environment to converge, which can be time-consuming and costly. Balancing exploration and exploitation can be challenging, especially in dynamic wind conditions. Ensuring safety and stability during RL training is required, as exploring untested actions may lead to undesirable system behavior.

Nevertheless, data-driven MPC can have a few advantages in wind farms and wind turbine control systems. First, wind farm and turbine control systems typically have access to a considerable amount of historical operational data. Data-driven MPCs use data to build accurate system models and optimize control actions based on past behavior. This historical data can provide valuable insights into system dynamics. On the other hand, model-free RL typically learns from scratch through trial and error, which can be inefficient and time-consuming. Second, wind turbine and wind farm control systems have various physical and operational constraints and safety limits. Data-driven MPC can easily incorporate these constraints into the optimization problem, ensuring that the control actions generated are within safe and feasible ranges. On the other hand, model-free RL may require additional effort and design considerations to handle constraints effectively.

Moreover, wind conditions are inherently uncertain, and wind turbine and wind farm control systems need to handle these uncertainties effectively. Data-driven MPC can benefit from continuous model updates using real measured data, and its robustness to model uncertainties allows it to adapt to changing conditions and disturbances. Aditionally, data-driven MPC provides practical and theoretical guarantees on performance and stability under certain assumptions [115]. These guarantees are valuable in wind farms and wind turbine control systems, where ensuring reliable and consistent operation is critical. Conversely, RL typically needs to provide such performance guarantees, making ensuring system stability and safety more challenging.

Meta-heuristic optimization techniques

Furthermore, the incorporation of meta-heuristic optimization techniques techniques, including Particle Swarm Optimization (PSO), Genetic Algorithms (GA), Simulated Annealing (SA), Ant Colony Optimization (ACO), Differential Evolution (DE), and Grey Wolf Optimizer (GWO), has opened up possibilities for advancing wind turbine and wind farm control. When combined with machine learning methods, these techniques offer a powerful means to tackle complex and multi-objective optimization challenges in wind energy systems.

Particle Swarm Optimization (PSO) and Genetic Algorithms (GA), inspired by natural processes, have appeared as powerful optimization approaches. They contribute to several critical aspects of wind energy control. They have been used vastly to fine-tune control parameters, such as optimizing rotor speed, pitch angle, yaw angle, and other variables to maximize power output while considering operational constraints and uncertainties. They have been used to optimize wind farm wake behavior, minimizing losses and enhancing overall energy capture, considering factors like wind direction, turbine spacing, and terrain. PSO and GA aid in model calibration and validation, improving simulation accuracy and control strategy reliability [116–118].

Considering the unpredictability and nonlinearity of wind energy, where multiple objectives often clash, PSO and GA still provide promising multi-objective optimization solutions. They unveil trade-off solutions known as Pareto fronts, providing decision-makers with a spectrum of optimal choices. Additionally, these techniques are scalable to large wind farms, efficiently exploring extensive search spaces for real-time decision-making. They also smoothly integrate with machine learning models, optimizing neural networks or reinforcement learning hyperparameters to enhance model performance and control effectiveness. Moreover, PSO and GA handle non-convex optimization problems effectively, overcoming local optima and reducing computational complexity [119].

Particle Swarm Optimization (PSO) is often the preferred choice for optimizing wind turbine and wind farm control systems because of its simplicity of implementation, computational efficiency, and minimal hyperparameters, making it accessible and fast. While not guaranteed, it often converges to global or near-global optimum solutions. Furthermore, its suitability for continuous optimization problems, robustness to noise, and parallelizability solidify its position in wind energy control systems. However, choosing the right optimization algorithm requires careful consideration of the specific problem's characteristics, fitness landscape, and available computational resources. Depending on complexity and requirements, alternatives such as Genetic Algorithms or Differential Evolution may warrant exploration.

1.4.4 Health monitoring methods

Health monitoring is another essential area of research in the maintenance and operation of wind turbines. It involves monitoring various components and systems of wind turbines to detect faults, diagnose problems, and predict potential failures. In real-world scenarios, various factors, such as temporary events or the natural aging process, make wind turbine parts susceptible to malfunctions and defects. These issues can result in interruptions to the system and financial setbacks [120]. Anomalies in wind turbine performance that are unforeseen can be classified as either faults or failures. A fault is identified when there is an undesirable deviation in the system's structure or parameters from its expected state, while a failure is characterized by a system or component's inability to carry out its intended function [120]. Figure 1.11 illustrates a pie chart indicating the distribution of common faults found in wind turbines.

Machine learning techniques have gained significant attention in wind turbine health monitoring due to their ability to analyze large amounts of sensor data [121, 122]. A valuable strategy to detect faults is to compare the actual wind turbine behavior with its nominal, healthy behavior. To that end, a digital twin - a digital model that mimics the behavior of the real-world wind turbine - can help. How can one build a digital twin? This can be based on data, eventually merged with a physics-based model, to optimize model parameter values so that the mathematical model corresponds with the real-world sensor data. To build such a model, one can use supervised learning, i.e., find data-driven model parameters, and/or use system identification techniques, i.e., find system model parameters and, eventually, system model structures. This leads to a mathematical model in engineering, often called a surrogate model. Figure 1.12 shows how anomaly detection can be performed based on real-time sensor data and a wind turbine digital twin. General Electric and Siemens are examples of companies that follow a strategy to use digital twins towards detecting anomalies. An overview of the commonly used machine learning approaches in wind turbine health monitoring is as follows:

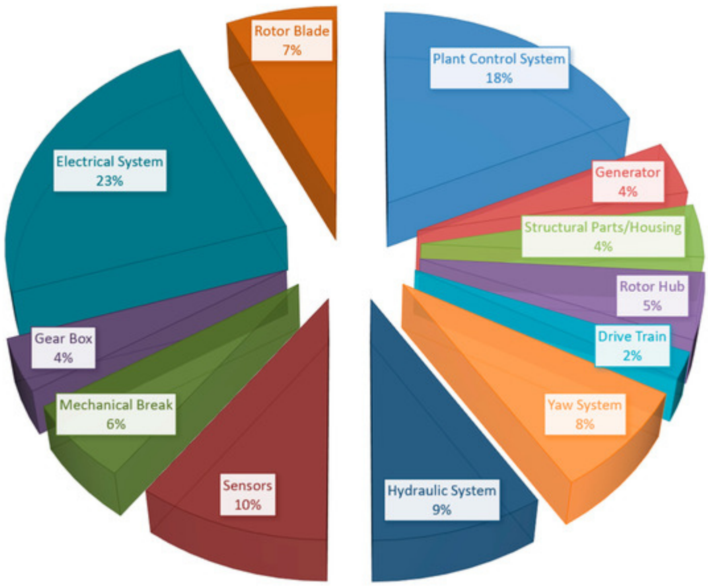

Figure 1.11: Typical malfunctions in wind turbines [120].

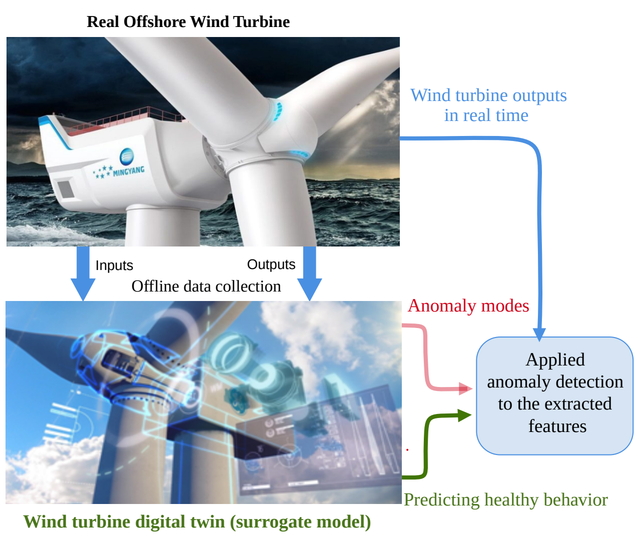

Figure 1.12: Machine learning-based anomaly detection.

- Supervised Learning: Supervised learning algorithms are trained on labeled datasets to learn patterns and make predictions. In wind turbine health monitoring, supervised learning techniques can be used for fault classification, anomaly detection, and remaining useful life (RUL) prediction. Key steps in applying supervised learning include data preprocessing, feature engineering, model training, and model evaluation. Commonly used algorithms include decision trees, random forests, support vector machines (SVM), and neural networks [121, 123].

- Unsupervised Learning: Unsupervised learning algorithms are utilized when labeled data is scarce or unavailable. These techniques aim to identify patterns, clusters, or anomalies in the data without explicit guidance. Unsupervised learning approaches can be employed for fault detection, data clustering, and outlier identification in wind turbine health monitoring. Clustering algorithms like k-means and hierarchical clustering, as well as dimensionality reduction techniques such as principal component analysis (PCA), are commonly used on this basis [121, 122, 124].

- Ensemble Techniques: Ensemble techniques combine multiple individual machine learning models to improve prediction accuracy and robustness. They can be utilized in wind turbine health monitoring to boost fault classification, anomaly detection, and RUL prediction. Ensemble methods, such as bagging and boosting, aggregate predictions from multiple models or train multiple models with different subsets of data to achieve better overall performance [125].

- Transfer Learning: Transfer learning is a technique where knowledge gained from one task or domain is applied to another related task or domain. In wind turbine health monitoring, transfer learning can be beneficial when labeled data is limited. Retrained models from similar applications or domains can be used as a starting point for training on wind turbine data, allowing for faster convergence and improved performance [126–128].

Health monitoring considering ancillary service provision:

Health monitoring is crucial for detecting anomalies during wind turbine provision of ancillary services, ensuring reliable operation. Detecting anomalies at an early stage can prevent severe damage and minimize downtime, reducing repair costs and maintaining continuous service provision [129]. Anomalies in wind turbine operation can impact performance when providing ancillary services. Health monitoring systems analyze real-time data to assess power output, pitch angle, rotor speed, and vibrations, promptly addressing deviations. These services are vital for grid stability and reliability [130].

However, when wind turbines provide ancillary services, several challenges are associated with wind turbine health monitoring. Ancillary services may involve deviations from normal turbine operation, making fault detection more challenging. Differentiating between normal variations related to ancillary service provision and actual faults requires practically efficient algorithms that can accurately distinguish between the two. This requires careful consideration of the operational characteristics and behavior of the turbine during ancillary service provision. Moreover, developing accurate and robust machine learning models for wind turbine health monitoring typically requires labeled training data.

However, obtaining labeled data for rare or specific fault scenarios during ancillary service provision can be challenging. Limited availability of labeled data can impact the performance and accuracy of the health monitoring system, requiring alternative approaches such as transfer learning or physics-informed deep learning modeling techniques. More importantly, wind turbines are complex systems with intricate interactions between various components and subsystems. The dynamic nature of these systems, coupled with changing wind conditions during ancillary service provision, makes it challenging to develop accurate models and algorithms for health monitoring. Capturing the dependencies and dynamics of the system accurately requires evolved modeling techniques and algorithms that can handle nonlinearities and time-varying conditions.

Addressing these challenges requires a combination of domain knowledge, improved data analytic techniques, and a multidisciplinary approach. Developing robust health monitoring systems that can effectively monitor wind turbines while providing ancillary services requires continuous research and innovation to overcome these challenges and ensure the reliable and efficient operation of wind turbine systems.

1.5 Objectives, challenges and contributions

The previous sections provide an introduction to the field of wind energy conversion systems: their operation and how they contribute to ancillary services with frequency containment reserve. We discussed the intricacies they face, demanding adaptive operational strategies, especially when integrating into electrical power systems. Data-driven methodologies can help in the modeling, control, and health monitoring to ultimately further optimize the operation of wind energy conversion systems that deliver FCR. The main objective of this dissertation is to find such strategies both on a wind farm supervisory control level as locally in a wind turbine control system and a wind turbine health monitoring system. In this dissertation, we use FAST and FLORIS simulators, cfr. Section 1.1.3, to assess the performance of the presented methodologies. The specific objectives, challenges, and thesis contributions for each area are outlined below:

1.5.1 Wind farm supervisory control

Objective: The fundamental goal of the proposed wind farm supervisory control is to maximize wind farms' overall performance efficiency and economic benefits in both reserve and energy markets. This is achieved through the optimal allocation of Frequency Containment Reserve (FCR) among wind turbines utilizing active wake control, taking into account the inherent uncertainties related to intermittent wind power, wind direction changes, and grid frequency fluctuations.
Challenges:

1. *Optimal scheduling:* Wind farms must provide day-ahead energy and reserve commitments schedules, cfr.1.2.3. Accurate forecasting of wind power output is critical to avoid imbalances between scheduled and actual generation. This can lead to financial damages or nonoptimal contributions to the energy market. Moreover, wind farms face risks confronting specific energy and reserve schedules due to the uncertainty associated with wind power generation. Deviations from the scheduled output can lead to financial losses or market penalties.

2. *Uncertainties in intermittent wind power and grid frequency:* Wind power generation is inherently stochastic and intermittent, making it challenging to predict the precise amount of energy a wind farm can produce at any given time. Developing control strategies that can adapt to these fluctuations is essential, as mentioned in Section 1.2.5, for effective integration into the power grid. Furthermore, in FCR provision wind farms need to actively respond to the grid's frequency changes

and ensure a stable and reliable power supply. Developing control algorithms that can achieve grid compatibility under varying frequency conditions is necessary.

3. *Complex aerodynamics of wake formation:* The interaction between wind turbines within a wind farm results in wake formation, reducing the downstream turbines' efficiency, cfr. 1.1.3. Developing optimal control mechanisms and adaptive operational strategies is required to manage wake effects and maximize power generation. Moreover, changes in wind direction and reserve provision alter wind farms' wake behavior and impact the performance of wind turbines, affecting the distribution of wake and the overall power output of the wind farm. Addressing the optimal distribution of power reserve considering wind direction variability and uncertainties associated with wind and grid frequency is essential for optimizing energy production and facilitating grid integration.

Contribution:

Chapter 2 of the thesis presents significant contributions. It introduces a new wind farm operational strategy optimizing FCR provision while managing aerodynamic wake formation and addressing challenges related to varying wind speed/direction, grid frequency uncertainties, and energy/reserve scheduling. This work uses a two-stage stochastic programming approach to realize these goals, as shown in Fig. 1.6.

1.5.2 Wind turbine local control

Objective: The wind farm supervisory level from Section 1.5.1 delivers setpoints to the local wind turbines. The main objective here is to create and deploy sophisticated algorithms that ensure robust, optimal performance and safe operation for individual wind turbines. These algorithms enable the turbines to dynamically provide FCR across all operational regions, including partial and full load regions, considering transition zones. These algorithms need to be adaptable and capable of handling the challenges posed by varying turbulent wind conditions.

Challenges:

1. *Nonlinearities in wind turbine dynamics:* Wind turbines exhibit nonlinear behavior influenced by various factors such as aerodynamic characteristics, fluctuating wind speeds, and mechanical components, cfr. 1.1.3. As a result, developing control strategies that can anticipate and account for these nonlinearities becomes indispensable for ensuring stable and efficient turbine operation while considering physical constraints

and restrictions. These strategies must possess the ability to predict and incorporate the complex interactions within the system and its control sequences to identify optimal control actions that enhance the overall performance of the turbines.

2. *Grid frequency changes and stochastic wind speed variations:* Wind turbines need to react to control setpoints decided at the wind farm supervisory control level and face regulating operation and proportionally responding to grid frequency fluctuations, cfr. 1.5. This necessitates an adaptive control design that adequately copes with determined power reserves, which must be adjusted according to the wind turbine's operating condition. Designing control algorithms capable of effectively adapting to these stochastic variations while ensuring safe, robust, and optimal performance poses significant challenges that demand attention and resolution.

Contribution:

Chapter 3 introduces a robust data-driven MPC approach for wind turbine control, enhancing power reference tracking. This work starts from the schematic shown in Fig. 1.9, employing optimal cooperation between pitch and torque control systems, considering FCR provision in turbulent and high-speed wind conditions, where wind turbines will be exposed to adverse mechanical loadings, leading to minimization of mechanical loads posed on the blade pitch mechanism.

Chapter 4 proposes an adaptive strategy that can effectively contribute to all operating conditions, improving FCR provision through generator torque control addressing grid frequency changes and wind variations. The proposed method also suggests an adaptive reserve deployment even in the below-rated wind speed, instead of having a fixed reserve proposed in chapter 3, which results in wind turbine efficiency and stability improvement.

1.5.3 Wind turbine health monitoring

Objective: The primary objective of wind turbine health monitoring is to acquire methods and procedures that precisely assess the condition of wind turbines, particularly in the context of grid integration. To strengthen the monitoring and detection of anomalies in wind turbine operation, data-driven methodologies are developed. We particularly look into comparing turbine sensor data with surrogate models. This is to ensure optimal performance and minimize downtime.

Challenges: Section 1.4.4 has already covered the challenges associated with monitoring the health of wind turbines. This thesis will now focus on addressing the primary challenges as follows:

1. *Overall health monitoring:* Overcoming the limitations of traditional methods by developing integrated and multi-dimensional health monitoring approaches to assess the wind turbine's overall performance and health, considering complex interactions and dependencies among subsystems.

2. *Efficient model fusion:* Facilitating wind turbine health monitoring by exploring efficient model fusion between physics-based techniques and data-driven approaches to manage multiple models, ensuring a cooperative and coherent view of the turbine's condition despite diverse data sources and sensor measurements.

3. *Curtailment-induced degradation:* Addressing the critical gap in wind turbine health monitoring research related to degradation scenarios caused by curtailment operations. Developing methodologies to detect and quantify the effects of curtailment-induced degradation on wind turbine health, ensuring effective maintenance decisions and optimal operation.

Contribution:

Chapter 5 presents a hybrid physics-based deep learning framework to predict wind turbines' overall performance. This framework predicts electrical power and rotational speed while considering the stochastic nature of wind speed and intricate correlations between pitch-generator torque control sequences and system responses in turbulent wind conditions. Additionally, the chapter explores a self-learning iterative framework that improves classifier performance by dynamically updating newly labeled anomalies based on past successful classifications. The study considers various anomalies and degradation scenarios to effectively address the complexities present in wind turbine performance under varying grid requirements and operating conditions.

By addressing the above-mentioned challenges, this thesis aims to enhance wind energy conversion systems' performance, reliability, and grid integration.

1.6 Thesis outline

The following chapters of the thesis contain the research results of this PhD. Combined, these results answer the objectives defined above. Figure 1.13 illustrates the coupling of the different chapters in this thesis. Chapter 2 starts with the optimal FCR allocation on the wind farm level. These provide setpoints to the wind turbine local controller for full load region (Chapter 3) and partial/full load (Chapter 4). In Chapter 5, wind turbine health monitoring is considered to strengthen the operations. The methodologies developed in these chapters are data-driven to be adaptive without losing track of the physical behavior of wind farms and turbines. In each chapter, we analyze the performance of the methodologies on simulation data.

Chapter 2: Wind Farm Supervisory Control Level: Optimal Allocation of FCR Considering Wake Effect

The chapter presents a novel operation strategy for wind farms (WFs), aiming to optimize the provision of FCR while simultaneously controlling wake formation. The power reserve allocation is dynamically determined at the wind farm supervisory control level, taking into account factors such as intermittent wind power, wind direction, grid frequency variability, and the complex aerodynamics of wake formation. A two-stage stochastic programming approach is employed to support decision-making for optimal contributions to day-ahead energy/FCR markets, considering sub-hourly wind power and grid frequency uncertainties. To reduce computational complexity, a data-driven surrogate model of wake formation is integrated into the optimizer. This surrogate model utilizes a neural network trained on the Gauss-Curl-Hybrid wake model in FLORIS, enabling rapid estimation of wake control parameters such as optimal yaw angles and axial induction factors. A coevolutionary-based multi-objective particle swarm optimization technique is utilized to search for the optimal deloading of wind turbines, maximizing total power production and kinetic energy while minimizing wake. The proposed algorithm's performance is evaluated using the C-Power wind farm in the North Sea as a case study. Simulation results demonstrate the effectiveness of the proposed algorithm in improving the overall performance of the wind farm under different operational conditions, showcasing its potential for improving FCR provision and optimizing wake control.

Chapter 3: Wind Turbine Local Control Level: Predictive and Optimal Activation of FCR

The chapter focuses on applying neural network-based Model Predictive Control (MPC) to enhance the performance of wind turbine (WT) control systems in providing frequency control ancillary services to the grid. A closed-loop Hammerstein structure is utilized to approximate the behavior of a 5MW floating offshore wind turbine with a Permanent Magnet Synchronous Generator (PMSG). Multilayer perceptron neural networks are employed to estimate the aerodynamic behavior of the nonlinear steady-state part, while the linear AutoRegressive with Exogenous input (ARX) model is used to identify the linear time-invariant dynamic part. The Cascade Hammerstein design is used to simplify online linearization at each operating point, avoiding the need for nonlinear optimization. The proposed algorithm utilizes quadratic programming to obtain control actions, eliminating the necessity for nonlinear optimization. The designed control system provides a fast and stable response to grid frequency variations with optimal pitch and torque cooperation. The performance of the MPC is compared with the gain-scheduled proportional-integral (PI) controller. Results demonstrate the effectiveness of the designed control system in providing FCR and frequency regulation in the future of power systems.

Chapter 4: Wind Turbine Local Control Level: Adaptive Activation of FCR

This chapter presents an adaptive operational strategy at wind turbines (WTs) local control level to provide FCR while considering the unpredictable behavior of grid frequency and wind speed. The strategy involves estimating an adaptive reserve margin based on short-term grid frequency predictions and using a real-time look-up table to adjust the reserve margin and control setpoints in an FCR supplementary control loop. The study evaluates the strategy's performance for fixed and percentage power reserve methods and applies gain scheduled fuzzy-PI control for reliable FCR provision in turbulent winds. The proposed strategy demonstrates optimal response to grid frequency changes and effectively smoothens out power fluctuations while improving generator speed regulation. The fuzzy-PI control approach performs well in all operating regions and reserve modes, providing stable control in the presence of turbulent wind speeds. The study concludes that the proposed operational strategy is cost-effective, adaptable to various operating conditions, and can be integrated into existing pitch and torque control systems of WTs for optimal FCR provision.

Chapter 5: Wind Turbine Health Monitoring: Anomaly/Degradation Detection Considering Curtailment

This chapter addresses the challenge of assessing the overall condition of wind turbines (WT) in operation, particularly when they provide ancillary services and operate under curtailment mode. A novel physics-informed learning framework is proposed to accurately approximate the time-varying correlation between control sequences and system response, capturing the aerodynamic nonlinearity of the NREL 5MW offshore WT. A computationally efficient weakly supervised approach is introduced to detect degradations and anomalies considering curtailment, using a hybrid structure and support vector machine for classification in both the time and frequency domain. An iterative learning framework is implemented to update the selected classifier dynamically, enabling it to learn from new anomalies during active operations. The proposed method accounts for uncertainties in the system, such as wind stochasticity and power curve variations, as well as different sparsity levels in the datasets. The results of the proposed approach demonstrate its potential in enhancing health monitoring performance, leading to more efficient and accurate assessments of the overall condition of wind turbines.

Chapter 6: Conclusion and Future Work

The concluding chapter summarizes the research outcomes presented in the thesis and provides a cohesive overview of the contributions made in each chapter. It highlights the key findings, addresses the research objectives, and discusses the potential future research directions and challenges.

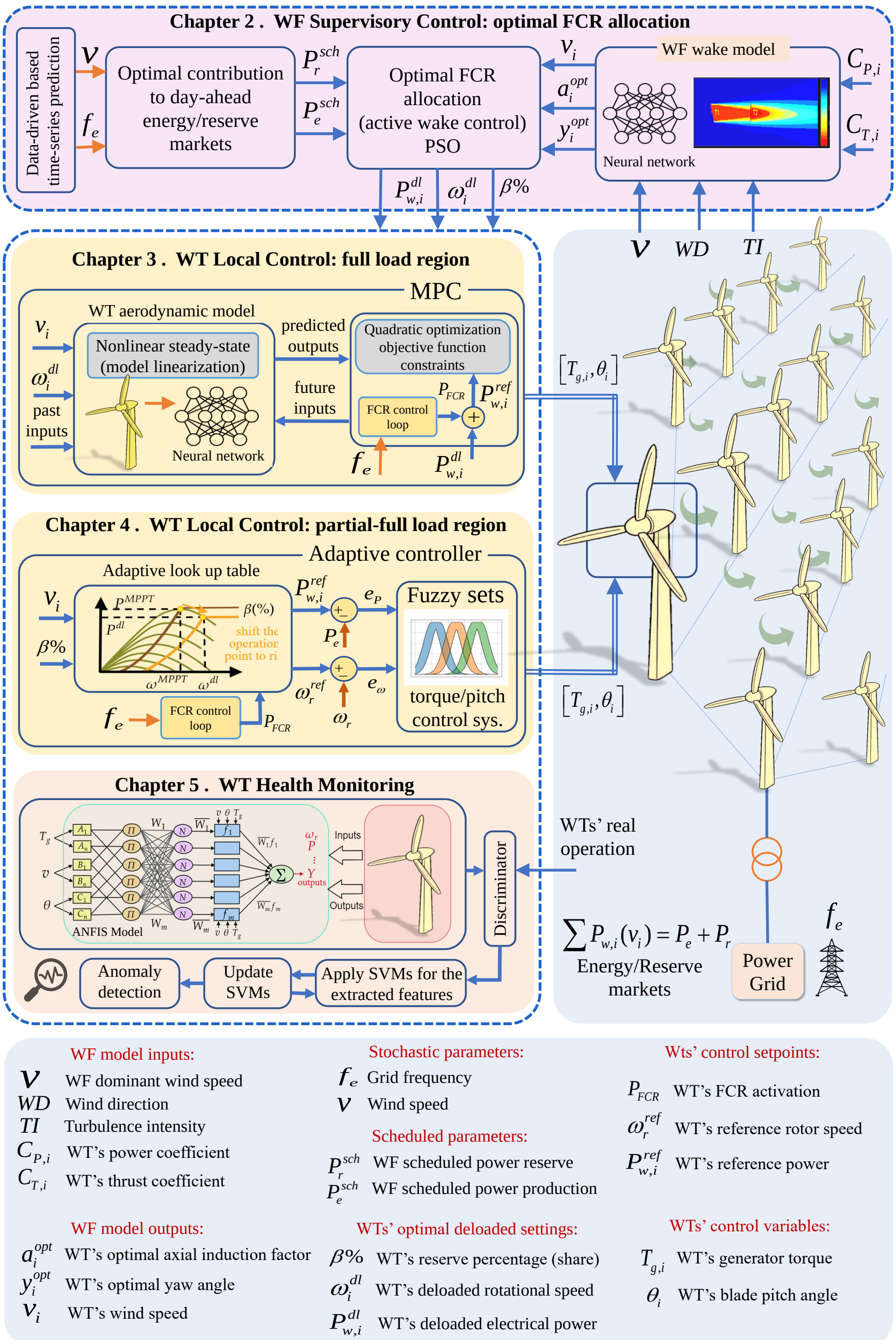

Figure 1.13: Overview of the chapters in this dissertation.

Bibliography

[1] O. H. Hohmeyer and S. Bohm, "Trends toward 100% renewable electricity supply in germany and europe: a paradigm shift in energy policies," *Wiley Interdisciplinary Reviews: Energy and Environment*, vol. 4, no. 1, pp. 74–97, 2015.

[2] R. Al-Farsi and M. Hayyan, "Paving the way for advancement of renewable energy technologies using deep eutectic solvents: A review," *Renewable and Sustainable Energy Reviews*, vol. 184, p. 113505, 2023.

[3] R. Asghar, M. J. Anwar, H. Wadood, H. Saleem, N. Rasul, and Z. Ullah, "Promising features of wind energy: A glance overview," in *2023 4th International Conference on Computing, Mathematics and Engineering Technologies (iCoMET)*, pp. 1–6, IEEE, 2023.

[4] A. İlhan, H. Zontul, S. Tümse, M. Bilgili, and B. Şahin, "Flow analyses of diffuser augmented wind turbines," *Energy Sources, Part A: Recovery, Utilization, and Environmental Effects*, vol. 0, no. 0, pp. 1–25, 2021.

[5] Y. Kumar, J. Ringenberg, S. S. Depuru, V. K. Devabhaktuni, J. W. Lee, E. Nikolaidis, B. Andersen, and A. Afjeh, "Wind energy: Trends and enabling technologies," *Renewable and Sustainable Energy Reviews*, vol. 53, pp. 209–224, 2016.

[6] A. Martinez and G. Iglesias, "Mapping of the levelised cost of energy for floating offshore wind in the european atlantic," *Renewable and Sustainable Energy Reviews*, vol. 154, p. 111889, 2022.

[7] C.-b. Li, G.-s. Lu, and S. Wu, "The investment risk analysis of wind power project in china," *Renewable Energy*, vol. 50, pp. 481–487, 2013.

[8] S. Jaber, "Environmental impacts of wind energy," *Journal of Clean Energy Technologies*, vol. 1, no. 3, pp. 251–254, 2013.

[9] G. Van Hoey, F. Bastardie, S. N. Birchenough, A. De Backer, A. B. Gill, S. De Koning, S. Hodgson, S. M. Chai, J. Steenbergen, E. Termeer, *et al.*, *Overview of the effects of offshore wind farms on fisheries and aquaculture*. Publications Office of the European Union, 2021.

[10] S. Wang and S. Wang, "Impacts of wind energy on environment: A review," *Renewable and Sustainable Energy Reviews*, vol. 49, pp. 437–443, 2015.

[11] H. Díaz and C. G. Soares, “Review of the current status, technology and future trends of offshore wind farms,” *Ocean Engineering*, vol. 209, p. 107381, 2020.

[12] “Global offshore wind report 2023.” `https://gwec.net/globalwindreport2023/`. 2023.

[13] L. Sens, U. Neuling, and M. Kaltschmitt, “Capital expenditure and levelized cost of electricity of photovoltaic plants and wind turbines–development by 2050,” *Renewable Energy*, vol. 185, pp. 525–537, 2022.

[14] A. Sedaghat, A. Hassanzadeh, J. Jamali, A. Mostafaeipour, and W.-H. Chen, “Determination of rated wind speed for maximum annual energy production of variable speed wind turbines,” *Applied energy*, vol. 205, pp. 781–789, 2017.

[15] K. Lebling, M. Ge, K. Levin, R. Waite, J. Friedrich, C. Elliott, C. Chan, K. Ross, F. Stolle, and N. Harris, “State of climate action: assessing progress toward 2030 and 2050,” *World Resources Institute (WRI), Washington, DC*, 2020.

[16] M. D. Esteban, J. J. Diez, J. S. López, and V. Negro, “Why offshore wind energy?,” *Renewable energy*, vol. 36, no. 2, pp. 444–450, 2011.

[17] E. P. Soares-Ramos, L. de Oliveira-Assis, R. Sarrias-Mena, and L. M. Fernández-Ramírez, “Current status and future trends of offshore wind power in europe,” *Energy*, vol. 202, p. 117787, 2020.

[18] S. Breyer, M. Cornet, J. Pestiaux, and P. Vermeulen, “The socio-economic impact of the belgian offshore wind industry,” *The Belgian Offshore Platform (BOP). URL: http://www. belgianoffshoreplatform. be/app/uploads/The-socio-economic-impact-ofthe-belgian-offshore-wind-industry. pdf*, 2017.

[19] A. I. Lillebø, C. Pita, J. G. Rodrigues, S. Ramos, and S. Villasante, “How can marine ecosystem services support the blue growth agenda?,” *Marine Policy*, vol. 81, pp. 132–142, 2017.

[20] S. Degraer, R. Brabant, B. Rumes, and L. Vigin, *Environmental Impacts of Offshore Wind Farms in the Belgian Part of the North Sea: Getting ready for offshore wind farm expansion in the North Sea.* 03 2023.

[21] S. Wang, Y. Huang, L. Li, C. Liu, and D. Zhang, “Dynamic analysis of wind turbines including nacelle–tower–foundation interaction for condition of incomplete structural parameters,” *Advances in Mechanical Engineering*, vol. 9, no. 3, p. 1687814017692940, 2017.

[22] E. Hernandez-Estrada, O. Lastres-Danguillecourt, J. B. Robles-Ocampo, A. Lopez-Lopez, P. Y. Sevilla-Camacho, B. Y. Perez-Sariñana, and J. R. Dorrego-Portela, "Considerations for the structural analysis and design of wind turbine towers: A review," *Renewable and Sustainable Energy Reviews*, vol. 137, p. 110447, 2021.

[23] M. R. Islam, Y. Guo, and J. Zhu, "A review of offshore wind turbine nacelle: Technical challenges, and research and developmental trends," *Renewable and Sustainable Energy Reviews*, vol. 33, pp. 161–176, 2014.

[24] F. K. Moghadam and A. R. Nejad, "Evaluation of PMSG-based drive-train technologies for 10-MW floating offshore wind turbines: Pros and cons in a life cycle perspective," *Wind Energy*, vol. 23, no. 7, pp. 1542–1563, 2020.

[25] P. J. Schubel and R. J. Crossley, "Wind turbine blade design review," *Wind engineering*, vol. 36, no. 4, pp. 365–388, 2012.

[26] X.-x. Yin, Y.-g. Lin, W. Li, Y.-j. Gu, X.-j. Wang, and P.-f. Lei, "Design, modeling and implementation of a novel pitch angle control system for wind turbine," *Renewable Energy*, vol. 81, pp. 599–608, 2015.

[27] Q. Yang, X. Jiao, Q. Luo, Q. Chen, and Y. Sun, "L1 adaptive pitch angle controller of wind energy conversion systems," *ISA transactions*, vol. 103, pp. 28–36, 2020.

[28] J. Yang, L. Fang, D. Song, M. Su, X. Yang, L. Huang, and Y. H. Joo, "Review of control strategy of large horizontal-axis wind turbines yaw system," *Wind Energy*, vol. 24, no. 2, pp. 97–115, 2021.

[29] Y. Inoue, S. Morimoto, and M. Sanada, "Control method for direct torque controlled pmsg in wind power generation system," in *2009 IEEE International Electric Machines and Drives Conference*, pp. 1231–1238, IEEE, 2009.

[30] H. Bailey, K. L. Brookes, and P. M. Thompson, "Assessing environmental impacts of offshore wind farms: lessons learned and recommendations for the future," *Aquatic biosystems*, vol. 10, no. 1, pp. 1–13, 2014.

[31] S. M. Maxwell, F. Kershaw, C. C. Locke, M. G. Conners, C. Dawson, S. Aylesworth, R. Loomis, and A. F. Johnson, "Potential impacts of floating wind turbine technology for marine species and habitats," *Journal of Environmental Management*, vol. 307, p. 114577, 2022.

[32] T. Ackermann, "Transmission systems for offshore wind farms," *Wind power in power systems*, pp. 479–503, 2005.

[33] R. Taninoki, K. Abe, T. Sukegawa, D. Azuma, and M. Nishikawa, "Dynamic cable system for floating offshore wind power generation," *SEI Technical review*, vol. 84, no. 53-58, p. 146, 2017.

[34] S. Rahman, I. Khan, H. I. Alkhammash, and M. F. Nadeem, "A comparison review on transmission mode for onshore integration of offshore wind farms: Hvdc or hvac," *Electronics*, vol. 10, no. 12, p. 1489, 2021.

[35] E. Apostolaki-Iosifidou, R. Mccormack, W. Kempton, P. Mccoy, and D. Ozkan, "Transmission design and analysis for large-scale offshore wind energy development," *IEEE Power and Energy Technology Systems Journal*, vol. 6, no. 1, pp. 22–31, 2019.

[36] H. Lee and D.-J. Lee, "Wake impact on aerodynamic characteristics of horizontal axis wind turbine under yawed flow conditions," *Renewable Energy*, vol. 136, pp. 383–392, 2019.

[37] Y. Yuan and J. Tang, "Adaptive pitch control of wind turbine for load mitigation under structural uncertainties," *Renewable Energy*, vol. 105, pp. 483–494, 2017.

[38] C. Zhu, Y. Qiu, Y. Feng, T. Wang, and H. Li, "Combined effect of passive vortex generators and leading-edge roughness on dynamic stall of the wind turbine airfoil," *Energy Conversion and Management*, vol. 251, p. 115015, 2022.

[39] T. Kim, A. M. Hansen, and K. Branner, "Development of an anisotropic beam finite element for composite wind turbine blades in multibody system," *Renewable Energy*, vol. 59, pp. 172–183, 2013.

[40] B. Sanderse, S. Van der Pijl, and B. Koren, "Review of computational fluid dynamics for wind turbine wake aerodynamics," *Wind energy*, vol. 14, no. 7, pp. 799–819, 2011.

[41] D. Mehta, A. Van Zuijlen, B. Koren, J. Holierhoek, and H. Bijl, "Large eddy simulation of wind farm aerodynamics: A review," *Journal of Wind Engineering and Industrial Aerodynamics*, vol. 133, pp. 1–17, 2014.

[42] J. M. Jonkman, M. L. Buhl, *et al.*, *FAST user's guide*, vol. 365. National Renewable Energy Laboratory Golden, CO, USA, 2005.

[43] A. J. Coulling, A. J. Goupee, A. N. Robertson, J. M. Jonkman, and H. J. Dagher, "Validation of a fast semi-submersible floating wind turbine numerical model with deep wind test data," *Journal of Renewable and Sustainable Energy*, vol. 5, no. 2, 2013.

[44] G. M. Stewart, M. A. Lackner, A. Robertson, J. Jonkman, and A. J. Goupee, "Calibration and validation of a fast floating wind turbine model of the deepcwind scaled tension-leg platform," in *ISOPE International Ocean and Polar Engineering Conference*, pp. ISOPE–I, ISOPE, 2012.

[45] F. González-Longatt, P. Wall, and V. Terzija, "Wake effect in wind farm performance: Steady-state and dynamic behavior," *Renewable Energy*, vol. 39, no. 1, pp. 329–338, 2012.

[46] R. Shakoor, M. Y. Hassan, A. Raheem, and Y.-K. Wu, "Wake effect modeling: A review of wind farm layout optimization using jensen's model," *Renewable and Sustainable Energy Reviews*, vol. 58, pp. 1048–1059, 2016.

[47] M. T. van Dijk, J.-W. van Wingerden, T. Ashuri, and Y. Li, "Wind farm multi-objective wake redirection for optimizing power production and loads," *Energy*, vol. 121, pp. 561–569, 2017.

[48] C. Cossu, "Wake redirection at higher axial induction," *Wind Energy Science*, vol. 6, no. 2, pp. 377–388, 2021.

[49] J. Annoni, P. M. Gebraad, A. K. Scholbrock, P. A. Fleming, and J.-W. v. Wingerden, "Analysis of axial-induction-based wind plant control using an engineering and a high-order wind plant model," *Wind Energy*, vol. 19, no. 6, pp. 1135–1150, 2016.

[50] P. Gebraad, P. Fleming, S. A. Ning, and J.-W. van Wingerden, "Floris," tech. rep., National Renewable Energy Lab.(NREL), Golden, CO (United States), 2014.

[51] P. Fleming, J. King, C. J. Bay, E. Simley, R. Mudafort, N. Hamilton, A. Farrell, and L. Martinez-Tossas, "Overview of floris updates," in *Journal of Physics: Conference Series*, vol. 1618, p. 022028, IOP Publishing, 2020.

[52] T. Acker and A. H. Chime, "Wind modeling using WindPro and WAsP software," *Norther Arizon University, USA*, vol. 1560000, no. 8.8, p. 510, 2011.

[53] H. Johlas, L. A. Martínez-Tossas, D. Schmidt, M. Lackner, and M. J. Churchfield, "Large eddy simulations of floating offshore wind turbine wakes with coupled platform motion," in *Journal of Physics: Conference Series*, vol. 1256, p. 012018, IOP Publishing, 2019.

[54] S. Ott and M. Nielsen, "Developments of the offshore wind turbine wake model fuga," *E-0046 Report*, 2014.

[55] S. Asiaban, N. Kayedpour, A. E. Samani, D. Bozalakov, J. D. De Kooning, G. Crevecoeur, and L. Vandevelde, “Wind and solar intermittency and the associated integration challenges: A comprehensive review including the status in the belgian power system,” *Energies*, vol. 14, no. 9, p. 2630, 2021.

[56] S. W. Ali, M. Sadiq, Y. Terriche, S. A. R. Naqvi, M. U. Mutarraf, M. A. Hassan, G. Yang, C.-L. Su, J. M. Guerrero, *et al.*, “Offshore wind farm-grid integration: A review on infrastructure, challenges, and grid solutions,” *IEEE Access*, vol. 9, pp. 102811–102827, 2021.

[57] P. Bousseau, R. Belhomme, E. Monnot, N. Laverdure, D. Boëda, D. Roye, and S. Bacha, “Contribution of wind farms to ancillary services,” *Cigre*, vol. 21, pp. 1–11, 2006.

[58] H. Liu and Z. Chen, “Contribution of vsc-hvdc to frequency regulation of power systems with offshore wind generation,” *IEEE Transactions on Energy Conversion*, vol. 30, no. 3, pp. 918–926, 2015.

[59] R. T. Pinto, P. Bauer, S. F. Rodrigues, E. J. Wiggelinkhuizen, J. Pierik, and B. Ferreira, “A novel distributed direct-voltage control strategy for grid integration of offshore wind energy systems through mtdc network,” *IEEE Transactions on Industrial Electronics*, vol. 60, no. 6, pp. 2429–2441, 2012.

[60] B. Kanna and S. N. Singh, “Towards reactive power dispatch within a wind farm using hybrid pso,” *International journal of electrical power & energy systems*, vol. 69, pp. 232–240, 2015.

[61] J. D. Hunt, B. Zakeri, A. G. de Barros, W. Leal Filho, A. D. Marques, P. S. F. Barbosa, P. S. Schneider, and M. Farenzena, “Buoyancy energy storage technology: An energy storage solution for islands, coastal regions, offshore wind power and hydrogen compression,” *Journal of Energy Storage*, vol. 40, p. 102746, 2021.

[62] A. Kaushal and D. Van Hertem, “An overview of ancillary services and hvdc systems in european context,” *Energies*, vol. 12, no. 18, p. 3481, 2019.

[63] Y. G. Rebours, D. S. Kirschen, M. Trotignon, and S. Rossignol, “A survey of frequency and voltage control ancillary services—part i: Technical features,” *IEEE Transactions on power systems*, vol. 22, no. 1, pp. 350–357, 2007.

[64] Y. G. Rebours, D. S. Kirschen, M. Trotignon, and S. Rossignol, "A survey of frequency and voltage control ancillary services—part ii: Economic features," *IEEE Transactions on power systems*, vol. 22, no. 1, pp. 358–366, 2007.

[65] W. Sun, C.-C. Liu, and S. Liu, "Black start capability assessment in power system restoration," in *2011 IEEE Power and Energy Society General Meeting*, pp. 1–7, IEEE, 2011.

[66] M. Adibi and N. Martins, "Power system restoration dynamics issues," in *2008 IEEE power and energy society general meeting-conversion and delivery of electrical energy in the 21st Century*, pp. 1–8, IEEE, 2008.

[67] W. Liu, Y. Liu, and L. Wu, "Model predictive control based voltage regulation strategy using wind farm as black-start source," *IEEE Transactions on Sustainable Energy*, vol. 14, no. 2, pp. 1122–1134, 2023.

[68] "European network of transmission system operators for electricity." `https://www.entsoe.eu/`. Accessed on 30th June 2023.

[69] "European wind energy association." `https://www.ewea.org/`. Accessed on 30th June 2023.

[70] "Belpex." `https://www.belpex.be/`. Accessed: June 30, 2023.

[71] "ELIA." `https://www.elia.be/`. Accessed: June 30, 2023.

[72] R. A. Al-Lawati, J. L. Crespo-Vazquez, T. I. Faiz, X. Fang, and M. Noor-E-Alam, "Two-stage stochastic optimization frameworks to aid in decision-making under uncertainty for variable resource generators participating in a sequential energy market," *Applied Energy*, vol. 292, p. 116882, 2021.

[73] N. Kayedpour, J. D. De Kooning, A. E. Samani, F. Kayedpour, L. Vandevelde, and G. Crevecoeur, "An optimal wind farm operation strategy for the provision of frequency containment reserve incorporating active wake control," *IEEE Transactions on Sustainable Energy*, 2023.

[74] Z. Zhou, J. Zhang, P. Liu, Z. Li, M. C. Georgiadis, and E. N. Pistikopoulos, "A two-stage stochastic programming model for the optimal design of distributed energy systems," *Applied Energy*, vol. 103, pp. 135–144, 2013.

[75] Z. Wu, P. Zeng, X.-P. Zhang, and Q. Zhou, "A solution to the chance-constrained two-stage stochastic program for unit commitment with wind energy integration," *IEEE Transactions on Power Systems*, vol. 31, no. 6, pp. 4185–4196, 2016.

[76] M. A. Hayes, L. A. Hooton, K. L. Gilland, C. Grandgent, R. L. Smith, S. R. Lindsay, J. D. Collins, S. M. Schumacher, P. A. Rabie, J. C. Gruver, *et al.*, "A smart curtailment approach for reducing bat fatalities and curtailment time at wind energy facilities," *Ecological Applications*, vol. 29, no. 4, p. e01881, 2019.

[77] "Electric Insights." `https://reports.electricinsights.co.uk/q4-2020/record-wind-output-and-curtailment/`. Accessed: June 30, 2023.

[78] G. Gust, T. Brandt, S. Mashayekh, M. Heleno, N. DeForest, M. Stadler, and D. Neumann, "Strategies for microgrid operation under real-world conditions," *European Journal of Operational Research*, vol. 292, no. 1, pp. 339–352, 2021.

[79] G. Lalor, A. Mullane, and M. O'Malley, "Frequency control and wind turbine technologies," *IEEE Transactions on power systems*, vol. 20, no. 4, pp. 1905–1913, 2005.

[80] K. Vidyanandan and N. Senroy, "Primary frequency regulation by deloaded wind turbines using variable droop," *IEEE transactions on Power Systems*, vol. 28, no. 2, pp. 837–846, 2012.

[81] I. Erlich and M. Wilch, "Primary frequency control by wind turbines," in *IEEE PES general meeting*, pp. 1–8, IEEE, 2010.

[82] G. Shu-Feng, Z. Jie-Tan, A. Philip, H. Li-Li, and J. Jing, "A review of wind turbine deloaded operation techniques for primary frequency control in power system," in *2018 China International Conference on Electricity Distribution (CICED)*, pp. 63–71, IEEE, 2018.

[83] Y. Fu, Y. Liu, L.-l. Huang, F. Ying, and F. Li, "Collection system topology for deep-sea offshore wind farms considering wind characteristics," *IEEE Transactions on Energy Conversion*, vol. 37, no. 1, pp. 631–642, 2021.

[84] A. S. Ahmadyar and G. Verbič, "Coordinated operation strategy of wind farms for frequency control by exploring wake interaction," *IEEE Transactions on Sustainable Energy*, vol. 8, no. 1, pp. 230–238, 2016.

[85] L. Abualigah, R. A. Zitar, K. H. Almotairi, A. M. Hussein, M. Abd Elaziz, M. R. Nikoo, and A. H. Gandomi, "Wind, solar, and photovoltaic renewable energy systems with and without energy storage optimization: A survey of advanced machine learning and deep learning techniques," *Energies*, vol. 15, no. 2, p. 578, 2022.

[86] L. Sun and F. You, "Machine learning and data-driven techniques for the control of smart power generation systems: An uncertainty handling perspective," *Engineering*, vol. 7, no. 9, pp. 1239–1247, 2021.

[87] J. Park and K. H. Law, "A data-driven, cooperative wind farm control to maximize the total power production," *Applied Energy*, vol. 165, pp. 151–165, 2016.

[88] L. Zheng, W. Hu, and Y. Min, "Raw wind data preprocessing: A data-mining approach," *IEEE Transactions on Sustainable Energy*, vol. 6, no. 1, pp. 11–19, 2014.

[89] X. Xiao, J. Liu, D. Liu, Y. Tang, and F. Zhang, "Condition monitoring of wind turbine main bearing based on multivariate time series forecasting," *Energies*, vol. 15, no. 5, p. 1951, 2022.

[90] A. Lenzi, J. Bessac, and M. Anitescu, "Power grid frequency prediction using spatiotemporal modeling," *Statistical Analysis and Data Mining: The ASA Data Science Journal*, vol. 14, no. 6, pp. 662–675, 2021.

[91] J. Wang and J. Hu, "A robust combination approach for short-term wind speed forecasting and analysis–combination of the arima (autoregressive integrated moving average), elm (extreme learning machine), svm (support vector machine) and lssvm (least square svm) forecasts using a gpr (gaussian process regression) model," *Energy*, vol. 93, pp. 41–56, 2015.

[92] I. Tyass, A. Bellat, A. Raihani, K. Mansouri, and T. Khalili, "Wind speed prediction based on seasonal arima model," in *E3S Web of Conferences*, vol. 336, p. 00034, EDP Sciences, 2022.

[93] S. Grossberg, "Recurrent neural networks," *Scholarpedia*, vol. 8, no. 2, p. 1888, 2013.

[94] J. Gu, Z. Wang, J. Kuen, L. Ma, A. Shahroudy, B. Shuai, T. Liu, X. Wang, G. Wang, J. Cai, *et al.*, "Recent advances in convolutional neural networks," *Pattern recognition*, vol. 77, pp. 354–377, 2018.

[95] M. F. Azeem, M. Hanmandlu, and N. Ahmad, "Generalization of adaptive neuro-fuzzy inference systems," *IEEE Transactions on Neural Networks*, vol. 11, no. 6, pp. 1332–1346, 2000.

[96] B. Mathew Nkurlu, C. Shen, S. Asante-Okyere, A. K. Mulashani, J. Chungu, and L. Wang, "Prediction of permeability using group method of data handling (gmdh) neural network from well log data," *Energies*, vol. 13, no. 3, p. 551, 2020.

[97] M.-D. Liu, L. Ding, and Y.-L. Bai, "Application of hybrid model based on empirical mode decomposition, novel recurrent neural networks and the arima to wind speed prediction," *Energy Conversion and Management*, vol. 233, p. 113917, 2021.

[98] Y. Yan, X. Wang, F. Ren, Z. Shao, and C. Tian, "Wind speed prediction using a hybrid model of EEMD and LSTM considering seasonal features," *Energy Reports*, vol. 8, pp. 8965–8980, 2022.

[99] N. Kayedpour, J. D. De Kooning, A. E. Samani, L. Vandevelde, and G. Crevecoeur, "An adaptive operational strategy for enhanced provision of frequency containment reserve by wind turbines: Data-driven based power reserve adjustment," *Electric Power Systems Research*, vol. 223, p. 109564, 2023.

[100] N. Kayedpour, J. D. De Kooning, A. E. Samani, L. Vandevelde, and G. Crevecoeur, "An adaptive operational strategy for enhanced provision of frequency containment reserve by wind turbines: Data-driven based power reserve adjustment," *Electric Power Systems Research*, vol. 223, p. 109564, 2023.

[101] Z. Ti, X. W. Deng, and H. Yang, "Wake modeling of wind turbines using machine learning," *Applied Energy*, vol. 257, p. 114025, 2020.

[102] A. Marvuglia and A. Messineo, "Monitoring of wind farms' power curves using machine learning techniques," *Applied Energy*, vol. 98, pp. 574–583, 2012.

[103] R. Meka, A. Alaeddini, and K. Bhaganagar, "A robust deep learning framework for short-term wind power forecast of a full-scale wind farm using atmospheric variables," *Energy*, vol. 221, p. 119759, 2021.

[104] D. Collet, M. Alamir, D. Di Domenico, and G. Sabiron, "Data-driven fatigue-oriented mpc applied to wind turbines individual pitch control," *Renewable Energy*, vol. 170, pp. 1008–1019, 2021.

[105] J. de Jesus Barradas-Berglind, R. Wisniewski, and M. Soltani, "Fatigue damage estimation and data-based control for wind turbines," *IET Control Theory & Applications*, vol. 9, no. 7, pp. 1042–1050, 2015.

[106] A. Kusiak, Z. Song, and H. Zheng, "Anticipatory control of wind turbines with data-driven predictive models," *IEEE Transactions on Energy Conversion*, vol. 24, no. 3, pp. 766–774, 2009.

[107] X. Yin, W. Zhang, Z. Jiang, and L. Pan, "Data-driven multi-objective predictive control of offshore wind farm based on evolutionary optimization," *Renewable Energy*, vol. 160, pp. 974–986, 2020.

[108] X. Yin and X. Zhao, "Data driven learning model predictive control of offshore wind farms," *International Journal of Electrical Power & Energy Systems*, vol. 127, p. 106639, 2021.

[109] N. Kayedpour, A. E. Samani, J. D. De Kooning, L. Vandevelde, and G. Crevecoeur, "Model predictive control with a cascaded hammerstein neural network of a wind turbine providing frequency containment reserve," *IEEE Transactions on Energy Conversion*, vol. 37, no. 1, pp. 198–209, 2021.

[110] M. Ławryńczuk, "A family of model predictive control algorithms with artificial neural networks," *International Journal of Applied Mathematics and Computer Science*, vol. 17, no. 2, pp. 217–232, 2007.

[111] J. Xie, H. Dong, and X. Zhao, "Data-driven torque and pitch control of wind turbines via reinforcement learning," *Renewable Energy*, 2023.

[112] J. Xie, H. Dong, X. Zhao, and A. Karcanias, "Wind farm power generation control via double-network-based deep reinforcement learning," *IEEE Transactions on Industrial Informatics*, vol. 18, no. 4, pp. 2321–2330, 2021.

[113] P. Chen and D. Han, "Reward adaptive wind power tracking control based on deep deterministic policy gradient," *Applied Energy*, vol. 348, p. 121519, 2023.

[114] J. D. Martín-Guerrero and L. Lamata, "Reinforcement learning and physics," *Applied Sciences*, vol. 11, no. 18, p. 8589, 2021.

[115] J. Berberich, J. Köhler, M. A. Müller, and F. Allgöwer, "Data-driven model predictive control with stability and robustness guarantees," *IEEE Transactions on Automatic Control*, vol. 66, no. 4, pp. 1702–1717, 2020.

[116] H. Jiang, J. Wang, J. Wu, and W. Geng, "Comparison of numerical methods and metaheuristic optimization algorithms for estimating parameters for wind energy potential assessment in low wind regions," *Renewable and Sustainable Energy Reviews*, vol. 69, pp. 1199–1217, 2017.

[117] P. Lu, L. Ye, Y. Zhao, B. Dai, M. Pei, and Y. Tang, "Review of metaheuristic algorithms for wind power prediction: Methodologies, applications and challenges," *Applied Energy*, vol. 301, p. 117446, 2021.

[118] E. H. Houssein, "Machine learning and meta-heuristic algorithms for renewable energy: a systematic review," *Advanced Control and Optimization Paradigms for Wind Energy Systems*, pp. 165–187, 2019.

[119] J. C. S. Chavez, A. Zamora-Mendez, M. R. A. Paternina, J. F. Y. Heredia, and R. Cardenas-Javier, "A hybrid optimization framework for the non-convex economic dispatch problem via meta-heuristic algorithms," *Electric Power Systems Research*, vol. 177, p. 105999, 2019.

[120] Z. Gao and X. Liu, "An overview on fault diagnosis, prognosis and resilient control for wind turbine systems," *Processes*, vol. 9, no. 2, p. 300, 2021.

[121] A. Stetco, F. Dinmohammadi, X. Zhao, V. Robu, D. Flynn, M. Barnes, J. Keane, and G. Nenadic, "Machine learning methods for wind turbine condition monitoring: A review," *Renewable energy*, vol. 133, pp. 620–635, 2019.

[122] B. Z. Cunha, C. Droz, A.-M. Zine, S. Foulard, and M. Ichchou, "A review of machine learning methods applied to structural dynamics and vibroacoustic," *Mechanical Systems and Signal Processing*, vol. 200, p. 110535, 2023.

[123] T. Regan, C. Beale, and M. Inalpolat, "Wind turbine blade damage detection using supervised machine learning algorithms," *Journal of Vibration and Acoustics*, vol. 139, no. 6, p. 061010, 2017.

[124] W. Yang, C. Liu, and D. Jiang, "An unsupervised spatiotemporal graphical modeling approach for wind turbine condition monitoring," *Renewable energy*, vol. 127, pp. 230–241, 2018.

[125] S. N. Pichika, G. Meganaa, S. G. Rajasekharan, and A. Malapati, "Multi-component fault classification of a wind turbine gearbox using integrated condition monitoring and hybrid ensemble method approach," *Applied Acoustics*, vol. 195, p. 108814, 2022.

[126] H. Ren, W. Liu, M. Shan, and X. Wang, "A new wind turbine health condition monitoring method based on vmd-mpe and feature-based transfer learning," *Measurement*, vol. 148, p. 106906, 2019.

[127] Y. Zhu, C. Zhu, J. Tan, Y. Tan, and L. Rao, "Anomaly detection and condition monitoring of wind turbine gearbox based on lstm-fs and transfer learning," *Renewable Energy*, vol. 189, pp. 90–103, 2022.

[128] W. Chen, Y. Qiu, Y. Feng, Y. Li, and A. Kusiak, "Diagnosis of wind turbine faults with transfer learning algorithms," *Renewable Energy*, vol. 163, pp. 2053–2067, 2021.

[129] W. Yang, P. J. Tavner, C. J. Crabtree, Y. Feng, and Y. Qiu, "Wind turbine condition monitoring: technical and commercial challenges," *Wind Energy*, vol. 17, no. 5, pp. 673–693, 2014.

[130] B. Karthikeya and R. J. Schütt, "Overview of wind park control strategies," *IEEE Transactions on Sustainable Energy*, vol. 5, no. 2, pp. 416–422, 2014.

Chapter 2

Wind Farm Supervisory Control: Optimal FCR Allocation Considering Wake Effect

This chapter addresses the challenges discussed in Secion 1.5.1 by presenting an innovative operational strategy for wind farms. The primary focus of this strategy is twofold: first, optimizing the provision of Frequency Containment Reserve (FCR), and second, effectively managing wake formation. The proposed approach involves determining the reserve and deloading percentage $\beta\%$ for individual wind turbines based on pre-defined optimal wake-controlled parameters. Additionally, set points for deloaded power and rotational speed are established for each wind turbine within the wind farm layout to achieve these objectives.

The power reserve allocation is dynamically determined at the supervisory control level, considering various factors such as intermittent wind power, wind direction, grid frequency variability, and the intricate aerodynamics involved in wake formation. To support decision-making for optimal contributions to day-ahead energy/FCR markets, a two-stage stochastic programming approach, cfr. Figure 1.6, is employed, which accounts for uncertainties in sub-hourly wind power and grid frequency.

To tackle computational complexity, the optimizer incorporates a data-driven surrogate model of wake formation. This surrogate model utilizes a neural network trained on the Gauss-Curl-Hybrid wake model in FLORIS, allowing for rapid estimation of wake control parameters, including optimal yaw angles and axial induction factors. By integrating this surrogate model, the algorithm can efficiently optimize the control of wakes.

To search for the optimal deloading of wind turbines, the proposed algorithm employs a coevolutionary-based multi-objective particle swarm optimization technique. This technique maximizes total power production and kinetic energy while minimizing the impact of the wake. By considering these objectives simultaneously, the algorithm enhances the overall performance of the wind farm.

The effectiveness of the proposed algorithm is evaluated through a case study conducted on the C-Power wind farm in the North Sea. Simulation results demonstrate that the algorithm significantly improves the wind farm's performance under different operational conditions. By highlighting the supervisory control level's role in optimizing the provision of FCR and controlling wake formation, the study showcases the algorithm's potential to enhance wind farm efficiency and reliability.

The contents of this chapter are published in IEEE Transactions on Sustainable Energy [1].

An Optimal Wind Farm Operation Strategy for the Provision of frequency Containment Reserve Incorporating Active Wake Control

Nezmin Kayedpour, Arash E. Samani, Farjam Kayedpour, Jeroen D. M. De Kooning, Lieven Vandevelde, and Guillaume Crevecoeur

Published in "IEEE Transactions on Sustainable Energy", 2023

Abstract *This study proposes a novel operation strategy for wind farms' optimal frequency Containment Reserve (FCR) provision that simultaneously distributes FCR and optimally controls wake formation. The power reserve allocation is dynamically decided at the wind farm supervisory control level, considering the intermittent wind power and direction, grid frequency stochasticity, and the aerodynamic complexity of the wake. A two-stage stochastic programming approach supports decision-making for an optimal contribution to day-ahead energy/FCR markets considering sub-hourly wind power and grid frequency uncertainty. Moreover, a novel method is used to reduce the computational complexity by employing a data-driven surrogate model of wake formation in the optimizer. This surrogate model consists of a neural network trained on the Gauss-Curl-Hybrid wake model in FLORIS. This deep learning approach allows fast estimation of the wake control parameters, i.e., the optimal yaw angles and axial induction factors. Then, a coevolutionary-based multi-objective particle swarm optimization searches for the optimal deloading of the WTs and maximizes the total power production and kinetic energy while minimizing wake. The performance of the proposed algorithm is evaluated on the C-Power wind farm in the North Sea. Simulation results demonstrate its effectiveness in improving the wind farm's overall performance for different operational conditions.*

2.1 Introduction

The European Union (EU) is dedicated to becoming the global leader in decarbonizing the power system. Wind power is essential in reaching the EU carbon-neutral target by 2050 [2]. However, effective integration of wind energy into the power system can raise concerns about grid stability and reliability due to the intrinsic stochastic nature of wind [3]. The primary reason for the blackout events on 9 August 2019 in the UK was the sudden decline in frequency beyond the regulation capability of system inertia [4]. As a result, there is a significant demand from Transmission System Operators (TSO) for wind energy sources to play an active role in balancing the grid through market participation and provision of ancillary services such as frequency control, which traditionally have been provided by conventional power plants. [5]. Nevertheless, how to effectively incorporate the ability to provide frequency support into the reliable and optimal operation of the system, accurately schedule the products of the frequency support, and efficiently distribute the power reserve within wind farms (WF) are still open challenges. This study aims to fill these gaps by proposing an optimal operation strategy considering all mentioned criteria.

Ancillary markets and other grid-balancing mechanisms have already been created for renewable energy sources in European countries. The participation of wind energy in reserve markets in Great Britain and Spain is analyzed in [6], and recommendations are made to support future development. [7] also explored the potential of wind power to enter the Swedish ancillary service markets, considering technical requirements and the potential financial impacts on a WF. The Belgian TSO has reported that offshore wind is expected to play a significant role in the Belgian power system in the near future [8]. Although wind energy has the capability to enter these markets, still some uncertainty regarding optimal contribution exists. A differentiated pricing scheme was used in [9] to propose a market mechanism design for inertia and primary frequency response, taking into account the energy market in which the system operator will participate in the joint market with a combined clearing process. While the methods described in [9,10] have not considered the day-ahead scheduling, [10] leverages field-measured data to examine the frequency support capacity of a WF, and discusses the uncertainty of wind and frequency constraints. [11–13] discussed optimal bidding and scheduling strategies that optimize hour-ahead, intraday, and day-ahead operations while incorporating a shared frequency regulation reserve plan for wind, photovoltaic, and thermal power. However, these studies did not take into account the real-time dynamic interactions inside or between these energy sources. An advanced day-ahead bidding strategy for wind power producers is proposed in [14], considering the wind speed and system frequency uncertainties as stochastic inputs and a confidence level on the real-time reserve provision. In [15], optimal bidding strategies in the real-time electricity market are investigated for wind power generation using a bi-level stochastic optimization framework that maximizes profit by determining the optimal bidding quantity. However, the optimal distribution of the scheduled reserve among Wind Turbines (WT), taking into account the aerodynamic complexity of these sources, has not been considered by [14, 15].

Another critical element needed to facilitate wind integration into power systems is an advanced WF supervisory operation strategy that guarantees the optimal provision, allocation, and activation of power reserve in different operating conditions [16]. In a two-stage economic dispatch model, [17] and [18] incorporate wind power reserve but yet overlook the optimal reserve allocation in WFs. More recent studies suggested novel WF control strategies and approaches for enhancing the grid support, such as self-control via diode rectifier-based high voltage alternating current (HVAC) transmission system [19], error-based active disturbance rejection control for WT power regulation [20], deloading and curtailment methods [21, 22] that maintain an adequate power reserve for delivering an automatic and fast response to the TSO's demands. [23] introduced a scheme for model predictive control that harmonizes the functioning of offshore WTs and offshore DC collection grid capacitors to offer rapid inertia and primary frequency support. Nevertheless, the need for power reserve and frequency support amplifies the intricacies of WFs with linked aerodynamic systems, necessitating a more comprehensive examination. Studies have been carried out focusing on the aerodynamic coupling between WTs and their wake formation, which creates a wind energy deficit between the wind-leaving turbine (upstream WT) and the wind-arriving turbine (downstream WT). This phenomenon makes it difficult to determine exact energy extractions and justify the WFs' optimal contribution to frequency regulations [24].

Further studies have focused on determining the effectiveness of including inertial response and frequency control techniques, considering the apparent limitations of WFs compared to traditional power plants [25–27]. Applying these techniques often reduces wind energy production by a certain level of efficiency loss. [28] addressed harvesting maximum kinetic energy during the deloading control strategy using a game theory-based optimal control framework, which distributedly adjusts WTs' rotor speeds in a WF layout. Additional studies propose coordinated control approaches for WFs providing frequency control considering wake interactions inside the WF. In [29], a coordinated WF operation strategy is proposed that, instead of seeking to maximize the power generation of WTs individually, ensures the maximization of the rotational kinetic energy while maintaining the optimal WF's overall performance. A control algorithm is suggested in [30] to distribute the power reserve, aiming to minimize the wake effects and maximize the reserve capacity.

The mentioned studies either covered optimal bidding problems in the market or investigated WF optimal operation strategies without considering wake effects or market constraints. Although some research reveals optimization methods that can coordinate WTs and enable them to provide ancillary services optimally, time-efficient optimization approaches are lacking, considering the high complexities involved in wake models. In addition, the stochastic behavior of wind and grid frequency forms a perpetually varying environment, requiring online and dynamic strategies that can cope with high aerodynamic complexity and variability. This study aims to overcome the limitations of current approaches by developing an integrated algorithm that can effectively tackle the primary challenges associated with WF providing FCR, particularly when there are no ideal energy storage systems in place. The proposed algorithm will take an active approach to ensure that FCR provision is optimized at scheduling and activation levels. In [29, 31] and [32], the FCR provision was optimally distributed in a WF, taking into account wake interaction, using the Jensen wake model. However, the wake or wake-controlled parameters were not actively controlled as part of the optimization. The primary novelty of this article is to integrate active control of the wakes in the operation strategy, such that FCR distribution and wake control are optimized simultaneously. However, the integration of active wake control significantly increases the complexity of the optimization problem compared to [29], and [32]. This is resolved by the secondary novelty of this work, i.e., using a data-driven surrogate model of the wake formation in the optimizer, resulting in a computationally efficient optimal operation strategy. Moreover, the Gauss-Curl-Hybrid (GCH) wake model in the FLORIS wake simulator is used to generate the dataset instead of the simplified Jensen wake model. The contributions of this paper are three-fold:

1. A two-stage stochastic programming is proposed to optimize the contribution of a WF to the day-ahead energy and FCR markets while considering uncertainties related to wind speed and grid frequency. The approach involves using the Group Method of Data Handling (GMDH), a data-driven time-series prediction technique, to predict wind speed and grid frequency and calculate expected values for different scenarios.

2. An optimization framework incorporating active wake control is then suggested to dynamically distribute the pre-scheduled optimal power reserve among the WTs, restricted by optimal wake-controlled parameters (yaw angles and axial induction factors), which are being calculated and updated for varying operating conditions using a computationally efficient approach involving deep learning neural networks.

3. The integrated algorithm of optimal power reserve allocation is realized by proposing an adaptive WT local control system that can cope with the set points decided at the supervisory control level to adjust the power reserve margin based on the optimally estimated deloaded percentage.

The rest of this paper is organized as follows: § II propose the formulation of the WF operation strategy. § III introduces the stochastic programming framework for offering an optimal FCR provision based on wind and grid frequency prediction. § IV formulates the optimal operation strategy and allocation of power reserve by maximizing WF power production and total kinetic energy. § V provides an overview of the outcomes and results, while § VI summarises and concludes the paper.

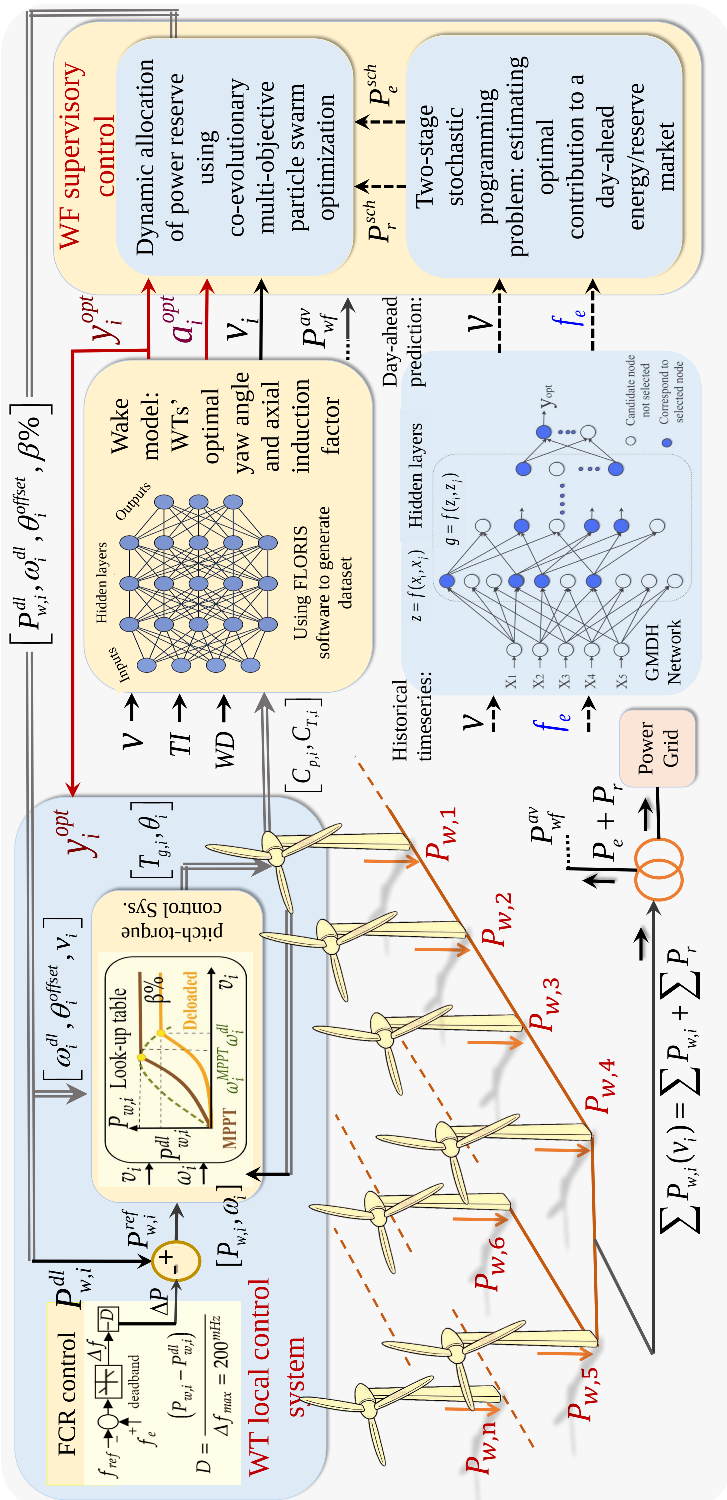

Figure 2.1: Proposed optimal operation strategy providing FCR.

2.2 Overview of the WF operation strategy

The proposed operational strategy is shown in Fig. 2.1. The presented concept relies on a two-step sequential framework. In the primary step, a two-stage stochastic programming problem estimates the WF's optimal contribution to the day-ahead energy and reserve markets, considering wind and grid frequency uncertainties. In the first stage, the model determines the optimal decision variables P_e^{sch} and P_r^{sch} based on the available information at the time of decision-making, such as the forecasted wind power output v and the grid frequency f_e employing the Group Method of Data Handling (GMDH), a data-driven time-series prediction technique. The decision variables include the amount of energy and reserve and the bids submitted to the market. In the second stage, the model takes into account the uncertainties associated with wind power generation and grid frequency, which can affect the actual outcomes of the first-stage decisions. The model considers a set of scenarios that represent different possible realizations of these uncertainties and evaluates the outcomes of the first-stage decisions under each scenario. The evaluation criteria include the expected profit, the risk of violating the reserve requirements, and the cost of deviation from the scheduled energy and reserve productions. The final decision is then made by considering the trade-off between the expected profit and the risk of violating the reserve requirements while ensuring the reliability of the WF operation.

Among different reserve products, this study only focuses on frequency Containment Reserve (FCR), formerly known as the primary control, which helps maintain the stability of the power grid by providing a rapid response to sudden changes in frequency. The FCR provision is responsible for keeping the power system's frequency within an acceptable range, $\Delta f = 200\ mHz$ around the nominal frequency of $f_{ref} = 50\ Hz$, and reacting proportionally to the frequency changes. Automatic and manual frequency Restoration Reserves (aFRR, mFRR) are other ancillary services, formerly known as secondary and tertiary control. Fig. 2.2 shows the provision and activation of these services. The aFRR and mFRR are reserve capacities that play a crucial role in maintaining the stability of the power grid by restoring the system's frequency to its nominal value in the event of a disturbance. While the aFRR is automatically activated, the mFRR requires manual activation. This study considers FCR provision, which can introduce considerable challenges on WFs integrated control systems.

Once an ideal reserve P_r^{sch} has been determined in the day-ahead market, the subsequent stage involves the utilization of a second-layer optimization algorithm to actively allocate the scheduled power reserve among the WTs. This process involves the efficient computation of optimal wake-controlled parameters, such as optimal yaw angles y_i^{opt} and axial induction factors a_i^{opt}, through

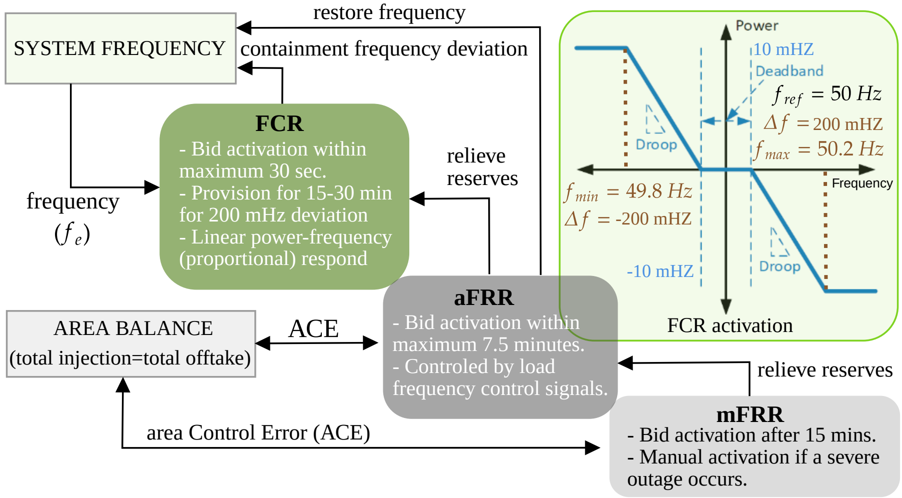

Figure 2.2: Provision of ancillary services.

the use of an Adaptive Network-based Fuzzy Inference System (ANFIS) framework. The ANFIS structure is capable of learning and replicating the wake behavior of the WF in various wind speeds, directions, and turbulence intensities (TI). The allocation of power reserve will be realized by sending WTs' setpoints, i.e., deloaded rotational speed ω_i^{dl}, and blade pitch offset θ_i^{offset}, and deloaded power $P_{w,i}^{dl}$, to the WTs' local control systems. After optimally deciding the WT's adjustable power reserve margin, the WT's look-up table will be adapted considering the estimated deloading percentage β. Eventually, activating FCR will be carried out by responding to frequency changes Δf through an FCR supplementary control loop.

2.3 Optimal FCR contribution

As mentioned, the proposed stochastic optimization framework aims to determine the strategic bidding for the scheduled reserve quantity in the day-ahead market at the market-clearing price and in a non-price-making position. Once the WF operator decides the bidding quantity, it will not be allowed to change its decision the next day against the signed corresponding transaction agreement. Therefore, a two-stage stochastic optimization process is formulated to support the decision-maker during the different stages considering the market restrictions. This strategy helps the operator make an optimal decision considering the day-ahead electricity and reserve transactions (first stage) and aids in optimizing tomorrow's real-time operations (second stage).

The GMDH method, which is a form of nonlinear regression, acts as a semi-supervised deep learning technique that can self-organize the predictive distribution of stochastic variables. By driving the optimal polynomial network structure, it can accurately reveal the approximated function and predict future values based on historical datasets. The GMDH time series prediction approach involves utilizing polynomial functions to express the general relationship between delayed inputs and output variables, known as the Volterra function series or the Kolmogorov-Gabor polynomial function expressed by:

$$y = a_0 + \sum_{i=1}^{m} a_i x_i + \sum_{i=1}^{m}\sum_{j=1}^{m} a_{ij} x_i x_j + \sum_{i=1}^{m}\sum_{i=1}^{m}\sum_{k=1}^{m} a_{ijk} x_i x_j x_k \tag{2.1}$$

In the given equation, the response variable is represented by 'y', while the vector of lagged time series to be regressed is represented by 'x'. The letter 'm' denotes the number of variables, and the weighting factors are represented by the coefficients a_0, a_i, a_{ij} and a_{ijk}. For this research, the quadratic K-G polynomial has been utilized and represented in the following form:

$$z = f(x_i, x_j) = b_0 + b_1 x_i + b_2 x_j + b_3 x_j x_i + b_4 x_i^2 + b_5 x_j^2 \tag{2.2}$$

The GMDH framework can be trained to learn the relationship between different lags using a function f. To accomplish this, a stochastic approximation algorithm is proposed, which is based on a multilayer network. Each layer of the network uses various component subsets of the polynomial function, with the output of the last layer being used as input for the next layer. The algorithm conducts regression polynomials of all possible combinations of two independent variables from a total of n inputs in the first layer. The minimum activation function is a second-order polynomial, but higher orders can be used to find the optimal complexity. A threshold is used to limit the number of solutions and to find the best structure based on an external criterion.

The grid frequency estimation is performed using the least-squares regression method over a period of five years of historical data from January 2015 to October 2019 with a 10-seconds time interval obtained from the website of the Belgian TSO Elia [33]. The wind speed dataset for the same period with a 15-minute sampling interval is obtained from a global weather API [34]. The prediction horizon is set to 24 hours with five delayed inputs. Fig. 2.3 illustrates the stochastic input parameters of the proposed problem. The quarter-hourly-based average grid frequency is estimated using the K-means algorithm that finds the average center of clusters located outside of the deadband zone. Also, around 400 wind speed scenarios are considered based on the historical data set. A scenario reduction suggested in [35] is used to reduce the computational complexity of the problem. The nonlinearity of the available WF power production considering wind speed, direct and turbulence intensity is estimated as follows:

$$P_{\mathrm{wf}} = \begin{cases} 0\ \mathrm{MW} & , \quad 0 < \mathrm{v} < \mathrm{v_w^{ci}} \\ a\,v^3 + b\,v^2 + c\,v + d\ \ \mathrm{MW} & , \quad \mathrm{v_w^{ci}} \leqslant \mathrm{v} \leqslant \mathrm{v_w^{n}} \\ 149.73\ \ \mathrm{MW} & , \quad \mathrm{v_w^{n}} \leqslant \mathrm{v} \leqslant \mathrm{v_w^{cu}} \end{cases} \tag{2.3}$$

where $v_{\mathrm{w}}^{\mathrm{ci}}$, $v_{\mathrm{w}}^{\mathrm{cu}}$ and $v_{\mathrm{w}}^{\mathrm{n}}$ are respectively the cut-in, cut-out and nominal wind speeds in m/s. P_{wf} is the WF total electrical power in MW. a, b, c, and d are the parameters of a cubic polynomial fitted to the data. A deep learning time-series forecasting method is conducted using the GMDH to compute each scenario's expected value [36].
The bidding decision variables of electricity production P_e^{sch} and reserve P_r^{sch} are first-stage decision variables that should be scheduled a day before the activation. Once the WF owner decides on the FCR contribution, it will not be allowed to change its decision the next day. Therefore, the second stage should consider the possible scenarios and their expected values. The optimization framework and the constraints are:

$$\max \begin{bmatrix} \left(P_e^{\mathrm{sch}} \cdot \lambda_e^{\mathrm{sch}} + P_r^{\mathrm{sch}} \cdot \lambda_r^{\mathrm{sch}}\right) \cdot \Delta T + \\ \mathrm{E}_s\left((\Delta P_e(s) \cdot \lambda_{\Delta e} + \Delta P_r(s) \cdot \lambda_{\Delta r}) \cdot \Delta T\right) \end{bmatrix} \tag{2.4}$$

$$P_{\mathrm{wf}} = P_r(s) + P_e(s) \tag{2.5}$$

$$\Delta P_e = \left|P_e(s) - P_e^{\mathrm{sch}}\right| \ \ , \ \ \Delta P_r = \left|P_r(s) - P_r^{\mathrm{sch}}\right| \tag{2.6}$$

$$\Delta P_e(s) \cdot \lambda_{\Delta e} = \Delta P_e^{+}(s) \cdot \lambda_{\Delta e}^{+} + \Delta P_e^{-}(s) \cdot \lambda_{\Delta e}^{-} \tag{2.7}$$

$$\Delta P_r(s) \cdot \lambda_{\Delta r} = \Delta P_r^{+}(s) \cdot \lambda_{\Delta r}^{+} + \Delta P_r^{-}(s) \cdot \lambda_{\Delta r}^{-} \tag{2.8}$$

$$P_r^{\mathrm{sch}} = 200\mathrm{mHz} \cdot K \ \ (K \text{ is droop constant}) \tag{2.9}$$

$$P_r(s) = \Delta f \cdot K \ \ , \ \ \Delta f = f_e - f_{\mathrm{ref}} \ (f_{\mathrm{ref}} \text{ is 50 Hz}) \tag{2.10}$$

where $P_r(s)$ and $P_e(s)$ are stochastic parameters, λ_e^{sch} and λ_r^{sch} are the electricity and reserve prices respectively. $\mathbb{E}_S$ is the probability of scenario s. $\Delta {P_e}^{+}(s)$, $\Delta {P_e}^{-}(s)$, $\Delta {P_r}^{+}(s)$ and $\Delta {P_e}^{+}(s)$ are additional and deficiency of power injection to the grid and reserve provision. $\lambda_{\Delta e}^{-}$, $\lambda_{\Delta e}^{+}$, $\lambda_{\Delta r}^{-}$ and $\lambda_{\Delta r}^{+}$ are revenue and penalty for additional power and reserve injected to the grid as well. The optimization will be carried out for 24 hours, considering market parameters on a quarter-hourly basis. ΔT is the time interval for electricity injection and frequency regulation, i.e., 15 minutes. The TSO has different mechanisms to penalize providers if they violate their scheduled reserve contributions based on the contracted agreement. The imbalance in energy settlement takes place in real-time on a quarter-hourly basis. Consequently, the energy provider gets a

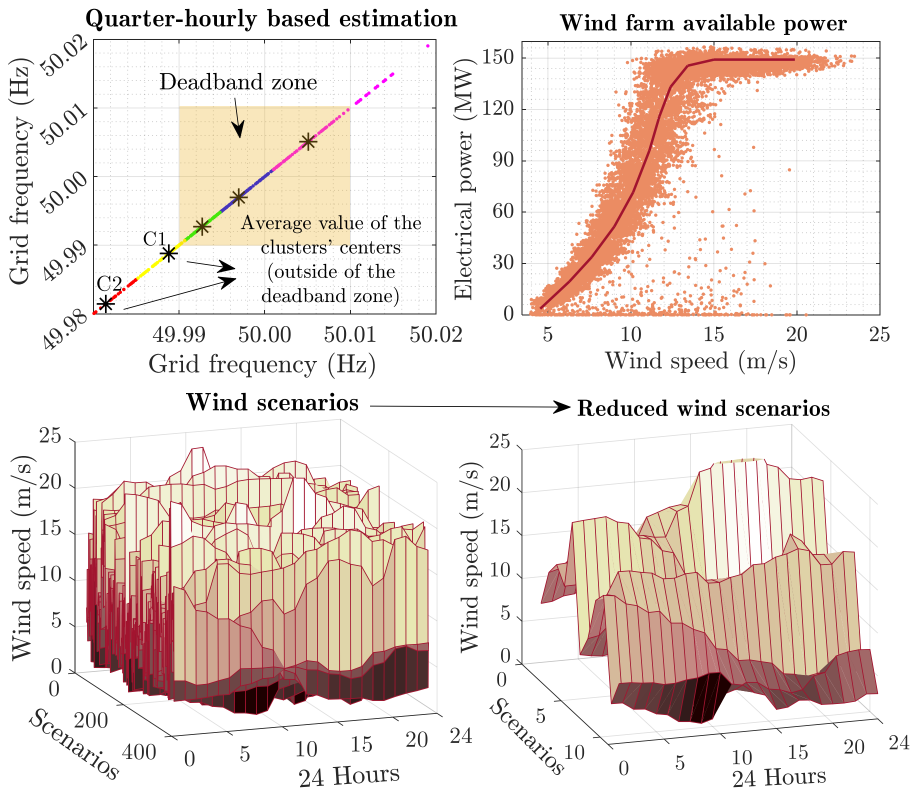

Figure 2.3: Stochastic parameters based on historical datasets.

reduced revenue and penalty for its positive and negative deviation at each settlement course when the generated power is higher than the scheduled power as follows:

$$\lambda_{\Delta e}^{+} = \lambda_{e}^{\text{sch}} - \alpha \quad ; \quad \lambda_{\Delta e}^{-} = \lambda_{e}^{\text{sch}} + \alpha \tag{2.11}$$

$$\lambda_{\Delta r}^{-} = 0.2 \cdot \Theta \cdot \lambda_{r}^{\text{M}} \quad ; \quad \lambda_{\Delta r}^{+} = 0 \tag{2.12}$$

$$\Theta = \frac{P_{r}^{\text{sch}} - P_{r}}{P_{r}^{\text{sch}}} \tag{2.13}$$

where α is an additional incentive component, which depends on the average of the absolute values of the System Imbalance (SI) of the current and the previous imbalance settlement period [37]. Θ is the failure factor, which increases by the difference between the scheduled FCR and the activated one, i.e., P_r. λ_r^{M} is the total remuneration for the FCR awarded for month M [38]. The objective function (2.4) is subject to the following boundary conditions:

First stage:

$$0 \leqslant P_{e}^{\text{sch}} \leqslant P_{\text{wf}}^{\max} \quad ; \quad 0 \leqslant P_{r}^{\text{sch}} \leqslant \frac{P_{e}^{\text{sch}}}{2} \tag{2.14}$$

$$P_e^{\text{sch}} + P_r^{\text{sch}} \leqslant P_{\text{wf}}^{\max} \tag{2.15}$$

Second stage:

$$0 \leqslant P_e(s) \leqslant P_{\text{wf}}^{\text{av}} \quad ; \quad 0 \leqslant P_r(s) \leqslant \frac{P_{\text{r}}(s)}{2} \tag{2.16}$$

$$\Delta P_e^{+}(s) = P_e(s) - P_e^{\text{sch}} \quad \text{if} \quad P_e(s) > P_e^{\text{sch}} \tag{2.17}$$

$$\Delta P_r^{+}(s) = P_r(s) - P_r^{\text{sch}} \cdot \Delta f \quad \text{if} \quad P_r(s) > P_r^{\text{sch}} \tag{2.18}$$

$$\Delta P_e^{-}(s) = P_e(s) - P_e^{\text{sch}} \quad \text{if} \quad P_e(s) \leqslant P_e^{\text{sch}} \tag{2.19}$$

$$\Delta P_r^{-}(s) = P_r(s) - P_r^{\text{sch}} \cdot \Delta f \quad \text{if} \quad P_r(s) \leqslant P_r^{\text{sch}} \tag{2.20}$$

where the piece-wise linearization of the P_{wf} given in (2.3) is used to find the optimal solutions. The constraints (2.14) and (2.15) limit the scheduled electricity and reserve contribution to the WF's maximum capacity. The constraints (2.16) restrict the electricity and reserve activation to the available WF output power. The half capacities in (2.14) and (2.16) guarantee the upward and downward regulations when the grid frequency drops or goes above 50 Hz, considering the deadband zone. The constraints in (2.16) are the limitations for electricity injection and reserve activation. The constraints (2.17) to (2.20) are considered for penalizing the electricity extra injection/off-takes and over/under reserve activations against the schedule.

2.4 Optimal operation strategy

2.4.1 Wind farm operation

When the total available power $P_{\text{wf}}^{\text{av}}$ is higher than the scheduled power reserve P_r^{sch}, the WF is able to deliver FCR in response to the grid frequency variations. The extra power that should be arranged among N WTs can be referred to as the WF deloaded power:

$$P_{\text{wf}}^{\text{dl}} = P_{\text{wf}}^{\text{av}} - P_r^{\text{sch}} \quad ; \quad P_{\text{wf}}^{\text{av}} = \sum_{i=1}^{N} P_{w,i}(v_i) \tag{2.21}$$

and v_i is the wind speed experienced by each turbine. The electrical power of each WT and the rotor thrust can be expressed as:

$$P_{w,i} = \frac{1}{2}\rho R^2 v_i^3 C_P(\lambda_i, \theta_i) \tag{2.22}$$

$$F_{w,i} = \frac{1}{2}\rho R^2 v_i^2 C_T(\lambda_i, \theta_i) \tag{2.23}$$

where ρ is the air density and R is the blade length. $C_P(\lambda_i, \theta_i)$ and $C_T(\lambda_i, \theta_i)$ are the power and thrust coefficients that vary with the individual tip speed ratio

$\lambda_i = R\omega_i/v_i$ and blade pitch angle θ_i. An empirical $C_p(\lambda, \theta)$ equation can also be found in literature [39], with an exponential form as follows:

$$C_P(\lambda, \theta) = c_1 \left(\frac{c_2}{\lambda_J} - c_3\theta - c_4 \right) e^{\frac{-c_5}{\lambda_J}} \tag{2.24}$$

$$\frac{1}{\lambda_J} = \frac{1}{\lambda + c_6} - \frac{c_7}{\theta^3 + 1} \tag{2.25}$$

where coefficients $c_1, ..., c_6$ for MW size WTs are 0.22, 116, 0.4, 5, 12.5, 0.088, and 0.035 respectively [40]. The thrust coefficient is modeled by a second-order polynomial function obtained from a wide range of simulations carried out using the NREL 5-MW offshore baseline WT:

$$C_T(\lambda, \theta) = \varepsilon_1 + \varepsilon_2\theta + \varepsilon_3\lambda + \varepsilon_4\theta^2 + \varepsilon_5\theta\lambda + \varepsilon_6\lambda^2 \tag{2.26}$$

where $\varepsilon_1, ..., \varepsilon_6$ are -0.1854, 0.0308, 0.161, 0.0002, -0.0133, and -0.0054, respectively. These results are derived for the robust fitness to the Least Absolute Residuals (LAR) with 0.9985 R-square and 0.067 RMSE.

2.4.2 Estimating wake formation

The conventional WF control approach relies on the WTs operating in Maximum Power Point Tracking (MPPT) mode without considering wake minimization strategies. However, in this study, two major optimal control approaches are considered, i.e., Axial Induction Control (AIC) and Wake Redirection Control (WRC). The AIC strategy reduces the upstream WTs' thrust force and controls wake formation by adjusting their axial induction factor by offsetting the blade pitch angle or tip speed ratio. The WRC strategy aims to steer the wakes away from downstream WTs by operating the WTs with a yaw misalignment [41]. To achieve axial induction-based control, the free-streamed WTs need to be operated outside their aerodynamic maximum by increasing the blade pitch angle or reducing the tip-speed ratio (operating at a suboptimal working point). This reduces the WT power P_w and the magnitude of the rotor's thrust force, which depends on the thrust coefficient. The power coefficient C_P and thrust coefficient C_T of the 5-MW offshore turbine as a function of the pitch angle and tip speed ratio are shown in Fig. 2.4. The power and thrust coefficients can also be expressed as functions of axial induction factor a_i and nacelle yaw angle y_i (yaw misalignment) as follows:

$$C_P = 4a_i(\cos y_i - a_i)^2 \tag{2.27}$$

$$C_T = 4a_i\sqrt{\sin^2 y_i + (\cos y_i - a_i)^2} \tag{2.28}$$

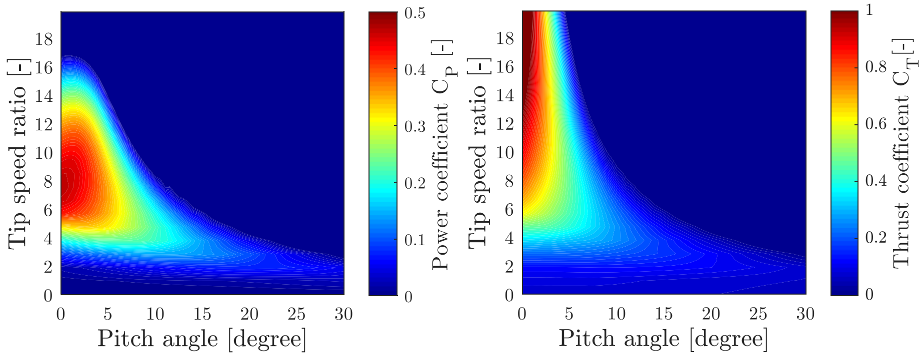

Figure 2.4: 5-MW WT Power and thrust coefficients.

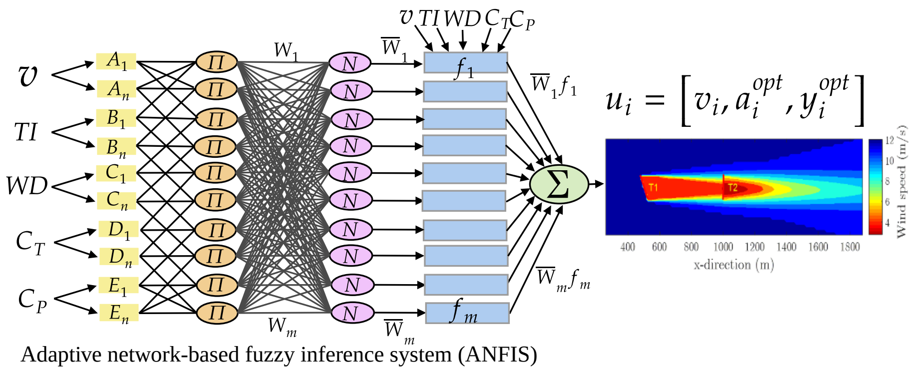

Figure 2.5: The ANFIS structure, estimating optimal wake-controlled parameters under AIC and WRC strategies.

The derivation of (2.27) and (2.28) involves using the axial momentum and the Glauert theory, which are widely used in theoretical models for predicting WT performance [42, 43]. The energy extraction by the turbine blades causes a reduction in the wind velocity at the turbine rotor disk. The average wind velocity at the turbine can be calculated by the axial induction factor $a_i \in [0, 1/3]$. The maximum C_P is determined by taking the derivative of the power coefficient (2.27) with respect to a_i and setting it equal to zero $\frac{\partial C_P}{\partial a_i} = 0$. In accordance with the Betz limit, $C_{P,max} = 16/27$ is the maximum theoretically possible rotor power coefficient [44]. Therefore, the maximum C_P can be achieved when $a_i = 1/3$ and zero degrees yaw misalignment y_i. Accordingly, from (2.28), the thrust coefficient for an ideal WT fully aligned with the wind, i.e., $y_i = 0$, is equal to $4a_i(1 - a_i)$. C_T has a maximum of 1.0 when $a = 0.5$ and the downstream velocity is zero. At maximum power output $a = 1/3$, C_T has a value of 8/9.

In order to identify optimal setpoints for WTs that provide FCR, it is crucial to rapidly report the WF's optimal aerodynamic couplings and wake information. To accomplish this, a deep learning approach has been proposed that can model the WF's flow fields and accurately approximate turbine wake information. The Gauss-Curl-Hybrid wake model available in the FlOw Redirection and Induction in Steady State (FLORIS) simulation software is employed, which combines the Gaussian wake model and the curl wake model to accurately predict the wind speed deficit and turbulence intensity in the wake of a WT. The model also considers the effects of ambient turbulence and the coupling between C_P and C_T to maximize power production while minimizing the wake effects with the following objective function:

$$\begin{aligned} \max_{y_i, a_i} \quad & \sum_{i=1}^{N} P_{w,i}(a_i, y_i, v, \textit{WD}) \\ \text{s.t.} \quad & -50.0^\circ \leq y_i \leq 50.0^\circ \\ & 0.0 \leq a_i \leq 0.3333 \end{aligned} \tag{2.29}$$

Optimal yaw angles y_i^{opt} and axial induction a_i^{opt} factors are estimated under AIC and WRC strategies in different wind conditions. Furthermore, extensive simulations are carried out offline to train and test the ANFIS structure shown in Fig.2.5. After training the ANFIS model with the obtained dataset, it can accurately replicate and mimic the complex wake deficits of a W for a wide range of conditions, including wind speeds, turbulence intensities, WDs, and turbine performance parameters such as C_P and C_T. By using these inputs, the model is capable of approximating the waked control operation and predicting the optimal values of v_i, y_i^{opt}, and a_i^{opt} for individual turbines within the W. Using the ANFIS model to estimate wake-controlled parameters allows for the rapid optimization of W performance by finding the optimal setpoints for individual turbines to contribute to frequency control reserves. Although the contracted scheduled reserve cannot be changed and must be respected hourly, the optimal allocation of power reserve can be actively updated when the wind field and wake formation vary.

2.4.3 Deloading strategy

WFs can provide power reserve and frequency control response (FCR) above nominal wind speeds. However, at wind speeds below the rated value, it may be necessary to deload some WTs to meet the promised FCR provision in case the grid frequency drops and extra power needs to be injected into the grid. Fig.2.6 shows that the deloaded operation of a WT can be achieved by shifting the operating point to the left or right of the maximum power point [45, 46]. This process creates a reserve margin by varying the active power between P^{dl} and P^{MPPT}, achieved by changing the rotor speed between ω^{dl} and ω^{MPPT}. It is

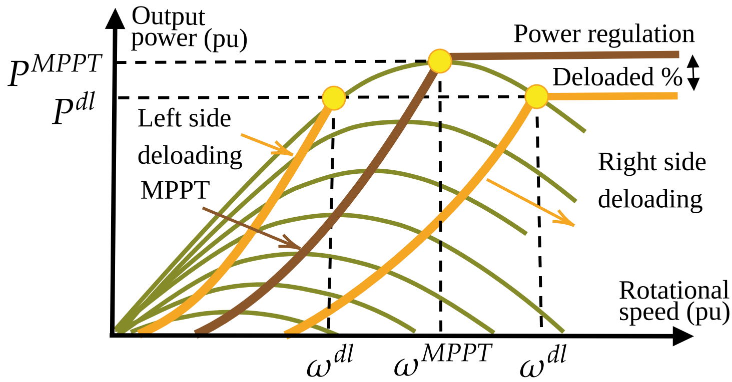

Figure 2.6: WT MPPT and deloaded power curves.

preferred to shift the operating point to the right to prevent a decrease in kinetic energy, which is beneficial for an inertial response, and restrict the wake deficit while activating FCR. An adaptive look-up table is included in the supplementary control loop, as shown in Fig. 2.1, for estimating the deloaded power reference P^{dl}, capture and reflect the time-varying characteristic of the proposed power reserve, and to adjust the rotational speed dynamically. In this method, the reserve margin β represents the deloading percentage that specifies the upper limit of generated power and the saving margin that must be maintained as a constant power reserve. During low-frequency periods, utilizing the generation margin thus created, the WT active power can be controlled by varying the rotor speed between ω^{dl} and ω^{MPPT}. The pitch control system will also be activated to adjust the limitations of the axial induction factor a_i^{opt} to restrict the wake deficit. Moreover, the kinetic energy stored in rotating masses of WTs can also be released for the inertial response as further system support.

2.4.4 Optimization problem

The scheduled reserve capacity should be optimally distributed depending on the location of each turbine within a farm and the airflow deficits caused by upstream turbines operating with a higher rotational speed than MPPT. Therefore, optimal rotor speed estimation can be achieved by considering the conflict between maximum generated power, complex interactions among WTs, and maximizing kinetic energy, which can be formulated as follows:

$$E_{w,i} = \frac{1}{2} J_i \omega_i^2 \tag{2.30}$$

where J_i is the inertia of each turbine. The objective of the optimization problem is to maximize the total kinetic energy of the WF $E_{w,i}$ and the total output power of the WF $\sum P_{w,i}$. This can be achieved by operating some of the

WTs in a sub-optimal operation mode, such that minimum wake deflection is produced. Consequently, the optimization problem for the optimal deloading control of WTs is given by:

$$\max_{\omega_i, \theta_i} \{f_1, f_2\} \qquad \omega_i, \theta_i \in \mathbb{R} \tag{2.31}$$

$$f_1 = \sum_{i=1}^{N} P_{w,i}(v_i, C_P(\omega_i, \theta_i)) \quad , \quad f_2 = \sum_{i=1}^{N} E_{w,i}(\omega_i) \tag{2.32}$$

s.t.

$$\underline{\omega_i} \leqslant \omega_i^{\mathrm{MPPT}} \leqslant \omega_i^{dl} \leqslant \overline{\omega_i} \tag{2.33}$$

$$\underline{\theta_i} \leqslant \theta_i^{\mathrm{offset}} \leqslant \overline{\theta_i} \tag{2.34}$$

$$C_{P_{w,i}}(\omega_i, \theta_i) \leqslant C_P(a_i^{\mathrm{opt}}, y_i^{\mathrm{opt}}) \tag{2.35}$$

$$C_{T_{w,i}}(\omega_i, \theta_i) \leqslant C_T(a_i^{\mathrm{opt}}, y_i^{\mathrm{opt}}) \tag{2.36}$$

$$\sum_{i=1}^{N} P_{w,i}^{\mathrm{dl}} = \sum_{i=1}^{N} P_{w,i}(v_i) - P_r^{\mathrm{sch}} \tag{2.37}$$

where $P_{w,i}$ and $E_{w,i}$ are given in (2.22) and (2.30) respectively. Constraints (2.33) and (2.34) limit the deloaded rotational speed and blade pitch angle offset to the allowable range. The maximum rotor speed is determined by the DC-link voltage of the power electronic converter, and the minimum rotor speed corresponds to the optimal tip speed ratio in MPPT mode. The constraints (2.35) and (2.36) ensure that the optimal power coefficient and thrust force of each WT are limited by the estimated optimal axial induction factors a_i^{opt} and yaw angles y_i^{opt} for the current wake formation given by the ANFIS model. These two constraints restrict the feasible space for searching the optimal rotor speed and blade pitch offset based on the unique wake formation caused by different scenarios of wind speed, direction, and TI. The constraint (2.37) also ensures maintaining the scheduled power reserve that has been foreseen for the WF to provide in the day-ahead market, which is discussed in (2.3). The optimal reserve allocation can be achieved by acting individually on pitch and torque control, ensuring sub-optimal operation for a given v_i, y_i^{opt} and a_i^{opt}, which are estimated by the method discussed in 2.4.2.

The proposed optimization problem aims to find the optimal rotational speed and blade pitch angle offset of the WTs to achieve the scheduled power reserve while actively updating the optimal wake-controlled parameters for different wind scenarios during the operating hour. Algorithm 1 outlines the optimal power reserve allocation and deployment, taking into account the operation and wake constraints specified in (2.33-2.37). Since activating the power reserve will dynamically impact the wake-controlled parameters, the

Algorithm 1 WT optimal power reserve allocation

Require: given historical datasets of gird frequency and wind speed, WF geometry, market clearance prices, system constraints, day-ahead forecasts, scenario selection.
Ensure:
for each hour τ of the operating day **do**
  At the beginning of the τth hour:
  Estimate quarter-hourly grid frequency fluctuations.
  Use k-means clustering:
  selecting the cluster centroids to represent Δf.
  Find wind scenarios $s_1, \ldots, s_K$ from uncertainty set $\mathcal{S}$.
  Estimating the expected value E_{s_K} of:
  reduced set of scenarios for wind speed.
  for $k = 1, \ldots, K$ **do**
    Solve the second-stage problem:

$$z_k = \max g(P_e(s), P_r(s), \mathrm{E}_{s_K})$$

    Solve the first-stage problem:

$$\max f(P_e^{\mathrm{sch}}, P_r^{\mathrm{sch}}) + \frac{1}{K}\sum_{k=1}^{K} z_k \quad \text{s.t.}(2.5 - 2.20)$$

    Solve the MINLP problem using a suitable solver.
  end for
  submit the optimized bid P_r^{sch} for the 24-hour horizon.
During the whole hour:
  for each τ' of the operating hour **do**
    Measure $v, \textsc{ti}, \textsc{wd}$
    Update the optimal wake-controlled parameters:
    approximating $v_i, a_i^{\mathrm{opt}}, y_i^{\mathrm{opt}}$ using ANFIS model.
    Solving (2.31) with constraints (2.33-2.37).
    Return ω_i^{dl} and $\beta_i^{\mathrm{offset}}$
  end for
end for

choice of shifting the operating point to the right side of the MPPT curve is made to not only increase kinetic energy for the inertial response but also restrict the wake-controlled parameters to stay within the predefined optimal ranges given in (2.35). At the same time, (2.36) ensures an optimal blade pitch offset that reduces the turbulence generated by the turbine and minimizes wake effects on downstream WTs while the WT activates FCR through the torque control system. This happens because of the unique nonlinear relationship between pitch and torque, which can only be fully controlled when the rotational speed exceeds the MPPT limit or when the wind speed goes above the rated value (the mentioned nonlinearities are visually illustrated in Fig.2.4). Therefore, although the pitch and torque control systems interact dynamically, wake formation will be actively controlled at the WT local control system by keeping the rotational speed variations in the right-side deloading zone (using an adaptive look-up table) while the blade pitch offset guarantees the optimal wake coordination when rotor speed changes due to the FCR activation in real-time.

It is worth mentioning that additional constraints and optimization objectives can be incorporated into the proposed problem formulation to further improve the system's performance. For instance, one can consider minimizing the cost of energy production by reducing mechanical loads and turbine wear and tear. This study mainly considered power production and kinetic energy, which mainly impact the WF's overall performance and wake mitigation. Moreover, different optimization algorithms can be explored to solve the problem efficiently, such as genetic algorithms, particle swarm optimization(PSO), or simulated annealing. This study considered multi-objective PSO to deal with the nonlinear optimization problem.

2.5 Case study and simulation results

2.5.1 Optimal scheduled reserve

One of the most critical issues with the bidding strategies of WTs is the stochasticity of wind power and grid frequency. If the decision-maker offers a too-high bidding quantity, the operator will not be able to satisfy grid requirements at low wind speeds and will be subject to penalties. However, a low reserve bidding quantity leads to extra wind power curtailment and declines in revenue. The proposed optimization strategy compromises between an aggressive and a conservative decision with a high or low bidding quantity, considering the quarter-hourly based penalties and revenues defined by the TSO. Fig. 2.7 shows the estimated wind and grid frequency variations for a day in January 2020 and the calculated 24-hour optimal bidding schedule when the electricity and FCR prices are competitive (electricity and reserve were considered at

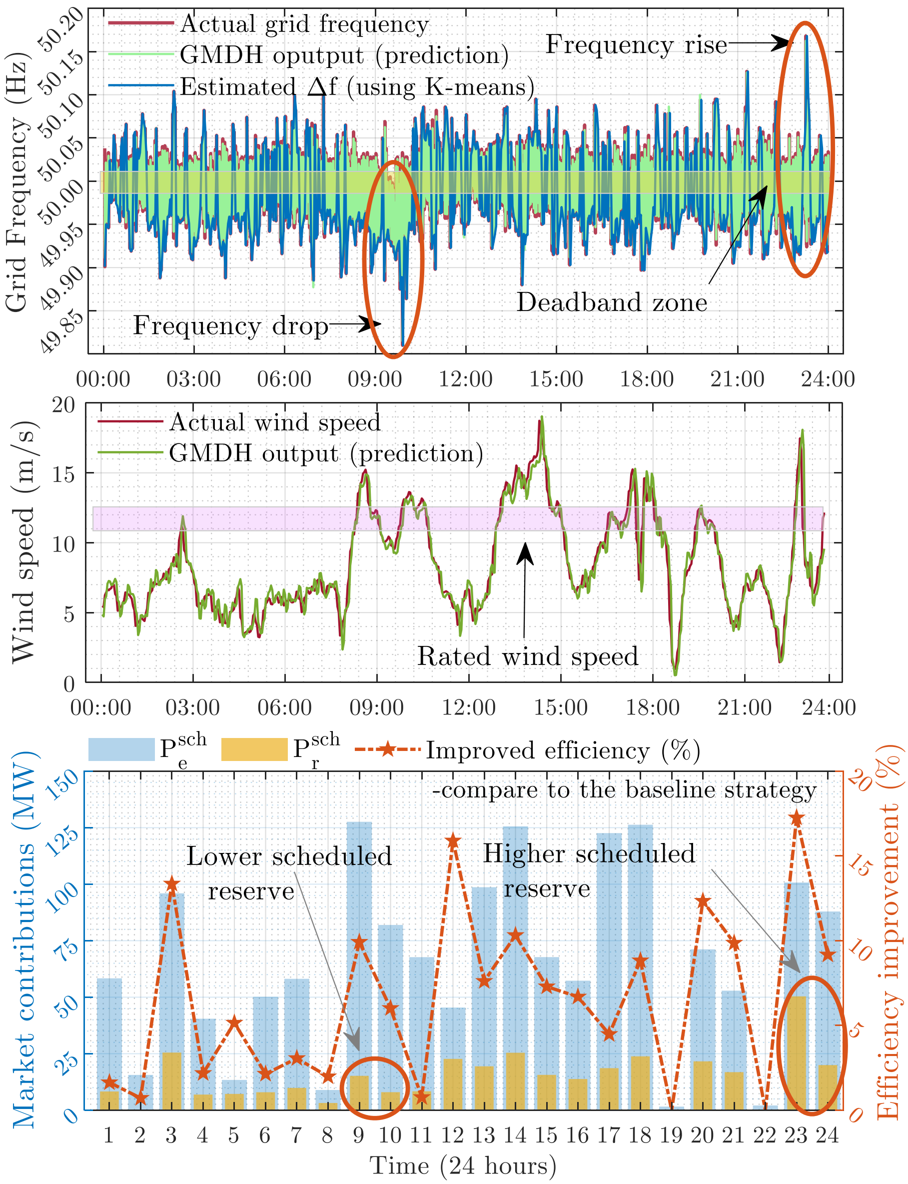

Figure 2.7: Estimated scheduled energy and reserve contribution. The time resolution of grid frequency and wind speed datasets is 10 seconds and 15 minutes, respectively.

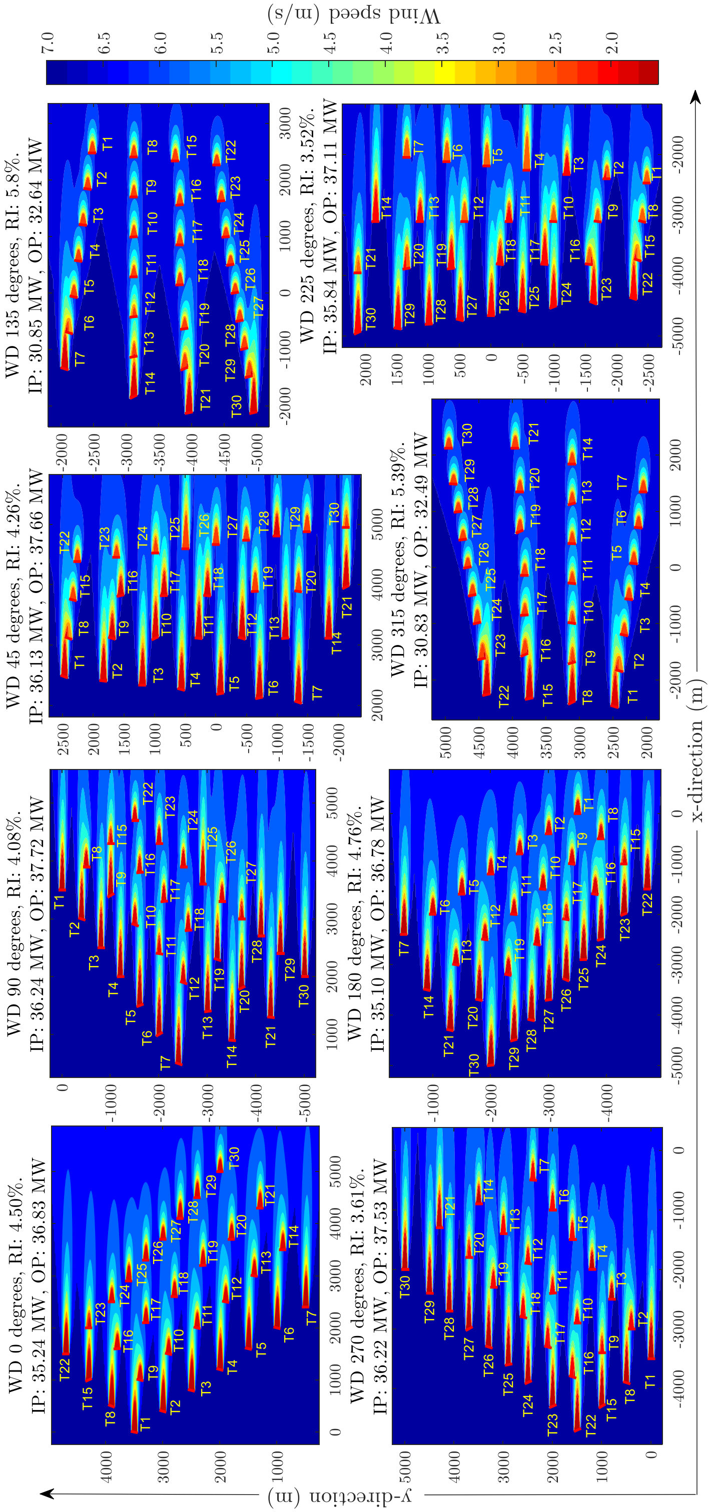

Figure 2.8: WF's wake modeling under the applied AIC and WRC strategies for 7 m/s wind speed and 5% TI.

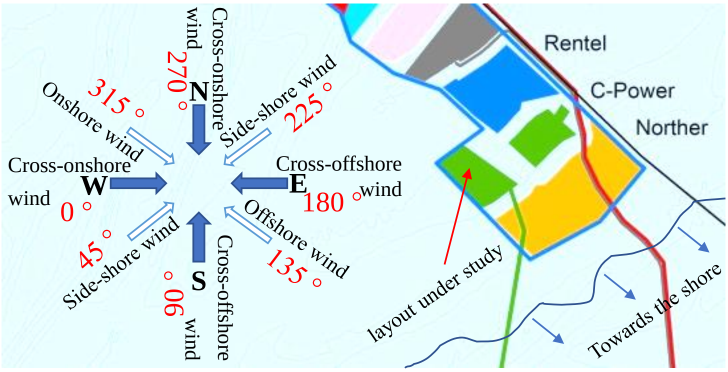

Figure 2.9: The WF layout in the North Sea.

the lowest and highest prices according to the energy market in 2019-2020). A windy day ($TI > 15\%$) is considered for studying different bidding scenarios. The proposed strategy is compared with the baseline approach, in which the WT contributes 10% of its capacity in the FCR market without considering the variability of wind and grid frequency, and the efficiency improvement is estimated, respectively. As Fig. 2.7 shows, higher contributions in both the energy and FCR are decided when the expected wind speed reaches the rated region. However, the lower or higher contribution in the day-ahead market is scheduled according to the estimation of maximum grid frequency deviation. For instance, although the wind speed goes above 11.4 m/s around 9:00-10:00h, a very low reserve bid is set due to the expected drop in grid frequency to avoid any penalty in case of a demanded upward regulation. In contrast, a higher contribution is set for reserve provision around 23:00-24:00h due to a rise in grid frequency considering the maximum possible downward regulation (reimbursing the curtailment by offering the FCR provision).

2.5.2 Wake modeling and optimal reserve allocation

This section evaluates the performance of the proposed optimal strategy for the 9.86 MW reserve provision that is decided around 7:00, where the mean wind speed is 7 m/s, and TI is 5%. Based on the results given in Fig.2.7, the optimal scheduled reserve around 7:00 clock is set to 9.86 MW when the average expected available wind power, considering different wake scenarios, is 38.13 MW. The studied wind directions WD are also illustrated in Fig.2.9, which addresses the geographic coordinates and indicates the onshore, offshore, side-shore, cross-offshore, and cross-onshore winds. Fig. 2.8 illustrates the WF modeling under the applied AIC and WRC strategies for the wind directions specified in Fig. 2.9, and power Relative Increase (RI) that percentiles the increase of Optimal Power (OP) based on the Initial Power (IP), where WTs greedily maximize their output power without considering negative impacts of

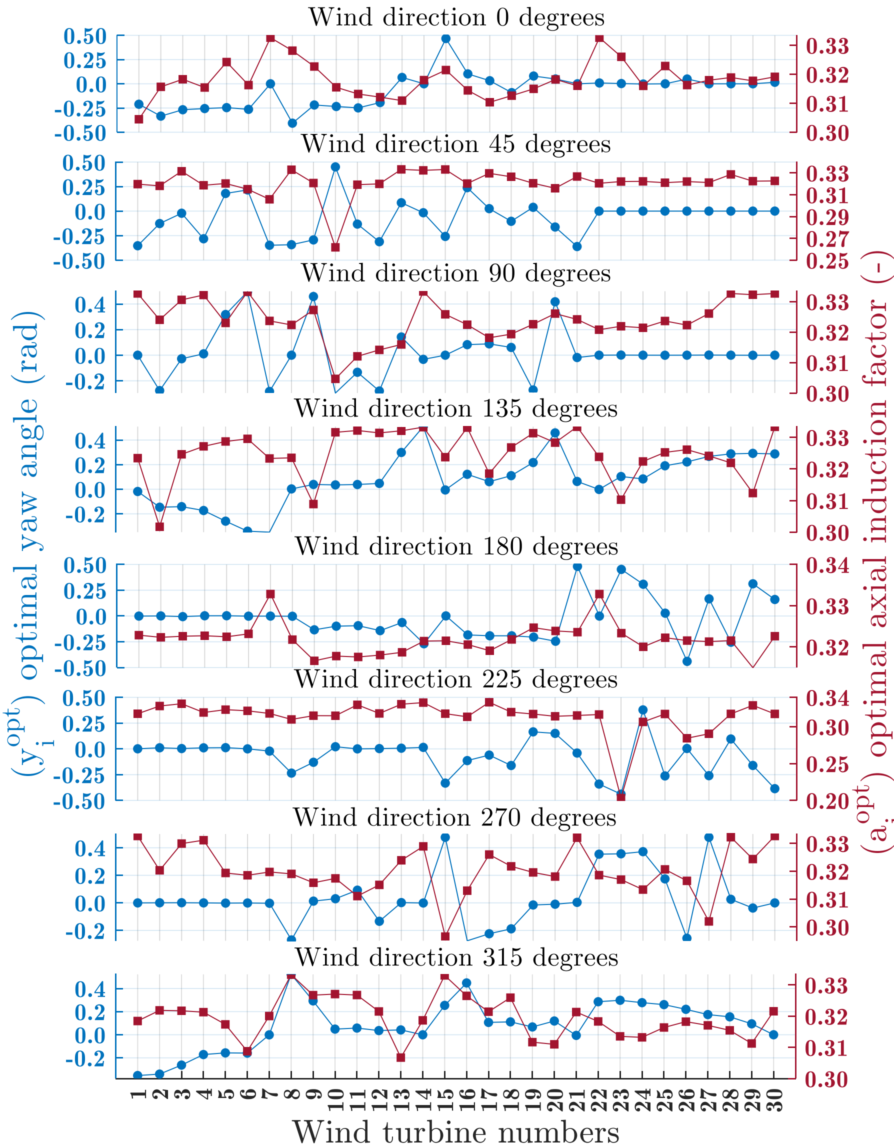

Figure 2.10: Estimated optimal wake-controlled parameters.

the wake. The AIC approach involves adjusting the axial induction factor of each WT to mitigate the wake effects generated by upstream turbines. By optimizing the axial induction factor, AIC limits the excessive reduction in power output of downstream turbines, preventing significant loss due to wake effects. On the other hand, WRC adjusts the yaw angle of each WT to redirect the wake away from downstream turbines and reduce wake-induced power losses in the wind farm. As illustrated in Fig. 2.8, depending on the wind direction and the specific wake formation, the optimal wake-controlled parameters, i.e., yaw angles and axial induction factors, can be very different for various scenarios of wind direction. Therefore, The optimization problem (2.31) should be rapidly updated to find the optimal distribution of the power reserve in a varying wind condition. The computationally efficient estimation of WFs' optimal wake-controlled parameters, discussed in 2.4.2, are given in Fig.2.10, corresponding to the WF wake modeling under AIC and WRD strategies. The obtained wake information and optimal scheduled reserve can be fed into the optimization problem (2.31) to search for the optimal solutions, i.e., optimal deloaded rotor speeds and blade pitch angles (pitch offsets), maximizing the total power production and the kinetic energy. A co-evolutionary multi-swarm particle swarm optimizer based on crowding distance archival management is applied to find solutions in rapidly changing environments (the implementation of the proposed algorithm is given in 2). In this algorithm, each particle is evaluated for its fitness values with respect to two objective functions, f_1 and f_2. External archives $A_1,\dots,A_K$ are used to store the non-dominated solutions encountered so far, and the best positions from these archives are used to update the particles in each iteration. The algorithm terminates after a maximum number of iterations T, and the final Pareto optimal set S and Pareto front F are generated by merging the external archives and selecting the non-dominated solutions, respectively. The function NonDominatedSort performs non-dominated sorting of the solutions in $A_k \cup P$ and returns the non-dominated solutions in A_k. After updating A_k, the algorithm checks if the size of A_k has exceeded the archive size K. If the size of A_k is greater than K, the crowding distance of solutions in A_k is calculated based on the f_1 and f_2 values. The solutions with the lowest crowding distance are then removed until the size of A_k is equal to K. This ensures that the external archive maintains a diverse set of non-dominated solutions by promoting well-spaced solutions in the objective space. Fig. 2.11 illustrates the optimal solutions and Pareto fronts for the cross-offshore, cross-onshore, and offshore wind, which have the maximum, medium, and minimum kinetic capacity, respectively. It also shows that the maximum power production without any FCR provision should ensure 60% of the maximum total kinetic energy that can be released in inertial support. Also, the maximum total kinetic energy can only be achieved in the cross-offshore and cross-onshore wind by 45% deloading WTs (increasing the WTs' rotational speeds up to 45%). It can be comprehended that yawing upstream WTs control wake deflections. Also, the upstream WTs' axial induction factors are set to a lower value compared to the other WTs, which are less located in each other's stream with minimum wake overlaps. For instance, the axial induction factor of the upstream T1 (with maximum wake overlap) is set to 0.305 in the cross-onshore wind (WD0°). However, since T7 and T22 are almost decoupled from the WF wake, they are allowed to operate at their maximum capacity. The estimated power reserve is optimally distributed among the WTs by shifting their

Algorithm 2 Co-evolutionary PSO with crowding distance archival management for bi-objective optimization

Require: Initial population of particles P, maximum number of iterations T, archive size K, fitness function $f_1(\cdot)$ and $f_2(\cdot)$
Ensure: Pareto optimal set S and Pareto front F
Initialize P and K external archives $A_1, \ldots, A_K$ with empty solutions
for $t = 1, \ldots, T$ **do**
    for $p \in P$ **do**
        Evaluate the fitness values of particle p:
        $f_1(p), f_2(p) \leftarrow f_1(p), f_2(p)$
        for $k = 1, \ldots, K$ **do**
            Update external archive A_k with the non-dominated solutions from the current population and the archive itself:
            $A_k \leftarrow \text{NonDominatedSort}(A_k \cup P)$
            if $|A_k| > K$ **then**
                Calculate crowding distance of solutions in A_k using the f_1 and f_2 values
                Remove solutions with the lowest crowding distance until $|A_k| = K$
            end if
        end for
    end for
    for $p \in P$ **do**
        Select a random external archive A_k
        Update particle p using the best position from A_k:
        $p.v \leftarrow w \cdot p.v + c_1 \cdot rand() \cdot (pbest - p) + c_2 \cdot rand() \cdot (best_{A_k} - p)$
        $p.x \leftarrow p.x + p.v$
    end for
end for
Generate the Pareto optimal set S by merging the solutions in the external archives $A_1, \ldots, A_K$:
$S \leftarrow A_1 \cup \cdots \cup A_K$
Generate the Pareto front F by selecting the non-dominated solutions from S:
$F \leftarrow p \in S : \nexists p' \in S^*$ such that:
$f_1(p') \leq f_1(p)$ and $f_2(p') \leq f_2(p)$

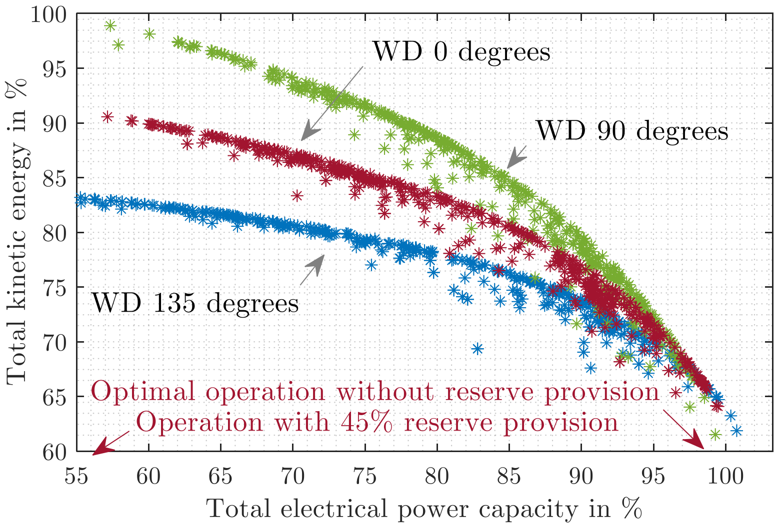

Figure 2.11: The Pareto front of the optimal solutions over the iterations of the bi-objective optimization problem.

rotational speeds to the right side of the MPPT curve shown in Fig.2.6.

Moreover, the algorithm searches for the optimal individual blade pitch offset to ensure that the estimated WTs' optimal axial induction factors are respected. The total WF output should be deloaded by 19.86%. The Pareto front determines the maximum kinetic energy in different wind directions, the optimal deloaded rotational speeds, and the blade pitch offsets for the WTs. Fig.2.12 shows the power reserve allocation and presents the percentual share of each WT, identifying the WTs' deloading portion. For instance, T7 and T22 have the maximum share of FCR provision in the cross-onshore wind (WD0°) because they almost have no conflict with their neighboring WTs. Therefore, increasing their rotational speed will not cause wake disruption for their neighbors, and for the same reason, no blade pitch offset is required. However, as Fig.2.8 also visually confirms, T1 in the same wind direction can cause a significant wake for T9. Therefore, it plays a minimum contribution to FCR provision, and its operation will be limited by the optimal axial induction factor, which is achieved by a blade pitch offset of 1.6°. Taking advantage of the superior computational efficiency of the PSO and the proposed ANFIS model, the optimal power reserve allocation can be instantly updated by any changes in the dominant wind speed, direction, or TI. The performance of the proposed strategy is estimated and compared with the baseline strategy, where 15% reserve power is distributed evenly regardless of wake interactions. Furthermore, the simulations are carried out with different wind speeds and TIs concerning the dominant inflow wind direction [47] given in Fig.2.13. The results confirm

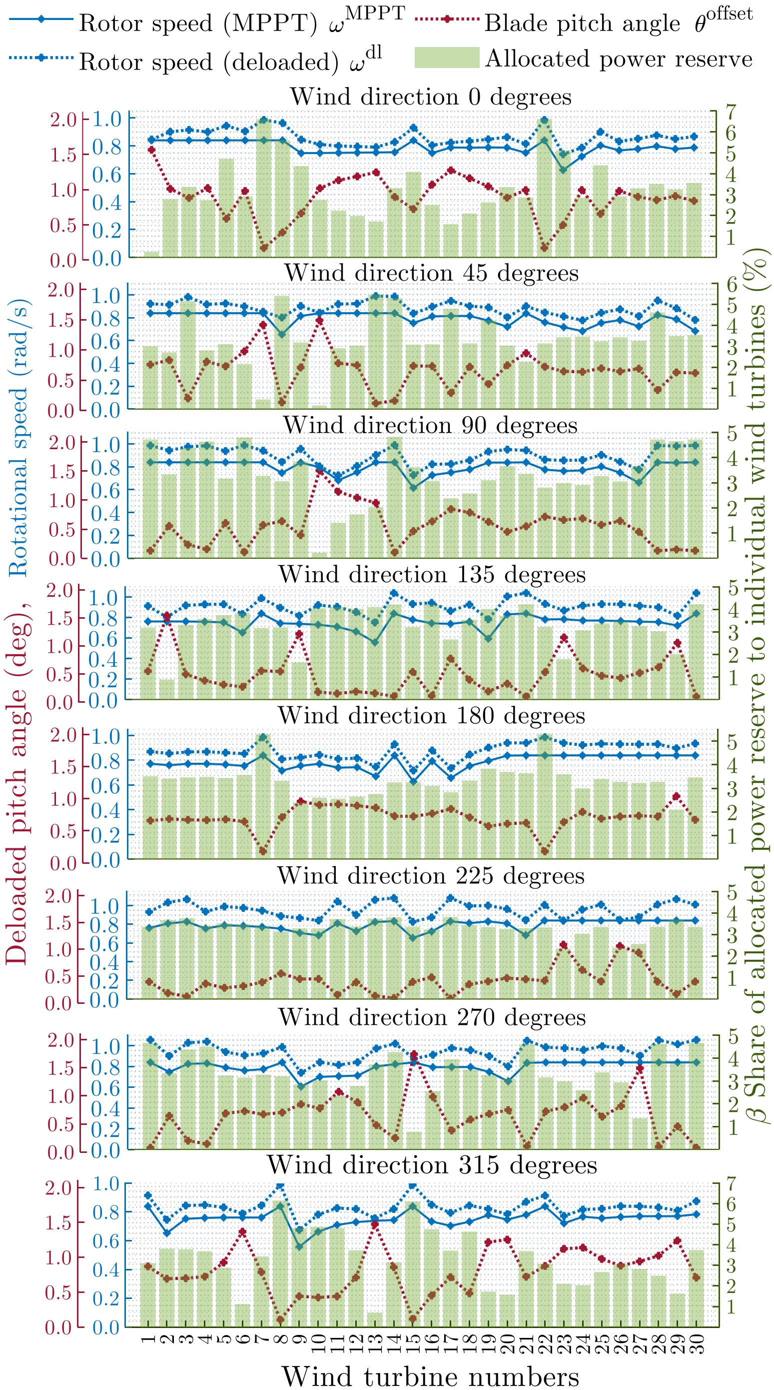

Figure 2.12: Optimal power reserve allocation for 7 m/s 5% TI wind speed, and 9.86 MW scheduled reserve.

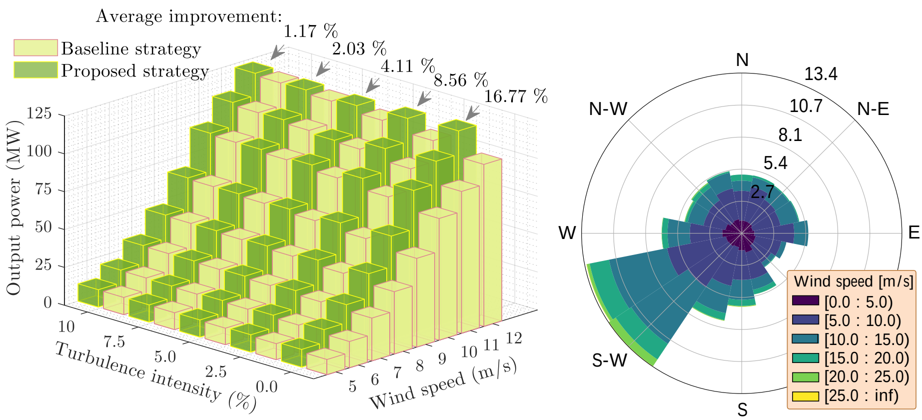

Figure 2.13: Performance of the proposed strategy for the S-W (side-shore) wind and wind rose for the C-Power layout.

the overall improvement and higher effectiveness at lower TIs, which cause stronger uniform wake formations and can play a significant role in the optimal allocation of power reserve.

Moreover, the dynamic behavior of the WF and the activation of the scheduled symmetric reserve have been investigated based on the carried-out wake analysis. Fig. 2.14 depicts the active operation of the WF, which provides 9.86 MW symmetric FCR under turbulent wind conditions. The frequency profile utilized in this study is designed to simulate the worst-case scenario and is not representative of natural grid frequency behavior. This profile includes a significant drop from 50.2 to 49.8 Hz over 500 seconds to ensure the system can adequately respond to both upward and downward regulation during extreme conditions. The study examines the results of the dominant wind speed profile (maximum wind speed experienced by T1-7, T9-14, and T21) for the side-shore wind coming from the southwest with 7 m/s mean and 5% turbulence intensity (TI). T8 and T20 experience a minimum wind speed of 5.46 m/s through the wake deficit. The rest of the WTs receive reduced wind speeds between 7 and 5.46 m/s.

The WF's total power production has been estimated using the baseline control strategy that distributes the power reserve equally among WTs and the proposed optimal method that actively controls the wake and optimally allocates the scheduled reserve to WTs. As Fig. 2.14 visually depicts, although the efficiency improvement of the proposed strategy is practically greater than the baseline method, it can be noticed that it is more significant when the wind speed drops below the mean value. This is the direct effect of the active wake-controlled approach, which reduces the adverse impact of wakes and ensures the efficiency of the WTs at lower wind speeds. The deployment of the FCR, be-

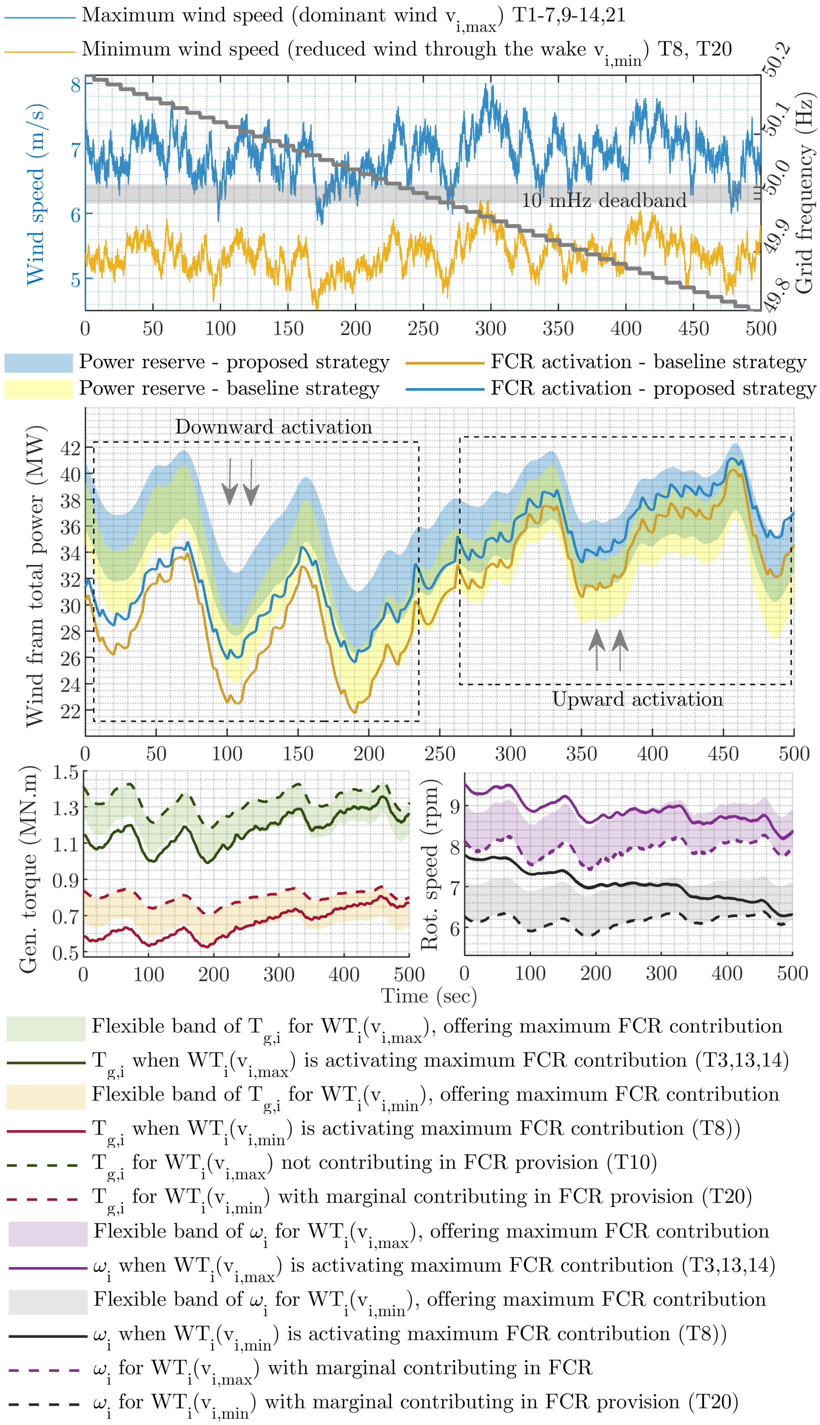

Figure 2.14: Dynamic operation of WF activating 9.86 MW symmetric FCR for side-shore wind from the southwest.

sides adjusting the blade pitch offset, yaw angle, and axial induction factor, dynamically involves regulating the WT's rotational speed and generator torque. Although FCR activation generally can be carried out through both pitch and torque control systems, in this study, to avoid introducing excessive mechanical loads on the WTs' blade's root and the tower, the FCR activation is done solely by adjusting the generator torque, and the pitch blade offset only keeps the WT operation in the acceptable optimal wake condition. These control actions and rotational speed variation between MPPT and deloaded operation (flexible band of ω_i) are also shown in Fig.14 for the maximum and minimum wind speeds with full and marginal FCR activations in different reserve allocations.

The optimization algorithm proposed in this study typically assigns a lower reserve to WTs located in the wake. Nevertheless, if the optimal yaw angle sufficiently redirects the wake and preserves wind speed, these turbines may also contribute to FCR provision. For instance, T8 receives a reduced mean wind speed of 5.44 m/s. However, with 50°yaw misalignment, its wake is redirected, and therefore, increasing its rotational speed up to 5% does not significantly reduce wind speed for T15 in its downstream path. Nevertheless, T20 is marginally involved in FCR contribution ($\beta < 3$) since its optimal yaw angle is decided for 25°, and its rotor speed increment can cause a significant wake for T29 and T28. Since wind direction changes can be frequent in the North Sea and alters the wake behavior, the proposed operation strategy suggests updating the power reserve allocation on a minutes scale (60 seconds $< \tau' <$ 600 seconds) to allow the WTs to optimize their power output in response to wind changing conditions and sub-hourly reserve schedules planned in the day-ahead market.

2.6 Conclusions

This study proposes an operating strategy for WFs with optimal distribution of FCR. The studied algorithm supports optimal decision-making in the day-ahead market using the two-stage stochastic programming method considering data-driven wind speed forecasting and grid frequency for determining an hourly-based optimal scheduled reserve. Moreover, an optimization problem is formulated to dynamically allocate the estimated scheduled reserve among the WTs by actively minimizing wake interactions and maximizing WT's total electrical power and kinetic energy. A deep learning approach is suggested for computationally efficient estimation of the WT wake behavior under axial induction and wake redirection control strategies. The trained ANFIS model can mimic the WT's aerodynamic complexity in varying wind speed/direction and turbulence intensity and provides the optimization problem with appropriate constraints. The WT's desired control set points at the supervisory level will be determined by searching for the WTs' optimal deloading percentage, rotational speed, and blade pitch offset, leading to a relative increase in total generated power. The C-Power WT layout is studied to explore the aerodynamic coupling behavior in different wind directions. The creation of wake forms can significantly change the optimal allocation of power reserve and share of each WT in providing FCR. Results suggest that the proposed optimal operational framework can optimize the WTs' overall performance, especially in less turbulent conditions, and benefit WF owners willing to contribute to the day-ahead market without relying on a perfect storage system.

Bibliography

[1] N. Kayedpour, J. D. M. De Kooning, A. E. Samani, F. Kayedpour, L. Vandevelde, and G. Crevecoeur, "An optimal wind farm operation strategy for the provision of frequency containment reserve incorporating active wake control," *IEEE Transactions on Sustainable Energy*, pp. 1–14, 2023.

[2] T. Muneer, E. Jadraque Gago, and S. Etxebarria Berrizbeitia, "Wind energy and solar pv developments in the eu," in *The Coming of Age of Solar and Wind Power*, pp. 139–177, Springer, 2022.

[3] X. Yuan, C.-W. Su, M. Umar, X. Shao, and O.-R. LOBONŢ, "The race to zero emissions: Can renewable energy be the path to carbon neutrality?," *Journal of Environmental Management*, vol. 308, p. 114648, 2022.

[4] ESO, "Technical report on the events of 9 august 2019.."

[5] D.-Y. Li, P. Li, W.-C. Cai, Y.-D. Song, and H.-J. Chen, "Adaptive fault-tolerant control of wind turbines with guaranteed transient performance considering active power control of wind farms," *IEEE Transactions on Industrial Electronics*, vol. 65, no. 4, pp. 3275–3285, 2017.

[6] C. Edmunds, S. Martín-Martínez, J. Browell, E. Gómez-Lázaro, and S. Galloway, "On the participation of wind energy in response and reserve markets in great britain and spain," *Renewable and Sustainable Energy Reviews*, vol. 115, p. 109360, 2019.

[7] H. Wiklund, "The potential of wind power on the swedish ancillary service markets," 2021.

[8] ELIA, "Study on the future design of the ancillary service of voltage and reactive power control," 2018.

[9] K. Li, H. Guo, X. Fang, S. Liu, F. Teng, and Q. Chen, “Market mechanism design of inertia and primary frequency response with consideration of energy market,” *IEEE Transactions on Power Systems*, 2022.

[10] H. Li, Y. Qiao, Z. Lu, B. Zhang, and F. Teng, “Frequency-constrained stochastic planning towards a high renewable target considering frequency response support from wind power,” *IEEE Transactions on Power Systems*, vol. 36, no. 5, pp. 4632–4644, 2021.

[11] Y. Ma, Z. Hu, and Y. Song, “Hour-ahead optimization strategy for shared energy storage of renewable energy power stations to provide frequency regulation service,” *IEEE Transactions on Sustainable Energy*, vol. 13, no. 4, pp. 2331–2342, 2022.

[12] S. Zhu, H. Wang, W. Wang, and X. Chang, “A combined day-ahead and intraday optimal scheduling strategy considering the joint frequency regulation reserve scheme among wind, photovoltaic and thermal power,” *Frontiers in Energy Research*, vol. 10, p. 1965, 2023.

[13] A. E. Samani, N. Kayedpour, F. Kayedpour, J. D. De Kooning, G. Crevecoeur, and L. Vandevelde, “An optimal operation strategy for collaborative flexibility provision of a carbon capture and utilization process with wind energy,” *IEEE Transactions on Sustainable Energy*, 2023.

[14] S. A. Hosseini, J.-F. Toubeau, Z. De Greve, and F. Vallée, “An advanced day-ahead bidding strategy for wind power producers considering confidence level on the real-time reserve provision,” *Applied Energy*, vol. 280, p. 115973, 2020.

[15] Z. Zhang and Z. Chen, “Optimal wind energy bidding strategies in real-time electricity market with multi-energy sources,” *IET Renewable Power Generation*, vol. 13, no. 13, pp. 2383–2390, 2019.

[16] A. Žertek, G. Verbič, and M. Pantoš, “Optimised control approach for frequency-control contribution of variable speed wind turbines,” *IET Renewable power generation*, vol. 6, no. 1, pp. 17–23, 2012.

[17] M. Hedayati-Mehdiabadi, P. Balasubramanian, K. W. Hedman, and J. Zhang, “Market implications of wind reserve margin,” *IEEE Transactions on Power Systems*, vol. 33, no. 5, pp. 5161–5170, 2018.

[18] M. Hedayati-Mehdiabadi, K. W. Hedman, and J. Zhang, “Reserve policy optimization for scheduling wind energy and reserve,” *IEEE Transactions on Power Systems*, vol. 33, no. 1, pp. 19–31, 2017.

[19] H. Xiao, X. Huang, Y. Huang, and Y. Liu, "Self-synchronizing control and frequency response of offshore wind farms connected to diode rectifier based hvdc system," *IEEE Transactions on Sustainable Energy*, vol. 13, no. 3, pp. 1681–1692, 2022.

[20] C. Huang and H. Zhao, "Error-based active disturbance rejection control for wind turbine output power regulation," *IEEE Transactions on Sustainable Energy*, 2023.

[21] S. Boersma, B. Doekemeijer, S. Siniscalchi-Minna, and J. van Wingerden, "A constrained wind farm controller providing secondary frequency regulation: An les study," *Renewable energy*, vol. 134, pp. 639–652, 2019.

[22] A. K. Bhyri, N. Senroy, and T. K. Saha, "Enhancing the grid support from dfig-based wind farms during voltage events," *IEEE Transactions on Power Systems*, 2023.

[23] Z. Zhang, P. Kou, Y. Zhang, and D. Liang, "Coordinated predictive control of offshore dc collection grid and wind turbines for frequency response: A scheme without secondary frequency drop," *IEEE Transactions on Sustainable Energy*, 2023.

[24] M. De-Prada-Gil, C. G. Alías, O. Gomis-Bellmunt, and A. Sumper, "Maximum wind power plant generation by reducing the wake effect," *Energy conversion and management*, vol. 101, pp. 73–84, 2015.

[25] M. Dreidy, H. Mokhlis, and S. Mekhilef, "Inertia response and frequency control techniques for renewable energy sources: A review," *Renewable and Sustainable Energy Reviews*, vol. 69, pp. 144–155, 2017.

[26] A. Fernández-Guillamón, E. Gómez-Lázaro, E. Muljadi, and Ángel Molina-García, "Power systems with high renewable energy sources: A review of inertia and frequency control strategies over time," *Renewable and Sustainable Energy Reviews*, vol. 115, p. 109369, 2019.

[27] M. Kheshti, S. Lin, X. Zhao, L. Ding, M. Yin, and V. Terzija, "Gaussian distribution-based inertial control of wind turbine generators for fast frequency response in low inertia systems," *IEEE Transactions on Sustainable Energy*, 2022.

[28] J. Zhang, Y. Li, Z. Xu, D. Qi, and C. Li, "Game theory-based optimal deloading control of wind turbines under scalable structures of wind farm," *IET Cyber-Physical Systems: Theory & Applications*, vol. 3, no. 4, pp. 224–231, 2018.

[29] A. S. Ahmadyar and G. Verbič, “Coordinated operation strategy of wind farms for frequency control by exploring wake interaction,” *IEEE Transactions on Sustainable Energy*, vol. 8, no. 1, pp. 230–238, 2016.

[30] S. Siniscalchi-Minna, F. D. Bianchi, M. De-Prada-Gil, and C. Ocampo-Martinez, “A wind farm control strategy for power reserve maximization,” *Renewable energy*, vol. 131, pp. 37–44, 2019.

[31] Z. Zhang, M. Zhou, Z. Wu, S. Liu, Z. Guo, and G. Li, “A frequency security constrained scheduling approach considering wind farm providing frequency support and reserve,” *IEEE Transactions on Sustainable Energy*, vol. 13, no. 2, pp. 1086–1100, 2022.

[32] X. Lyu, Y. Jia, and Z. Xu, “A novel control strategy for wind farm active power regulation considering wake interaction,” *IEEE Transactions on Sustainable Energy*, vol. 11, pp. 618–628, 2020.

[33] ELIA, “Transparency on grid data.”

[34] W. API, “Sub-hourly historical weather.”

[35] K. C. Sharma, P. Jain, and R. Bhakar, “Wind power scenario generation and reduction in stochastic programming framework,” *Electric Power Components and Systems*, vol. 41, no. 3, pp. 271–285, 2013.

[36] N. Kayedpour, A. E. Samani, J. D. De Kooning, L. Vandevelde, and G. Crevecoeur, “A data-driven approach using deep learning time series prediction for forecasting power system variables,” in *2019 IEEE 2nd International Conference on Renewable Energy and Power Engineering (REPE)*, pp. 43–47, IEEE, 2019.

[37] Elia, “Day-ahead balance obligation of the balance responsible parties.”

[38] Elia, “Terms and conditions for balancing service providers for frequency containment reserve (FCR).”

[39] J. D. M. De Kooning, L. Gevaert, J. Van de Vyver, T. L. Vandoorn, and L. Vandevelde, “Online estimation of the power coefficient versus tip-speed ratio curve of wind turbines,” in *IECON 2013-39th Annual Conference of the IEEE Industrial Electronics Society*, pp. 1792–1797, IEEE, 2013.

[40] M. Carpintero-Renteria, D. Santos-Martin, A. Lent, and C. Ramos, “Wind turbine power coefficient models based on neural networks and polynomial fitting,” *IET Renewable Power Generation*, vol. 14, no. 11, pp. 1841–1849, 2020.

[41] S. Boersma, B. M. Doekemeijer, P. M. Gebraad, P. A. Fleming, J. Annoni, A. K. Scholbrock, J. A. Frederik, and J.-W. van Wingerden, "A tutorial on control-oriented modeling and control of wind farms," in *2017 American control conference (ACC)*, pp. 1–18, IEEE, 2017.

[42] T. Burton, N. Jenkins, D. Sharpe, and E. Bossanyi, *Wind energy handbook*. John Wiley & Sons, 2011.

[43] K. S. Heck, H. M. Johlas, and M. F. Howland, "Modelling the induction, thrust and power of a yaw-misaligned actuator disk," *Journal of Fluid Mechanics*, vol. 959, p. A9, 2023.

[44] J. F. Manwell, J. G. McGowan, and A. L. Rogers, *Wind energy explained: theory, design and application*. John Wiley & Sons, 2010.

[45] K. Vidyanandan and N. Senroy, "Primary frequency regulation by deloaded wind turbines using variable droop," *IEEE transactions on Power Systems*, vol. 28, no. 2, pp. 837–846, 2012.

[46] X. Ge, X. Zhu, Y. Fu, Y. Xu, and L. Huang, "Optimization of reserve with different time scales for wind-thermal power optimal scheduling considering dynamic deloading of wind turbines," *IEEE Transactions on Sustainable Energy*, 2022.

[47] D. Allaerts, S. V. Broucke, N. van Lipzig, and J. Meyers, "Annual impact of wind-farm gravity waves on the belgian–dutch offshore wind-farm cluster," in *Journal of physics: conference series*, vol. 1037, p. 072006, IOP Publishing, 2018.

Chapter 3

Data-driven Model Predictive Control for Wind Turbines providing FCR

The previous Chapter 2 focused on the optimal operation strategy for wind farms participating in a reserve market and determining wind turbines' setpoints. In this chapter, we address the challenges of FCR activation at the wind turbine local control level, starting from the optimal power reserve, allocation, and the delivered set points such as P^{dl}, which are decided at the wind farm level, see also Figure 1.13. As mentioned in Section 1.5.2, wind turbines exhibit nonlinear behavior, necessitating the development of advanced control strategies that ensure stable and efficient wind turbine operation. These strategies must effectively handle varying control setpoints, decided at the wind farm supervisory level while activating FCR and maximizing energy production with optimal control efforts. These strategies must accurately predict and incorporate the complex interactions within the system to identify optimal control actions that consider system physical constraints and limitations and enhance overall turbine performance.

Building on the previous chapter's findings and given the ability of data-driven model predictive controllers (MPC) to adapt and capture nonlinear behavior, see Section 1.4.3 and Figure 1.9, this chapter delves into the application of neural network-based Model Predictive Control (MPC) to enhance the performance of wind turbine control systems in delivering frequency control ancillary services to the grid. Our primary focus lies in improving the wind turbine's response at above-rated wind speeds, presenting a robust and efficient solution for future power systems. The studied data-driven-based MPC can effectively manage the nonlinear behavior of wind turbines, enabling them to provide precise frequency control support while operating under stochastic turbulent wind conditions.

This study employs a closed-loop Hammerstein structure to approximate the behavior of a 5MW floating offshore wind turbine equipped with a Permanent Magnet Synchronous Generator (PMSG). Within this structure, multilayer perceptron neural networks are utilized to estimate the aerodynamic behavior of the nonlinear steady-state part. In addition, the linear AutoRegressive with Exogenous input (ARX) model is utilized to identify the linear time-invariant dynamic part. This combination allows for an accurate representation of the turbine's behavior.

The studied Cascade Hammerstein approach simplifies online linearization at each operating point without resorting to nonlinear optimization. This streamlines the process and eliminates the need for computationally expensive nonlinear optimization. Moreover, the proposed algorithm employs quadratic programming to derive control actions, effectively removing the necessity for nonlinear optimization. This ensures a fast and stable response to grid frequency variations, enabling optimal pitch and torque cooperation. This control approach at the wind turbine level is able to interact with the wind farm supervisory control level, which oversees the overall operation of the wind farm. The supervisory control level coordinates and manages the individual turbines to achieve optimal performance and desired system-wide outcomes.

We compare the performance of the presented data-driven MPC with a (PI) controller. The results demonstrate the effectiveness of the designed control system in delivering FCR and frequency regulation services. Furthermore, the MPC-based control system showcases improved performance and outperforms the traditional PI controller in terms of response speed, stability, and accuracy.

The adoption of this advanced control strategy promises significant advancements in wind turbine technology, leading to enhanced grid stability and optimal utilization of wind energy resources. The study highlights the potential of the proposed neural network-based Model Predictive Controller to enhance the smooth contribution of wind farms in reserve markets. Combining innovative control techniques with the inherent benefits of wind energy presents a promising pathway toward achieving a greener and more efficient power grid.

The contents of this chapter are published in IEEE Transactions on Energy Conversion [1].

Model Predictive Control with a Cascaded Hammerstein Neural Network of a Wind Turbine Providing Frequency Containment Reserve

Nezmin Kayedpour, Arash E. Samani, Jeroen D. M. De Kooning, Lieven Vandevelde, and Guillaume Crevecoeur

Published in ”IEEE Transactions on Energy Conversion”, 2021

Abstract:*This article presents an application of neural network-based Model Predictive Control (MPC) to improve the wind turbine control system's performance in providing frequency control ancillary services to the grid. A closed-loop Hammerstein structure is used to approximate the behavior of a 5MW floating offshore wind turbine with a Permanent Magnet Synchronous Generator (PMSG). The multilayer perceptron neural networks estimate the aerodynamic behavior of the nonlinear steady-state part, and the linear AutoRegressive with Exogenous input (ARX) is applied to identify the linear time-invariant dynamic part. Using the specific structure of the Cascade Hammerstein design simplifies the online linearization at each operating point. The proposed algorithm evades the necessity of nonlinear optimization and uses quadratic programming to obtain control actions. Eventually, the proposed control design provides a fast and stable response to the grid frequency variations with optimal pitch and torque cooperation. The performance of the MPC is compared with the gain-scheduled proportional-integral (PI) controller. Results demonstrate the effectiveness of the designed control system in providing Frequency Containment Reserve (FCR) and frequency regulation in the future of power systems.*

3.1 Introduction

Modern wind turbines are designed to operate over a wide range of wind speeds to make wind energy more cost-effective. However, these wind energy sources generate fluctuating power due to their dependency on intermittent and variable wind. This issue hinders adequate retaining levels of reliability and stability of the power grid and the balance of electricity supply-demand. Hence, the integration of wind energy into the power system meets significant challenges without addressing this issue [2].

While offshore wind farms are growing in size, the need arises for these sources to take part in grid balancing and stabilization, e.g., by providing ancillary services [3]. The Frequency Containment Reserve (FCR), formerly known as the primary frequency reserve, is used to limit the frequency deviation caused by the sudden changes in the generation or load. Offshore wind turbines offer the potential for providing FCR since the wind flow is less variable compared to inland wind farms where obstacles may divert the wind flow [4], and specifically in above-rated wind speeds. However, the wind turbine control system's capability in providing FCR is challenged by the frequent changes in operating points and delivering a fast optimal response in the presence of varying wind speed. These challenges need to be addressed in order to increase the further share of wind power in the future power system [5].

Over the past decades, the wind turbine control system's primary goal was rotor speed regulation and maximum power point tracking with a Proportional-Integral (PI) design. However, current wind turbines are needed to satisfy the grid code technical requirements and additional operating conditions demanded by transmission system operators [6–8]. Some studies suggest that torque control and pitch control can act as frequency regulation schemes [9–11]. One approach is that the wind turbine operates in the MPPT mode, and the inertia characteristics can answer the power response to frequency variations on a short time scale. However, this strategy may cause system instability due to the rapid variations in the rotational speed of the wind turbine [12]. Another scheme is that the wind turbine does not operate in MPPT mode but instead operates at the suboptimal operating limit by under-speeding or over-speeding control methods to obtain a power reserve for frequency regulation [13, 14]. As a counterpoint, providing power reserve with de-loaded wind turbines in below-rated wind speed result in a reduced energy yield. On the other hand, the frequency control scheme, which only relies on the pitch control system, does not necessarily regulate the frequency variations to a full extent due to the typical delay of the pitch actuator [11]. Thus, the need arises for an advanced control design with varying control policies to cope with the system's complexity, physical constraints, and the intermittent nature of wind, enabling the wind turbine to provide FCR by taking advantage of the optimal interaction between pitch and torque control.

In recent years, advanced optimal control methods such as Linear Quadratic Gaussian (LQG), fuzzy logic, and $H\infty$ have been applied in wind turbine control systems concerning the power grid integration [15–18]. Despite the robust behavior of these controllers in maximizing energy conversion, frequency regulation, or even structural load mitigation, the control performance can still be improved further, which can be attributed to the intrinsic nonlinearity of the system and/or the difficulties to incorporate physical constraints. Model-based Predictive Control (MPC) is becoming increasingly popular in wind energy applications. It possesses the inherent ability to deal with multi-input multi-output systems and constraints imposed on manipulated variables [19]. Additionally, MPC can be made robust to plant uncertainties [11] and measurement uncertainties [20]. Finally, MPC has the ability to incorporate wind speed estimation [20].

Linear MPC based on a linearized wind turbine model has been widely used because it requires less programming and computational power than scheduled MPC or nonlinear adaptive MPC. For instance, [19] claims that the implementation of a linear MPC algorithm, based on linearization along with a single operating point, can achieve a suitable performance in the entire range of wind turbine operation, as long as the underlying design is robustly made. However, the parametric uncertainties in the model and the presence of disturbances can significantly affect the underlying robustness and may degrade MPC's performance in the whole operating range [21,22].

Scheduled MPC can realize significant load mitigation and reliable power reference tracking throughout the entire operating region [23]. Soliman et al. proposed in [24] an MPC technique for controlling a variable-speed variable-pitch wind turbine that switches between multiple linear models that each are valid at different operating points. However, when designing scheduled MPC, varying operating conditions impose difficulties on a smooth switching performance, especially in the transition between partial load region and full load region where the control variable changes between torque and pitch. In [25] Ebadollahi et al. introduce a new soft-switching multiple MPC based on the gap metric and Kalman filter estimator for reduction of torque oscillation but only in the partial load region. Moreover, nonlinear MPC applications with a nonlinear optimization algorithm have become increasingly performant but are still computationally demanding. In their implementation, control actions need to be taken within a bounded time that is not always met [26]. Artificial Neural Networks offer the advantage of learning from sensory data to optimize the wind turbine's performance in stochastic conditions and fasten computing the control actions [27,28].

The purpose of this study is to improve the capability of an offshore floating wind turbine in providing FCR, based on cooperation between the torque and the pitch controller, by taking advantage of data-driven techniques and optimal predictive control. The primary reserve is achieved through a balance type control, where an absolute power set-point is chosen below the available power [7,8,29]. In this case, the turbine will produce maximum output power up to the desired power set-point and responds to the grid frequency changes by tracking the reference power through optimal performance of pitch and torque.

In this research, a 5MW offshore floating wind turbine is firstly simulated by using the Fatigue Aerodynamic Structure and Turbulence (FAST) software provided by the National Renewable Energy Laboratory (NREL) [30,31]. Next, the nonlinear approximations and linear modeling have been carried out based on the simulations' obtained datasets in a turbulent wind condition, which can strongly detail the wind turbine's nonlinear dynamics. Subsequently, a neural network-based MPC algorithm, proposed in [32], is implemented, and its control performance in providing FCR is evaluated. The proposed derivative-free optimization method uses neural networks to relax the need for an analytical model of a large-sized wind turbine, which would require the high numerical effort of computational fluid dynamics. [33].

To circumvent using nonlinear optimization methods, we have applied a linearization, based on Taylor series expansion, around the operating point such that a quadratic optimization problem can be formulated. For this purpose, the AutoRegressive with Exogenous input (ARX) model is used as a linear function of the calculated future input sequence. The calculated control inputs should satisfy the physical limitations of pitch and torque. Therefore, the determined vectors of constraints are projected onto the set of feasible solutions. Finally, a frequency profile is used to test the proposed design's effectiveness in power reference tracking through a comparative study. The simulation results confirmed that the proposed control approach has the ability to provide transient and steady-state power reference tracking and effectively improve the stabilization of the active power control with an optimal and secure operation of the wind turbine.

The article is organized as follows: The 5MW wind turbine dynamic model and the baseline control structure are discussed in section II. Section III introduces the data-driven model approximation based on the cascade Hammerstein structure using multilayer perceptron (MLP) neural networks and linear ARX underpinning the proposed MPC structure. Section IV formulates the proposed control strategy. The controller performance assessment and clarification are given in section V. Discussion and conclusions are drawn in section VI.

3.2 Wind turbine design

3.2.1 Wind turbine dynamic model

The wind energy conversion system includes wind turbine dynamics and a PMSG with a power electronic converter that subsequently converts the mechanical energy into electrical power. The aerodynamic power of the turbine rotor P_a is a function of power coefficient and wind speed.

$$P_a = \frac{1}{2}\rho\pi R^2 v_w^3 C_p(\lambda, \theta_c) \tag{3.1}$$

where R, v_w, and ρ are the blade radius, wind speed, and air density, respectively. The power coefficient $C_p(\lambda, \theta_c)$ is a function of tip speed ratio and collective pitch angle θ_c. The tip speed ratio λ is defined as the ratio of rotor speed Ω_r at the tip of blades to the wind speed $\lambda = R\Omega_r/v_w$. Figure 3.1 shows the power coefficient of the NREL 5MW offshore wind turbine as a function

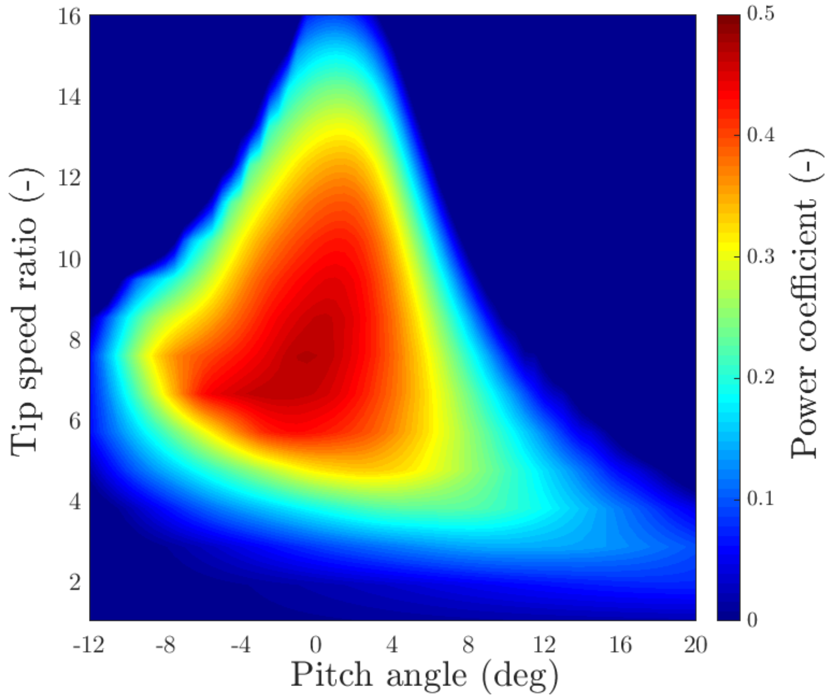

Figure 3.1: NREL 5-MW offshore wind turbine power coefficient as a function of tip speed ratio and pitch angle.

of tip speed ratio and pitch angle. The maximum power coefficient of 0.48 is achieved at the pitch angle of 0 and a tip speed ratio of 7.5.

The NREL 5-MW offshore wind turbine, with given parameters in Table 3.1, can be controlled by means of three kinds of manipulative inputs, i.e., nacelle yaw angle, pitch angle, and generator torque T_g. In this work, it is assumed that there is no changing direction in wind speed; hence the nacelle yaw angle actuator is disabled, and both torque and pitch control systems with the baseline PI controller are used to control the aerodynamic power capture and rotational speed. The dynamic equation of the wind turbine is described by

$$T_a - T_g = F\Omega_r + J\frac{d\Omega_r}{dt} \tag{3.2}$$

with J being the moment of inertia, F is the viscous friction coefficient and $T_a = \frac{P_a}{\Omega_r}$ is the mechanical torque. Furthermore, the electric output power of the generator is defined as follows:

$$P_g = \eta_g T_g \Omega_r \tag{3.3}$$

where η_g is the generator efficiency. The FAST 5-MW baseline wind turbine model is coupled to a generator and converter model implemented in Matlab/Simulink. The generator is a direct-drive PMSG, which is modeled with an equivalent scheme in the rotating reference frame, as presented in [34]. The efficiency curve is included in the model as a function of different operating points. This model offers a realistic representation of the dynamics and losses of the machine since it includes machine inductances, armature reaction effect, stator copper losses, and iron core losses. The generator control is a field orientation control, which offers direct control of the generator torque by regulating the q-axis current to a set-point value while keeping the d-axis current at zero. The power-electronic converter is not modeled up to the switching level, but an efficiency curve is included. The efficiency curve is obtained from a separate Simulink model, including both conduction and switching losses, in which the converter was modeled up to the switching level [35].

Table 3.1: NREL 5 MW Wind Turbine Parameters

Parameters	Values
Rated Power	5 MW
Rotor Orientation	Upwind
Configuration	3 Blades
Control	Variable Speed, Collective Pitch
Cut-In, Rated, Cut-Out Wind Speed	3 m/s, 11.4 m/s, 25 m/s
Cut-In, Rated Rotor Speed	6.9 rpm, 12.1 rpm
Rated Tip Speed	80 m/s

3.2.2 The baseline control design

The pitch and torque baseline controllers are designed to work under specific wind conditions. The operating mode depends on the wind speed and can be divided into four operating regions [30]. In the first two regions where the wind speed is below the rated value, the pitch angle is kept in an optimal position to extract the maximum aerodynamic power while the generator torque varies proportionally to the square of the generator speed as follows:

$$T_{\mathrm{g-ref}}(t) = K_{\mathrm{opt}}\Omega_r^2 \tag{3.4}$$

where K_{opt} is calculated by the maximum power coefficient $C_{\mathrm{p-Max}}$ curve and the optimal tip speed ratio.

$$K_{\mathrm{opt}} = \frac{1}{2}\rho\pi R^5 \frac{\mathrm{C}_{\mathrm{p-Max}}}{\lambda_{\mathrm{opt}}^3} \tag{3.5}$$

In region two, a cascaded control system is designed to control the rotational speed by regulating the generator torque. The outer PI controller is the (slow) power controller providing the reference signal to the inner current controller. The fast inner PI control loop regulates the generator current by rectifier control. A predefined lookup table determines the reference signal of the cascaded control system. The lookup table is generated from the power-speed curves obtained through simulations. The third region, known as the transition mode between the second and fourth regions, can be considered an extension of the second region. In this region, the main concern is to regulate generator speed at rated power by using pitch control. Finally, in the fourth region, where the wind speed is above the rated value, the main control objective is to regulate power capture at the rated power by means of pitch control. In this region, the constant PI gains are not adequate for effective speed control due to aerodynamic power's sensitivity to the blade pitch angle, which considerably varies during the active power control [31]. However, since pitch sensitivity and blade pitch angle are nearly linear, the gain scheduling is implemented based on the gain correction factor determined from pitch sensitivity analysis. The gain-scheduled proportional-integral (PI) pitch controller is developed at each operating point to cope with this nonlinear aerodynamic sensitivity. The blade-pitch sensitivity is calculated for the NREL 5-MW model by performing a linearization analysis in FAST.

Furthermore, to be able to provide FCR, a supplementary control loop is required to control the active power output responding to grid frequency changes. In [8], three de-loading modes, based on the torque-speed tracking controller, are presented. In this study, the first mode is used, which reserves a constant percentage of rated power, and enables the wind turbine to track the power command based on absolute de-loaded power when the wind speed is above the rated value. In this case, the turbine will produce maximum output power up to the desired power set-point. On the other hand, there would be no available reserve margin when the wind speed is below the rated value, and the wind turbine only operates in MPPT mode.

3.2.3 Wind estimation

In this article, the proposed MPC strategy uses the preview of the wind speed over the prediction horizon. The rotor inflow wind speed is simulated by TurbSim [36]. In reality, LIDAR systems are capable of scanning the incoming raw wind data and extract the wind estimation [37]. We used a data-driven approach for carrying out the short-term prediction of wind speed with data collected at 10-millisecond sample time. A Group Method of Data Handling (GMDH) is used as a semi-supervised deep learning tool that automatically self-organizes the predictive distribution of variables. GMDH is a nonlinear regression method capable of driving the best polynomial network structure to predict future values from the historical time-series [38].

3.3 Model approximation

3.3.1 Neural cascade Hammerstein model

As discussed in [39,40], the Hammerstein structure can represent the dynamics of the wind turbine by connecting the static nonlinear mapping in series with a Linear Time-Invariant (LTI) subsystem. Therefore, the nonlinear steady-state part and a linear dynamic part are defined separately. The simulated datasets for the neural approximation include the inputs of the nonlinear steady-state subsystem (wind speed, tip-speed ratio, and pitch angle), and the main outputs are the rotor torque and rotor thrust, which are given by the following equations:

$$T_a = \frac{1}{2}\rho\pi R^3 v_w^2 C_T(\lambda, \theta_c) \tag{3.6}$$

$$F_a = \frac{1}{2}\rho\pi R^2 v_w^2 C_F(\lambda, \theta_c) \tag{3.7}$$

where C_T and C_F are the torque and thrust coefficients. The cascaded structure of the Hammerstein model is depicted in Figure 3.2. The input signals are the vector of aerodynamic variables, and the wind speed is the measured disturbance, while the output signals of the consecutive networks $x_r(K)$ are known as the auxiliary variables in the Hammerstein model and can be defined as follows:

$$x_r(K) = w_0^{2,r} + \sum_{i=1}^{k^s} w_i^{2,r} \varphi(z_i^r(K)) \tag{3.8}$$

where $\varphi : \mathbb{R} \rightarrow \mathbb{R}$ is the nonlinear transfer function, K the sampling instant and $z_i^r(K)$ the sum of the input signals $u(K)$ connected to the ith node ($i = 1, , k^s$) given by

$$z_i^r(K) = w_{i,0}^{1,r} + w_{i,1}^{1,r}\theta_c(K) + w_{i,2}^{1,r}\lambda(K) + w_{i,3}^{1,r}v_w(K) \tag{3.9}$$

From (3.8) and (3.9), the following outputs of rotor torque and rotor thrust can be derived

$$x_r(K) = w_0^{2,r} + \sum_{i=1}^{k^s} w_i^{2,r} \varphi\left(\begin{array}{c} w_{i,0}^{1,r} + w_{i,1}^{1,r}\theta_c(K) \\ +w_{i,2}^{1,r}\lambda(K) + w_{i,3}^{1,r}v_w(K) \end{array}\right) \tag{3.10}$$

where i is the number of nodes in each layer, r is denoting the outputs of the neural networks (rotor torque and rotor thrust), and j is indicating the input variables, including pitch angle, tip speed ratio, and the estimation of wind speed, which is considered as measured disturbances. Weights of the first layer and second layer are denoted by $\omega_{i,j}^{1,r}$ and $\omega_i^{2,r}$.

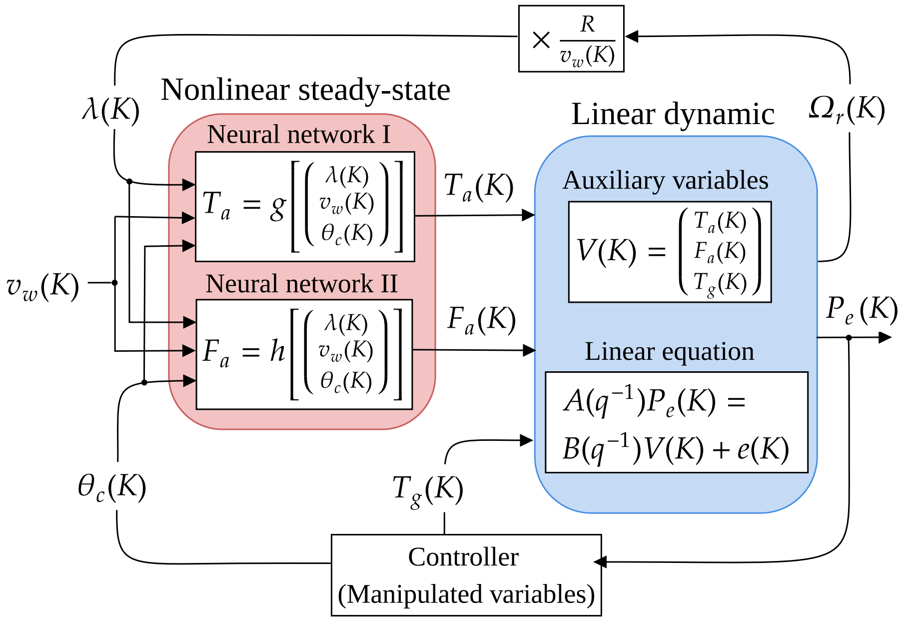

Figure 3.2: Wind turbine cascaded Hammerstein Structure.

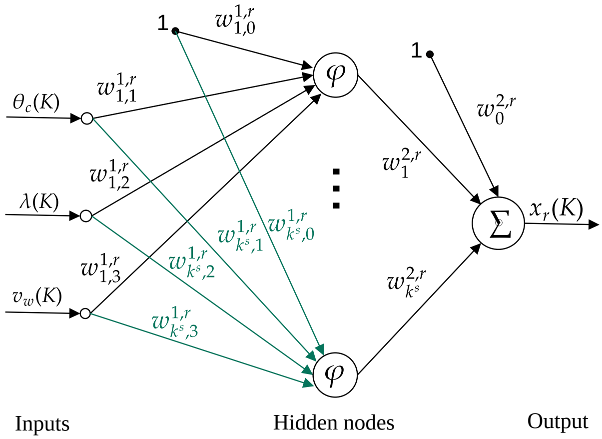

Figure 3.3: The neural network's structure used in the Hammerstein model

3.3.2 Nonlinear steady state approximation

The nonlinear part is approximated by the function $g : \mathbb{R}^{n_x} \rightarrow \mathbb{R}^{n_r}$ and $h : \mathbb{R}^{n_x} \rightarrow \mathbb{R}^{n_r}$, by using the MLP neural network with $k^s = 10$ hidden nodes in the first layer and 1 node in the second layer. The neural network's structure is shown in Figure 3.3. The neural networks have the ability to learn the sophisticated nonlinear relationships among the inputs and accurately capture the essential aerodynamic behavior of the system in turbulent wind conditions. The datasets, including the input variables and the outputs of the nonlinear dynamic part, are obtained from simulation and randomly divided into the train, validation, and test datasets. 70% of the datasets are used to train the MLPs, and 30% of the datasets are used for test and validation. The statistical results, i.e., mean square error (MSE), error mean, and error standard deviation (StD), are given in Table 3.2. The results of the nonlinear approximation for the tested dataset are depicted in Figure 3.4, showing an effective and accurate performance of the MLPs.

Table 3.2: Validation of Nonlinear Steady-state Approximation

	Rotor torque (T_a)			Rotor thrust (F_a)		
Dataset	MSE	Error Mean	Error StD	MSE	Error Mean	Error StD
Train	59.6	0.04	7.72	275.08	-0.01	16.58
Validation	64.9	0.35	8.05	258.59	0.20	16.08
Test	70.4	-0.19	8.39	303.40	-0.35	17.42
All	62.0	0.05	7.87	276.86	-0.03	16.64

3.3.3 Linear approximation

The LTI subsystem must include the aerodynamics of the drivetrain, the generator, and the rotor dynamics. Therefore, the inputs of the linear dynamic part consist of the rotor thrust, the rotor torque, and generator torque, while the electrical power is considered as the output. A linear data-based approximation approach is proposed, based on a low-order linear ARX model, which involves detecting the system structure by finding the regressors with the highest contribution to the output. Figure 3.5 illustrates the result of the linear estimation using ARX with the fourth-order polynomial function, including the mean-square error (MSE) and the final prediction error (FPE). The auxiliary variables and the equation of the linear dynamic part can be defined by (3.11) and (3.12)

$$V(K) = \begin{bmatrix} x_r(K) & T_g(K) \end{bmatrix} \tag{3.11}$$

$$A(q^{-1})p_e(K) = B(q^{-1})V(K - n_k) + e(K) \tag{3.12}$$

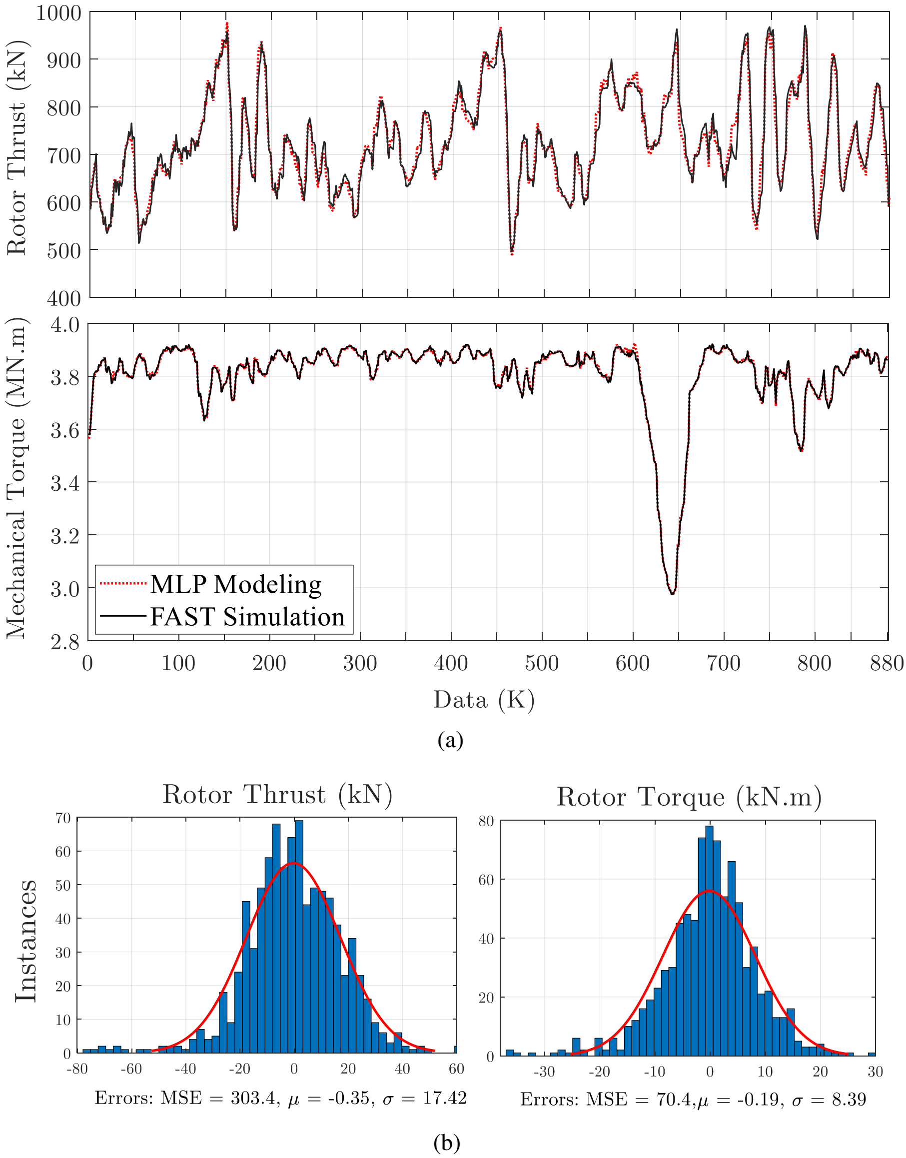

Figure 3.4: (a) Approximation of nonlinear steady-state part using MLP, (b) Histogram of errors related to the model approximation.

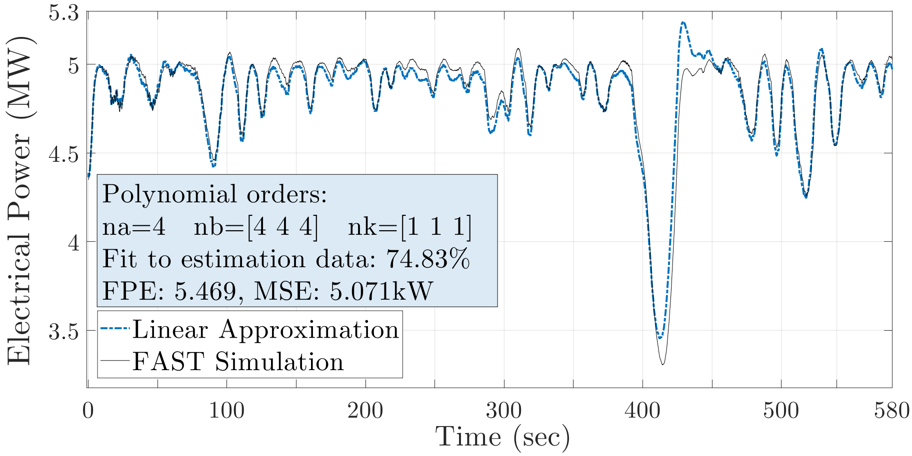

Figure 3.5: Estimation of linear dynamic part using ARX.

where the parameters of A and B consist of polynomials of the time delay operator q^{-1} defined by (3.13), n_a and n_b are the constants that define the order of the LTI subsystem dynamics. The delayed order n_k is the number of input samples that occur before the input affects the output, called the system's dead time. $e(K)$ is white-noise disturbance.

$$\begin{aligned} A(q^{-1}) &= 1 + a_1 q^{-1} + \dots + a_{n_a} q^{-n_a} \\ B(q^{-1}) &= b_1 q^{-1} + \dots + b_{n_b} q^{-n_b} \end{aligned} \tag{3.13}$$

From (3.12) and (3.13), the consecutive outputs of the Hammerstein model can be calculated as follows:

$$P_e(K) = \sum_{r=1}^{n_r} \sum_{l=1}^{n_b} b_l(K) V(K-1) - \sum_{l=1}^{n_a} a_l(K) P_e(K-1) \tag{3.14}$$

The Hammerstein model's accuracy can be improved by increasing the number of hidden layers in the neural network structure. Also, by increasing the order of the polynomial function estimating the linear dynamic behavior. In this work, the model complexity is kept as simple as possible to have a good balance between the accuracy and computational complexity of the numerical optimizer.

3.4 Proposed control strategy

3.4.1 MPC algorithm based on neural Hammerstein model

This section discusses the MPC algorithm based on the neural Hammerstein model, including predicting the outputs, the definition of the cost function, and online linearization. The general structure of the presented algorithm to control the wind turbine energy conversion system is shown in Figure 3.6. The vector of decision variables is calculated at each sampling instant by using quadratic optimization. Also, the coefficients of the linear approximation of the neural Hammerstein model are calculated numerically based on the Taylor series expansion formula and can be represented as follows:

$$\begin{aligned} a_l(K) &= a_l \\ b_l(K) &= \sum_{r=1}^{n_r} b_l \sum_{i=1}^{k^s} \omega_i^{2,r} \frac{d\varphi(z_i^r(K-l))}{dz_i^r(K-l)} \omega_{i,n}^{1,r} \end{aligned} \tag{3.15}$$

Coefficients in (3.15) are calculated for all $l = 1, \ldots, n_b$ and $n = 1, \ldots, n_x$. It is noteworthy to mention that the coefficients of the linearized model $a_l(K)$ and $b_l(K)$ depend on the current operation point. In contrast, the constants a_l and b_l denote the parameters of the linear dynamic part of the model. However, thanks to the cascaded Hammerstein structure, the linear part of the model equals the linearized model's parameter at the current operating point for sampling instant K. More details can be found in [32]. Therefore, the predicted output trajectory

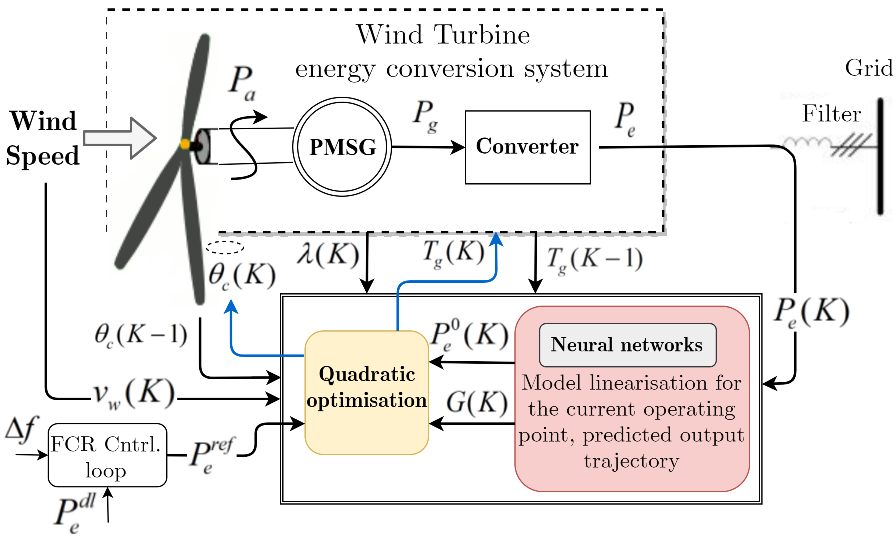

Figure 3.6: The structure of the MPC algorithm with nonlinear prediction and linearization for current operating point.

($p = 1, \ldots, N$ with prediction horizon N) can be calculated as follows:

$$
\begin{aligned}
&p_e^0(K+p|K) = \\
&\sum_{r=1}^{n_r}\sum_{l=1}^{n_b} b_l \left(w_0^{2,r} + \sum_{i=1}^{k^s} w_i^{2,r} \varphi \left(\begin{array}{c} w_{i,0}^{1,r} + w_{i,1}^{1,r}\theta_c(K-1) \\ +w_{i,2}^{1,r}\lambda_g(K-1) \\ +w_{i,3}^{1,r} v_w(K-l+p|K) \end{array} \right)\right) \\
&+\sum_{l=1}^{n_b} b_l \left(T_g(K-1)\right) - \sum_{l=1}^{n_a} a_l P_e^0(K-l+p|K)
\end{aligned}
\tag{3.16}
$$

Equation (3.16) can be obtained from (3.11), which defines the vector of axillary variables, and (3.14). The predicted electrical power is given by (3.17), which consists of two parts; the first part is a function of the currently calculated control action of pitch and torque, whereas the second part, given by (3.16), depends on the past measurements of manipulated variables and tip speed ratio.

$$\hat{P}_e(K) = G(K)\Delta u(K) + P_e^0(K) \tag{3.17}$$

where $\Delta u(K)$ is the vector of manipulated variables and is given by:

$$
\Delta u(K) = \begin{bmatrix} \Delta\theta_c(K|K) \\ \cdots \\ \Delta\theta_c(K+N_u-1|K) \\ \Delta T_g(K|K) \\ \cdots \\ \Delta T_g(K+N_u-1|K) \end{bmatrix} \tag{3.18}
$$

The dynamic matrix $G(K)$ is of dimensionality $N \times n_u N_u$ (N_u and n_u are the preset control horizon and the number of manipulated variables) consists of the step response coefficients of the linear part of the Hammerstein model, which is computed for each operating point.

3.4.2 Cost function and Constraints

As mentioned in section 3.2.2, an available power reserve is needed to be able to provide FCR. As illustrated in Figure 3.7, the generated output power needs to be curtailed to enable the wind turbine to provide an adequate amount of FCR in response to frequency deviations. A corresponding change in active power output is directly proportional to Δf, which is the difference between the nominal frequency $f_{\text{ref}} = 50\ Hz$ and the real-time frequency f_{actual}, with a droop coefficient of D. The relationship between active power changes and grid frequency deviations can be expressed as follows:

$$\Delta P = -D\Delta f \tag{3.19}$$

where Δf is the incremental change in frequency and ΔP is the incremental change in power [41]. The operating power reference P_e^{ref} of the deloaded wind turbine is calculated by:

$$P_e^{\text{ref}} = P_e^{\text{dl}} + \Delta P \tag{3.20}$$

The aim is to operate the wind turbine in a suboptimal mode through the deloaded control strategy so that a certain amount of reserve is always available to supply additional active power in case of frequency deviations in a way that the droop response will adjust the reference power.

Finally, the general MPC optimization task can be defined as the quadratic optimization problem given by (3.21). The first term of the cost function $J(K)$ drives the electrical output towards the desired power reference, and the second term seeks to minimize variations of the control inputs.

$$\begin{gathered}\min_{\substack{\Delta u(K)\\ \varepsilon^{\min}(k),\varepsilon^{\max}(k)}} \quad J(K)\\ J(K) = \left\{\begin{array}{l} \left\|P_e^{\text{ref}}(k) - G(K)\Delta u(K) - P_e^0(K)\right\|_M^2 \\ + \left\|\Delta u(K)\right\|_R^2 \\ +\rho^{\min}\left\|\varepsilon^{\min}(k)\right\|^2 + \rho^{\max}\left\|\varepsilon^{\max}(k)\right\|^2 \end{array}\right\}\end{gathered} \tag{3.21}$$

subject to

$$\begin{array}{l} \theta_c^{\min} \leq \theta_c(K) \leq \theta_c^{\max} \\ -\Delta\theta_c^{\max} \leq \Delta\theta_c(K) \leq \Delta\theta_c^{\max} \\ 0 \leq T_g(K) \leq {T_g}^{\max} \\ -\Delta {T_g}^{\max} \leq \Delta T_g(K) \leq \Delta {T_g}^{\max} \\ P_e^{\min} - \varepsilon^{\min}(k) \leq \hat{P}_e(K) \leq P_e^{\max} + \varepsilon^{\max}(k) \\ \varepsilon^{\min}(k) \geq 0, \varepsilon^{\max}(k) \geq 0 \end{array} \tag{3.22}$$

where $\theta_c^{\min}$, $\theta_c^{\max}$, $\Delta\theta_c^{\max}$, ${T_g}^{\min}$, ${T_g}^{\max}$,and $\Delta {T_g}^{\max}$ are the constraints imposed on the magnitude and the increments of the blade collective pitch angle and the generator torque respectively. In the optimization problem, to avoid the feasible set becoming empty, the hard output constraints can be violated by the factors ($\varepsilon^{\min}(k)$, $\varepsilon^{\max}(k)$), which determine the degree of constraint violation for the consecutive sampling instant over the prediction horizon and $\rho^{\min}$, $\rho^{\max} \geq 0$ are penalty coefficients. The diagonal matrices M and R are constantly and independently considered for the whole prediction and control horizons. The control parameters and the imposed constraints on the manipulated variables are given in Table 3.3.

The stability of the proposed MPC for wind turbine active power control can be analyzed in terms of practical stability. A very detailed analysis of the quadratic MPC with a discrete-time system can be found in [42] based on the definitions of the positively invariant set and the practical-Lyapunov function.

Table 3.3: Control Parameters and Constraints

Parameters	Values	Definitions
$\theta_c^{\max}$	90º	Maximum blade pitch
$\theta_c^{\min}$	0º	Minimum blade pitch
$\Delta\theta_c^{\max}$	8 º/s	Maximum blade pitch rate
$\Delta\theta_c^{\min}$	-8 º/s	Minimum pitch rate
$T_g{}^{\max}$	4,704 kNm	Rated generator torque
$\Delta T_g{}^{\max}$	150 kNm/s	Maximum generator torque rate
$\Delta T_g{}^{\min}$	-150 kNm/s	Minimum generator torque rate
N	10 s	Prediction horizon
N_u	3 s	Control horizon
M	1.48	Weighting factor
R	1.13	Weighting factor

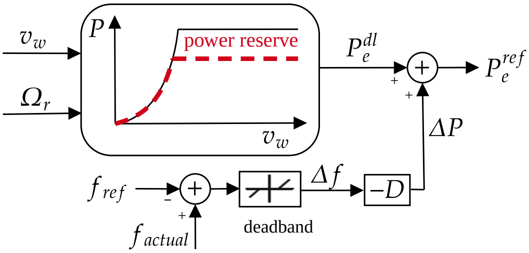

Figure 3.7: FCR control loop.

Another very detailed analysis regarding the application issues of MPC control for Hammerstein systems is presented in [43]. A short review of MPC algorithms' stability and robustness with nonlinear models, including the specific structure of the Hammerstein model, is given in [32]. It has been discussed that the stability of the proposed MPC degrades into the feasibility of the cost function optimization process, i.e., whether a solution to the optimization problem exists. It is only required to calculate a feasible solution for stability, which satisfies all the optimization problem constraints in (21). Hence, it is not essential to find the global or even a local minimum of the optimization problem at each sampling instant. Alternatively, the calculated value of the cost function necessitates being decreasing in consecutive iterations. Although this may result in a suboptimal solution and may not lead to ideal control performance, it will guarantee the close loop stability on account of choosing the finite set control principles, which can be a great advantage of the proposed strategy.

Moreover, to prevent excessive computation time, the repetitions are set to last for a fixed number of iterations. As a result, the execution of the MPC algorithm, running on an Intel(R) Core(TM) i7-7820 2.9 GHz CPU with 8 Gb

RAM, takes less than 120 milliseconds for the maximum number of iterations ensuring shorter computational time at each time step concerning the sampling time.

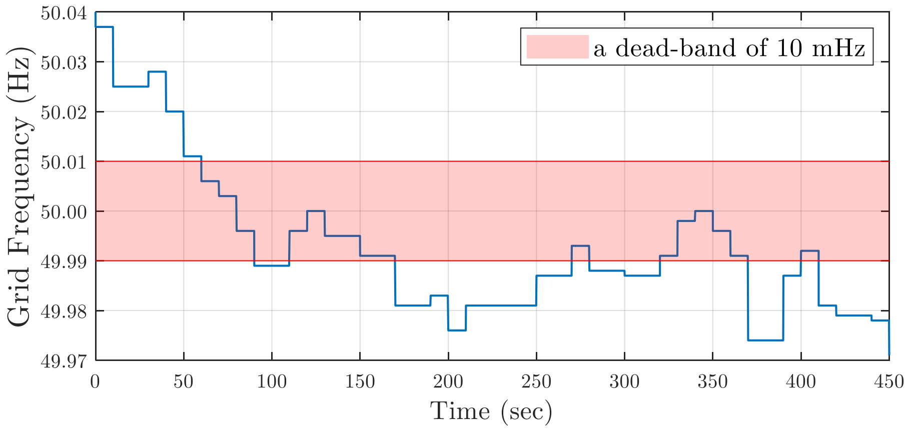

Figure 3.8: Frequency deviation for 450 seconds provided by ELIA (the Belgian transmission system operator).

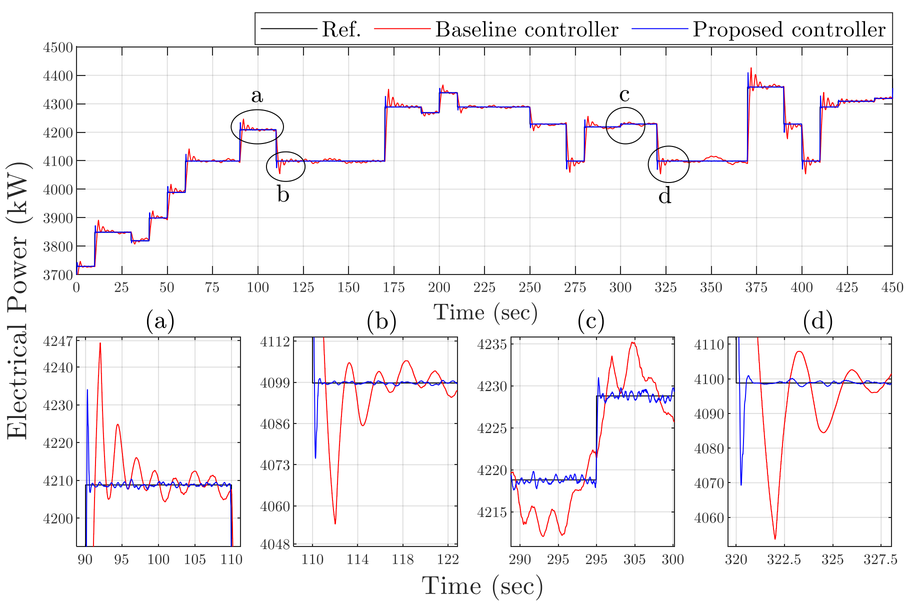

Figure 3.9: Wind turbine output power providing FCR.

3.5 Verification and results

In this section, we compare the results of the two control systems developed to achieve the active power control of the wind turbine, which is providing FCR. Their capability of tracking the desired power reference command by actuating the generator torque and the collective blade pitch angles is tested. Belgian TSO calculates the moving average of 10 seconds to examine whether at least 90% of the requested FCR volume is successfully delivered. In this study, a frequency profile from [44], as shown in Figure 3.8 with 450 seconds of the grid frequency and 10 seconds time interval, is used to test the proposed design's effectiveness in power reference tracking. Moreover, the GMDH is used to have a ten-second forecast of wind speed. Therefore, with the knowledge of the plant's dynamics, the prediction horizon is set to 10 seconds such that the dynamic model gives a good estimation. A longer prediction horizon has not been considered to avoid excessive propagation of the prediction error.

Furthermore, the simulations have been carried out for the control horizon set to 10 to 50% of the prediction horizon (1s, 2s, ..., 5s). A time interval of 3s is an acceptable response and does not pose an overly enormous computational burden. Moreover, the weighting coefficients are chosen to balance the manipulated variables' increments and the reference tracking performance. The weighting matrices are set to the values given in Table 3.3 to force the Hessian matrix to be positive-definite, in which the quadratic programming has a unique solution when no constraints are defined. In this article, the wind turbine's contribution has been set to 1 MW for a 200 mHz symmetric FCR with a predefined dead band of 10 mHz. The de-loaded power setpoint P_e^{dl} has been set to 4.1 MW. Both of the proposed and baseline controllers respond to the frequency profile shown in Figure 3.8. Extensive simulations are carried out with the wind turbine subject to realistic turbulent wind speed. A realization of turbulent wind speed is used, with 10.9% turbulence intensity (TI) and 15.3 m/s mean wind speed, to ensure that the wind turbine operates in the full load region. The results of the proposed MPC design are compared with the gain scheduling PI as the baseline controller. Figure 3.9 illustrates the performance of both controllers in power reference tracking. The Root Mean Square Error (RMSE) and Standard Deviation (StD) are commonly used to evaluate the reference tracking miss-match. The RMSE and StD values of the electrical power in the baseline strategy are 678.86 and 775.12 Watt respectively, while in the proposed strategy, these values are reduced to 36.48 and 238.77 Watt respectively. One can observe that the proposed controller ensures a stable active power response compared to the gain-scheduled PI with significantly improved tracking performance. The corresponding pitch and generator torque actions together with rotational speed are given in Figure 3.10 a-c, respectively. Due to the ability of the proposed control strategy to utilize a wind speed estima-

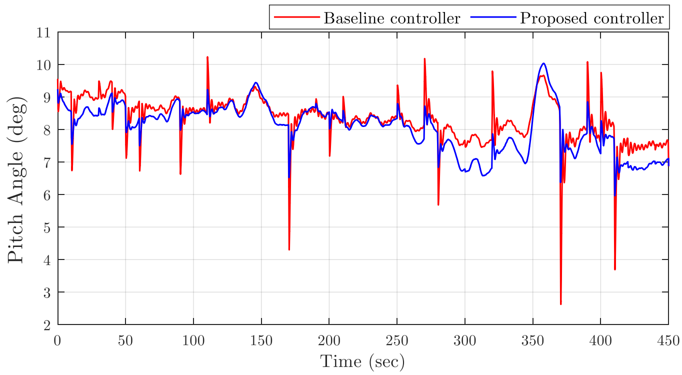

(a)

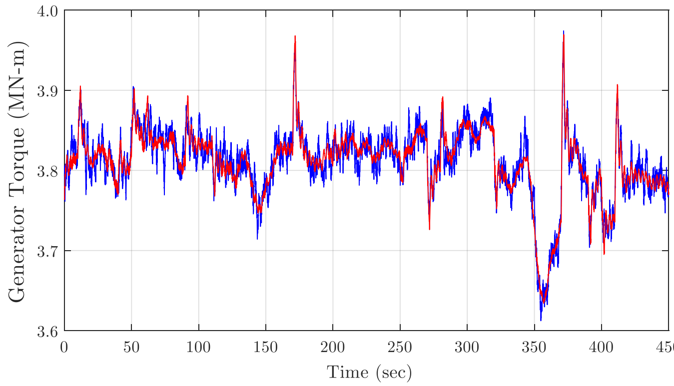

(b)

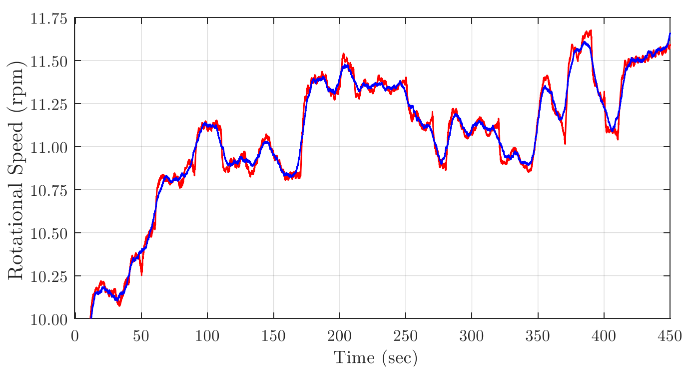

(c)

Figure 3.10: The performance of two control strategies for a wind speed of 15.3 m/s with 10% TI (a) Optimal behavior of pitch, (b) Generator torque reaction, (c) Rotational speed

.

tion and predict the optimal solution, the operation of the pitch angle is minimized. Therefore, the dynamics of the pitch system decrease as well, which may positively affect the life of the pitch mechanism and decrease maintenance costs. Also, we added a penalized soft constraint to the MPC algorithm in a way that the proposed controller will not allow the electrical power to exceed 5% of the rated value. Due to the added penalized soft constraint, the generator torque would slow down the over-speeding wind turbine varying in small perturbations. The smoother rotor speed might also offer a damping effect on the drivetrain torsional vibrations [45].

The FAST simulator is based on blade element momentum theory and includes many features such as distributed mass and stiffness of the blades and tower, dynamic wake effects, and hub and blade tip losses. In this article, the wind turbine blade and bending moments have been monitored to examine the impact of the proposed control strategy on the wind turbine structural loads. As expected, due to the minimization of the pitch action, Figure 3.11 shows a significant reduction in the amplitude of tower bending moments and an average reduction of blade root out-of-plane moment, while no meaningful reduction can be found in the blade root in-plane bending moment. Also, the proposed control design does not increase blade root edgewise and flapwise bending moments. The RMS values of the applied loads are given in Table 3.4. Although the structural load mitigation was not the main objective of the proposed control design, as a side outcome, a reduction of mechanical loads (compared with the baseline control scheme) can be achieved due to the optimization of the blade control action in response to grid frequency changes.

Table 3.4: The RMS of Applied Loads

RMS Value Bending Moment (MN.m)	Baseline Controller	Proposed Controller
Blade Root In-Plane	2.79	2.75
Blade Root Out-of-plane	8.10	7.34
Tower Base Fore-Aft	53.41	49.15
Tower Base Side-to-Side	5.15	2.40

The droop constant is increased up to 100% to monitor the proposed scheme's performance near the constraints. The test results are depicted in Figure 3.12 for a time interval of 10 seconds. The pitch and torque variability determine the optimum operating point for the MPC controller. Figure 3.12 shows the upper and lower limits of pitch and torque rate, rate, illustrating the wind turbine's degree of controllability. The optimization algorithm enables the proposed design to reach the torque rate limit at a faster rate than the

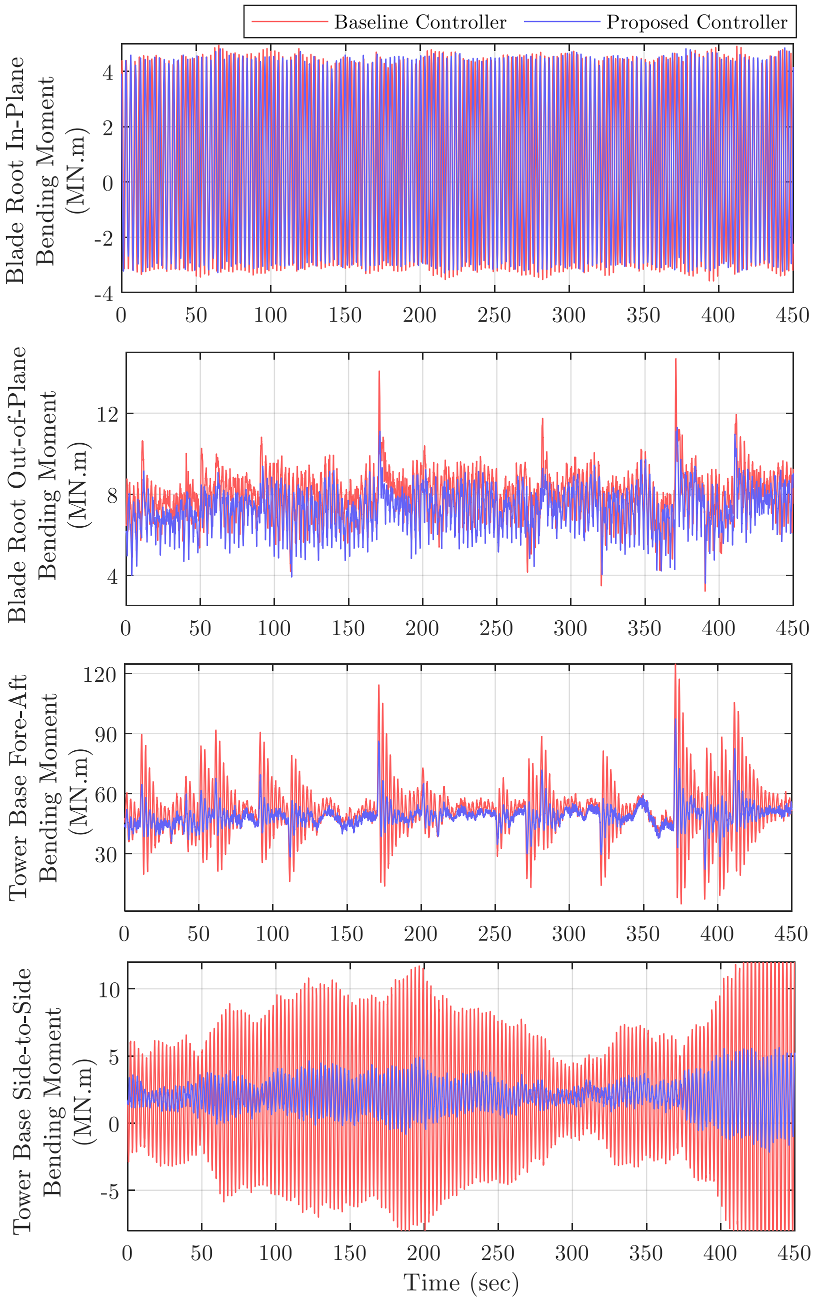

Figure 3.11: Wind turbine applied loads under baseline and proposed control strategies.

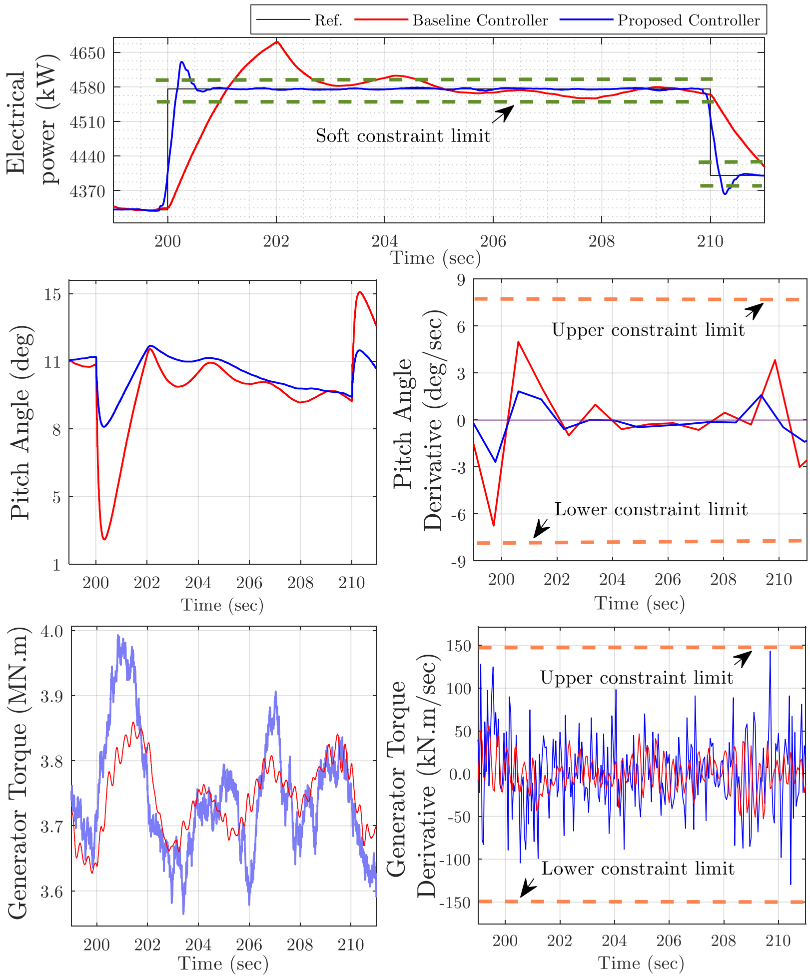

Figure 3.12: Operation around constraints

baseline controller while optimizing the pitch rate. As shown in Figure 3.12, the torque rate of the MPC at 210 seconds approaches its upper limit and supports the slow dynamics of the pitch to maintain the power reference tracking with the small overshoot. The advantage of the designed MPC is that the constraint limits can be synthetically adjusted to reduce the manipulated variables' control action or improve the power reference tracking based on the physical and operational conditions. For instance, the pitch rate constraints can be more restricted to avoid extreme actions of the pitch. Although this might result in poor reference tracking, the excessive mechanical loads will be mitigated due to pitch movement minimization.

Furthermore, the proposed MPC algorithm aims to ignore the wind disturbances that appear in periodic fluctuations of wind shear instead of trying

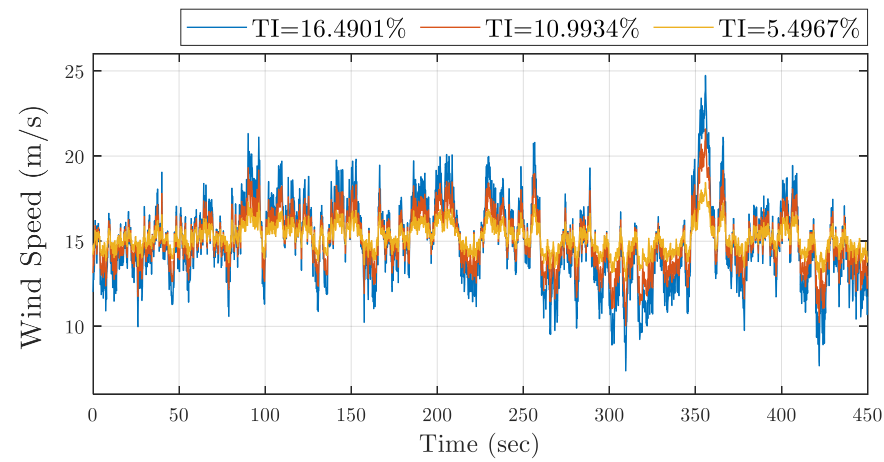

Figure 3.13: Wind speed with different turbulence intensities.

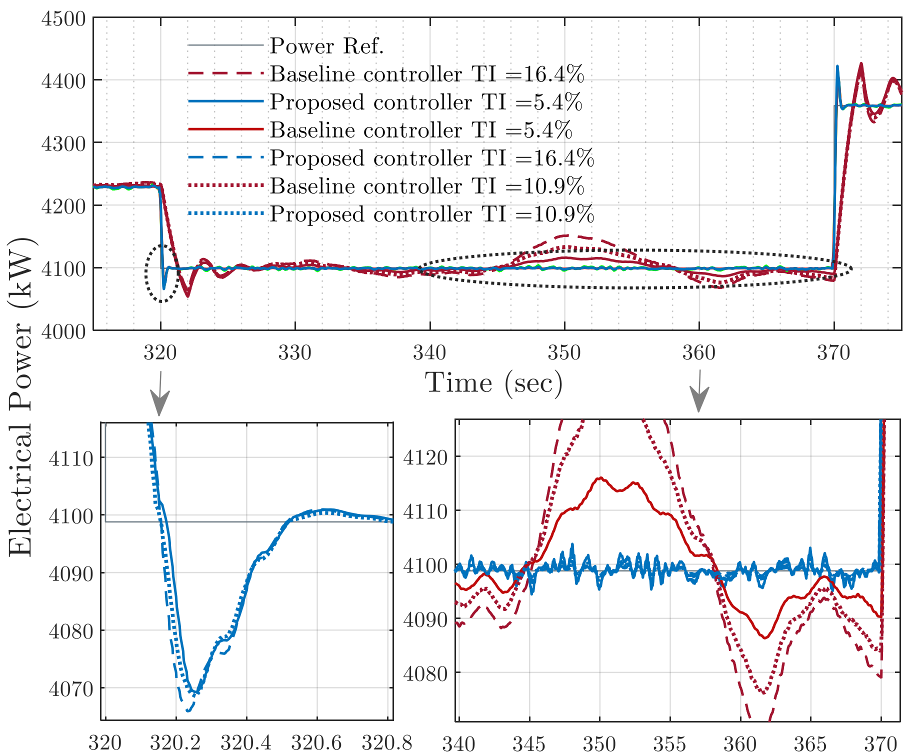

Figure 3.14: Robustness of the proposed controller in the presence of turbulent wind.

to reject them, which results in less control action in pitch and optimal torque behavior. Finally, the inflow wind speed with three different Turbulence Intensities (TI), shown in Figure 3.13, is applied to both controllers. The robust performance of the proposed controller against the variant TI is demonstrated in Figure 3.14. Another finding is that the uncertainties in wind estimation do not deteriorate the overall performance of the proposed controller, even in the presence of unexpected TI.

3.6 Conclusion and discussion

In this article, the proposed MPC enables the offshore wind turbine to provide FCR by tracking a power reference signal, given by the supplementary control loop, with an optimal pitch and torque action. The power reference tracking following a frequency disturbance has been introduced, and the robust performance of the proposed controller has been compared with the baseline controller. The proposed controller offers a stable response to frequency changes and significantly enhanced the capability of reference tracking. The stability of the control system is conducted from the system's behavior during the simulations. Moreover, the results confirm the robust performance of the proposed controller in the presence of turbulent wind. Using the neural Hammerstein model increases the accuracy of the closed-loop system approximation. The online linearization makes it possible to use a reliable quadratic programming method and eliminates the necessity of repeating nonlinear optimization at each sampling instant. The obtained results showed that the proposed approach was able to provide FCR despite the uncertainties in terms of wind speed measurements and turbulence intensity.

Contributing to frequency regulation services may cause an increase in the blade and tower mechanical loads, leading to fatigue failures, which is an economic disincentive due to lifetime reduction. On the other hand, increasing the penetration of renewable sources has led some countries, e.g., Ireland and the UK, to set specific requirements and grid codes for wind power generating units to provide ancillary services. Therefore, employing the proposed predictive control algorithm, which is able to offer the power reserve with minimized power error and mechanical loads, can be an inspiration for many wind energy operators and encourage manufacturers for further investments.

In the future of this research, more uncertainty sets such as wind gusts and the associated controller parameters that might be corrupted with contingencies could be computed offline for the different wind speed scenarios. Therefore, an online computational adjustment could be carried out to secure the system's behavior in all operating conditions.

Bibliography

[1] N. Kayedpour, A. E. Samani, J. D. De Kooning, L. Vandevelde, and G. Crevecoeur, "Model predictive control with a cascaded hammerstein neural network of a wind turbine providing frequency containment reserve," *IEEE Transactions on Energy Conversion*, vol. 37, no. 1, pp. 198–209, 2021.

[2] D.-A. Ciupăgeanu, G. Lăzăroiu, and L. Barelli, "Wind energy integration: Variability analysis and power system impact assessment," *Energy*, vol. 185, pp. 1183–1196, 2019.

[3] C. Edmunds, S. Martín-Martínez, J. Browell, E. Gómez-Lázaro, and S. Galloway, "On the participation of wind energy in response and reserve markets in Great Britain and Spain," *Renewable and Sustainable Energy Reviews*, vol. 115, p. 109360, 2019.

[4] V. Gevorgian, M. Singh, and E. Muljadi, "Variable frequency operations of an offshore wind power plant with HVDC-VSC," tech. rep., National Renewable Energy Lab.(NREL), Golden, CO (United States), 2011.

[5] S. I. Abouzeid, Y. Guo, H.-C. Zhang, and X. Ma, "Improvements in primary frequency regulation of the grid-connected variable speed wind turbine," *IET Renewable Power Generation*, vol. 13, no. 3, pp. 491–499, 2018.

[6] M. Tsili and S. Papathanassiou, "A review of grid code technical requirements for wind farms," *IET Renewable Power Generation*, vol. 3, no. 3, pp. 308–332, 2009.

[7] Z. Wu, W. Gao, T. Gao, W. Yan, H. Zhang, S. Yan, and X. Wang, "State-of-the-art review on frequency response of wind power plants in power systems," *Journal of Modern Power Systems and Clean Energy*, vol. 6, no. 1, pp. 1–16, 2018.

[8] E. Ela, V. Gevorgian, P. Fleming, Y. Zhang, M. Singh, E. Muljadi, A. Scholbrook, J. Aho, A. Buckspan, L. Pao, *et al.*, "Active power controls from wind power: Bridging the gaps," tech. rep., National Renewable Energy Lab (NREL), Golden, CO (United States), 2014.

[9] R. M. Kamel, A. Chaouachi, and K. Nagasaka, "Three control strategies to improve the microgrid transient dynamic response during isolated mode: A comparative study," *IEEE Transactions on Industrial Electronics*, vol. 60, no. 4, pp. 1314–1322, 2012.

[10] X. Tang, M. Yin, C. Shen, Y. Xu, Z. Y. Dong, and Y. Zou, "Active power control of wind turbine generators via coordinated rotor speed and pitch angle regulation," *IEEE Transactions on Sustainable Energy*, vol. 10, no. 2, pp. 822–832, 2018.

[11] H. Wang, J. Yang, Z. Chen, W. Ge, Y. Ma, Z. Xing, and L. Yang, "Model predictive control of PMSG-based wind turbines for frequency regulation in an isolated grid," *IEEE Transactions on Industry Applications*, vol. 54, no. 4, pp. 3077–3089, 2018.

[12] C. Luo, H. Banakar, B. Shen, and B.-T. Ooi, "Strategies to smooth wind power fluctuations of wind turbine generator," *IEEE Transactions on Energy Conversion*, vol. 22, no. 2, pp. 341–349, 2007.

[13] S. De Rijcke, P. Tielens, B. Rawn, D. Van Hertem, and J. Driesen, "Trading energy yield for frequency regulation: optimal control of kinetic energy in wind farms," *IEEE Transactions on Power Systems*, vol. 30, no. 5, pp. 2469–2478, 2014.

[14] H. Wang, Z. Chen, and Q. Jiang, "Optimal control method for wind farm to support temporary primary frequency control with minimised wind energy cost," *IET Renewable Power Generation*, vol. 9, no. 4, pp. 350–359, 2014.

[15] E. B. Muhando, T. Senjyu, A. Uehara, T. Funabashi, and C.-H. Kim, "LQG design for megawatt-class WECS with DFIG based on functional models' fidelity prerequisites," *IEEE Transactions on Energy Conversion*, vol. 24, no. 4, pp. 893–904, 2009.

[16] H. Bevrani and P. R. Daneshmand, "Fuzzy logic-based load-frequency control concerning high penetration of wind turbines," *IEEE Systems Journal*, vol. 6, no. 1, pp. 173–180, 2011.

[17] X. Yin, X. Tong, X. Zhao, and A. Karcanias, "Maximum power generation control of a hybrid wind turbine transmission system based on H∞ loop-shaping approach," *IEEE Transactions on Sustainable Energy*, vol. 11, no. 2, pp. 561–570, 2019.

[18] H. Camblong, I. Vechiu, A. Etxeberria, and M. Martinez, "Wind turbine mechanical stresses reduction and contribution to frequency regulation," *Control Engineering Practice*, vol. 30, pp. 140–149, 2014.

[19] L. Henriksen, *Model Predictive Control of Wind Turbines*. PhD thesis, Technical University of Denmark, 2011.

[20] M. Mirzaei, M. Soltani, N. K. Poulsen, and H. H. Niemann, “An MPC approach to individual pitch control of wind turbines using uncertain LiDAR measurements,” in *2013 European Control Conference (ECC)*, pp. 490–495, IEEE, 2013.

[21] M. Mirzaei, N. K. Poulsen, and H. H. Niemann, “Robust model predictive control of a nonlinear system with known scheduling variable and uncertain gain,” *IFAC Proceedings Volumes*, vol. 45, no. 13, pp. 616–621, 2012.

[22] M. A. Evans, M. Cannon, and B. Kouvaritakis, “Robust MPC tower damping for variable speed wind turbines,” *IEEE Transactions on Control Systems Technology*, vol. 23, no. 1, pp. 290–296, 2014.

[23] A. Kumar and K. Stol, “Scheduled model predictive control of a wind turbine,” in *47th AIAA aerospace sciences meeting including the new horizons forum and aerospace exposition*, p. 481, 2009.

[24] M. Soliman, O. Malik, and D. T. Westwick, “Multiple model predictive control for wind turbines with doubly fed induction generators,” *IEEE Transactions on Sustainable Energy*, vol. 2, no. 3, pp. 215–225, 2011.

[25] S. Ebadollahi and S. Saki, “Wind turbine torque oscillation reduction using soft switching multiple model predictive control based on the gap metric and kalman filter estimator,” *IEEE Transactions on Industrial Electronics*, vol. 65, no. 5, pp. 3890–3898, 2017.

[26] D. Schlipf, D. J. Schlipf, and M. Kühn, “Nonlinear model predictive control of wind turbines using LiDAR,” *Wind energy*, vol. 16, no. 7, pp. 1107–1129, 2013.

[27] D.-A. Ciupăgeanu, G. Lăzăroiu, V. Berbece, M. Tîrşu, and V. Galbură, “Modeling and control of a low power wind turbine,” in *2018 International Conference on Development and Application Systems (DAS)*, pp. 26–30, IEEE, 2018.

[28] A. P. Marugán, F. P. G. Márquez, J. M. P. Perez, and D. Ruiz-Hernández, “A survey of artificial neural network in wind energy systems,” *Applied energy*, vol. 228, pp. 1822–1836, 2018.

[29] J. Van de Vyver, J. D. M. De Kooning, B. Meersman, T. L. Vandoorn, and L. Vandevelde, “Optimization of constant power control of wind turbines to provide power reserves,” in *2013 48th International Universities' Power Engineering Conference (UPEC)*, IEEE, 2013.

[30] J. Jonkman, S. Butterfield, W. Musial, and G. Scott, "Definition of a 5-MW reference wind turbine for offshore system development," tech. rep., National Renewable Energy Lab (NREL), Golden, CO (United States), 2009.

[31] J. M. Jonkman, "Dynamics modeling and loads analysis of an offshore floating wind turbine," tech. rep., National Renewable Energy Lab.(NREL), Golden, CO (United States), 2007.

[32] M. Ławryńczuk, *Computationally efficient model predictive control algorithms*. Springer, 2014.

[33] L. M. Tossas and S. Leonardi, "Wind turbine modeling for computational fluid dynamics," *National Renewable Energy Laboratory (NREL), Technical Report No. NREL/SR-5000-55054*, 2013.

[34] J. D. M. De Kooning, J. Van de Vyver, B. Meersman, and L. Vandevelde, "Maximum efficiency current waveforms for a PMSM including iron losses and armature reaction," *IEEE Transactions on Industry Applications*, vol. 53, no. 4, pp. 3336–3344, 2017.

[35] J. D. M. De Kooning, T. L. Vandoorn, J. Van de Vyver, B. Meersman, and L. Vandevelde, "Displacement of the maximum power point caused by losses in wind turbine systems," *Renewable Energy*, vol. 85, pp. 273–280, 2016.

[36] B. Jonkman and M. Buhl Jr, "Turbsim user's guide, National Renewable Energy Laboratory golden," tech. rep., CO, Technical Report NREL/TP-500-39797, 2006.

[37] A. Rettenmeier, O. Bischoff, M. Hofsäß, D. Schlipf, J. Trujillo, and M. Kühn, "Wind field analyses using a nacelle-based LiDAR system," in *Proc. European Wind Energy Conference*, 2010.

[38] N. Kayedpour, A. Ebneali Samani, J. D. M. De Kooning, L. Vandevelde, and G. Crevecoeur, "A data-driven approach using deep learning time series prediction for forecasting power system variables," in *IEEE 2nd International Conference on Renewable Energy and Power Engineering*, 2019.

[39] G. Van der Veen, J.-W. van Wingerden, and M. Verhaegen, "Global identification of wind turbines using a Hammerstein identification method," *IEEE Transactions on Control Systems Technology*, vol. 21, no. 4, pp. 1471–1478, 2012.

[40] G. J. van der Veen, J.-W. van Wingerden, P. A. Fleming, A. K. Scholbrock, and M. Verhaegen, "Global data-driven modeling of wind turbines in the presence of turbulence," *Control Engineering Practice*, vol. 21, no. 4, pp. 441–454, 2013.

[41] Y.-Q. Bao and Y. Li, "On deloading control strategies of wind generators for system frequency regulation," *International Transactions on Electrical Energy Systems*, vol. 25, no. 4, pp. 623–635, 2015.

[42] R. P. Aguilera and D. E. Quevedo, "Stability analysis of quadratic MPC with a discrete input alphabet," *IEEE Transactions on Automatic Control*, vol. 58, no. 12, pp. 3190–3196, 2013.

[43] H. Bloemen, T. Van den Boom, and H. Verbruggen, "Model-based predictive control for Hammerstein systems," in *Proceedings of the 39th IEEE Conference on Decision and Control (Cat. No. 00CH37187)*, vol. 5, pp. 4963–4968, IEEE, 2000.

[44] "Elia.be, Belgian TSO providing transparency on grid data."

[45] A. D. Wright and L. Fingersh, "Advanced control design for wind turbines; part i: control design, implementation, and initial tests," tech. rep., National Renewable Energy Lab (NREL), Golden, CO (United States), 2008.

Chapter 4

Adaptive Control Strategy Supporting Varying Reserve for Wind Turbines providing FCR

The previous Chapter 3 was focused on optimally providing FCR using a data-driven MPC. The data-driven aspect was focused on accelerating the underlying optimal control problem considering the nonlinearity of the system. As seen in Figure 1.13, see also the previous chapter, an FCR control loop lets the data-driven MPC control the power reference reacting to grid frequency changes in the above-rated turbulent wind condition by considering a fixed power reserve margin. In this chapter, we dive further into the local FCR control loop that can cope with altering reserve margin in partial and full load regions, providing adaptive torque and pitch control actions. Here, we start with a low-level PI controller and show how adaptation can be implemented on wind turbines. The seamless integration of these strategies with the wind farm's supervisory control level enables a harmonized and optimized approach to control actions and FCR provision in a wide range of operating conditions, maximizing Wind farms' overall efficiency and compatibility, making them a compelling choice for sustainable energy production.

So, this chapter focuses on the implementation of adaptive deloading strategies, as presented in Section 1.3.1, with particular emphasis on addressing the second challenge discussed in Section 1.5.2. The proposed adaptive operational strategy is designed to be integrated at the local control level of wind turbines with the primary objective of providing FCR while adhering to optimal setpoints as defined in Chapter 2. These optimal setpoints, such as the varying deloading percentage ($\beta\%$), are determined at the wind farm supervisory level.

To evaluate the strategy's performance, the study considers fixed and percentage power reserve methods. Additionally, gain scheduled fuzzy-PI control is applied to ensure reliable FCR provision in turbulent wind conditions. The proposed strategy exhibits an optimal response to grid frequency changes, effectively mitigates power fluctuations, and enhances generator speed regulation.

Compared to the MPC approach presented in Chapter 2, the adaptive operational strategy in this chapter offers complementary advantages. While MPC provides a comprehensive and accurate representation of the turbine's behavior, the adaptive strategy excels in all operating regions and reserve modes. It ensures stable control even in the presence of turbulent wind speeds, making it a reliable choice for wind turbines operating in variable wind speeds, constantly switching between partial and full load regions. Furthermore, the proposed strategy is cost-effective, adaptable to various operating conditions, and can seamlessly integrate into existing pitch and torque control systems of WTs for optimal FCR provision.

In this approach, the adaptive operational strategy at the local control level of wind turbines interacts with the wind farm's supervisory control level through the decided reserve percentage $\beta\%$, deloaded rotational speed ω_i^{dl} and power $P_{w,i}^{\mathrm{dl}}$ similar to the MPC controller discussed in the previous chapter that follows the specified deloaded power $P_{w,i}^{\mathrm{dl}}$. The wind farm can achieve optimal FCR provision and enhanced performance in all operating regions by integrating the proposed control approaches discussed in Chapters 3 and 4. This integration allows for the effective coordination of control actions across the wind farm, maximizing the overall system performance.

Moreover, the study encompasses the development of an optimal and adaptive deloading strategy to support FCR provision for individual wind turbines, takes into account the unpredictable behavior of grid frequency and wind speed. The strategy involves estimating an adaptive reserve margin, utilizing short-term grid frequency predictions, to dynamically adjust the reserve margin and control setpoints within an FCR supplementary control loop. By incorporating grid frequency prediction, the adaptive deloading strategy ensures that the wind turbine efficiently responds to changes in grid frequency and wind conditions. This flexibility not only facilitates seamless FCR provision but also maintains operational efficiency by optimizing the turbine's power output in alignment with the wind farm's overall objectives.

The comprehensive and adaptive operational strategy presented in this chapter showcases its potential to significantly enhance wind turbine performance across all operating regions by providing reliable FCR. Notably, both control strategies discussed in chapter 2 and chapter 3 mutually complement each other, resulting in a powerful combined solution for wind farm control. The combination of these strategies excels in delivering reserves efficiently in all operating regions, even in the presence of turbulent wind conditions, highlighting their robustness.

Finally, the smooth incorporation of these strategies into the wind farm's supervisory control system creates a synchronized and efficient method for implementing control actions. This fusion guarantees cost-effective FCR provision and bolsters adaptability across various operational scenarios. Through collaborative coordination, these strategies synergistically enhance the wind farm's efficiency and stability, solidifying their appeal as a sustainable energy production solution.

The contents of this chapter are published in ELECTRIC POWER SYSTEMS RESEARCH [1].

An Adaptive Operational Strategy for Enhanced Provision of Frequency Containment Reserve by Wind Turbines: data-driven based power reserve adjustment

Nezmin Kayedpour, Arash E. Samani, Jeroen D. M. De Kooning, Lieven Vandevelde, and Guillaume Crevecoeur

Published in "Electric Power Systems Research", 2023

Abstract:*Due to the growing penetration of renewables, Wind Turbines (WT) are becoming increasingly crucial for grid balancing services, such as Frequency Containment Reserve (FCR). This study proposes an adaptive operational strategy that optimally accommodates the power reserve and controls the active power based on grid frequency uncertainties and stochastic wind variations. The proposed approach includes an end-to-end solution, considering fixed and percentage reserve methods, from estimating an appropriate reserve margin to the real-time computation of generator torque and pitch control setpoints in response to grid frequency variations. A real-time look-up table is incorporated to actively adjust the reserve and adapt the deloading rotor speed-power curve based on a short-term estimation of the grid frequency using a deep-learning technique. Applying the proposed strategy improves WTs' FCR contribution by at least 3.3 times reserve in MW. Moreover, adaptive fuzzy-PI pitch-torque controllers are suggested to enhance the WT dynamic response and ensure smooth provision of FCR. Simulation results of a 5MW-NREL offshore model show the improvement of the fuzzy-PI in power reference tracking, rotor speed regulation, and average studied mechanical load parameters in the range of 2.14-11.69%, 11.1%, and 8.81%, respectively, for an average of 250 kW reserve, confirming an overall improvement.*

4.1 Introduction

Wind energy conversion systems are among the most promising technologies that support a low-carbon energy system. The installed wind power capacity has grown substantially during the last couple of decades [2]. This capacity has been increased up to 837 GW by the end of 2022 [3]. Approximately 12.4% of the new capacity is installed in the last year, only 1.8% lower than 2020's record year [3]. Offshore wind energy is expected to supply around 30% of the electricity demand by 2050, representing at least 50% of the total energy mix [4]. However, extensive penetration of wind sources into the power grid seriously affects the power system's frequency stability. The primary reason for the blackout events on 9 August 2019 in the UK was the sudden decline in frequency beyond the regulation capability of system inertia [5]. The unpredictability, stochastic, and highly fluctuating nature of wind energy with less directly coupled inertia are the main reasons that result in the grid's inertia degradation consequently [6]. Therefore, system operators require to involve wind energy sources in providing ancillary services. These ancillary products can be in the form of hierarchical frequency control, including Frequency Containment Reserve (FCR), automatic Frequency Restoration Reserve (aFRR), and manual Frequency Restoration Reserve (mFRR) [7, 8]. Many Wind Turbine (WT) manufacturers have already rolled out enhanced control systems that include the functionality of inertial and frequency response [9]. However, developing methodologies to improve the capability of providing active power control and frequency regulation is an active field of research, both in academia and industry [10–13]. This article mainly focuses on the FCR provision, in which an operating reserve is required for constant containment of frequency deviations from the nominal value to maintain the power balance in the aggregate synchronous grid.

Numerous investigations have been performed to focus on the possibility of WTs participating in frequency containment reserve through active power control. In order to improve the frequency regulation capability, an available power reserve is needed for actively responding to grid frequency changes. Therefore, the WT's power output must be deloaded by specific percentages [14]. However, the deloading strategies are not yet perfectly developed for WTs in different wind speed zones and operating conditions. In [15], the operating wind speed is divided into low, medium, and high zones, and a deloading strategy for WTs is developed to perform differentiated reserve capacity allocation. The power reserve in different operating conditions can be obtained by derating/deloading the WT through the pitch controller (above-rated wind speed), lowering the torque, and operating on a suboptimal tip-speed ratio (below-rated wind speed). The realizations of deloading operation in DFIG-Based WTs, which can be done via rotor over speeding control (converter controlled) and pitch angle control (actuator controlled), are discussed in [16]. Recently, the active power control provision for Variable-Speed WTs has been studied in [10], improving the primary frequency contribution considering WT's health condition. Moreover, adaptive frequency control strategies in isolated power [17] and in a grid-connected system under power imbalance conditions [18] are studied considering wind fluctuations and power smoothing.

Furthermore, advanced control approaches such as multiple-input multiple-output Linear Quadratic Gaussian (LQG) controller and Model Predictive controller are employed to improve the frequency regulation in [19, 20]. Fuzzy Inference System (FIS)-based methods can also offer adaptive control performance, especially when an operation strategy should be applied in varying operating regions. In [21], a hybrid control method based on a Fuzzy-Proportional Integral Derivative (Fuzzy-PID) control strategy is applied for a pitch system of an offshore WT with a direct-driven Permanent Magnet Synchronous Generator (PMSG). In [22], a novel Fuzzy-Proportional-Integral (Fuzzy-PI) pitch control is proposed to improve the power adjustment, resulting in decreased fatigue loads of the tower base and the blade root by up to 21.53% in normal turbulent wind conditions and by up to 18.14% in extremely turbulent wind conditions. Recently, a fuzzy logic-based linear quadratic regulator (LQRF) control algorithm for a variable-speed variable-pitch WT was introduced in [23], which can reduce the tower vibrations by up to 12.50% and improve the power regulation by 38.93% depending on the operating region. In [24], the fuzzy logic pitch controller performance is optimized by applying a genetic algorithm.

Although the discussed control approaches can improve WTs performance in grid balancing services, as evidenced by the literature, most existing methods rely on constant deloading techniques. However, this approach may not be optimal in terms of reserved power margin and contribution to the energy market. Nevertheless, WT characteristics show that different power margins and variable deloading approaches enable wind energy conversion systems to participate optimally in frequency support. The use of a constant deloading factor may result in non-optimal operation and infeasibility for varying grid frequency scenarios. Additionally, when the frequency exceeds 50 Hz, further deloading is required, which can be disadvantageous for wind farm owners. These limitations of the constant deloading approach can be effectively addressed by varying the deloading factor based on the grid frequency to optimize the available power margin. In [25], the advantages, disadvantages, and practical uses of variable and adaptive frequency regulation methods for WTs are compared and analyzed. More recent studies, [26, 27] attempt to adjust the deloading level of the WT generations in a real-time framework. However, these adjustments and adaptive approaches are mainly according to the wind speed, regardless of the grid frequency behavior, and the activation of power reserve, which depends on a complex cooperation between renewables, thermal power units, and demand response. These existing studies also overlook the importance of adaptiveness of power reserve and adjustment of unit deloading operation in response to grid frequency stochasticity, which is crucial for improving the flexibility of FCR provision. Therefore, a lack of emphasis can be observed in the literature regarding the adaptive operation of WTs with varying power reserves for different frequency scenarios. Such an approach has the potential to optimize deloading operations and maximize wind power production. To address this issue, our study proposes a dynamic deloading strategy that operates WTs with real-time and adaptive margin estimation based on the grid frequency variations across different wind speed zones. By adopting this approach, we aim to enhance the flexibility and efficiency of FCR provision from wind power plants.

This study introduces a novel adaptive deloading scheme that utilizes an intelligent adaptation approach. It takes into account the variability of wind, the need for adapting the deloading margin in the partial load region to wind speed, and proposes an adaptive deloading method that optimizes the deloading of active power while considering grid frequency stochasticity. The suggested deloading framework is investigated for fixed and percentage reserve strategies. In the fixed reserve mode, also known as delta mode, a fixed amount of reserve is set, while in percentage reserve mode, the reserve margin corresponds to a percentage of the available wind power [9]. The reserve margin should be adequately estimated to avoid an over-deloading performance. The deloading margin can be set to the output level of WTs in a dynamic way adapting to the time-varying stochastic wind speed and grid frequency. It prevails over the dynamic trade-off concern of frequency regulation and output maximization of wind power. To do so, real-time power system frequency information that shows the balance between generation and demand should be estimated using a historical time-series data set to reflect the frequency variations and features, such as Nadir. An accurate system frequency observation is required to estimate the adequate power reserve, which will likely be activated in the next window of the prediction horizon. To address the limitations of the nonlinear deloading approach, we also suggest an adaptive look-up table that can adjust the wind turbine's rotational speed and calculate the reference deloaded power with respect to the estimated wind speed in partial and full load regions. This study further discusses an end-to-end operation strategy that enables a wind turbine coupled with a Permanent Magnet Synchronous Generator (PMSG) to provide FCR by first analyzing the power system frequency using the Group Method of Data Handling (GMDH) as a data-driven time-series prediction approach. Secondly, estimating the power reserve that can be adapted to the grid frequency variations. Thirdly, estimating the generator torque and pitch control setpoints by considering a real-time look-up table that adaptively justifies the rotor speed and electrical power operating curve considering varying wind speeds. Fourthly, employing advanced control approaches to constantly operate the WT with adaptive scheduled gains. Since the wind turbine needs to operate under varying conditions and activate different power reserves, fuzzy-PI pitch and torque controllers are designed to achieve an adaptive gain scheduling performance. Finally, comprehensive simulations are presented for different operating conditions under various scenarios of wind and frequency to evaluate the performance of the proposed end-to-end operation strategy.

This study is arranged as follows: Section II presents the 5MW WT dynamic and baseline control designs. The proposed adaptive reserve strategy and deloading methods are discussed in section III. Section IV introduces the adaptive fuzzy-PI pitch and speed control design. The controller performance assessment and clarification are given in section V. Discussion and conclusions are presented in section VI.

4.2 Wind turbine baseline control system

This work studies a 5MW NREL offshore WT model, which has a conventional variable-speed, variable blade-pitch-to-feather configuration. The baseline controller, consisting of a gain-scheduled PI, has been implemented according to the control design section introduced in [28]. The baseline control

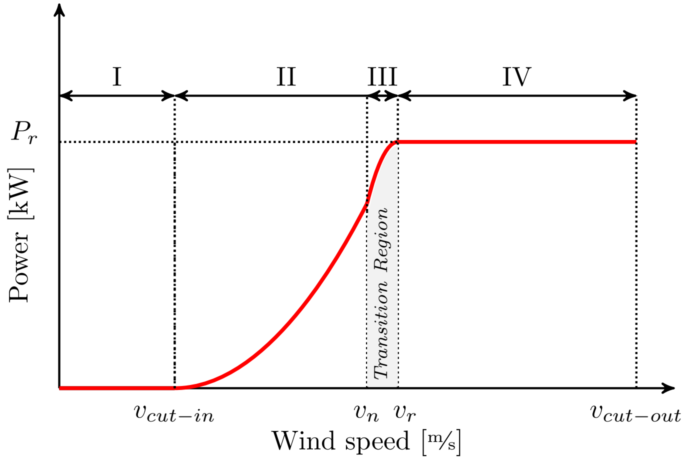

Figure 4.1: Wind turbine operating regions.

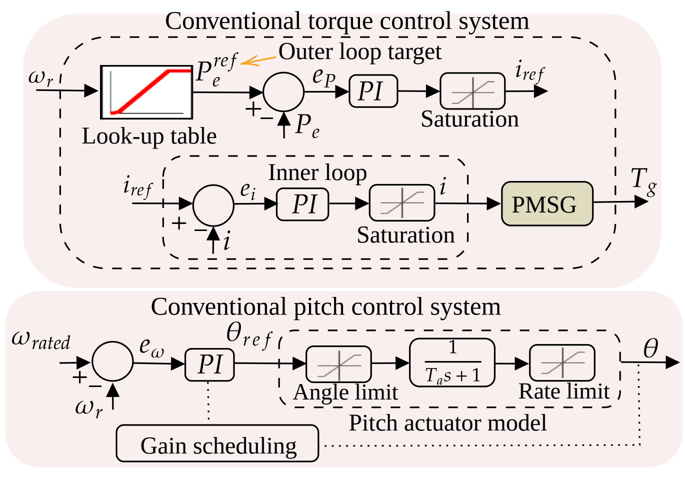

Figure 4.2: Wind turbine baseline control system.

system relies on a generator-torque controller and a full-span rotor-collective blade-pitch controller. The two essential control systems are designed to work independently in all operating regions. As shown in Figure4.1, the operating mode depends on the wind speed and can be divided into four regions. In the first two regions where the wind speed is below the rated value, the pitch angle is kept in an optimal position, and the generator-torque controller aims to maximize power capture. This is known as the Maximum Power Point Tracking (MPPT) mode. The third region, the transition zone, can be considered an extension of the second. In this region, the primary objective is to regulate generator speed at rated power using a pitch control system. The blade-pitch controller aims to regulate generator speed in the fourth region, where the wind speed is above the rated value. In general, the nonlinear relationship between aerodynamic power P_a and wind speed v can be formulated as follows:

$$P_a = \frac{1}{2}\rho R^2 \pi v^3 C_p(\lambda, \theta) \tag{4.1}$$

$$\lambda = \frac{\omega_r R}{v} \tag{4.2}$$

where C_p is the power coefficient, ρ is the air density, R is the blade length and θ is the pitch angle of the blade. λ is the tip-speed ratio, which is a function of wind and rotational speed, v, and ω_r, respectively. The mechanical torque can be formulated as follows:

$$T_m = \frac{1}{2\lambda}\rho R^3 \pi v^2 C_p(\lambda, \theta) \tag{4.3}$$

The mechanical equation of motion is given by:

$$T_m - T_g = J\frac{\mathrm{d}\omega_r}{\mathrm{d}t} + F\omega_r \tag{4.4}$$

where, J is the moment of inertia, F is the viscous friction coefficient, and T_g is the electromagnetic torque from the generator. FAST implements Blade Element Momentum (BEM) and simulates nonlinear aerodynamics. It also determines structural response to wind-inflow conditions in time, which is advantageous for developing control designs and analysis [29, 30].

In this article, the direct-drive PMSG is also modeled with an equivalent scheme in the rotating reference frame, as suggested in [31]. The machine's realistic dynamics and losses, including machine inductances, the armature reaction effect, stator winding copper losses, and iron core losses, are considered and included in the efficiency curve. The dynamic equivalent model of the PMSG can be formulated in the q,d rotating reference frame:

$$V_d = R_s I_d + L_d\frac{\mathrm{d}I_d}{\mathrm{d}t} - N_P \omega_r L_q I_q \tag{4.5}$$

$$V_q = R_s I_q + L_q \frac{dI_q}{dt} + N_P \omega_r (L_d I_d + \Phi_m) \tag{4.6}$$

where, R_s is the stator-winding resistance, L_d and L_q are the d-axis and q-axis stator-inductances, Φ_m is the flux linkage, V_d and I_d are d-axis stator voltage and current, respectively, V_q and I_q are q-axis stator voltage and current, respectively, and N_p is the pole pair number. The generator torque and electrical power can be calculated as follows:

$$T_g = \frac{3}{2} N_p \left[\Phi_m I_q + (L_d - L_q) I_d I_q \right] \tag{4.7}$$

$$P_e = \frac{3}{2} \left[V_d I_d + V_q I_q \right] \tag{4.8}$$

The generator control uses field orientation, i.e., the torque is controlled by regulating the q-axis current while maintaining the d-axis current at zero. It is out of the scope of the current work to use a full-switching model of the power-electronic converter. Instead, an efficiency curve is obtained from a separate Simulink model to represent its losses realistically. The Simulink model includes conduction and switching losses up to the switching level [32]. No additional control actions, such as startup sequences, shutdown sequences, and safety functions, are considered. The nacelle-yaw control system is not included in the analysis as it is deemed too slow to contribute to FCR activation, as this requires sufficiently fast power control. Figure 4.2 shows the baseline control system that regulates the rotational speed with an outer control loop based on power and an inner torque control loop. The outer proportional-integral (PI) controller loop is the (slow) power controller giving the reference signal to the (fast) inner control loop, regulating the generator current through control of the active rectifier. A pre-defined look-up table determines the reference signal of the cascaded control system. The look-up table is created from the power-speed curves obtained through simulations. The gain-scheduled PI pitch controller, shown in Figure 4.2, is developed at each operating point to cope with the nonlinear aerodynamic sensitivity. The blade-pitch sensitivity is calculated for the 5MW NREL turbine model by performing a linearization analysis in FAST [33].

In this study, the aerodynamic forces on the blades and the tower are obtained from AeroDyn, based on Automated Dynamic Analysis of Mechanical Systems (ADAMS), and integrated into FAST. The land-based version of the NREL 5-MW baseline is employed for offshore floating systems, which incorporates several degrees of freedom (DOF), i.e., two flapwise and one edgewise bending mode DOF for the blades, one variable generator speed DOF, one driveshaft torsional DOF, and two fore-aft and two side-to-side bending mode DOFs for the tower [33].

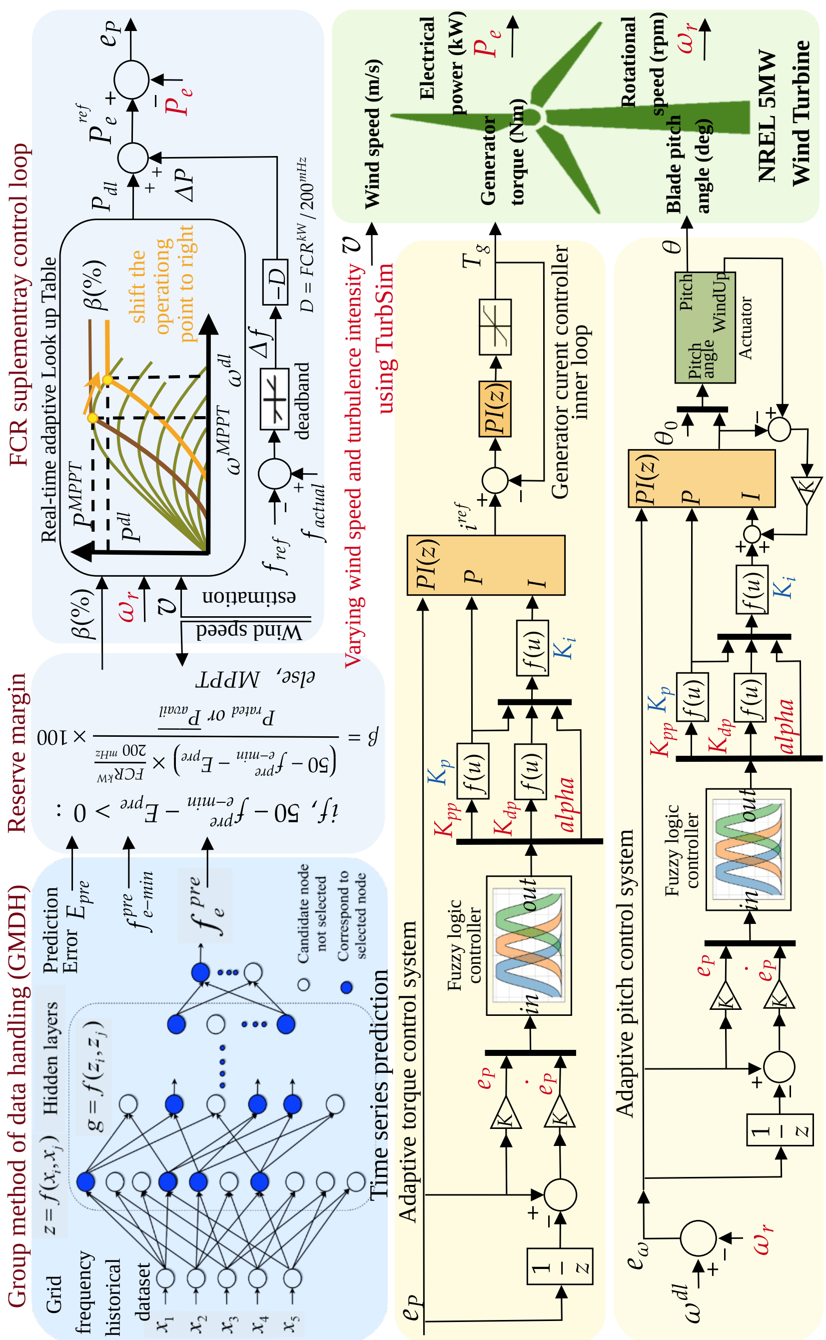

Figure 4.3: Proposed control architecture and the FCR supplementary control loop.

4.3 Methodology

The control scheme discussed in this section, shown in Figure 4.3, aims to enable WTs to operate in FCR provision in scenarios where both upward and downward products need to be supported simultaneously. Upward reserve power refers to the additional power needed to be injected into the grid when the electricity demand exceeds the available supply. This can happen when there is a sudden increase in demand or a decrease in supply due to unexpected power plant outages or transmission line faults. On the other hand, downward reserve power refers to the power that needs to be reduced or curtailed when the electricity supply exceeds the demand. This can happen when there is excess electricity production due to favorable weather conditions or the unexpected absence of large industrial loads. In such cases, the WT cannot operate in Maximum Power Point Tracking (MPPT) mode and must be deloaded. However, the control scheme allows the WT to be deloaded only to the extent necessary to satisfy the predicted request for the expected horizon. The proposed scheme estimates a varying reserve margin based on the grid frequency prediction, which provides control setpoints to the pitch and torque control setpoints. This adaptive control structure can cope with the estimated reserve and adjust the WT operation accordingly. An adaptive fuzzy gain scheduling PI control algorithm is suggested to follow the electrical power and rotational speed in all operating regions. This control algorithm adjusts the gain of the PI controller based on the operating conditions of the WT. The PI controller is responsible for regulating the electrical power output of the WT by adjusting the pitch and torque control systems.

4.3.1 Reserve margin estimation and Grid frequency prediction

To provide FCR, the measured grid frequency is converted into a frequency response, considering a deadband of 10mHz, through a corresponding change in active power output ΔP, which is proportional to grid frequency deviations Δf ($f_{\text{ref}} = 50\ Hz$) with a droop coefficient D. The promised reserve contribution must be respected once the wind farm decision-maker selects the reserve bids based on probable wind speed scenarios and FCR prices in the day-ahead reserve market. Therefore, the decided droop coefficient D should be maintained for a 200 mHz symmetric product with a frequency deviation of 40.8 to 50.2 Hz under any circumstances. However, the grid frequency distributions for the last five years, shown in Figure 4.4, indicate the grid frequency varies with less strong deviations (49.94 to 50.06 Hz). Thus, this study suggests an optimal but still conservative approach that considers an adequate reserve margin for the potential activation by adapting the reserve margin β to the lowest expected frequency drop f_{e-min}^{pre} for a short-term

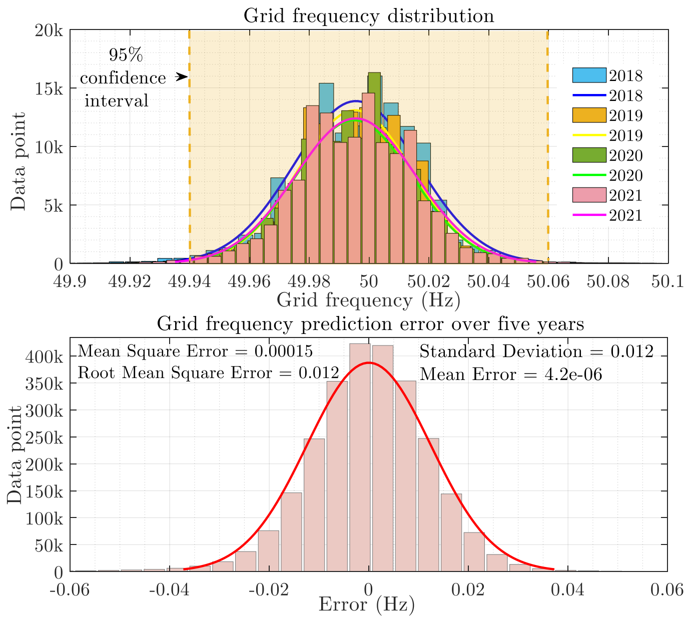

Figure 4.4: Grid frequency distribution and prediction error.

prediction horizon. Then, as indicated in Figure 4.3, the reserve margin will be decided considering f_{e-min}^{pre} and the prediction error E_{pre}.

In this study, a nonlinear regression method is employed as a semi-supervised deep learning tool that automatically self-organizes the predictive distribution of variables. GMDH can drive the best polynomial network structure to accurately reveal the approximated function and predict future values from historical datasets. The GMDH time series prediction considers a general relationship between delayed inputs and output variables in the form of polynomial functions, which is referred to as the Volterra function series or the Kolmogorov-Gabor polynomial function expressed by:

$$f_e^{pre} = a_0 + \sum_{i=1}^{m} a_i x_i + \sum_{i=1}^{m}\sum_{j=1}^{m} a_{ij} x_i x_j + \sum_{i=1}^{m}\sum_{i=1}^{m}\sum_{k=1}^{m} a_{ijk} x_i x_j x_k \tag{4.9}$$

where f_e^{pre} is the response variable that indicates grid frequency prediction, x is the vector of lagged time series to be regressed, m is the number of variables, and a_0, a_i, a_{ij} and a_{ijk} are the weighting factors. In this study, the quadratic K-G polynomial is employed in the form of:

$$z = f(x_i, x_j) = b_0 + b_1 x_i + b_2 x_j + b_3 x_j x_i + b_4 x_i^2 + b_5 x_j^2 \tag{4.10}$$

The GMDH structure can be trained to realize the relationship among the

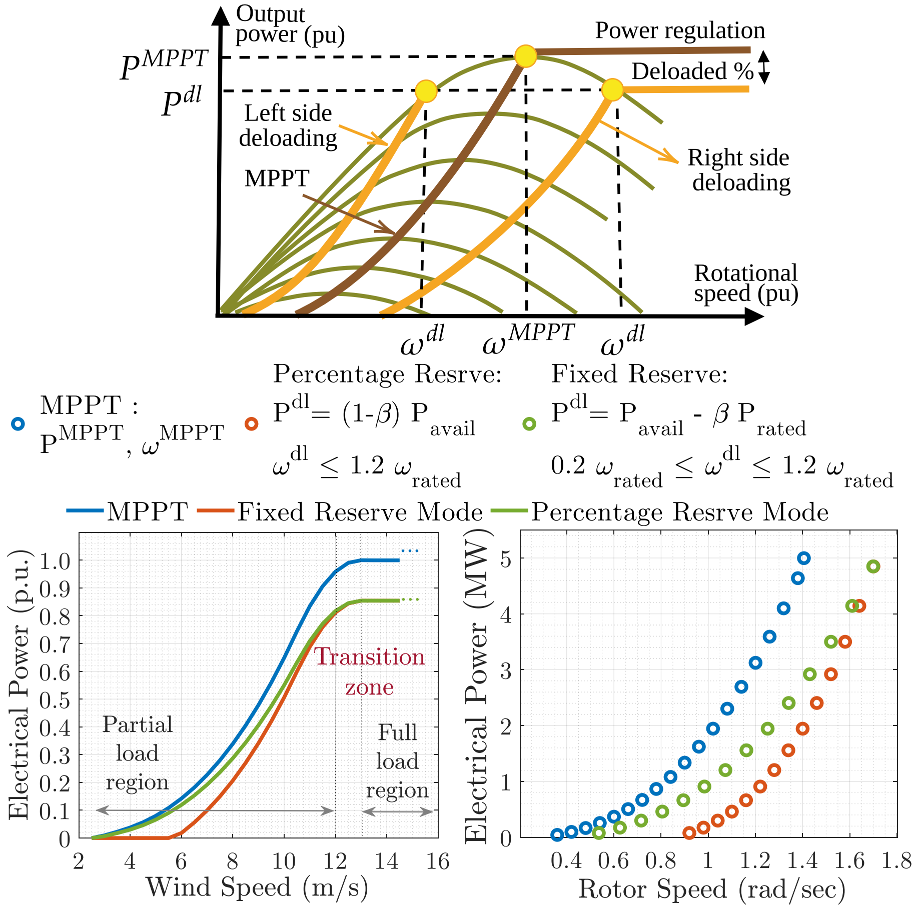

Figure 4.5: Rotor speed adjustment for WT deloading operation (top), Power curve as a function of wind speed (bottom-left), Calculation of power reference and rotational speed for deloaded operation (bottom-right).

lags with the function f. The proposed stochastic approximation algorithm is developed based on a multilayer network using various component subsets of the polynomial function for each layer. In this algorithm, the output obtained from the last layer will be set as a new input variable for the next layer. All possible tries of two independent variables are taken out of a total n inputs to conduct a regression polynomial in the form of (4.10) in the first layer. Therefore, the minimum activation function is the second-order polynomial, but it can be gradually increased to higher orders to find an architecture with optimal complexity. A threshold restricts the number of solutions using the external criterion to find the fittest structure. The parameters are estimated using the

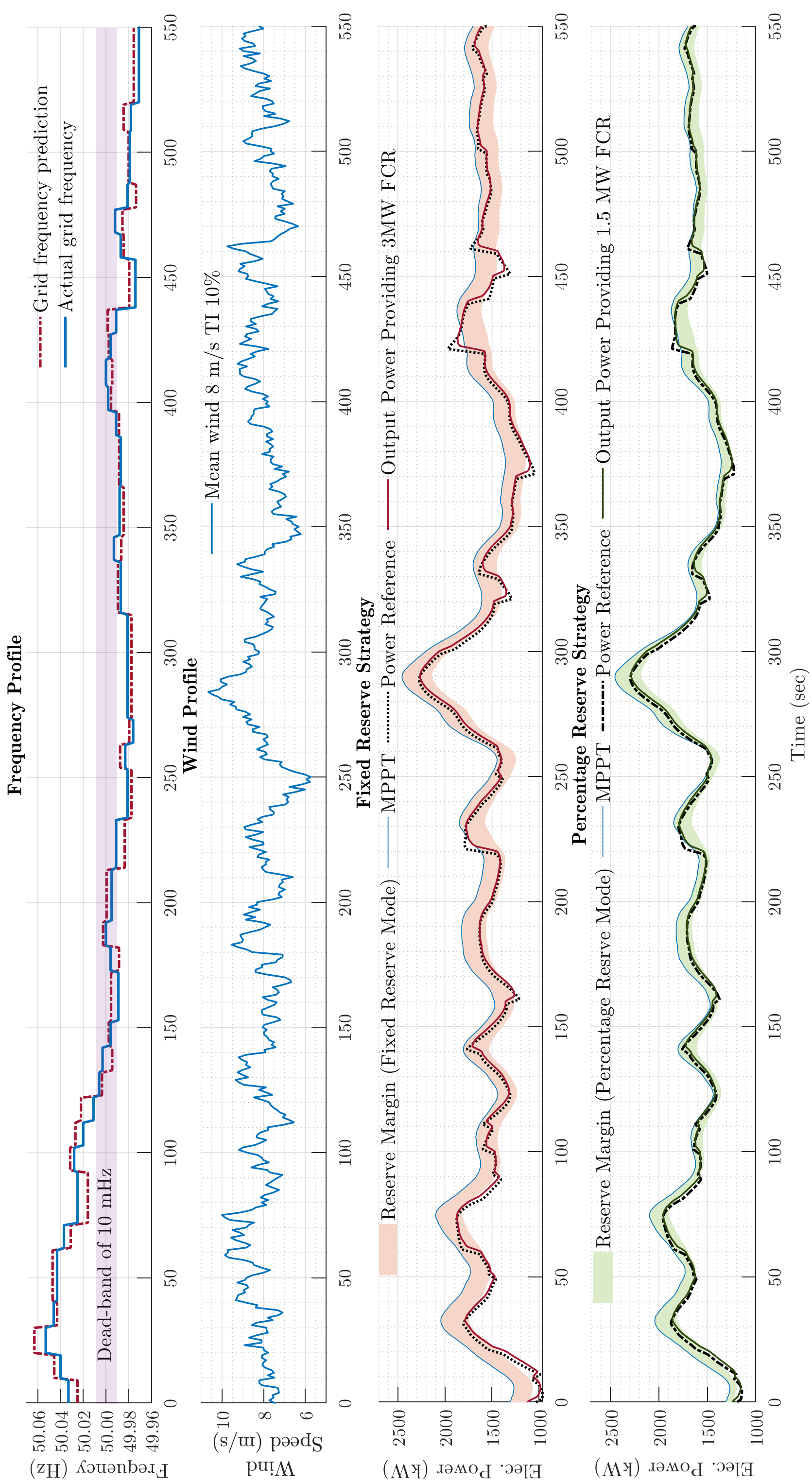

Figure 4.6: FCR provision under two power reserve strategies.

least-squares regression method over five years of the historical data set, i.e., from January 2017 to October 2022, with a 10-second sample time. The prediction horizon is set to 550s with five delayed inputs. The Mean, Root Mean Square Error (RMSE), Mean Square Error (MSE), and Standard Deviation (SD) of the absolute errors are the evaluation metrics used for assessing the results, which are given in Figure 4.4.

Although WTs usually participate in day-ahead or intra-day markets, where reserve provision must be estimated up to 24 hours or 6 hours before activation, the accurate and reliable prediction of grid frequency variations make it possible for the studied WT to contribute to the FCR market in real-time. Figure 4.4 demonstrates the distribution of grid frequency variations for 120 mHz over the last five years, taking into account a 95% confidence interval. This highlights the potential of the proposed strategy for enabling WTs to improve their FCR contribution by at least 3.3 times power reserve in a conservative and reliable manner compared to conventional approaches. This strategy involves utilizing advanced predictive algorithms that take into account upward and downward activations in different wind speeds and turbulence intensities. By incorporating the predictive model into a real-time adaptive look-up table that can actively adapt the reserve margin by adjusting the electrical power and rotational speed, WTs can participate more effectively in the regulation market and generate additional revenue streams for wind farm operators.

4.3.2 Power reserve strategies

The estimated reserve margin can be achieved through three main deloading strategies introduced in [34], e.g., derating, fixed power reserve, and percentage reserve control modes. The baseline pitch controller is the same for the three deloading types, whereas the generator-torque controller is slightly different. Figure 4.5 shows a deloaded power curve and the steady-state power capture of each power reserve strategy. The WT is able to satisfy the scheduled FCR at the above-rated wind speed. However, it is required to deload the wind turbines at below-rate wind speeds by shifting the WT operating point towards the left or right of the maximum power point [35]. Thus, a reserve margin will be created by flexibly varying the active power between P^{dl} and P^{MPPT} through changing the rotor speed between ω^{dl} and ω^{MPPT}. This study suggests shifting the operating point to the right to avoid reducing the kinetic energy, which is beneficial for inertial response [36]. Furthermore, an adaptive look-up table is incorporated into the supplementary control loop to capture and reflect the time-varying characteristic of the proposed power reserve. As Figure 4.3 serves, the deloaded power reference P^{dl} for operating under fixed and percentage reserve modes needs to be estimated by dynamically adjusting the rotational speed. In this method, the reserve margin β represents the portion of

P_{rated} (deloading percentage) that specifies the upper limit of generated power in MPPT for the fixed reserve mode. Thus, βP_{rated} represents the saving margin required to be maintained as a constant power reserve. In the percentage reserve mode, $(1-\beta)$ represents the fraction of the available power that can be captured in a way that the rest of capacity βP_{avail} can be maintained as a power reserve which is not constant and fixed but proportionally changes with the available power. Figure 4.6 shows the power output and the estimated β in both fixed and percentage strategies corresponding to the grid frequency profile by proportionally activating ΔP in a turbulent wind speed. In these simulations, the allowable range of suboptimal rotor speed ω^{dl} corresponds to P^{dl} should be respected, considering the highest permitted limit of rotational speed (determined by rated rotational speed ω_{rated}). In this case, the suboptimal rotor speed ω^{dl} is limited between $0.2\omega_{rated}$ and $1.2\omega_{rated}$ for the fixed reserve and $\omega^{dl} \leq 1.2\omega_{rated}$ for percentage reserve mode considering maximum 3 MW FCR contribution for 550s.

4.3.3 Adaptive fuzzy-PI control system

PI control is still one of the most successful controllers in industrial processes. However, it typically has poor control performance and stability issues for nonlinear and time-varying systems [37], especially when control actions are needed at different operating points with varying operating conditions and dynamic setpoints. The PI and fuzzy logic algorithm combination offers a promising alternative solution, in which gain parameters are adapted by weighting factors calculated through a fuzzy logic controller [38]. This research studies the performance of fuzzy-PI regulators for pitch and torque control systems in tracking the power reference providing FCR for varying reserve margins and deloading strategies. The derivative action is excluded as it causes an undesired reaction to high-frequency measurement noise.

Fuzzy-PI algorithm

The adaptive gain scheduling fuzzy-PI consists of three components: fuzzification, fuzzy inference system, and defuzzification. The fuzzification generally transforms definite and crisp inputs, errors, and derivative errors, into the form of a fuzzy set and a membership function. As Figure 4.7.a describes, any membership corresponds to a fuzzy set through linguistic marks, i.e., NB, NM, NS, Z, PS, PM, and PB, which stands for negative big, negative medium, negative small, zero, positive small, positive medium, and positive big, respectively [39, 40]. The FIS contains the control target derived from expert knowledge and fuzzy-based rules in the form of if-then. The transformation of the control quantity obtained by fuzzy rules into a distinct quantity is called de-

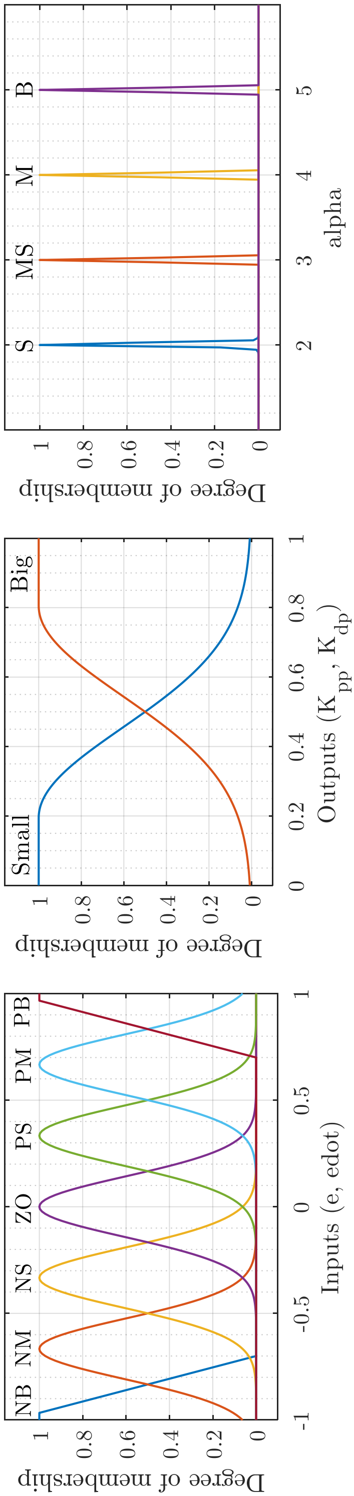

a. Membership function for error and error derivative, for K_{pp} and K_{dp}, and Singleton membership functions for α (left to right).

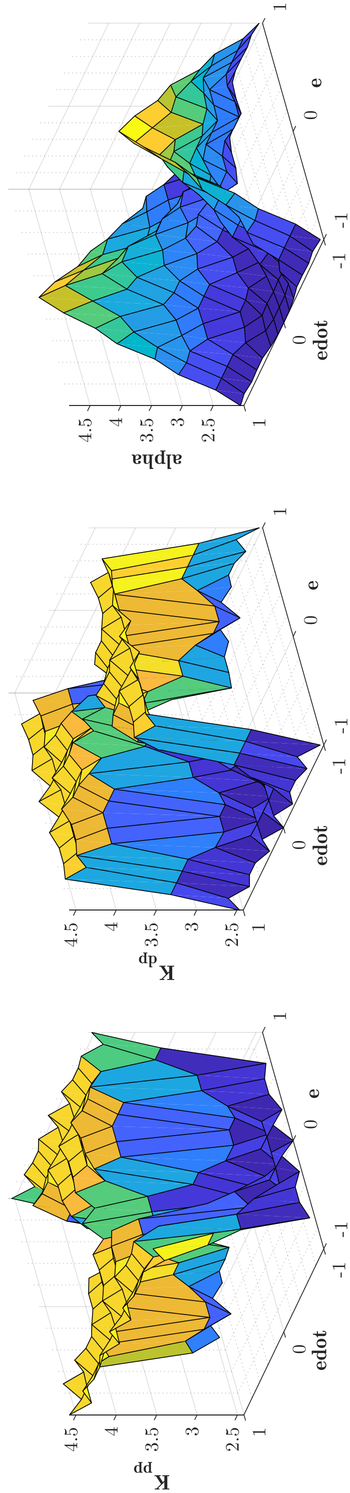

b. Surface view of the fuzzy rules

Figure 4.7: Fuzzy parameters.

fuzzification. This can be done by means of techniques such as centroid of area, a center of gravity, or the maxima method [41].

The control output and the formulation of fuzzy rules highly depend on the number of fuzzy subsets, such that choosing more fuzzy subsets would improve the control performance [40]. However, selecting a larger number of fuzzy sets would complicate the implementation due to the complex rule-making. In this article, the fuzzy subsets are divided into seven fuzzy subsets based on experience. The input membership functions for (error, derivative error) and the outputs are created with the Gaussian distribution. The singleton parameter α is created using the triangular-shaped membership functions. The membership functions and the corresponding rule surface as the function of inputs and outputs are shown in Figure 4.7.b. The corresponding rule surface shows the combination of all the membership functions and the corresponding rules that define how inputs are mapped to outputs. The rule surface determines the overall behavior of the fuzzy logic system. By defining the membership functions and fuzzy rules, the system can approximate nonlinear functions and handle uncertainty and imprecision in the input data. The ruled surface is typically defined using linguistic variables and fuzzy sets, and it can be visualized using a 3D surface plot or contour plot. The goal of the system is to map the inputs to the outputs in a way that best captures the underlying relationships between the variables. There are two sets of Gaussian membership functions to fuzzy-PI: the crisp values of the error and the error derivative. The fuzzy rules are designed to decide the output value for a given case of error and change in error.

Adaptive fuzzy-PI pitch and generator-torque controllers

Typically, the PI gains should be set to enhance the system's response speed and improve response accuracy. However, an excessive proportional parameter causes overshoot and system instability. Moreover, the model characteristics change dynamically and drive the system to different operation points. Therefore, an online adaptive gain scheduling PI is necessary for providing FCR due to the system's nonlinearity and the varying operational conditions. When providing FCR, the adaptive proportional and integral gains should be significant enough to respond quickly to the changes in the setpoint (when the error is significant). Then, after the power reference changes in reaction to the grid frequency (when the steady-state approaches), the proportional gain can decrease enough to ensure the system stability and avoid excessive overshoots, which negatively impact the mechanical loads. The following continuous transfer function can describe the PID controller:

$$G_c(s) = K_p \left(1 + \frac{1}{T_i s} + T_d s\right) \tag{4.11}$$

where K_p is a proportional gain. T_i and T_d are the integral and derivative time constants. The PI controller can also be defined in discrete time as follows:

$$u(k) = u(k-1) + K_p \Delta e(k) + K_i e(k) \tag{4.12}$$

The control signals $u(k)$ is determined by knowing the error $e(k)$ between the reference signal and the output of the plant, the change of error that discretely specified as $\Delta e(k) = e(k) - e(k-1)$, and K_p and K_i represent the proportional and integral gains respectively. Although the derivative gain is not considered in this article due to high-frequency measurement noise, it has been calculated since it is required to obtain the integral gain. As shown in Figure 4.3, the fuzzy inference system has two inputs ($e(k)$,$\Delta e(k)$) and two outputs (K_{pp},K_{dp}) that are within the predefined ranges $[K_{p,\min}, K_{p,\max}]$ and $[K_{d,\min}, K_{d,\max}]$ respectively. The fuzzy outputs are calculated using the normalization method, given in [42], as follows:

$$K_{pp} = (K_p - K_{p,\min})/(K_{p,\max} - K_{p,\min}) \tag{4.13}$$

$$K_{dp} = (K_d - K_{d,\min})/(K_{d,\max} - K_{d,\min}) \tag{4.14}$$

where K_{pp} and K_{dp} are defined based on the fuzzy rules. These are defined in the form of IF-THEN, introduced by [42], for gain scheduling, and can be formulated as follows:

$$\text{If} \quad \begin{array}{c} e \text{ is } A_i \\ \text{and} \\ \Delta e \; is \; B_i \end{array}, \quad \text{Then} \quad \begin{array}{c} K_{pp} \text{ is } C_i, \\ k_{dp} \text{ is } D_i, \\ \text{and} \\ \alpha = \alpha_i \end{array} \tag{4.15}$$

where A_i, B_i, C_i and D_i are fuzzy sets and α_i is a constant. The membership functions (MF) of these fuzzy sets for $e(k)$ and $\Delta e(k)$ are shown in Figure 4.7.a. Trapezoidal membership functions are used for (NB) and (PB), and Gaussian membership functions with the means of (-0.67,-0.33,0,0.33,0.67) and the same standard deviation of 0.14 are used for (NM, NS, ZO, PS, and PM). The grade of the membership function μ for these linguistic levels are defined as follows:

$$\begin{cases} \mu_{\mathrm{NB}}(x) = \begin{cases} 0, & x > -0.7 \\ \frac{0.97+x}{0.27}, & -0.97 \leqslant x \leqslant -0.7 \\ 1, & x < -0.97 \end{cases} \\ \mu_{\mathrm{PB}}(x) = \begin{cases} 0, & x < 0.7 \\ \frac{x-0.97}{0.27}, & 0.7 \leqslant x \leqslant 0.97 \\ 1, & x < 0.97 \end{cases} \end{cases} \tag{4.16}$$

$$
\begin{cases}
\mu_{\mathrm{NM}}(x) = e^{-\frac{(x+0.67)^2}{0.04}}, & x \in \mathbb{R} \\
\mu_{\mathrm{NS}}(x) = e^{-\frac{(x+0.33)^2}{0.04}}, & x \in \mathbb{R} \\
\mu_{\mathrm{ZO}}(x) = e^{-\frac{x^2}{0.04}}, & x \in \mathbb{R} \\
\mu_{\mathrm{PS}}(x) = e^{-\frac{(x-0.33)^2}{0.04}}, & x \in \mathbb{R} \\
\mu_{\mathrm{PM}}(x) = e^{-\frac{(x-0.67)^2}{0.04}}, & x \in \mathbb{R}
\end{cases}
\tag{4.17}
$$

The fuzzy sets C_i, and D_i can be specified as either Big or Small by combining two Gaussian membership functions (gauss2mf in Matlab), also known as the two-sided Gaussian composite membership function, which is shown in Figure 4.7. The grade of these membership functions are expressed as follows:

$$
\begin{aligned}
&\mu_{\mathrm{Small}}(x) = \mu_{\mathrm{Small-Left}}(x) \cdot \mu_{\mathrm{Small-Right}}(x) \\
&\qquad \begin{cases}
\mu_{\mathrm{Small-Left}}(x) = e^{-\frac{(x+0.195)^2}{0.135}}, & x \leqslant -0.195 \\
\mu_{\mathrm{Small-Right}}(x) = 1 - e^{-\frac{(x-0.195)^2}{0.135}}, & x \leqslant 0.195
\end{cases}
\end{aligned}
\tag{4.18}
$$

$$
\begin{aligned}
&\mu_{\mathrm{Big}}(x) = \mu_{\mathrm{Big-Left}}(x) \cdot \mu_{\mathrm{Big-Right}}(x) \\
&\qquad \begin{cases}
\mu_{\mathrm{Big-Left}}(x) = e^{-\frac{(x-0.8)^2}{0.135}}, & x \leqslant 0.8 \\
\mu_{\mathrm{Big-Right}}(x) = 1 - e^{-\frac{(x-1.195)^2}{0.135}}, & x \leqslant 1.195
\end{cases}
\end{aligned}
\tag{4.19}
$$

The proportional, derivative, and integral gains are given in (4.20), (4.21), and (4.22) and are determined using the method described in [42], which is based on the Ziegler-Nichols tuning technique.

$$K_p = K_{pp}(K_{p,\max} - K_{p,\min}) + K_{p,\min} \tag{4.20}$$

$$K_d = K_{dp}(K_{d,\max} - K_{d,\min}) + K_{d,\min} \tag{4.21}$$

$$K_i = \frac{{K_p}^2}{\alpha K_d} \quad \left(\alpha = \frac{T_i}{T_d}\right) \tag{4.22}$$

Relying on large-scale practices, the ranges of K_p and K_d are given as:

$$
\begin{aligned}
K_{p,\min} &= 0.32K_u \quad, \quad K_{p,\max} = 0.6K_u \\
K_{d,\min} &= 0.32K_uT_u \quad, \quad K_{d,\max} = 0.6K_uT_u
\end{aligned}
\tag{4.23}
$$

where K_u and T_u are the gain and the period of oscillation that are measured when the stability limit is reached under ultimate P-control, and the controller output would oscillate with a constant amplitude.

The values of K_u and T_u are estimated in uniform wind conditions. The gains for the pitch and generator-torque controller are set as 8.00 and 4.50, respectively. For the pitch controller, 10.67 and 5.06 are taken as oscillation periods. Note that α is a constant described by the singleton membership function and has an integer value in the range from 2 to 5 [42]. Figure 4.3 shows the implementation of the proposed fuzzy controller. Based on the values of the error and the change in error inputs of the pitch and electrical power, the fuzzy inference system determines the values of the proportional and integral gains. The output of the speed controller is the current reference of the generator. The proposed nonlinear adaptive fuzzy-PI gains change continuously to optimally track the reference signals, which vary rapidly due to the wind speed and grid frequency changes.

4.4 Simulation results

4.4.1 Control performance

In this section, the performance of the adaptive power reserve provision is evaluated. It also compares the adaptive gain scheduled fuzzy-PI with the baseline controller under the fixed and percentage reserve mode strategies. The simulations have been carried out in partial and full load regions under turbulent wind conditions to challenge the robustness of the proposed controller. The wind speed profile is generated based on the Von Karman model, using the scaling parameter from the standard IEC 61400-1, edition 3 [43]. Furthermore, a grid frequency deviation profile provided by the Belgian transmission system operator (Elia) [44] is used, which activates upward and downward regulations and lets the WT power reserve be adjusted based on the proposed method in 4.3.

Partial load region

For the simulations in the partial load region, the WT is exposed to an 8 m/s mean wind speed with 10% Turbulence Intensity (TI). Figure 4.8.a shows the activation of the power reserve in the partial load region. The proposed controller is able to track the power reference signal under both reserve strategies and activate FCR with optimal deloading reserve. The simulation time is considered 550s to better compare the controllers. The Root Mean Square Error (RMSE) of the electrical power is calculated as a performance criterion. For the baseline controller under the fixed mode strategy and percentage mode strategy, the RMSE is 50.30 and 32.53 kW, respectively. At the same time, this

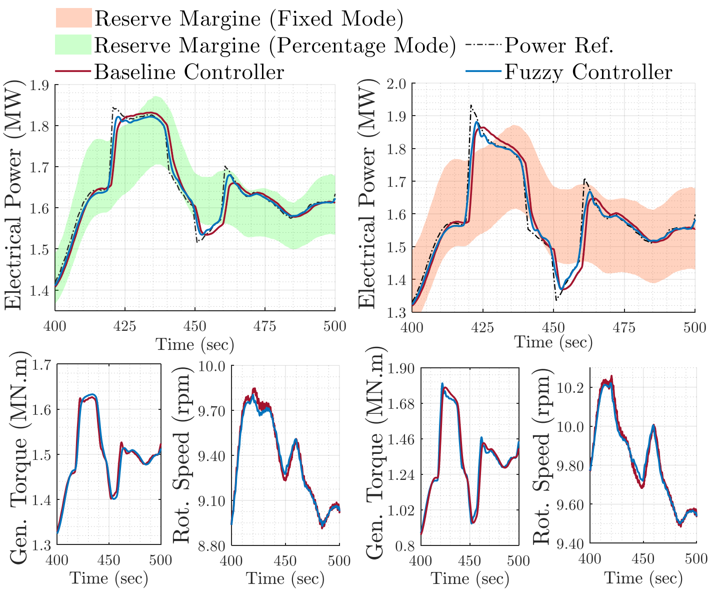

a. Performance of the proposed controller in power reference tracking and controlling generator torque and rotational speed.

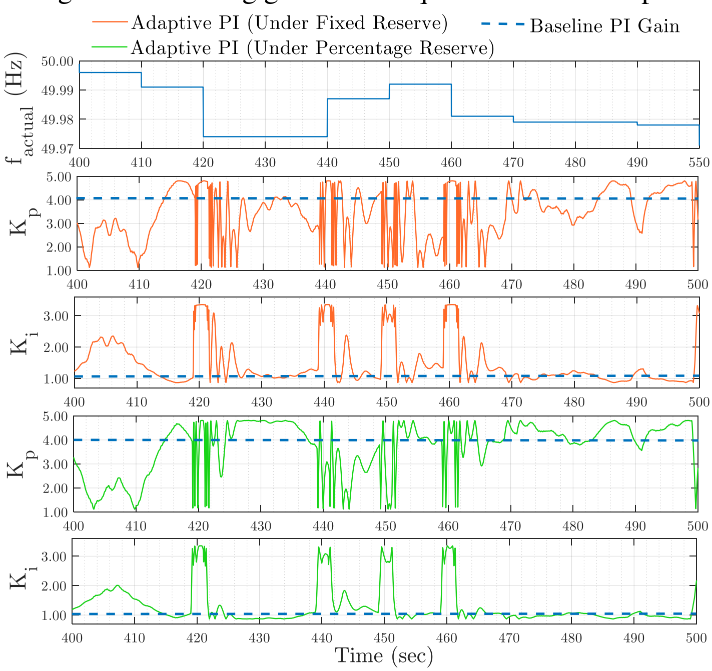

b. Adaptive fuzzy-PI gains (generator torque) versus baseline gains.

Figure 4.8: Activation of FCR in below-rated wind speed.

parameter is reduced to 21.08 and 14.18 kW, respectively, by using the fuzzy-PI controller. As the main control input, the generator torque and the rotational speed are monitored for all the abovementioned cases. The proposed controller has a fast and adequate response while giving smoother rotational speed with small oscillation damping. In the simulation, the estimated power reserve is adapted to a maximum of 5% of the available wind power for both strategies. However, due to the inertia of the rotating mass, it can be seen around the time of 425s that the electrical power for a short duration can react up to 7.5% of the total power.

Moreover, Figure 4.8.b shows the adaptive proportional and integral gains of the generator-torque controller delivered by the fuzzy algorithm for a simulation of 100s (between 400s to 500s) following both reserves strategies and the turbulent wind condition. Figure 4.8.b depicts that when the grid frequency changes, the fuzzy proportional and integral gains are increased adaptively to reach and recompense the new operating point that has been changed due to the new power reference set point provided by the supplementary control loop. The proposed controller's adaptiveness feature would let the generator torque change adequately and fast without causing the rotor to overspend.

Full load region

For wind speeds above the rated value, a derating control strategy is implemented in which the turbine will produce maximum power up to the desired power setpoint. In these simulations, an absolute power setpoint (maximum 95% of the rated power) is estimated to have a marginal reserve of a maximum of 250 kW for tracking the power signal, which proportionally corresponds to grid frequency changes. When the speed reaches the rated value, both percentage and reserve strategies can easily switch to the derating mode due to the constant rotational speed control. Figure 4.9.a illustrates the WT power reference tracking performance of the baseline and proposed fuzzy-PI controller in the above-rated wind speed, responding to the grid frequency profile that is already shown in Figure 4.6. The RMSE of the baseline controller is 25.93 kW, and this value is reduced to 20.58 kW when applying adaptive fuzzy-PI, which confirms that the proposed controller improves the control performance. Moreover, Figure 4.9.b depicts the pitch and generator torque behavior along with an improvement in rotor speed regulation in the case of employing the adaptive fuzzy-PI. The calculated RMSEs for the rotational speed under the proposed and baseline control strategies are 0.49 rpm and 0.8 rpm, respectively.

The aerodynamic power sensitivity to the collective blade pitch angle, $\delta P/\delta\theta$, is an aerodynamic property of the rotor that depends on the wind speed, rotor speed, and blade-pitch angle. This study calculates pitch sensitivity based on a linearization analysis in FAST with AeroDyn for the NREL offshore

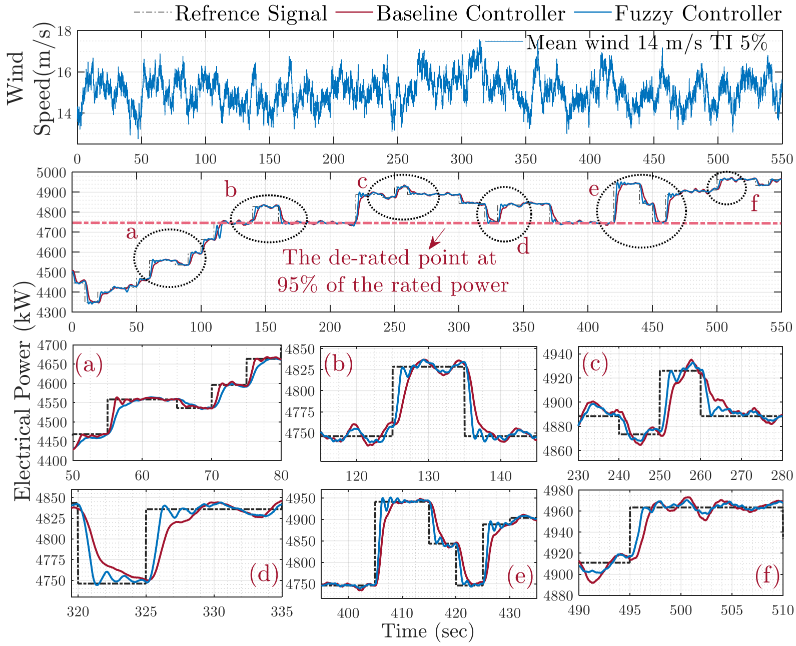

a. Power reference tracking of the proposed control system.

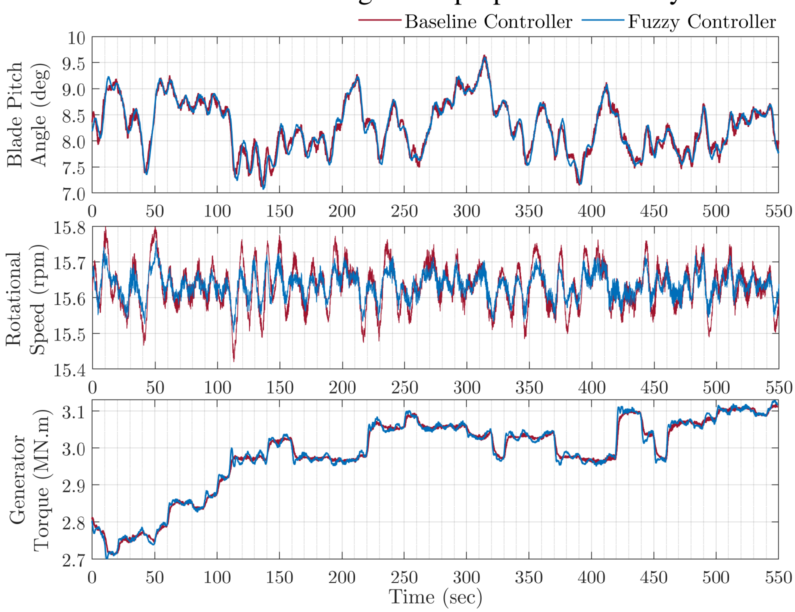

b. Performance of the pitch and generator torque and rotational speed of the proposed control system.

Figure 4.9: Activation of FCR in above-rated wind speed.

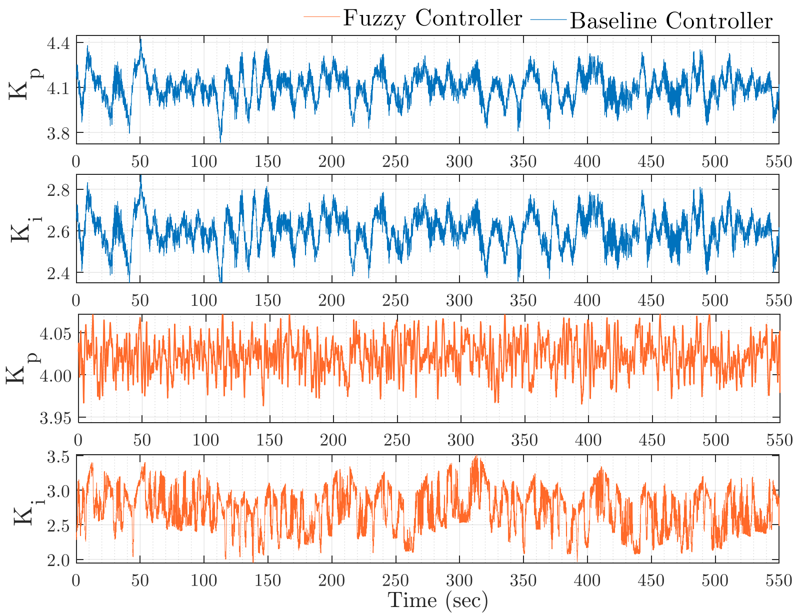

a. The pitch control system, adaptive fuzzy-PI gains versus baseline gains.

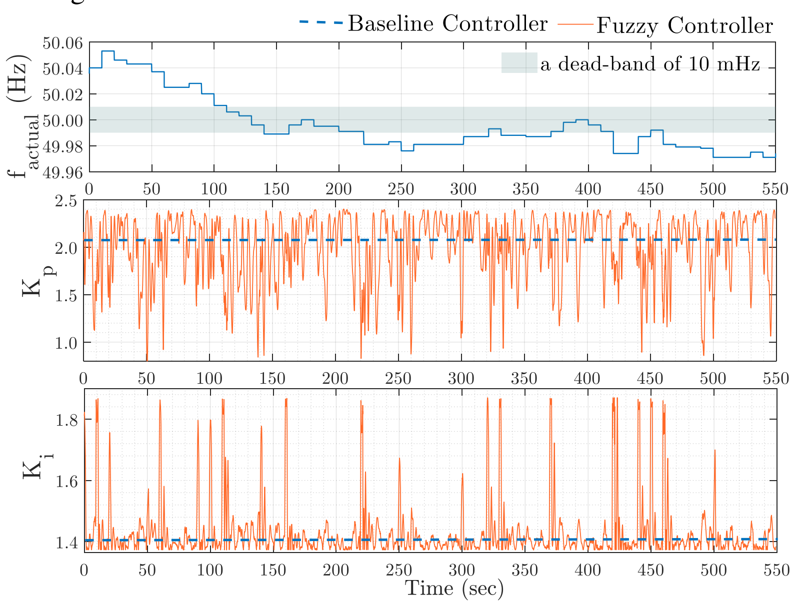

b. Generator torque, adaptive fuzzy-PI gains versus baseline gains.

Figure 4.10: Baseline and fuzzy controller gains in above-rated wind speed.

5MW WT baseline. The gain schedule PI as a baseline pitch controller is developed as suggested in [28]. The drivetrain gain and negative damping from the generator-torque controller in WT pitch control systems have been shown to have relatively small effects on the overall system behavior compared to other factors, such as wind speed and blade pitch angle sensitivity [45]. This is due to the fact that the drivetrain gain represents a minor source of system dynamics, and the negative damping term is typically small and can be compensated by the adaptiveness that the generator-torque PI controller can offer. Therefore, the PI gains are calculated by knowing the recommended response characteristics along with the gain-correction factor. However, in the proposed fuzzy approach, no pitch sensitivity is included. Instead, an improved adaptation of control gains is offered that only considers the speed tracking error and the rate of this error. On the other hand, the torque control system will be involved in FCR provision in all operating regions.

The power reference in the above-rated wind speed will be calculated through the supplementary control loop given in section 4.3. In the control scheme discussed, the de-loaded power reference P_{dl} is set to a fraction of the nominal power at rated wind speed P_{rated}, where the fraction β can vary between 0 and 1. In fact, the de-loaded power reference should be set to a maximum derated margin, which is determined based on a prediction of the grid frequency. This ensures that the power output of the wind turbine remains within acceptable limits while also maximizing the energy yield from the wind. The value of β determines the amount of power reduction required to provide the necessary downward reserve power while still maintaining the stability of the WT. In the simulations performed in this study, the maximum value of β considered was 0.05. This corresponds to a power reduction of 5% of the nominal power at rated wind speed. The value of β was chosen based on the estimated maximum expected deviation in the grid frequency profile, which was Δf_{max} = 43mHz in this study. The value of β can be adjusted for the specific amount of the FCR provision, which should be decided in the reserve market considering the electricity and reserve prices. By adjusting β, the WT can be deloaded to provide the necessary downward reserve power while maintaining the electrical grid's stability.

Figure 4.10.a shows the PI gains of the pitch of the fuzzy and baseline designs in responding to the grid frequency changes. The pitch controller's proportional and integral gains in the fuzzy approach are changing rapidly to offer a greater controlling and damping effect. Although no gain correction factor is considered based on the pitch control sensitivity, the proposed controller is able to regulate the rotational speed in turbulent wind conditions (wind speed varies between 12m/s to 18 m/s) by employing the fuzzy adaptive gains.

Figure 4.10.b shows the proportional and integral gains of the torque controller in the fuzzy approach, comparing the fixed gains in the baseline ap-

proach, adaptively reacting to the varying electrical power setpoint, which responds to the grid frequency changes for providing FCR. When the power setpoint changes at the transient moment, the value of the proportional gain should become reasonably significant, and the integral gain should be kept as small as possible to prevent an overshoot. When the steady-state approaches, the value of the proportional gain should decrease, and the value of the integral gain should increase to prevent further overshoots and oscillations. These conditions are well consolidated in the proposed fuzzy-based approach. Based on the simulation results that are reflected in Figures 4.9 and 4.10, the fuzzy-PI design has demonstrated better tracking and control performance compared to the baseline PI scheme.

4.4.2 Analysis of mechanical load

Partial load region

This subsection aims to investigate the proposed approach's impact on the WT's mechanical load under different power reserve strategies and control systems. The analysis considers the root mean square (RMS) values during the final 400s of the simulation, excluding the initial 150s, to account for any startup conditions that may affect the results. The studied parameters related to the structural behavior of WT involve the blade root out-of-plane bending moment, tower base fore-aft bending moment, and tower base side-to-side bending moment, which are all examples of the bending moments that wind turbine components can experience, which are the key metrics determining structural loading. The blade flapwise and edgewise bending moments are specific to the behavior of the wind turbine blades. The blade root pitching moment relates to the twisting or rotation of the blade around its longitudinal axis.

Figure 4.11.a displays the blade root out-of-plane, tower base fore-aft, and side-to-side bending moments for normal operation at MPPT mode and two reserve strategies. As expected, the cyclic loading significantly increases the amplitude of the blade root out-of-plane and tower base fore-aft bending moments, which will further escalate as the rotor speed increases. However, the amplitude of the tower base side-to-side bending moments decreases, as this bending moment depends on the torque induced by the roll motions at the top of the tower. In both strategies, the thrust force responsible for the fore-aft tower base bending moment increases while the torque moment decreases. This analysis helps explain the excessive mechanical loads observed in the fixed reserve strategy, which maintains a higher reserve than the percentage reserve strategy.

Figure 4.11.b presents the root mean square (RMS) values of other loading parameters, including blade root pitching, flapwise, and edgewise bending mo-

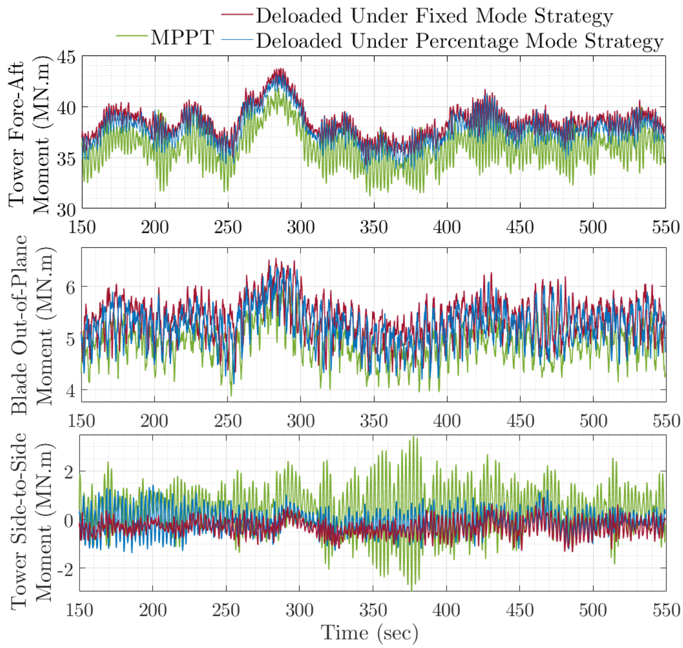

a. Time-series of mechanical loads in partial load region.

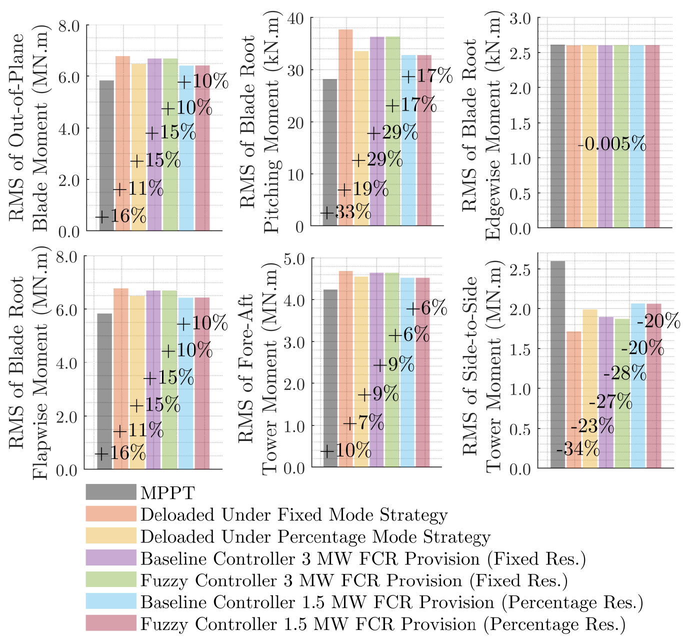

b. WT mechanical loads for FCR provision in partial load region.

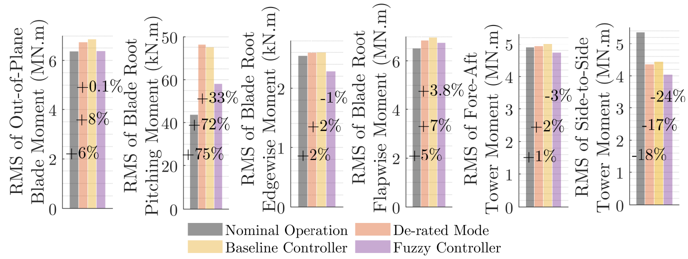

c. WT mechanical loads for FCR provision in full load region.

Figure 4.11: Mechanical load analysis

ments, for different control strategies. The monitoring is performed at turbulent wind speeds with a fixed pitch angle of zero degrees. The results indicate that the proposed control strategies have a negligible effect on the blade edgewise moment (around 0.005%). However, it is observed that the fixed reserve strategy causes an increase in blade root pitching and flapwise moments by 14% and 5%, respectively, compared to the percentage reserve mode. Although both reserve strategies increase most of the affected mechanical loading parameters, the adaptive fuzzy-PI control scheme applied at below-rated wind speeds does not add extra forces to the blade and tower base. The proposed control scheme slightly reduces the blade out-of-plane pitching and flapwise bending moments by around 5%, owing to the smooth regulation of the rotor speed and the adaptive response of the generator torque to the varying power setpoint. The adaptive fuzzy-PI controller outperforms the baseline PI controller in regulating the electrical power and achieving the least RMS of the mechanical loads in the below-rated wind speed. Overall, the fuzzy-PI controller has superiority over the baseline PI controller in adjusting the electrical power and achieving the least RMS of the mechanical loads in the below-rated wind speed.

Full load region

As shown in Figure 4.9.b, applying the fuzzy-PI can effectively decrease the frequent action of the pitch actuator while providing improved power reference tracking and better rotor speed regulation compared to the baseline method. The lowered pitch servos and blade actions result in reduced mechanical loads. Figure 4.11.c shows that the proposed method significantly reduced the out-of-plane and pitching moment, two critical load parameters that can cause fatigue damage to the blades. In nominal operation, the fuzzy-PI control strategy reduced the blade root edgewise moment by 7.9% and the pitching moment by 39% compared to the baseline method. In derated operation, the fuzzy-PI control strategy reduced the blade root edgewise and flapwise moments by 3%

and 3.2%, respectively, compared to the baseline method. Additionally, the proposed method reduces the tower fore-aft and side-to-side bending moments by 5% and 8%, respectively, more than the baseline approach. The proposed method causes torque and pitch controllers to cooperate effectively in providing active power regulation at the above-rated wind speed. Active power regulation plays a vital role in preventing mechanical loads from surpassing design limits, which can lead to turbine damage. By effectively managing these loads, we can significantly extend the remaining useful life of the wind turbine. The fuzzy-PI control strategy regulated the wind turbine's power output while keeping the mechanical loads within safe limits.

4.5 Conclusions

This article proposes an adaptive operational strategy for a WT to provide Frequency Containment Reserve (FCR) considering grid frequency and wind speed stochastic behavior. An adaptive reserve margin is estimated based on a short-term prediction of the grid frequency. To track the power reference signal with a varying reserve margin, a real-time look-up table is employed in an FCR supplementary control loop to adjust the reserve margin and the control setpoints adaptively. The performance of the suggested framework is investigated for two power reserve methods, i.e., fixed reserve and percentage reserve strategies. This study also addresses the gain scheduled fuzzy-PI design for adaptive and reliable control of a large offshore operation (partial and full load regions) providing FCR in turbulent winds. The proposed controller is applied to the FAST simulator, which offers detailed nonlinear aero-hydro-servo-elastic simulation in the time domain for analyzing the effectiveness of pitch and torque control systems. The suggested adaptive reserve strategy performs well in terms of optimal and adequate response to the grid frequency changes. Moreover, the application of fuzzy-PI pitch and torque controllers for the proposed control structure is able to smoothen out electrical power fluctuations in an active power control mode and improve robust regulation of generator speed. No adverse impacts were found on mechanical loads that might be increased in particular conditions when providing the power reserve for the active power regulation. The simulation results indicate the superior performance of the adaptive fuzzy-PI in all operating regions and for both reserve modes. Besides the effectiveness and compatibility of the fuzzy-PI in terms of power reference tracking, it results in an optimal control action of pitch and torque in the presence of turbulent wind speed in below and above-rated wind conditions without risking the control system's stability. A general conclusion of this study suggests that the proposed operational strategy using adaptive gain scheduling fuzzy-PI is applicable and beneficial for FCR provision due to its in-expensive and computationally reasonable cost and capability to cover a broad range of operating conditions. Although providing power reserve increases some mechanical loads, this could be compensated by the adaptive and smooth performance of the proposed scheme, especially at above-rated wind speed and for fixed power reserve mode in below-rated wind speed. The proposed operational strategy can efficiently be integrated into a WT's existing pitch and torque control systems, enabling them to provide FCR with optimal deloading margins and adaptively operate under different power reserve strategies.

Bibliography

[1] N. Kayedpour, J. D. De Kooning, A. E. Samani, L. Vandevelde, and G. Crevecoeur, "An adaptive operational strategy for enhanced provision of frequency containment reserve by wind turbines: Data-driven based power reserve adjustment," *Electric Power Systems Research*, vol. 223, p. 109564, 2023.

[2] J. Shair, X. Xie, L. Wang, W. Liu, J. He, and H. Liu, "Overview of emerging subsynchronous oscillations in practical wind power systems," *Renewable and Sustainable Energy Reviews*, vol. 99, pp. 159–168, 2019.

[3] GWEC (Global Wind Energy Council), "GLOBAL WIND REPORT," 2022.

[4] T. Muneer, E. Jadraque Gago, and S. Etxebarria Berrizbeitia, "Wind energy and solar pv developments in the eu," in *The Coming of Age of Solar and Wind Power*, pp. 139–177, Springer, 2022.

[5] ESO, "Technical report on the events of 9 august 2019.."

[6] J. Đaković, M. Krpan, P. Ilak, T. Baškarad, and I. Kuzle, "Impact of wind capacity share, allocation of inertia and grid configuration on transient RoCoF: The case of the Croatian power system," *International Journal of Electrical Power & Energy Systems*, vol. 121, p. 106075, 2020.

[7] E. Rebello, D. Watson, and M. Rodgers, "Ancillary services from wind turbines: automatic generation control (AGC) from a single Type 4 turbine," *Wind Energy Science*, vol. 5, no. 1, pp. 225–236, 2020.

[8] H. Algarvio, F. Lopes, A. Couto, and A. Estanqueiro, "Participation of wind power producers in day-ahead and balancing markets: An overview and a simulation-based study," *Wiley Interdisciplinary Reviews: Energy and Environment*, vol. 8, no. 5, p. e343, 2019.

[9] Z. Wu, W. Gao, T. Gao, W. Yan, H. Zhang, S. Yan, and X. Wang, "State-of-the-art review on frequency response of wind power plants in power systems," *Journal of Modern Power Systems and Clean Energy*, vol. 6, no. 1, pp. 1–16, 2018.

[10] S. Li, W. Wang, X. Zhang, S. Qin, and Y. Ying, "A novel primary frequency regulation strategy of wind farm based on wind turbine health condition," *IET Renewable Power Generation*, 2022.

[11] X. Bian, J. Zhang, Y. Ding, J. Zhao, Q. Zhou, and S. Lin, "Microgrid frequency regulation involving low-wind-speed wind turbine generators based on deep belief network," *IET Generation, Transmission & Distribution*, vol. 14, no. 11, pp. 2046–2054, 2020.

[12] Q. Yao, Y. Hu, H. Deng, Z. Luo, and J. Liu, "Two-degree-of-freedom active power control of megawatt wind turbine considering fatigue load optimization," *Renewable Energy*, vol. 162, pp. 2096–2112, 2020.

[13] X. Wang, Y. Wang, and Y. Liu, "Dynamic load frequency control for high-penetration wind power considering wind turbine fatigue load," *International Journal of Electrical Power & Energy Systems*, vol. 117, p. 105696, 2020.

[14] M. Cañas-Carretón and M. Carrión, "Generation capacity expansion considering reserve provision by wind power units," *IEEE Transactions on Power Systems*, vol. 35, no. 6, pp. 4564–4573, 2020.

[15] R. Prasad and N. P. Padhy, "Synergistic frequency regulation control mechanism for dfig wind turbines with optimal pitch dynamics," *IEEE Transactions on Power Systems*, vol. 35, no. 4, pp. 3181–3191, 2020.

[16] Z. Dong, Z. Li, Y. Dong, S. Jiang, and Z. Ding, "Fully-distributed deloading operation of dfig-based wind farm for load sharing," *IEEE Transactions on Sustainable Energy*, vol. 12, no. 1, pp. 430–440, 2020.

[17] A. Fernández-Guillamón, G. Martínez-Lucas, Á. Molina-García, and J. I. Sarasua, "An Adaptive Control Scheme for Variable Speed Wind Turbines Providing Frequency Regulation in Isolated Power Systems with Thermal Generation," *Energies*, vol. 13, no. 13, p. 3369, 2020.

[18] A. Fernández-Guillamón, J. Villena-Lapaz, A. Vigueras-Rodríguez, T. García-Sánchez, and Á. Molina-García, "An adaptive frequency strategy for variable speed wind turbines: application to high wind integration into power systems," *Energies*, vol. 11, no. 6, p. 1436, 2018.

[19] M. Khamies, G. Magdy, S. Kamel, and B. Khan, "Optimal model predictive and linear quadratic gaussian control for frequency stability of power systems considering wind energy," *IEEE Access*, vol. 9, pp. 116453–116474, 2021.

[20] N. Kayedpour, A. E. Samani, J. D. De Kooning, L. Vandevelde, and G. Crevecoeur, "Model predictive control with a cascaded hammerstein neural network of a wind turbine providing frequency containment reserve," *IEEE Transactions on Energy Conversion*, vol. 37, no. 1, pp. 198–209, 2021.

[21] L. Pan and X. Wang, "Variable pitch control on direct-driven PMSG for offshore wind turbine using Repetitive-TS fuzzy PID control," *Renewable Energy*, vol. 159, pp. 221–237, 2020.

[22] B. Xu, Y. Yuan, H. Liu, P. Jiang, Z. Gao, X. Shen, and X. Cai, "A Pitch Angle Controller Based on Novel Fuzzy-PI Control for Wind Turbine Load Reduction," *Energies*, vol. 13, no. 22, p. 6086, 2020.

[23] T. Jeon and I. Paek, "Design and Verification of the LQR Controller Based on Fuzzy Logic for Large Wind Turbine," *Energies*, vol. 14, no. 1, p. 230, 2021.

[24] Z. Civelek, "Optimization of fuzzy logic (Takagi-Sugeno) blade pitch angle controller in wind turbines by genetic algorithm," *Engineering Science and Technology, an International Journal*, vol. 23, no. 1, pp. 1–9, 2020.

[25] H. Wang, H. He, Z. Yang, G. Li, Z. Chen, J. Yang, G. Zhang, and H. Dong, "Frequency response methods for grid-connected wind power generations: A review," *Electric Power Systems Research*, vol. 221, p. 109396, 2023.

[26] X. Zhang, Y. Chen, Y. Wang, X. Zha, S. Yue, X. Cheng, and L. Gao, "Deloading power coordinated distribution method for frequency regulation by wind farms considering wind speed differences," *IEEE Access*, vol. 7, pp. 122573–122582, 2019.

[27] A. K. Mishra, P. Mishra, and H. Mathur, "A deep learning assisted adaptive nonlinear deloading strategy for wind turbine generator integrated with an interconnected power system for enhanced load frequency control," *Electric Power Systems Research*, vol. 214, p. 108960, 2023.

[28] J. Jonkman, S. Butterfield, W. Musial, and G. Scott, "Definition of a 5-MW reference wind turbine for offshore system development," tech. rep.,

National Renewable Energy Lab (NREL), Golden, CO (United States), 2009.

[29] J. M. Jonkman, M. L. Buhl, *et al.*, *FAST user's guide*, vol. 365. National Renewable Energy Laboratory Golden, CO, USA, 2005.

[30] P. J. Moriarty and A. C. Hansen, "AeroDyn theory manual," tech. rep., National Renewable Energy Lab., Golden, CO (US), 2005.

[31] J. D. M. De Kooning, J. Van de Vyver, B. Meersman, and L. Vandevelde, "Maximum efficiency current waveforms for a PMSM including iron losses and armature reaction," *IEEE Transactions on Industry Applications*, vol. 53, no. 4, pp. 3336–3344, 2017.

[32] J. D. M. De Kooning, T. L. Vandoorn, J. Van de Vyver, B. Meersman, and L. Vandevelde, "Displacement of the maximum power point caused by losses in wind turbine systems," *Renewable Energy*, vol. 85, pp. 273–280, 2016.

[33] J. Jonkman, S. Butterfield, W. Musial, and G. Scott, "Definition of a 5-MW Reference Wind Turbine for Offshore System Development," *Technical Report*, 2 2009.

[34] J. Aho, L. Pao, and P. Fleming, "An active power control system for wind turbines capable of primary and secondary frequency control for supporting grid reliability," in *51st AIAA Aerospace Sciences Meeting including the New Horizons Forum and Aerospace Exposition*, p. 456, 2013.

[35] X. Ge, X. Zhu, Y. Fu, Y. Xu, and L. Huang, "Optimization of reserve with different time scales for wind-thermal power optimal scheduling considering dynamic deloading of wind turbines," *IEEE Transactions on Sustainable Energy*, 2022.

[36] P. Fernández-Bustamante, O. Barambones, I. Calvo, C. Napole, and M. Derbeli, "Provision of frequency response from wind farms: A review," *Energies*, vol. 14, no. 20, p. 6689, 2021.

[37] J.-H. Urrea-Quintero, J. N. Fuhg, M. Marino, and A. Fau, "PI/PID controller stabilizing sets of uncertain nonlinear systems: an efficient surrogate model-based approach," *Nonlinear Dynamics*, pp. 1–23, 2021.

[38] K. Bedoud, M. Ali-rachedi, T. Bahi, and R. Lakel, "Adaptive fuzzy gain scheduling of PI controller for control of the wind energy conversion systems," *Energy Procedia*, vol. 74, pp. 211–225, 2015.

[39] A. G. Aissaoui, A. Tahour, N. Essounbouli, F. Nollet, M. Abid, and M. I. Chergui, "A Fuzzy-PI control to extract an optimal power from wind turbine," *Energy Conversion and Management*, vol. 65, pp. 688–696, 2013.

[40] G. Chen, T. T. Pham, and N. Boustany, "Introduction to fuzzy sets, fuzzy logic, and fuzzy control systems," *Appl. Mech. Rev.*, vol. 54, no. 6, pp. B102–B103, 2001.

[41] Y.-M. Wang, "Centroid defuzzification and the maximizing set and minimizing set ranking based on alpha level sets," *Computers & Industrial Engineering*, vol. 57, no. 1, pp. 228–236, 2009.

[42] Z.-Y. Zhao, M. Tomizuka, and S. Isaka, "Fuzzy gain scheduling of PID controllers," *IEEE Transactions on Systems, Man, and Cybernetics*, vol. 23, no. 5, pp. 1392–1398, 1993.

[43] B. J. Jonkman, "Turbsim User's Guide: Version 1.50," tech. rep., National Renewable Energy Lab.(NREL), Golden, CO (United States), 9 2009.

[44] "www.elia.be, Belgian TSO providing transparency on grid data."

[45] M. H. Hansen, A. Hansen, T. J. Larsen, S. Øye, P. Sørensen, and P. Fuglsang, "Control design for a pitch-regulated, variable speed wind turbine," 2005.

Chapter 5

Hybrid Physics-based Data-driven Modeling for Wind Turbine Health Monitoring

As discussed in previous chapters, data-driven methodologies can help in the modeling and control to optimize the operation of wind farms (Chapter 2) and wind turbines (Chapter 3 and 4) that deliver FCR. This chapter focuses on wind turbine health monitoring. As mentioned in Sections 1.4.4 and 1.5.3, assessing the overall condition of wind turbines (WTs) in operation poses a significant challenge due to their complex nature, which becomes even more intricate when WTs are simultaneously providing ancillary services and responding to grid requirements, especially under curtailment mode. Traditionally, multiple models are required to effectively evaluate the health condition of WTs, making the process cumbersome and impractical, particularly for large-scale wind farms. Moreover, conventional physics-based models often struggle to capture the full complexity of turbulent wind flows and the intricate aerodynamics of wind turbine blades under varying operating conditions. This is where hybrid physics-based data-driven methods come into play. They combine physics-based models with data-driven approaches, such as deep learning, to use the strengths of both approaches, improving the accuracy and reliability of predictive capabilities and ultimately leading to more efficient and cost-effective wind turbine condition monitoring purposes.

To address these challenges, this chapter proposes a novel hybrid physics-based deep learning framework that accurately approximates the time-varying correlation between control sequences and system response, capturing the aerodynamic nonlinearity of the NREL 5MW offshore WT. This framework introduces a layer of novelty by presenting a computationally efficient weakly supervised approach that utilizes the hybrid structure to detect degradations and anomalies, specifically considering curtailment operation.

To detect anomalies and degradation, a support vector machine is employed to classify extracted electrical power and rotational speed features in both the time and frequency domains. A wide range of anomalies and power depredations, such as PMSG abnormalities, pitch control failure, or yaw misalignment, will be evident in these two parameters. The proposed approach also incorporates an iterative self-learning framework that updates the selected classifier's hyperparameters dynamically during active operations, enabling it to learn from new and previously unseen anomalies. This adaptive learning process enhances the monitoring capabilities and ensures continuous improvement in anomaly detection.

Furthermore, the proposed method accounts for uncertainties in the system, such as wind stochasticity and power curve variations, and accommodates different sparsity levels in the datasets. This flexibility allows the approach to handle diverse operational scenarios and ensures its applicability in real-world wind farm conditions.

By employing this comprehensive approach, the proposed method significantly improves health monitoring performance, leading to a more efficient and accurate assessment of the overall condition of WTs. This is necessary for wind farm supervisory control level and grid integration improvement. The enhanced monitoring capabilities enable better decision-making at the supervisory control level, facilitating effective maintenance scheduling, optimizing power generation, and ensuring reliable grid integration. Ultimately, the proposed method contributes to the overall operational excellence of wind farms by improving health monitoring and enhancing the integration of WTs with the grid.

The contents of this chapter is currently under review [1].

Wind Turbine Hybrid Physics-based Deep Learning Model for a Health Monitoring Approach Considering Provision of Ancillary Services

Nezmin Kayedpour, Jixiang Qing, Jolan Wauters, Jeroen D. M. De Kooning, Ivo Couckuyt, and Guillaume Crevecoeur

Revised manuscript submitted to ”IEEE Transactions on Instrumentation and Measurement”

Abstract *Assessing the overall condition of wind turbines in operation is challenging due to their intricate nature. This becomes even more complicated when wind turbines provide ancillary services and respond to grid requirements under curtailment mode. Multiple models are required to effectively evaluate the wind turbines' healthy condition, which can be unmanageable and impractical, particularly for large-scale wind farms. This article proposes a novel hybrid physics-based deep learning framework to accurately approximate the time-varying correlation between control sequences and system response, reflecting the aerodynamic nonlinearity of the 5-megawatt offshore wind turbine model, designed and tested by the National Renewable Energy Laboratory (NREL). Another layer of this study's novelty relies on proposing a computationally efficient weakly supervised approach that employs the hybrid structure to detect degradations and anomalies considering curtailment operation. A self-learning classification approach is employed to iteratively update the best-tuned classifier, dynamically learning unforeseen abnormalities from brand-new anomalies during active operations. The proposed method deals with uncertainties in the system, such as wind stochasticity and power curve variations, including different sparsity levels in the datasets. The results of the proposed approach show promise in improving health monitoring performance, leading to a more efficient and accurate assessment of the overall condition of wind turbines.*

5.1 Introduction

the growing number of wind energy conversion systems, ensuring reliable operation that considers grid balancing provision through ancillary services while lowering maintenance costs and reducing downtime is necessary. However, wind turbines (WTs) are complicated systems containing multiple subsystems. Anomalies and faults can occur due to various factors, leading to failure. Therefore, it is crucial to have a condition monitoring system (CMS) that can detect these issues early on to improve the system's reliability and to lower the levelized cost Of energy (LCOE) [2].

The fast development of big data techniques plays an evolutionary role in WT Health monitoring and predictive maintenance strategies. In recent years, there has been a significant amount of research interest in monitoring the conditions of WTs using hybrid modeling, measured data, and deep learning methods to carry out a wide range of tasks, from detecting WT anomalies [2,3], gearbox fault diagnosis [4–8], blade icing detection [9, 10], and predicting failures [11] to estimating components remaining useful life [12–15].

Among the latest studies, some efforts aim to extract high-level features from data, obviating the need for specialized domain knowledge. In [16], a deep learning classifier for WT gearboxes employs a stacked auto-encoder. Similarly, [17] uses an adaptive algorithm to capture evolving sensor weights for WT health assessment. In [18], an interactive spatiotemporal model extracts features, while [19] introduces an adaptive gated attention mechanism for fault feature extraction. Nevertheless, emphasis is placed on achieving accurate modeling, given the intricate and aerodynamic nature of WT data connections to unveil hidden nonlinear patterns, ensuring an overall recognition of rapidly altering operating conditions, i.e., maximum power point tracking (MPPT) mode, power regulation and the transitions zone, and improving the overall effectiveness of WT condition monitoring, fault diagnosis, and lifetime prognosis [20].

Data-driven methods and sensor data analytics are powerful tools to mirror and predict the system performance [21]. A machine learning-based surrogate structure as a virtual model and a proxy to the actual high-fidelity model of an existing system can emulate the behavior of a physical system depending on the entity's design and operation. [22] proposes using a surrogate model to calculate extreme WT tower loads using various signals and a suitable simulation tool. Also, surrogate models based on polynomial chaos expansion (PCE) and Kriging are suggested in [23] to approximate WT fatigue loads. Long short-term memory (LSTM) is a recurrent neural network (RNN) that is often used in wind turbine surrogate modeling due to its ability to capture temporal dependencies and sequential patterns in time series data, which is common in wind turbine operational data [24, 25]. Another robust and effective method to estimate the nonlinear behavior of dynamical operations is the adaptive neuro-fuzzy inference system (ANFIS), which enables expressing uncertain circumstances in the form of rules by using the (if-then) decision-making mechanism [26]. ANFIS and fuzzy logic approaches can show superior performance, short execution time, and accuracy, especially in WT applications that possess stochastic aerodynamic characteristics [27, 28]. The introduction of convolutional neural network (CNN) has broadened the possibilities for time series prediction methods, and made them no longer limited to RNN. CNNs offer the advantage of parallel processing and the ability to expand their receptive fields. This capability allows CNNs to access a more comprehensive historical context, potentially mitigating issues associated with long-term dependencies. Temporal convolutional network (TCN) represents an advanced refinement of the CNN architecture. It does so by employing dilated causal convolutions to uncover important historical information [29]. Interestingly, enlarging the receptive field using dilated causal convolutions results in only a minor increase in the network's layer count and parameter complexity. As a result, TCN excels in the domain of time series prediction, surpassing the predictive capabilities of standard CNNs [29]. Promising outcomes of TCN in predictive tasks, such predicting RUL of rotating machinery and forecasting wind speed intervals for wind turbines are discussed in [30, 31]. The Transformer model is another deep learning architecture, which recently has become very popular due to its effectiveness in capturing long-range dependencies in sequences [32,33]. The attention-based Transformer model addresses some of the limitations of recurrent and convolutional neural networks in handling sequential data and is recently developed for remaining useful life (RUL) estimation approaches [34]. However, despite the mentioned benefits of Transformers, their adoption for real-time inference is hindered by demanding computational requirements [35]. This complexity in deployment poses a notable challenge for practical applications where data might be limited.

Nevertheless, applying pure data-driven techniques to WT modeling faces significant limitations, emerging from insufficient data quality and quantity of vital parameters like wind and rotor speed, power, and control performance metrics [36]. By juxtaposing power predictions with real-time data and combining physics-based and data-driven methods, a comprehensive and accurate representation of the turbine's behavior can result in successful flag-up deviations, particularly in scenarios involving stochastic processes or varying grid conditions. However, the current hybrid methods are also often focused on limited parameters and elements, solely on a few key components such as the gearbox, the generator, blade bearings, or power quality [37]. Furthermore, power prediction within WTs plays a pivotal role in wind energy management and power forecasting. When combined with data analysis and monitoring methods, this predictive capacity not only aids energy generation management and grid integration but also facilitates the detection and diagnosis of significant powertrain degradation and failures [37]. On the other hand, accurate modeling and a standalone condition monitoring system (CMS) for the entire WT can be costly, requiring extra investments [2]. While significant progress has been made through these techniques, a comprehensive evaluation of the entire WT is often challenging to attain [2, 38]. The issue becomes even more complex when the selected monitoring indicator fails to detect the fault signatures, as these could be masked by the condition parameters of another component or different operating policies, such as power degradation related to the Frequency Containment Reserve (FCR) provision [39], which has not been taken into consideration in the previous studies. Multiple models have been produced due to various studies attempting to tackle the issue by combining various methods that increase the system's complexities. However, they are found to be less efficient and more costly to manage, particularly in large floating offshore wind farms [40]. This underscores the need for an integrated approach that comprehensively addresses the intricacies and challenges of wind turbine health assessment and condition monitoring.

This study addresses three key challenges that hinder a comprehensive evaluation of wind turbine performance. Firstly, existing methods focusing on single turbine components fail to provide an overall performance assessment, disregarding complex interdependencies within the system [37]. Secondly, managing multiple models for different aspects of performance is often inefficient and computationally expensive [2]. Thirdly, the impact of wind turbine curtailment operations on system health for grid balancing purposes is often overlooked [41]. To bridge these gaps, we propose a hybrid framework that predicts the WT overall performance by coupling physical equations representing the estimation of controlled parameters responding to various operating conditions and a deep learning surrogate model predicting WT aerodynamic behavior, allowing a more accurate reflection of healthy behavior. We investigated the prediction capability of three different deep learning approaches suggested in the literature, i.e., ANFIS, LSTM, and TCN, ensuring the accuracy and computational efficiency of the surrogate model. This study particularly addresses the third gap by explicitly considering curtailment-related degradation that can be falsely detected as performance degradation or any other anomalies. Additionally, we employed a weakly supervised approach using limited labeled faulty data to address the challenges posed by supervised and unsupervised methods and their requirements of extensive labeled data, which are not always practically available [36, 42].

The key contributions of this article can be outlined as follows:

- A hybrid framework is proposed that accurately predicts the WT's overall healthy performance by approximating the electrical power and rotational speed, not only considering the stochastic nature of wind speed but also complex correlations between control sequences of pitch-generator torque and system response in turbulent wind. These parameters are physically described and integrated into a deep learning surrogate model to effectively capture the system's nonlinearities across various stochastic conditions and operational modes. Employing the proposed hybrid structure facilitates anomaly detection by distinguishing between normal and abnormal states, indicating deviations (residuals).

- A self-learned approach with an iterative framework is investigated that improves the classifier's performance by dynamically updating newly labeled anomalies from former successful classifications. Support Vector Machines (SVMs) are employed for classifying the faultiness and degradation, incorporating coherent features that can be extracted from the plant's main observables, i.e., electrical power, and rotational speed, in time and frequency domains for seamless integration into the system's condition indicators.

- This study also considers a wide range of anomalies and degradation scenarios, including degradation due to curtailment operations providing FCR, blade pitch control failure, yaw misalignment, and Permanent Magnet Synchronous Generator (PMSG) abnormalities. The suggested approach addresses the intricacies and inter-dependencies present in WT performance under varying grid requirements and operating conditions. The methodology's validation was performed on a realistic 5MW offshore floating wind turbine using the NREL FAST software. This simulation integrates detailed models of the wind turbine's nonlinear aerodynamics, providing a realistic environment for comprehensive assessment.

This article is organized as follows: Section II discusses the hybrid physics-based deep learning structure. Section III describes the proposed condition monitoring approach. The performance assessment, data, simulations, and results are presented in Section IV. Finally, in Section V, the findings are discussed, and conclusions are drawn.

5.2 Hybrid Physics-based deep learning model

5.2.1 Underlying WT physical system

This study employs a 5MW offshore WT with variable blade-pitch-to-feather configuration and an operational control approach based on power-production regulation using pitch and torque control systems. To accurately model the behavior of the WT, each subsystem is described and modeled separately. This involves developing a detailed model of the aerodynamics, control system, and electrical characteristics of the Permanent Magnet Synchronous Generator (PMSG). These models are then integrated into a closed-loop system to study WT's dynamic behavior in various operating conditions.

Dynamic model

To investigate the dynamic behavior of wind turbines, the study employs TurbSim to generate time series data for the three Cartesian wind components within a dimensional grid. This data is generated based on statistical models, effectively simulating the full-field wind speed distribution. Subsequently, the generated wind data undergoes analysis to assess its spectral and coherence properties in the frequency domain. By applying an inverse Fourier transform, the data is transformed into wind speed time series, a crucial preparatory step for its integration into the time domain-oriented FAST simulation tool. This comprehensive approach ensures the faithful representation of wind conditions, ultimately facilitating a robust exploration of wind turbine dynamics and performance [43,44]. The wind turbine captures a total amount of mechanical power P_m, and the mechanical torque T_m of the wind turbine can be described using the following relationships:

$$P_m = Av^3 C_p(\lambda, \theta), A = \frac{1}{2}\rho\pi R^2, \tag{5.1}$$

$$T_m = Av^3 C_p(\lambda, \theta) \cdot \frac{1}{\omega_r}, \tag{5.2}$$

where C_p represents the power coefficient, ρ is the air density, R denotes the blade length and θ is the pitch angle. The tip-speed ratio $\lambda = \omega_r R/\ v$ is a function of wind v and rotational speed ω_r. FAST implements the Blade Element Momentum (BEM) theory and simulates the nonlinear equations of motion. It also determines the WT's aerodynamic and structural response to wind-inflow conditions in time, which is advantageous for developing control designs and analysis [45].

Generator

The dynamic equivalent model of the PMSG can be formulated in the q,d rotating reference frame:

$$V_d = R_s I_d + L_d \frac{dI_d}{dt} - N_p \omega_r L_q I_q, \tag{5.3}$$

$$V_q = R_s I_q + L_q \frac{dI_q}{dt} + N_p \omega_r (L_d I_d + \Phi_m), \tag{5.4}$$

where R_s is the stator-winding resistance, L_d and L_q are the d-axis and q-axis stator-inductances and Φ_m is the flux linkage. V_d and I_d are the d-axis stator voltage and current. V_q and I_q are the q-axis stator voltage and current. N_p

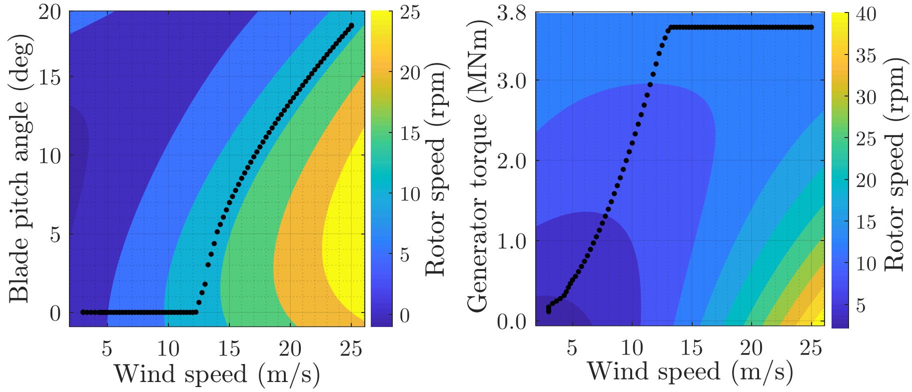

Figure 5.1: Nonlinear mapping between wind speed, WT generator torque, blade pitch angle, and rotational speed.

is the number of pole pairs. The generator torque and electrical power can be formulated as follows:

$$T_g = \frac{3}{2} N_P \left(\Phi_m I_q + (L_d - L_q) I_d I_q \right), \tag{5.5}$$

$$P_e = \frac{3}{2} [V_d I_d + V_{sq} I_{sq}]. \tag{5.6}$$

The wind turbine system's equation of mechanical motion is formulated as follows:

$$T_m - T_g = J \cdot \frac{d\omega_r}{dt} + B_f \cdot \omega_r, \tag{5.7}$$

where, J represents the overall moment of inertia, while B_f denotes the coefficient associated with viscous friction. The machine's realistic dynamics and losses, including machine inductances, the armature reaction effect, stator winding copper losses, and iron core losses, are considered and included in the efficiency curve as proposed in [46].

Control system and FCR provision

The WT control design includes two main controllers: a generator-torque controller and a full-span rotor-collective blade-pitch controller. These controllers operate across all operational regions. In wind speeds below the rated level, the pitch angle is set at zero degrees, and the torque controller optimally maximizes wind power extraction by keeping λ and consequently C_p at the optimal level, which is $C_p^{opt} = 0.482$ and $\lambda_{opt} = 7.55$ respectively. Conversely, for wind speeds above the rated level, the pitch controller maintains rotational speed using a gain-scheduled PI controller. In this operating region, there is no

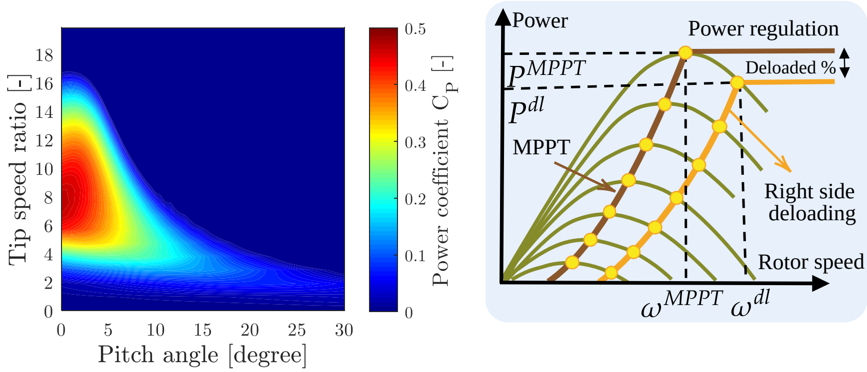

(a) (b)

Figure 5.2: a) WT optimal power coefficient for normal operation.
b) WT power modification for curtailed operation.

rotor acceleration by applying a rated generator torque T_{g-equ} that cancels the aerodynamic torques at equilibrium. Figure 5.1 illustrates the nonlinear relationships among wind speed, generator torque, blade pitch angle, and rotational speed. The pitch controller adapts to the nonlinear aerodynamic characteristics at different operating points, as determined through linearization analysis in FAST. The control system includes a transition zone between partial and full load to ensure a smooth transition between maximum power point tracking and power regulation. The pitch angle θ can be approximated considering the pitch control proportional K_p and integral K_i, to keep the rotational speed at the rated value ω_{ref}:

$$\theta \approx \theta_{\text{ref}} = K_p \delta\omega_r + K_i \int_0^t \delta\omega_r dt, \tag{5.8}$$

$$\delta\omega_r = \omega_{\text{ref}} - \omega_r, \tag{5.9}$$

where, ω_{ref} is the rated rotational speed of 12.1 rpm for 5MW offshore WT. The proportional K_p and integral K_i scheduled gains that are calculated by multiplying the gain correction factor $GK(\beta) = \frac{1}{1+\beta/\beta_K}$ to constant values, considering the aerodynamic pitch sensitivity of wind turbine $\delta P/\delta\beta$ [45]. Moreover, the control system also governs the yaw angle during normal operation, ensuring the nacelle remains aligned with the wind direction. This dynamic adjustment minimizes mechanical stress, enhances energy output, and mitigates potential damage from extreme wind conditions. In curtailment mode, wind turbines are intentionally operated at less than their maximum power output capacity. In curtailment mode, a power reserve is needed to let the WT respond to grid frequency variations with primary control architecture [47]. This means that the turbine's blades and generator torque are adjusted to capture less energy from the wind than they would at their optimal operating conditions. The power coefficient in curtailment mode C_p^{cur} would generally be lower than the optimal power coefficient C_p^{opt} in full-healthy operating mode by applying a deloaded factor β (in percentage) that determines WT contribution in FCR market, which can be formulated as follows:

$$C_p^{\text{cur}} = \beta \cdot C_P^{\text{opt}}. \tag{5.10}$$

Fig.5.2a shows wind turbine optimal power coefficient in relationship with tip speed ratio and blade pitch angle. To let the WT respond to grid frequency variations, a supplementary FCR control loop is used, and the rotor speed-power lookup table is modified by shifting the WT's operating point to the right side of the Maximum Power Point Tracking (MPPT) curve [48]. The curtailed operation lets the WT to regulate the deloaded power P^{dl}, considering the adjustment of rated rotor speed in deloading mode ($\delta\omega_r^{\text{dl}} = \alpha\omega_{\text{ref}} - \omega_r$), applying the deloaded generator torque T_{g-equ}^{dl}. Figure 5.2b shows WT power modification for curtailed operation as discussed in [47]. The WT overspeeding factor α ensures sufficient reserve at sub-optimal performance while enabling the WT to respond to grid frequency variations Δf proportionally, even when wind speed is at the below-rated value.

5.2.2 Hybrid framework

Recently, a robust baseline approach has been suggested in literature that leverages a predictive model and estimates a healthy power curve, achieving a normal behavior model (NBM) based on measured wind speeds for assessing the overall health condition of the entire WT [2]. However, several abnormalities can induce similar degradation impacts on the power curve while impacting rotational speed differently. For instance, increasing and decreasing rotor speed above or below rated wind speed has the same electrical power degradation effect. Therefore, yaw misalignment in below-rated wind conditions can be misinterpreted as curtailment degradation if we only consider the power cure prediction. However, observing the rotational speed more accurately indicates the related deviation. This is mainly because in yaw misalignment the rotor speed drops below the MPPT curve, while it will be moved to above the MPPT curve for curtailment reasons to avoid losing kinetic energy that can be used for supporting inertial response [47].

On the other hand, PMSG abnormalities are more evident by observing the electrical power, and they have less impact on the WT's rotational speed. Therefore, in the proposed hybrid framework, we suggest closely monitoring both the WT power and rotational speed to evaluate the overall performance of the WT in different operating conditions. Additionally, the proposed architecture aims to approximate the time-varying correlation between control inputs and system response while ensuring the process dynamics are enforced within the network. The baseline approach only considers wind speed as the main independent input. However, the mentioned controlled parameters can directly impact the aerodynamic nonlinearity of the system. They can be estimated by governing physical equations that provide the pitch and generator torque signals based on the central independent input, wind speed, and rotational speed as a feedback signal. The mathematical equations are adjusted to respond to wind speed variations, and the active power, which should be decided according to the power grid fluctuations at the supplementary FCR control loop. Then, a nonlinear mapping of multiple inputs, i.e., wind speed, blade pitch angle, and generator torque, into multiple outputs, i.e., rotor speed and mechanical power, is carried out by training a deep learning surrogate model, using a data-set gathered offline in various possible operating conditions.

Figure 5.3 presents the suggested hybrid framework alongside a black-box data-driven model. The baseline balck-box model predominantly relies on wind speed as its main input and is commonly studied in the literature as a benchmark for predicting WT power curve [49]. The hybrid model, on the other hand, goes a step further by estimating pitch and generator torque both below and above the rated wind speed, utilizing wind and rotor speed estimations. Subsequently, it predicts the aerodynamic behavior of the wind turbine by establishing a relationship between healthy control parameters and wind speed.

5.2.3 Structure of the surrogate models

Adaptive neuro-fuzzy inference system (ANFIS)

A hybrid learning algorithm of both the least-squares method and backpropagation learning is used to train the network and optimize the parameters of a fuzzy model capable of handling both quantitative and qualitative criteria. The nonlinear mapping is carried out using the Takagi–Sugeno inference model employing fuzzy if-then rules. In the fuzzification layer of the ANFIS structure, the Gaussian Membership Functions (MF) of the crisp inputs are created by:

$$\mu_{A_i}(T_g),\ \ \mu_{B_j}(v),\ \ \mu_{C_k}(\theta),\ \ i,j,k=1,...,n, \tag{5.11}$$

$$\mu_x = e^{-\left(x-\frac{a_i}{bi}\right)^2}, \tag{5.12}$$

where μ_{A_i}, μ_{B_j} and μ_{C_k} are the MFs of fuzzy sets, which have a Gaussian form characterized by the variance a_i and center b_i of the MF. In the rule layer, each node output is denoted by the fuzzy inference system representing the firing strength of a rule W_p, which is calculated by the multiplication of incoming signals (5.12). The purpose of the normalization layer is to normalize

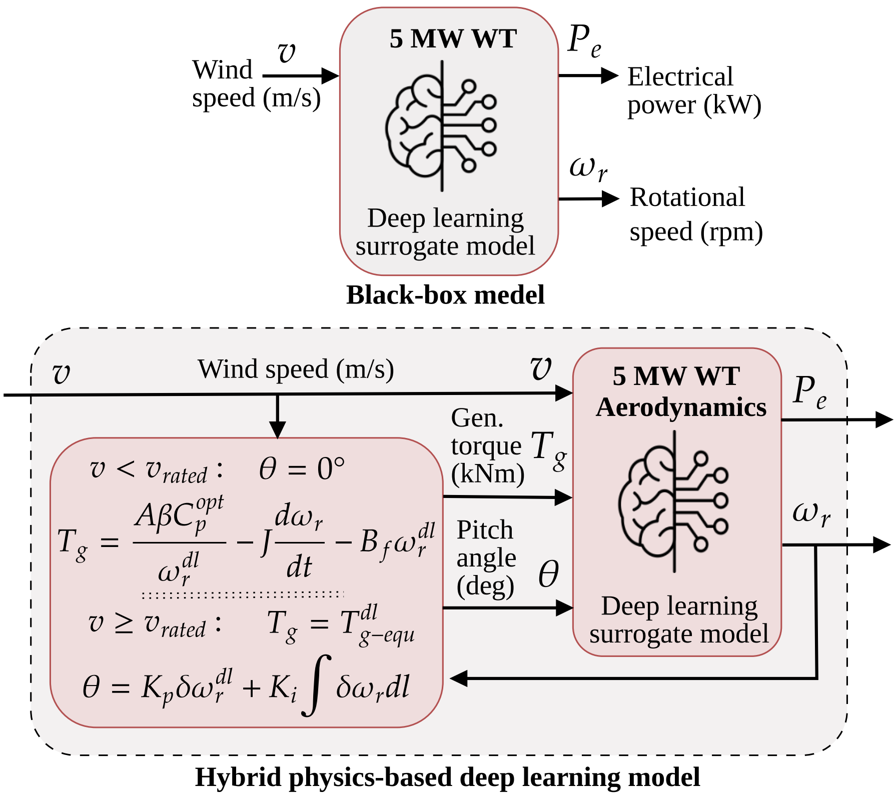

Figure 5.3: Proposed hybrid framework.

the weight function using (5.13).

$$W_p \begin{cases} \mu_{A_i}(T_g) \cdot \mu_{B_j}(v), \\ \mu_{B_j}(v) \cdot \mu_{C_k}(\theta), \\ \mu_{A_i}(T_g) \cdot \mu_{C_k}(\theta), \end{cases} \qquad i, j, k = 1, ..., n, \tag{5.13}$$

$$\bar{W}_p = \frac{W_p}{\Sigma W_p}, \quad p = 1, ..., m. \tag{5.14}$$

In the defuzzification layer, the output of nodes will be defined as the product of first order polynomials f_p and normalized firing strength $\bar{W}_p$, where f_p represents the fuzzy If–then rules:

$$\begin{aligned} &R1: \text{If } T_g = A_n \text{ and } v = B_n, \text{Then } f_n = \alpha_n T_g + \beta_n v + r_n, \\ &R2: \text{If } v = B_n \text{ and } \theta = C_n, \text{Then } f_m = \beta_n v + \gamma_n \theta + r_n \quad , \\ &R3: \text{If } T_g = A_n \text{ and } \theta = C_n, \text{Then } f_m = \alpha_n v + \gamma_n \theta + r_n \quad , \end{aligned}$$

where $\{\alpha, \beta, \gamma, r\}$ is the resultant attribute set, which belongs to each node. Finally, one node represents the sum layer, which calculates the total output

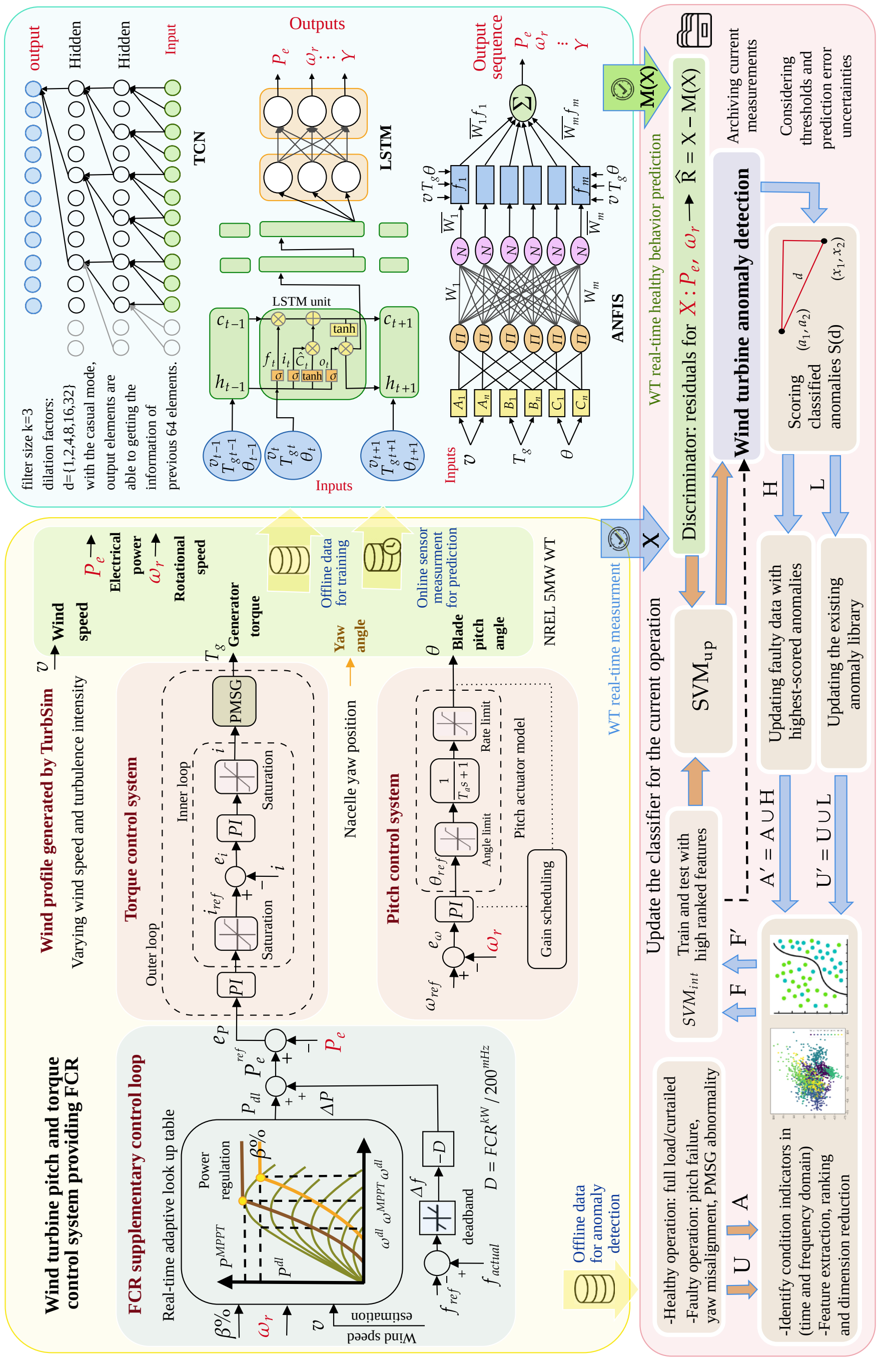

Figure 5.4: The proposed health monitoring framework using the hybrid model.

summation of all arriving signals by:

$$Y = \sum_{p=1}^{m} \bar{W}_p f_p. \tag{5.15}$$

In this study, the Fuzzy C-means (FCM) method is used to compute the membership degrees, minimizing the following objective function:

$$\mathcal{J}_q = \sum_{l=1}^{N} \sum_{s=1}^{G} u_{ls}^{q} \|x_l - G_s\|^2, \quad 1 < q < \infty, \tag{5.16}$$

where N is the size of the data set, q is a weighted index, u_{ls} is the degree of membership of x_l in the cluster q, which is lth of d-dimensional measured data. G_s is the d-dimension center of the cluster. A Genetic Algorithm (GA) is used to find the optimal weighting exponent q value for the FCM algorithm. The q value determines the fuzziness degree in the clustering process and affects the performance. The goal is to partition the dataset into the desired number of classes and to calculate the cluster centers and membership degrees that assign data points to clusters.

Long short-term memory (LSTM) network

The LSTM network is a Recurrent Neural Network (RNN) based architecture that has been commonly used for sequence regression-related application problems, e.g., [50, 51]. The main advantage of LSTM over standard RNN is that it is able to capture not only the short-term temporal relations in sequence but also the long-term relationship. This has been achieved by its specifically designed network structure, as illustrated in Fig.5.4. For a specific LSTM unit, if we denote the input at time step t as $\boldsymbol{X}_t := [v_t, T_{g_t}, \theta_t]$, the flow within the LSTM unit $\mathrm{LSTM} : \boldsymbol{X}_t \to \mathrm{LSTM}(\boldsymbol{X}_t)$ can be represented as:

$$\begin{aligned}
\boldsymbol{f}_t &= \sigma(\boldsymbol{W}_f[\boldsymbol{h}_{t-1}, \boldsymbol{X}_t] + \boldsymbol{b}_f),\\
\boldsymbol{i}_t &= \sigma(\boldsymbol{W}_i[\boldsymbol{h}_{t-1}, \boldsymbol{X}_t] + \boldsymbol{b}_i),\\
\hat{\boldsymbol{C}}_t &= \tanh\big(\boldsymbol{W}_{\hat{C}}[\boldsymbol{h}_{t-1}, \boldsymbol{X}_t] + \boldsymbol{b}_{\hat{C}}\big),\\
\boldsymbol{o}_t &= \sigma(\boldsymbol{W}_o[\boldsymbol{h}_{t-1}, \boldsymbol{X}_t] + \boldsymbol{b}_o),\\
\boldsymbol{C}_t &= \boldsymbol{f}_t \odot \boldsymbol{C}_{t-1} + \boldsymbol{i}_t \odot \hat{\boldsymbol{C}}_t,\\
\boldsymbol{h}_t &= \boldsymbol{o}_t \odot \tanh(\boldsymbol{C}_t),
\end{aligned} \tag{5.17}$$

where σ, tanh represents the sigmoid and tanh activation functions respectively; $\boldsymbol{W}_f, \boldsymbol{W}_o, \boldsymbol{W}_{\hat{C}}$ represent the weights and $\boldsymbol{b}_f, \boldsymbol{b}_i, \boldsymbol{b}_{\hat{C}}, \boldsymbol{b}_o$ denote the biases. $[\cdot]$ represents the concatenation operation and $\odot$ is the Hadamard product. $\boldsymbol{o}_t$ is the output gate's activation vector, $\boldsymbol{C}_t$ is the output cell state and $\boldsymbol{h}_t$ is the hidden state that will be provided for $t + 1$ steps recurrently. Importantly, we remark that $\boldsymbol{C}_t$ is the key factor that enables capturing long-term patterns. With the elaborated LSTM unit, in order to increase the flexibility of the network to capture the potential complex temporal correlations between the input and output of the surrogate model, we construct an LSTM-based network architecture illustrated in Fig.5.4: the constructed architecture consists of 3 LSTM layers, with two dense layers afterward. We note that this network architecture is empirically determined as leading to a satisfying performance in reality. For input $\boldsymbol{X}_t$ any time steps t, this architecture has the following output:

$$\boldsymbol{h}_t = \mathrm{LSTM}_3(\mathrm{LSTM}_2(\mathrm{LSTM}_1(\boldsymbol{X}_t))), \tag{5.18}$$

$$\boldsymbol{y}_t = \mathrm{Dense}_2(\mathrm{Dense}_1(\boldsymbol{h}_t)), \tag{5.19}$$

where LSTM gives one LSTM layer, Dense := $I(\boldsymbol{W}\boldsymbol{x} + \boldsymbol{b})$ represents one fully connected layer, where the linear activation function is used. One hundred twenty-eight hidden units within each LSTM layer are used for the other hyperparameter of the network. The hidden unit for the first dense layer is 128, and 3 for the second layer.

To optimize the weights of the proposed LSTM network architectures, we utilize the mean squared error as the objective function commonly used in a regression problem. The Adam optimizer [52] is utilized as a stochastic gradient-based optimizer. The model is implemented utilizing Keras under Tensorflow 2, and the parameters are trained with 100 epochs with a mini-batch size of 250.

Temporal convolutional neural network (TCN)

TCN is a convolutional type neural network. It works similarly to a standard convolutional neural network while the convolution operates on the time series. The convolutional kernel can either be causal (as depicted in Fig. 5.4), preventing any information leakage from the future time step, or use these parts of information if in a feasible scenario. With stacked dilated convolutions, the model is able to effectively expand the receptive field of the convolutional network, hence getting the information from a very long context. More formally, for a 1-dimensional time series input, and filters defined as $f \in \{0, , k-1\}$, the dilated convolution on an arbitrary element s of the sequence is defined as:

$$F(s) = \sum_{i=0}^{k-1} f(i) \cdot x_{(s-d \cdot i)} \tag{5.20}$$

where the element s will incorporate the information of the past up to $k(d-1)$ elements. For a more in-depth description of the neural network, we refer to the paper [29]. The TCN network structure to compare in this research consists of 3 stacked TCN layers. The filter size is set to 32, we use a kernel k with size 3, and a dilation of $d = \{1, 2, 4, 8, 16, 32, 64\}$ is utilized. For simplicity, not all hidden layers are shown in the TCN Structure in Fig. 5.4. A residual block is utilized (as shown in Fig. 1.b of [29]). After passing the 3 stacked TCN layers, a dense layer is set to extract the final output time series. We follow the same training routine as training LSTM and ANFIS models.

5.3 Health monitoring

This section introduces a health monitoring approach that utilizes the surrogate models proposed in Section 5.2.2 to assess the current condition of a WT and detect and diagnose anomalies. Figure 5.4 outlines the workflow of this approach, which commences with a data-gathering step that reflects the WT's operation under both healthy and faulty conditions. This step provides the model with measured data for anomaly detection and performance assessment. Once the surrogate model is created, the proposed hybrid structure can mimic the healthy behavior of the system and discern normal and abnormal behavior from the calculated deviations, i.e., the residuals. The next step involves using the extracted features that can be identified and incorporated into the system's condition indicators. A classifier is then trained using a small set of labeled anomaly data. In an iterative process, the highest-scored anomalies detected will be used to update the classifier by introducing more faulty sets to the initial dataset through an automatic or manual labeling method. Additionally, unknown anomalies (lowest or zero-scored data points) will be added to the existing library and updated by repeating the feature extraction and dimension reduction step. Finally, the classification model is updated using the brand-new archived dataset from the current operation, considering thresholds and the uncertainties of prediction errors. This updated model enables more accurate detection and diagnosis of anomalies in the system.

5.3.1 Anomaly and degradation scenarios

The suggested health monitoring approach is developed and assessed in various working conditions with different sources of faultiness, which have a high chance of occurrence and can be falsely interpreted as normal degradation in deloading operations with curtailment. As shown in Fig.5.5, two control failures, i.e., blade pitch angle and nacelle yaw position error, are considered, affecting the rotational speed and causing electrical power degradation in full and partial load regions, respectively. In this study, the blade pitch failure mode occurs when one or two blade pitch motor mechanisms fail to respond to the control signals, lock the blade at a certain position, and stop creating pitch-angle demands. Yaw misalignment is also implemented for yaw position errors from 5 to 20° when the WT is not fully facing the wind. This occurs when the wind direction changes and the yaw control system fails to orient the WT rotor towards the wind direction properly.

Moreover, PMSG abnormality is considered to assess the performance of the proposed condition monitoring approach in all operating regions. The presence of an electrical disturbance in the PMSG may occur at any operational condition and may interrupt or degrade electrical power. Abnormal behavior in the PMSG is attained by adding nontracked order and random noise to the back electromotive force (EMF) with a noise power of 1% to 5% of the EMF voltage and 10ms sample time. The data in healthy and faulty states are obtained by running numerous simulations in the incoming flow field with all operating ranges of wind speed and turbulence intensity levels of 5% to 15%. Figure 5.6 reveals the scatter plot of the WT healthy and 20% curtailed operation (β = 80%) as well as the mentioned anomalies with boxplots demonstrating the anomaly locality, distribution, and skewness. The electrical power degradation is evident in pitch failure and yaw misalignment in full load and partial regions. The PMSG abnormality subtly impacts the electrical power in all operating regions compared to the two other anomalies. However, its impact hardly appears in the rotational speed time-series signal.

5.3.2 Feature extraction and dimension reduction

When calculating condition indicators as summary statistics, it is crucial to consider the system features that differentiate normal operations from abnormal behaviors, including degradation in the form of curtailment. A good understanding of the system is necessary to select appropriate condition indicators in two or multiple dimensions, and some experimentation may be required. In

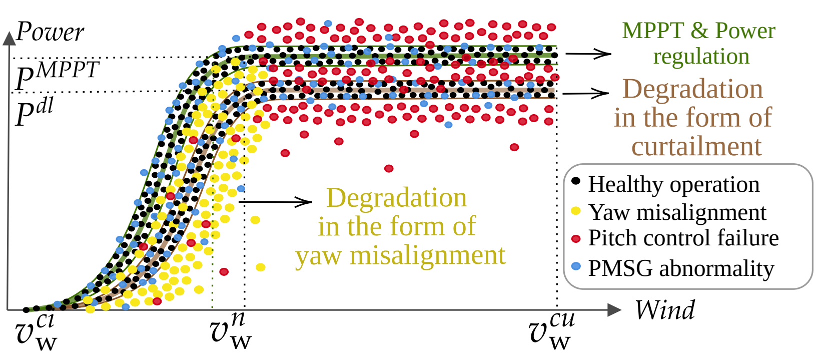

Figure 5.5: Degradation in the form of anomalies/curtailment.

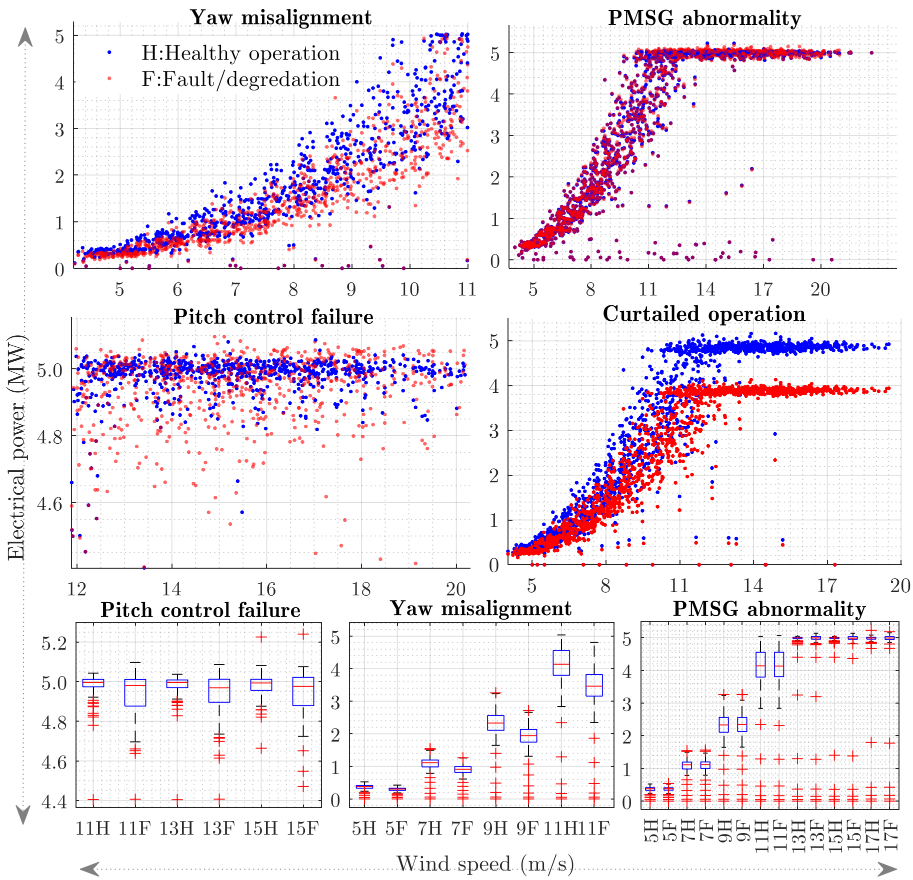

Figure 5.6: WT operation in abnormal conditions.

this study, we analyze several features in both the time and frequency domains for the electrical power and rotational speed signals, which can be combined to create condition indicators that capture the overall "unusualness" of the data. The effectiveness of each feature in differentiating normality and abnormality is estimated and ranked using one-way ANalysis Of VAriance (ANOVA) and Kruskal-Wallis [53]. Figure5.7 shows all the features used in this study, which are ranked by their importance. This work employs Principal Component Analysis (PCA) for efficiently reducing feature dimensions to enhance computational efficiency.

5.3.3 Classification

In this study, Support Vector Machines (SVM) are used to classify the obtained feature vectors, comparing the current observable value with the corresponding healthy value provided by the surrogate models. Then faulty conditions are

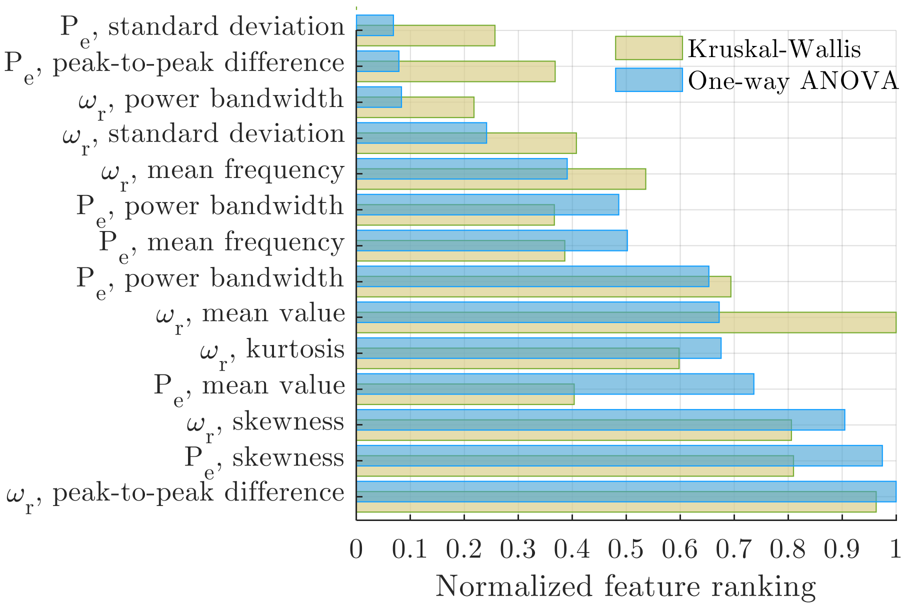

Figure 5.7: Features sorted by importance.

estimated and the occurred faultiness is identified. Different kernel functions, which map the input samples into a higher dimensional space using a nonlinear function $\phi(\cdot)$ and soft margin hyperplanes separating the data in the higher dimensional space, are considered. The SVM, in general, solves the following quadratic optimization problem:

$$\begin{aligned} \min_{W,b,\xi} \quad & \frac{1}{2}\|W\|_2^2 + C\sum_{i=1}^{N}\xi_i \\ s.t. \quad & y_i(W^T\Phi(x_i)+b) \geqslant 1-\xi_i \end{aligned} , \tag{5.21}$$

where (x_i, y_i) denotes the training set, ξ is the slack variable that allows the hard margin to be violated, W and b are N-dimensional vectors, and the offset defines the hyperplane equation. The parameter C controls the trade-off between achieving a larger margin and minimizing the number of misclassifications. Then, a kernel function $k(X_s, X_s')$ is explicitly defined to calculate the inner product in the image of the nonlinear mapping function $\xi(\cdot)$. The Gaussian, quadratic, and cubic kernel functions can be written as follows:

$$k(X_s, X_s') = \exp\left(-\frac{\|X_s - X_s'\|_2^2}{2\sigma}\right), \tag{5.22}$$

$$k(X_s, X_s') = 1 - \frac{\|X_s - X_s'\|_2^2}{\|X_s - X_s'\|_2^2 + C}, \tag{5.23}$$

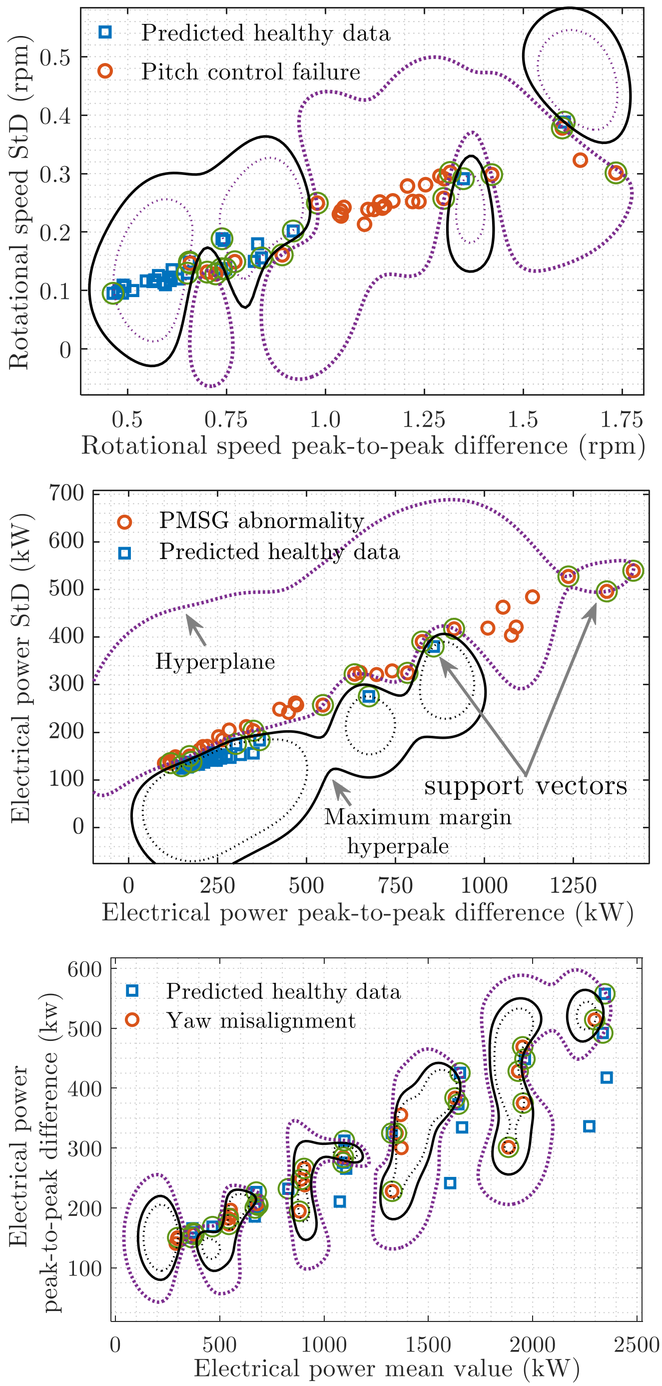

Figure 5.8: The SVM classification on lowest-ranked features.

$$k(X_s, X_s') = (X_s^T X_s' + 1)^3, \tag{5.24}$$

where X_s and X_s' are two arbitrary samples and σ is the kernel width. Fig.5.8 illustrates the two-dimensional condition indicators and the Gaussian kernel SVM classification performance for the lowest-ranked features, which have complex distributions. Although the proposed classifier is robust enough and still able to give appropriate boundaries, it results in local performance. Therefore, the first ten high-ranked features are selected to achieve global performance and reduce computational complexity. The hyperparameters are tuned to find a hyperplane that separates the data perfectly into faulty and healthy classes and reduces misclassification errors.

5.3.4 Enhancing Classification using surrogate model

The anomaly detection given in algorithm 3 aims to detect anomalies in measured data by utilizing the hybrid model that mimics the system behavior. After creating and training the surrogate model using the offline data, the residuals between the measured data and the hybrid model's predictions will be calculated. Then, features are then extracted from the residuals, and practical features are selected using one-way ANOVA. Condition indicators incorporating these features in the time and frequency domain are created, and an initial classifier, SVM_{int}, is trained using a small set of labeled anomalies under different operating conditions. The algorithm iteratively updates the classifier by selecting and adding the highest-scored anomalies to the labeled dataset, followed by retraining the classifier. The anomaly scoring relies on a distance-based scoring method in which the abnormalities are characterized by being significantly distant from the majority of the data points, considering the Euclidean distance metric. Then, unknown anomalies, identified as the lowest-scored data points, are added to the anomaly library and undergo feature extraction and dimension reduction. The SVM_{int} hyperparameters are updated based on the reduced feature set. The iteration continues until convergence is achieved. The final output is an updated self-learned classifier, SVM_{up}, capable of accurately detecting anomalies in the system. In general, the algorithm aims to improve the strength and effectiveness of the classifier over time by experiencing more abnormalities. The iterative nature of the algorithm allows the classifier to learn from new anomalies selected and added to the labeled dataset in each iteration. By continuously updating the classifier with increasing irregularities, it becomes more robust and adaptive to different types of abnormalities present in the system. This iterative learning process helps enhance the classifier's ability to detect anomalies and improve its overall performance over time.

Algorithm 3 Anomaly detection using surrogate model

Require: Measured data X, anomaly librery U

1: Create surrogate model M
2: Discriminator: Calculate residuals $\hat{R} \leftarrow (X - M(X))$
3: Extract features $F : f_1, ..., f_n$ from residuals $\hat{R}$
4: Apply one-way ANOVA to select effective features F
5: Create condition indicators I incorporating features F'
6: Train SVM_{int} using small set of labeled anomalies A for faulty scenarios from anomaly library U
7: Applying different kernel functions
8: Optimize SVM hyperparameters for the best kernel
9: **while** not converged **do**
10: Calculate anomaly scores S for all data points in X
11: Sort the data points in X based on their corresponding scores in S in **descending** order:
12: SortIndices $\leftarrow$ argsort(S)
13: Select the r highest-scored anomalies:
14: $H \leftarrow \{X[\text{SortIndices}[i]]\}_{i=1}^{r}$
15: Augment labeled dataset A with H to obtain A' :
16: $A' = A \cup H$
17: Update classifier SVM_{up} using A'
18: **end while**
19: Identify unknown anomalies: Sort the data points in X based on their corresponding scores in S in **ascending** order: SortIndices $\leftarrow$ argsort(S)
20: Select the r' lowes-scored anomalies:
21: $L \leftarrow \{X[\text{SortIndices}[i]]\}_{i=1}^{r'}$
22: Add L to the anomaly library $U' : U \cup L$
23: Perform feature extraction and dimension reduction on U to obtain reduced feature set F'
24: Update SVM_{int} hyperparameters
25: Repeat steps 8 to 15 **return** SVM_{up}

5.4 Simulation results

5.4.1 Prediction accuracy

In order to train the deep learning models, the time-consuming, computationally expensive simulations are carried out offline to generate a training dataset for numerous ranges of mean wind speed and turbulence intensities. The WT behavior is monitored for 600s in each simulation with a sampling rate of 100s. The steady-state operation of the WT is used for the training data. As a result,

Table 5.1: Predicting accuracy of the baseline black box Model vs. proposed hybrid physics-based deep learning model.

Model	Prediction Error of ω_r (rpm)		Prediction Error of P_e (kW)		Inference Time (Sec)
	Baseline	Hybrid	Baseline	Hybrid	
ANFIS-GP	0.40	0.1196	139.11	41.7667	0.53
ANFIS-SC	0.38	0.1263	137.47	42.6894	0.14
ANFIS-FCM	0.38	0.1321	134.11	45.3367	0.14
ANFIS-FCM/GA	0.31	0.0891	97.15	26.1521	0.41
LSTM	0.21	0.0704	74.82	16.8951	0.78
TCN	0.60	0.1528	176.21	103.63	0.25

894 training datasets are obtained, each having a length of 55000 samples. In order to provide a more efficient dataset for model training, each data sequence is truncated to new sequences, each with a length of 1000 samples, resulting in an expanded training data set with 49170 sequences. Finally, the LSTM and ANFIS models are trained using 100 epochs. In order to evaluate the performance of the models, we use another 100 original-length data as test data to measure the performance of the predictive model. The prediction results for the baseline black box model vs. the proposed hybrid physics-based deep learning model are given in Table 5.1, comparing the employed deep learning methods, i.e., ANFIS Grid Partitioning (GP), Subtractive Clustering (SC), Fuzzy C-Means (FCM), optimized FCM using Genetic Algorithm (GA), LSTM and TCN. The Root Mean Square Error (RMSE) of both observable predictions, i.e., rotational speed and electrical power, are quantified as follows:

$$\text{RMSE} = \frac{1}{55000}\sum_{t=1}^{55000}\left(\sqrt{\sum_{i=1}^{100}\left(y_{\text{predicted}} - y_{\text{target}}\right)^2}\right). \tag{5.25}$$

The ANFIS-based, LSTM, and TCN architectures demonstrate significantly reduced RMSE values for rotor speed and electrical power output within the hybrid framework, which integrates data-driven and physics-based information. This signifies a notable enhancement in predictive accuracy compared to the baseline black box model. Notably, the LSTM outperforms ANFIS and TCN in terms of accuracy. Introducing genetic algorithms (GA) to optimize FCM parameters notably boosts the accuracy and sensitivity of the ANFIS model while drastically reducing execution time. In the case of TCN, its performance excels when trained for extended epochs, and it can rival the LSTM when the number of epochs is increased to around 300. However, to mitigate over-fitting risks and ensure a fair comparison, we have maintained the number of training epochs at 100.

The improved accuracy across all deep learning approaches within the hybrid framework underscores the practicality and versatility of the proposed method. Nevertheless, selecting among these deep learning surrogate models should be influenced by the size of the training dataset and a trade-off between the required inference time and prediction accuracy. These findings highlight the superiority of the hybrid physics-based modeling approach, which adeptly captures the intricate dynamics of wind turbine systems, resulting in more precise predictions of rotor speed and power output compared to the baseline black box model, with a substantial 67.97% reduction in average RMSE.

The following subsection discusses the application of the proposed hybrid model in the anomaly detection framework for health monitoring purposes.

5.4.2 Anomaly detection performance

In this section, the healthy prediction of the ANFIS model is fed into the weakly supervised health monitoring method for two types of operating conditions. The first type represents the healthy and faulty operation of the WT in partial and full-load regions without considering the transition zone. The healthy predicted data needs to be differentiated from all the single anomalies or the combination of PMSG abnormalities with either pitch failure or yaw misalignment. The confusion matrices are shown in Fig.5.9, using the health codes, i.e., Healthy Operation including the curtailment (HO), PMSG Abnormality (PA), Pitch Failure (PF), and Yaw Misalignment (YM). These indicate the best performance of the updated SVM created by the proposed self-learning classification strategy, compared with the conventional classification approach that uses a Binary Decision Tree (BDT) to classify anomalies without considering the updated learning approach. Even though the BDT presents rather satisfactory accuracy among all applied classifiers (BDT and SVMs with different kernel functions discussed in Table5.2), the results show using the proposed approach with the updated SVM and Gaussian kernel function significantly improves anomaly detection performance.

The second type of data used for evaluating the proposed algorithm includes WT operation in the transition zone, where all the anomalies are likely to occur while the control system performance degrades due to the frequent switching between pitch and torque control mechanisms, supporting the FCR provision of the deloaded WT. The performance of the SVM with the best kernel functions, including execution time, minimum prediction speed, total misclassification cost, and minimum accuracy, are presented in Table 5.2. Moreover, the Receiver Operating Characteristic (ROC) curves and the area under the ROC curve (AUC) for different searched kernel functions are illustrated in Fig.5.10,

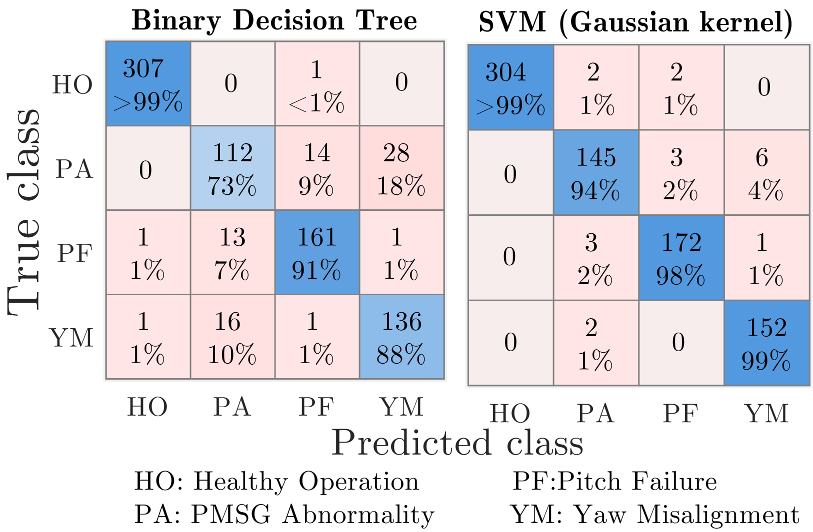

Figure 5.9: Performance of the classifiers for the first type data: the baseline approach with the BDT and the proposed approach with the self-learned SVM.

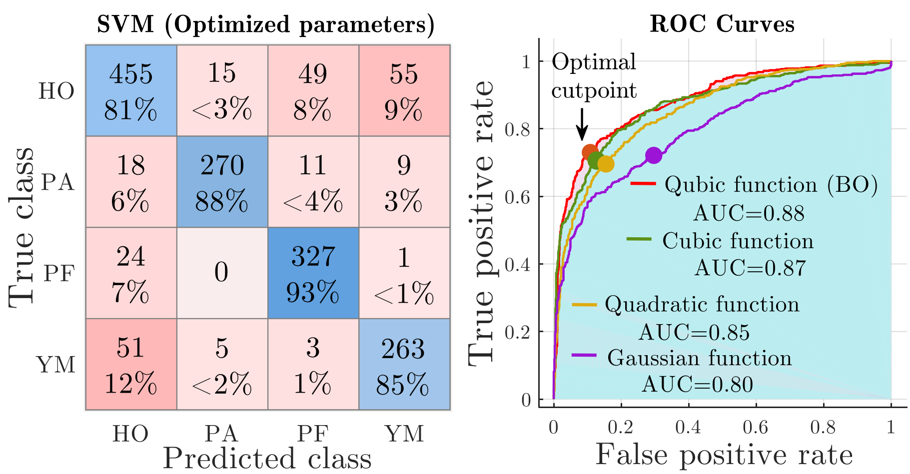

Figure 5.10: Anomaly detection for the second type data: the proposed approach with the self-learned SVM and optimized parameters.

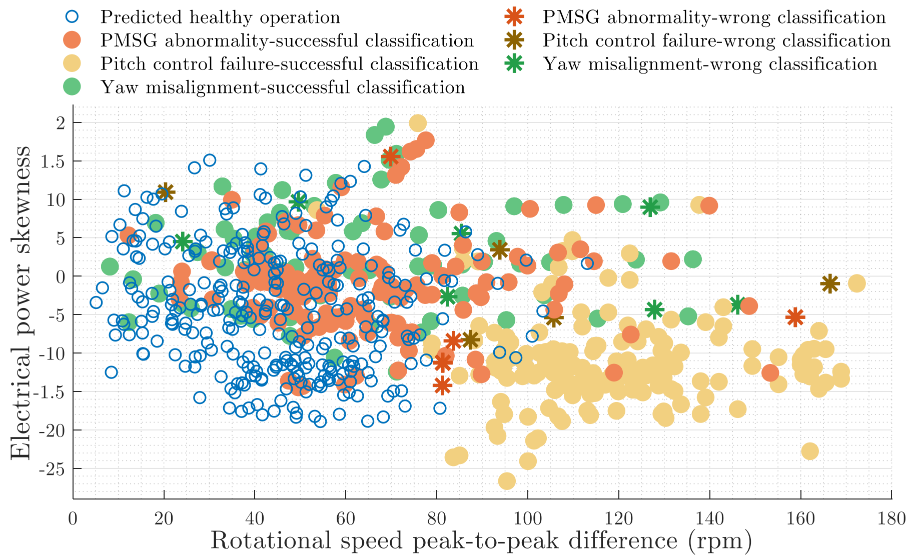

Figure 5.11: Anomaly detection for the first data type applying the proposed approach.

indicating that the cubic kernel function has the best performance. Applying the Bayesian Optimization (BO) algorithm, with a wide range of searches between 0.001 and 1000 for kernel scale and box constraint, can improve the search efficiency and increase the execution time, which may be less practical from a computational point of view. Fig.5.11 demonstrates successful classifications and highlights incorrect classifications within the scatter plot of the two-dimensional highest-ranked feature space. This showcases the robust performance of the proposed anomaly detection method, even when faced with challenges such as sparsity and lack of linearity in the data points.

The presence of successful classifications in the scatter plot validates the effectiveness of the proposed approach in accurately identifying healthy behaviors. The algorithm identifies and correctly classifies instances that exhibit patterns and characteristics indicative of normal behavior. This demonstrates the ability of the method to capture and understand complex relationships within the data despite the inherent challenges posed by sparsity and nonlinearity.

Additionally, incorrect classifications in the scatter plot highlight the method's ability to detect anomalies that deviate from the expected patterns. These incorrect classifications represent instances where the algorithm identifies data points as anomalous, even though they may appear similar to healthy data points that represent normal degradations due to TI and power curtailment. This demonstrates the algorithm's sensitivity to subtle variations and its capability to identify anomalies that might not be apparent through conventional methods. As the confusion matrix illustrates in Fig.5.10, a

Table 5.2: The SVM kernel tricks for the second type data

Kernel function	Execution time (sec)	Min prediction speed (obs/sec)	Total cost of misclassification	Minimum accuracy
Linear	6.061	16000	542	65.2%
Gaussian	3.279	11000	501	67.8%
Quadratic	19.235	12000	396	74.6%
Cubic	29.96	12000	332	78.7%
Cubic-BO	33.86	12000	293	81.2%

global optimization result is achieved by involving the kernel tricks for the updated SVM. The pitch failure detection shows outperformance, while the yaw misalignment detection has the lowest accuracy. The signal shapes of electrical power and rotational speed in yaw misalignment, unlike the PMSG abnormality and the pitch failure, do not deviate significantly. In the yaw misalignment scenario, the anomaly appears in the form of degradation and lower electrical power efficiency. Also, this kind of abnormality may occur because of aerodynamic degradation due to a high level of turbulence intensity or frequent transients from torque to pitch control action. Also, it can be challenging for the algorithm to distinguish the curtailment and the aerodynamic degradation from yaw misalignment in the transition zone. Nevertheless, by comparing the results shown in Fig.5.9 and 5.10, the proposed approach gives a better result for both data types. Although the second dataset type appears to be more challenging due to the inclusion of data from the transition zone, the proposed self-learn classification performance is still satisfactory compared to the baseline approach applied to the first dataset type without considering operations in the transition zone. This observation indicates the overall improvement of the proposed anomaly detection in the presence of different sparsity levels in the dataset and different degradation scenarios.

5.4.3 Time window and computational trade-offs

By decreasing the size of the sliding window over the observable signals and recording at a low sampling frequency, the detailed transient behavior of the system can be captured and predicted by the deep learning models and, therefore, automatically translated into features for a more realistic and improved classification. To comprehensively analyze the temporal dynamics of the system's behavior, it is essential to employ multiple time windows spanning from seconds to minutes. Shorter time windows prove more effective for identifying rapid fluctuations or anomalies, such as those associated with PMSG abnormal-

ities or degradations due to turbulent wind conditions, which can occur within a short time frame. In contrast, longer time windows offer a broader perspective, facilitating the detection of gradual performance decline or persistent issues like pitch or control failures.
Nevertheless, reducing the window's duration comes with a trade-off. It intensifies the computational workload and may hinder the optimization process when searching for the best SVM kernel hyperparameters. Thus, when applying the proposed approach, it is crucial to carefully consider the choice of the time window, taking into account the specific types of anomalies and a trade-off between accuracy and computational feasibility.

In our study, we experimented with various time windows, and the most favorable results emerged within the 10-50-second window range. The first data type exhibited the best performance with a 50-second time window. Remarkably, even when we reduced the time window to just 10 seconds for the second data type, we observed an improvement in classification performance. Therefore, since the proposed approach compromises fast and efficient computation, the ANFIS-FCM and SVM-Gaussian kernel function with the lowest predicting and execution time can be considered default settings for real-time health monitoring approaches. On the other hand, the LSTM and SVM-BO are better choices for a reasonably large window of time, i.e., more than 100s. These setting options can provide a human operator or a fully automated intelligent one with a practical tool to decide different arrangements depending on various operational conditions, which might lead to a more dedicated health monitoring system.

5.4.4 Limitations and future prospects

In future research, noteworthy challenges deserve closer attention. One significant challenge is data availability and quality for predicting healthy behavior, which needs a more thorough examination. This includes finding solutions for dealing with limited data, creating effective methods for marking unusual events during the initial stages of model training, and managing the computational demands of complex models, especially when working with larger wind farms. Moreover, the aging effects, another form of degradation, should be considered in predicting healthy operation. This means the hybrid model should be adjusted, knowing the aging factors, or updated using the most recent datasets. Addressing these challenges is fundamental for making progress in wind turbine health monitoring.
Additionally, applying the proposed methodology to different types of wind turbines and various environmental conditions can benefit transfer learning techniques, allowing the model to adapt to different situations. By understanding how to transfer and adjust knowledge across different types of turbines and en-

vironmental settings, it is possible to fully realize the potential of the proposed approach and make it useful in a broader range of real-world applications.

5.5 Conclusion

In conclusion, this study introduces a hybrid physics-based deep learning modeling approach that advances the field of wind turbine health monitoring and anomaly detection, particularly in the context of providing Frequency Containment Reserve (FCR). The contributions of this study are three-fold: First, a hybrid framework is presented that accurately predicts wind turbine health by capturing the intricate interplay between stochastic wind speed fluctuations and complex correlations between control sequences (pitch and generator torque) and system responses. The proposed hybrid structure's practicality in predicting two main observables, i.e., WT electrical power and rotational speed, shows improvements compared to the baseline black box approach. This modeling approach enhances anomaly detection by effectively distinguishing normal and abnormal states. Second, this research introduces a self-learning approach with an iterative framework, demonstrating notable improvements in classifier performance. For employing Support Vector Machines (SVM) classification, coherent features are extracted from crucial observables in both time and frequency domains, enhancing the accuracy of condition indicators. Third, a comprehensive range of anomaly and degradation scenarios are considered, including those resulting from curtailment operations for FCR provision, blade pitch control failures, yaw misalignment, and Permanent Magnet Synchronous Generator (PMSG) abnormalities. The results demonstrate that the proposed health monitoring approach has improved performance and can detect anomalies that may be falsely classified as healthy but still possess some level of degradation due to turbulent intensities or deloading operations for FCR provision.
This work generally contributes to advancing wind energy system monitoring and predictive maintenance strategies by comprehensively evaluating wind turbine health and performance. It considers intricate operational conditions and the interdependencies among control sequences, enhancing the interpretability of anomaly detection and management of wind energy conversion systems. However, challenges such as data constraints, labeling anomalies for initial training, and model complexity that can be computationally intensive for larger wind farms should be further investigated in future studies.

Bibliography

[1] N. Kayedpour, J. Qing, J. Wauters, J. D. M. De Kooning, I. Couckuyt, and G. Crevecoeur, "Wind turbine hybrid physics-based learning model for a

health monitoring approach considering provision of ancillary servicest," *IEEE Transactions on Instrumentation and Measurment*, 2023.

[2] F. Bilendo, H. Badihi, N. Lu, P. Cambron, and B. Jiang, "A normal behavior model based on power curve and stacked regressions for condition monitoring of wind turbines," *IEEE Transactions on Instrumentation and Measurement*, vol. 71, pp. 1–13, 2022.

[3] M. Wang, C. Wang, A. Hnydiuk-Stefan, S. Feng, I. Atilla, and Z. Li, "Recent progress on reliability analysis of offshore wind turbine support structures considering digital twin solutions," *Ocean Engineering*, vol. 232, p. 109168, 2021.

[4] Z. Wang, X. Jin, and Z. Xu, "An adaptive condition monitoring method of wind turbines based on multivariate state estimation technique and continual learning," *IEEE Transactions on Instrumentation and Measurement*, 2023.

[5] X. Yu, B. Tang, and K. Zhang, "Fault diagnosis of wind turbine gearbox using a novel method of fast deep graph convolutional networks," *IEEE Transactions on Instrumentation and Measurement*, vol. 70, pp. 1–14, 2021.

[6] L. Yang and Z. Zhang, "Wind turbine gearbox failure detection based on scada data: A deep learning-based approach," *IEEE Transactions on Instrumentation and Measurement*, vol. 70, pp. 1–11, 2020.

[7] G. Jiang, H. He, P. Xie, and Y. Tang, "Stacked multilevel-denoising autoencoders: A new representation learning approach for wind turbine gearbox fault diagnosis," *IEEE Transactions on Instrumentation and Measurement*, vol. 66, no. 9, pp. 2391–2402, 2017.

[8] L. Lu, Y. He, Y. Ruan, and W. Yuan, "Wind turbine planetary gearbox condition monitoring method based on wireless sensor and deep learning approach," *IEEE transactions on instrumentation and measurement*, vol. 70, pp. 1–16, 2020.

[9] L. Wang, Y. He, K. Shao, Z. Xing, and Y. Zhou, "An unsupervised approach to wind turbine blade icing detection based on beta variational graph attention autoencoder," *IEEE Transactions on Instrumentation and Measurement*, 2023.

[10] D. Zhang, W. Tian, X. Cheng, F. Shi, H. Qiu, X. Liu, and S. Chen, "Fedbip: A federated learning based model for wind turbine blade icing prediction," *IEEE Transactions on Instrumentation and Measurement*, 2023.

[11] Z.-X. Hu, Y. Wang, M.-F. Ge, and J. Liu, "Data-driven fault diagnosis method based on compressed sensing and improved multiscale network," *IEEE Transactions on Industrial Electronics*, vol. 67, no. 4, pp. 3216–3225, 2019.

[12] T. Xiahou, Z. Zeng, and Y. Liu, "Remaining Useful Life Prediction by Fusing Expert Knowledge and Condition Monitoring Information," *IEEE Transactions on Industrial Informatics*, vol. 17, no. 4, pp. 2653–2663, 2020.

[13] H. Zhao, H. Liu, Y. Jin, X. Dang, and W. Deng, "Feature extraction for data-driven remaining useful life prediction of rolling bearings," *IEEE Transactions on Instrumentation and Measurement*, vol. 70, pp. 1–10, 2021.

[14] Z. Kong, X. Jin, Z. Xu, and B. Zhang, "Spatio-temporal fusion attention: a novel approach for remaining useful life prediction based on graph neural network," *IEEE Transactions on Instrumentation and Measurement*, vol. 71, pp. 1–12, 2022.

[15] K. He, Z. Su, X. Tian, H. Yu, and M. Luo, "Rul prediction of wind turbine gearbox bearings based on self-calibration temporal convolutional network," *IEEE Transactions on Instrumentation and Measurement*, vol. 71, pp. 1–12, 2022.

[16] F. Cheng, J. Wang, L. Qu, and W. Qiao, "Rotor-current-based fault diagnosis for dfig wind turbine drivetrain gearboxes using frequency analysis and a deep classifier," *IEEE transactions on industry applications*, vol. 54, no. 2, pp. 1062–1071, 2017.

[17] J. Peng, A. Kimmig, Z. Niu, J. Wang, X. Liu, D. Wang, and J. Ovtcharova, "Wind turbine failure prediction and health assessment based on adaptive maximum mean discrepancy," *International Journal of Electrical Power & Energy Systems*, vol. 134, p. 107391, 2022.

[18] Q. Lyu, J. Liu, Y. He, X. Wang, and S. Wu, "Condition monitoring of wind turbines with implementation of interactive spatio temporal deep learning networks," *IEEE Transactions on Instrumentation and Measurement*, 2023.

[19] Z. Su, X. Zhang, Y. Han, S. Wang, and M. Luo, "Adaptive gated attention network with weighted metric enhancement for fault diagnosis of wind turbine gearbox," *IEEE Transactions on Instrumentation and Measurement*, 2023.

[20] H. Badihi, Y. Zhang, B. Jiang, P. Pillay, and S. Rakheja, "A comprehensive review on signal-based and model-based condition monitoring of wind turbines: Fault diagnosis and lifetime prognosis," *Proceedings of the IEEE*, vol. 110, no. 6, pp. 754–806, 2022.

[21] S. Chakraborty, S. Adhikari, and R. Ganguli, "The role of surrogate models in the development of digital twins of dynamic systems," *Applied Mathematical Modelling*, vol. 90, pp. 662–681, 2021.

[22] M. S. Nielsen and V. Rohde, "A surrogate model for estimating extreme tower loads on wind turbines based on random forest proximities," *Journal of Applied Statistics*, vol. 49, no. 2, pp. 485–497, 2022.

[23] R. M. Slot, J. D. Sørensen, B. Sudret, L. Svenningsen, and M. L. Thøgersen, "Surrogate model uncertainty in wind turbine reliability assessment," *Renewable Energy*, vol. 151, pp. 1150–1162, 2020.

[24] J. Lei, C. Liu, and D. Jiang, "Fault diagnosis of wind turbine based on Long Short-term memory networks," *Renewable energy*, vol. 133, pp. 422–432, 2019.

[25] H. Chen, H. Liu, X. Chu, Q. Liu, and D. Xue, "Anomaly detection and critical SCADA parameters identification for wind turbines based on LSTM-AE neural network," *Renewable Energy*, vol. 172, pp. 829–840, 2021.

[26] D. Karaboga and E. Kaya, "Adaptive network based fuzzy inference system (ANFIS) training approaches: a comprehensive survey," *Artificial Intelligence Review*, vol. 52, no. 4, pp. 2263–2293, 2019.

[27] M. Rezamand, M. Kordestani, R. Carriveau, D. S.-K. Ting, M. E. Orchard, and M. Saif, "Critical wind turbine components prognostics: A comprehensive review," *IEEE Transactions on Instrumentation and Measurement*, vol. 69, no. 12, pp. 9306–9328, 2020.

[28] X. Hu, Y. Li, L. Jia, and M. Qiu, "A Novel Two-stage Unsupervised Fault Recognition Framework Combining Feature Extraction and Fuzzy Clustering for Collaborative AIoT," *IEEE Transactions on Industrial Informatics*, 2021.

[29] S. Bai, J. Z. Kolter, and V. Koltun, "An empirical evaluation of generic convolutional and recurrent networks for sequence modeling," *arXiv preprint arXiv:1803.01271*, 2018.

[30] H. Sun, M. Xia, Y. Hu, S. Lu, Y. Liu, and Q. Wang, "A new sorting feature-based temporal convolutional network for remaining useful life prediction of rotating machinery," *Computers and Electrical Engineering*, vol. 95, p. 107413, 2021.

[31] Z. Gan, C. Li, J. Zhou, and G. Tang, "Temporal convolutional networks interval prediction model for wind speed forecasting," *Electric Power Systems Research*, vol. 191, p. 106865, 2021.

[32] E. G. S. Nascimento, T. A. de Melo, and D. M. Moreira, "A transformer-based deep neural network with wavelet transform for forecasting wind speed and wind energy," *Energy*, vol. 278, p. 127678, 2023.

[33] Y. Wang, H. Xu, M. Song, F. Zhang, Y. Li, S. Zhou, and L. Zhang, "A convolutional transformer-based truncated gaussian density network with data denoising for wind speed forecasting," *Applied Energy*, vol. 333, p. 120601, 2023.

[34] J. Zhang, X. Li, J. Tian, H. Luo, and S. Yin, "An integrated multi-head dual sparse self-attention network for remaining useful life prediction," *Reliability Engineering & System Safety*, vol. 233, p. 109096, 2023.

[35] L. Liu, Z. Qu, Z. Chen, F. Tu, Y. Ding, and Y. Xie, "Dynamic sparse attention for scalable transformer acceleration," *IEEE Transactions on Computers*, vol. 71, no. 12, pp. 3165–3178, 2022.

[36] X. Li and W. Zhang, "Physics-informed deep learning model in wind turbine response prediction," *Renewable Energy*, vol. 185, pp. 932–944, 2022.

[37] M. Benbouzid, T. Berghout, N. Sarma, S. Djurović, Y. Wu, and X. Ma, "Intelligent condition monitoring of wind power systems: State of the art review," *Energies*, vol. 14, no. 18, p. 5967, 2021.

[38] K. Zhang, B. Tang, L. Deng, and X. Yu, "Fault detection of wind turbines by subspace reconstruction-based robust kernel principal component analysis," *IEEE Transactions on Instrumentation and Measurement*, vol. 70, pp. 1–11, 2021.

[39] F. K. Moghadam, V. Chabaud, Z. Gao, and S. Chapaloglou, "Power train degradation modelling for multi-objective active power control of wind farms," *Forschung im Ingenieurwesen*, vol. 87, no. 1, pp. 13–30, 2023.

[40] A. Otter, J. Murphy, V. Pakrashi, A. Robertson, and C. Desmond, "A review of modelling techniques for floating offshore wind turbines," *Wind Energy*, vol. 25, no. 5, pp. 831–857, 2022.

[41] A. Castellani, S. Schmitt, and S. Squartini, "Real-World Anomaly Detection by Using Digital Twin Systems and Weakly Supervised Learning," *IEEE Transactions on Industrial Informatics*, vol. 17, no. 7, pp. 4733–4742, 2020.

[42] M. Zheng, J. Man, D. Wang, Y. Chen, Q. Li, and Y. Liu, "Semi-supervised multivariate time series anomaly detection for wind turbines using generator scada data," *Reliability Engineering & System Safety*, vol. 235, p. 109235, 2023.

[43] B. J. Jonkman, "TurbSim user's guide: Version 1.50," tech. rep., National Renewable Energy Lab.(NREL), Golden, CO (United States), 2009.

[44] B. Jonkman and L. Kilcher, "Turbsim user's guide: version 1.06. 00," *National Renewable Energy Laboratory: Golden, CO, USA*, 2012.

[45] J. Jonkman, S. Butterfield, W. Musial, and G. Scott, "Definition of a 5-MW reference wind turbine for offshore system development," tech. rep., National Renewable Energy Lab (NREL), Golden, CO (United States), 2009.

[46] J. D. M. De Kooning, T. L. Vandoorn, J. Van de Vyver, B. Meersman, and L. Vandevelde, "Displacement of the maximum power point caused by losses in wind turbine systems," *Renewable Energy*, vol. 85, pp. 273–280, 2016.

[47] N. Kayedpour, J. D. De Kooning, A. E. Samani, L. Vandevelde, and G. Crevecoeur, "An adaptive operational strategy for enhanced provision of frequency containment reserve by wind turbines: Data-driven based power reserve adjustment," *Electric Power Systems Research*, vol. 223, p. 109564, 2023.

[48] X. Ge, X. Zhu, Y. Fu, Y. Xu, and L. Huang, "Optimization of reserve with different time scales for wind-thermal power optimal scheduling considering dynamic deloading of wind turbines," *IEEE Transactions on Sustainable Energy*, vol. 13, no. 4, pp. 2041–2050, 2022.

[49] Y. Wang, X. Duan, R. Zou, F. Zhang, Y. Li, and Q. Hu, "A novel data-driven deep learning approach for wind turbine power curve modeling," *Energy*, vol. 270, p. 126908, 2023.

[50] D.-E. Choe, H.-C. Kim, and M.-H. Kim, "Sequence-based modeling of deep learning with LSTM and GRU networks for structural damage detection of floating offshore wind turbine blades," *Renewable Energy*, vol. 174, pp. 218–235, 2021.

[51] N. Zhang, S.-L. Shen, A. Zhou, and Y.-F. Jin, "Application of LSTM approach for modelling stress–strain behaviour of soil," *Applied Soft Computing*, vol. 100, p. 106959, 2021.

[52] D. P. Kingma and J. Ba, "Adam: A method for stochastic optimization," *arXiv preprint arXiv:1412.6980*, 2014.

[53] T. V. Hecke, "Power study of anova versus Kruskal-Wallis test," *Journal of Statistics and Management Systems*, vol. 15, no. 2-3, pp. 241–247, 2012.

Chapter 6

Conclusions and outlook

6.1 Conclusions

In conclusion, this thesis centers on data-driven-based adaptive and optimal operation strategies for wind energy conversion systems, recognizing their significance in the global energy transition and their potential for mitigating climate change. It acknowledges wind power's clean and abundant nature but highlights the challenges its intermittent and variable characteristics pose. The thesis emphasizes the need for advanced control strategies and monitoring techniques to ensure the reliable and efficient operation of wind energy conversion systems on a large scale, supporting ancillary services such as FCR.

Optimizing wind energy conversion systems necessitates pioneering methods that transcend traditional control and monitoring techniques to tackle the distinct features and intricacies linked to wind energy. As discussed in Sections 1.1.3 and 1.5, energy conversion systems' complexities require adaptable operational approaches, especially when integrating them into electrical power grids. Utilizing data-driven techniques holds promise for improving the modeling, control, and health monitoring aspects, ultimately enhancing the efficiency of FCR-delivering wind energy conversion systems.

This dissertation's primary aim is to identify and implement such strategies, both at the wind farm supervisory control level and within individual wind turbine control and health monitoring systems. Furthermore, this thesis research delves into hybrid methods, which possess the capacity to acquire insights from data, innovative control strategies, and monitoring methods to amplify the adaptive functionality of wind energy conversion systems, considering altering power reserve strategies in complex FCR markets, and surmounting the inherent hurdles presented by the fluctuations, intermittence, and unpredictability of grid frequency and wind patterns.

In the wind farm supervisory control domain, Chapter 2 proposes a novel operation strategy that optimizes the contribution of wind farms to reserve and energy markets. It introduces a scenario-based two-stage stochastic programming approach that considers uncertainties associated with intermittent wind power and the complex aerodynamics of wake formation. The research integrates a data-driven surrogate model of wake formation using an adaptive network-based fuzzy inference system (ANFIS). Employing the estimated wake-controlled parameters, an allocation problem searches for an optimal distribution of the scheduled reserve among wind turbines. The proposed algorithm showcases its potential to improve overall wind farm performance and enhance FCR provision while actively optimizing wake-controlled parameters.

Building upon the insights gained from wind farm supervisory control, cfr. Chapter 2, the thesis focuses on wind turbine local control to facilitate FCR activation at individual wind turbines. It develops advanced control algorithms that address various limitations, such as wind turbine nonlinearities, stochasticity of wind speed, and grid frequency, as discussed in Sections 1.5.2. Chapter 3 proposes a data-driven Model Predictive Control (MPC) approach that accurately predicts the turbine's aerodynamic behavior and provides optimal control actions in response to grid frequency variations in above-rated and turbulent wind conditions. The results given in Section 3.5 demonstrate the superior performance of the MPC approach compared to baseline proportional-integral (PI) controllers, enhancing power reference tracking, reducing mechanical loads, and ensuring grid stability within the confines of the test cases considered.

Furthermore, Chapter 4 introduces an adaptive operational strategy for providing FCR in both full and partial-load operating regions, supporting varying power reserve strategies. It employs a generator torque control system instead of a blade pitch control system, considering the unpredictable behavior of grid frequency and wind speed within the specific test cases. The research also presents an adaptive reserve margin estimation method based on short-term grid frequency predictions. It integrates gain-scheduled fuzzy-PI control to address the challenges highlighted in Section 1.3.1, improving FCR provision in turbulent wind conditions. Based on a 5MW-NREL offshore model, the simulation outcomes illustrate enhancements achieved with the fuzzy-PI approach in terms of power reference tracking, rotor speed regulation, and the average mechanical load parameters studied. These results collectively validate an overall enhancement in performance. This chapter demonstrates stable control performance in all operating regions and reserve modes, ensuring reliable operation and power regulation without excessive structural loads within the defined test scenarios.

Moreover, the effective incorporation of the control strategies explored in Chapters 3 and 4 into the wind farm's supervisory control framework outlined in Chapter 2 facilitates a cohesive and enhanced method for controlling operations and delivering FCR across various operational scenarios, as demonstrated within the parameters of the study. This approach aims to maximize the overall efficiency and adaptability of wind farms, positioning them as a compelling solution for sustainable energy generation.

Finally, Chapter 5 addresses the challenges of wind turbine health monitoring discussed in Section 1.5.3, by presenting a novel hybrid physics-based deep learning framework that significantly reduces the prediction error of wind turbine behavior compared to the baseline black-box method within the context of the study. The proposed algorithm is able to detect anomalies and degradations in wind turbine operation by approximating the time-varying correlation between wind turbine control sequences and system response. It utilizes a hybrid structure and support vector machine for classification, accounting for uncertainties such as wind stochasticity and power curve variations. The iterative learning framework enables dynamic updating of the classifier, improving its ability to learn from new anomalies during active operations within the defined test cases. This approach enhances the accuracy and efficiency of wind turbine health monitoring, leading to more efficient assessments of turbine conditions and reduced downtime based on the specific models and conditions used in the study.

This thesis provides a comprehensive approach to optimizing wind energy conversion systems by addressing key challenges in wind farm supervisory control, local control, and health monitoring. The research introduces novel strategies and techniques to enhance wind energy conversion systems' performance, reliability, and grid integration. By optimizing FCR provision, controlling wake formation, improving control strategies, and enhancing health monitoring techniques, this research contributes to a more sustainable and resilient future powered by wind energy. The outcomes of this research are beneficial and gainful for the efficient and reliable integration of wind power into the global energy landscape, promoting sustainability and reducing greenhouse gas emissions.

6.2 Future research

In the future, several interesting fields of research can contribute to improving offshore wind farm performance to efficiently contribute to the ancillary market. Here are some areas worth exploring:

6.2.1 Advanced Hybrid Control Strategy

The proposed data-driven MPC in this thesis, cfr. Chapter 3, employs historical and real-time data to learn a predictive model of the system dynamics. This model captures the relationships between control inputs, system states, and desired outputs. It provides a basis for predicting future system behavior and optimizing control actions to achieve specific objectives. In contrast, Reinforcement Learning (RL) employs an agent that interacts with the system and learns optimal control policies through trial and error. As discussed earlier in the introduction, the agent explores the system by taking action and receiving feedback in the form of rewards or penalties based on predefined performance criteria. By maximizing cumulative rewards, the RL agent iteratively improves its control strategies. To overcome the RL challenges mentioned in 1.4.3, such as robustness to uncertainties or incorporation of constraints, the hybrid control system can be suggested that combines the predictive capabilities of data-driven MPC with the adaptive learning of RL.

The MPC component provides a baseline control policy based on the learned system model, while the RL component continuously refines and adapts the control policy based on real-time feedback and exploration. During the training phase, the RL agent explores different control actions and observes the resulting system behavior. The agent adjusts its policy based on rewards and penalties, gradually improving its understanding of the system dynamics, finding optimal control strategies, and becoming more robust to uncertainties. Once the RL agent is trained, it can be deployed in real-time control scenarios. The agent interacts with the system, observes its current state, and selects control actions based on the learned policy.

The data-driven MPC component may still be utilized to provide initial control signals or as a fallback mechanism if the RL agent encounters unfamiliar situations. The hybrid system continues to adapt and learn during online operations. As the RL agent interacts with the system, it gathers new data and updates its control policy based on the observed outcomes. This adaptive learning enables the system to improve its performance over time and handle uncertainties or changes in the system dynamics. The performance of the hybrid control system is regularly evaluated and refined based on feedback from the actual system operation. The control policies and model parameters may be adjusted, and additional training data can be incorporated to enhance the system's effectiveness and robustness. The hybrid approach combining data-driven MPC and reinforcement learning (RL) can bring several benefits to wind turbine and wind farm applications:

By integrating data-driven MPC, the hybrid system can benefit from historical and real-time data to learn accurate predictive models of wind turbine behavior. This enables more precise control actions and better tracking of desired performance objectives, such as electrical power and rotational speed set points, induction factors, or mechanical loadings. The system can optimize control strategies based on learned system dynamics and historical data patterns.

Wind turbine and wind farm operations are subject to various uncertainties, including fluctuating wind conditions, mechanical loads, and system faults.

The RL component of the hybrid system allows for adaptive learning and control policy refinement, enabling the system to adapt to changing conditions and optimize control actions accordingly. This adaptability improves the system's ability to respond to uncertainties and disturbances. Wind turbines are exposed to varying wind conditions and changing power grid requirements, leading to mechanical loads, fatigue, and structural wear. The hybrid system can incorporate load reduction requirements into the control strategies.

Using the data-driven MPC to optimize control actions and RL to learn and adapt in real time, the system can effectively mitigate loads and reduce fatigue, improving turbine lifespan and reducing maintenance costs. The hybrid control system can enhance the wind farm's ability to participate in ancillary markets, such as frequency regulation or grid stability services. By optimizing control actions based on learned models and RL-based adaptation, the system can efficiently respond to grid demands, contribute to grid stability, and provide ancillary services, thereby increasing the economic value of wind farm operations.

The hybrid system can also use the data-driven surrogate models to monitor system behavior and identify potential faults or anomalies. The system can detect deviations and trigger appropriate actions by continuously comparing the predicted behavior with real-time measurements, such as fault detection, isolation, and fault-tolerant control strategies. RL can also adapt the control policies in the presence of faults to maintain system performance and safety. The hybrid control system can optimize wind turbines and wind farms' energy capture and power production. By learning and adapting control policies based on historical data and real-time feedback, the system can make more informed decisions regarding turbine operation, rotor speed, pitch control, and power set points. This optimization can lead to increased energy production, improved power quality, and better integration with the grid. Overall, the hybrid approach combining data-driven MPC and RL offers the potential for more accurate, adaptive, and efficient control of wind turbines and wind farms. It enables improved performance, load reduction, fault detection, uncertainty adaptability, and optimized energy capture, enhancing overall system operation, reliability, and economic benefits.

6.2.2 Integration of Energy Storage

The integration of energy storage systems, such as electrolyzers for hydrogen production, can be promising in improving offshore wind farm performance, particularly in providing ancillary services. Offshore wind farms face various challenges related to the intermittency of wind energy and the need for grid stability. By integrating energy storage systems like electrolyzers, offshore wind farms can store excess generated energy as hydrogen through the process of electrolysis. This stored hydrogen can be utilized for multiple purposes, contributing to improved performance and providing ancillary services. One significant benefit of electrolyzers and hydrogen production is their ability to address the intermittent nature of wind energy. During periods of high wind production, when the wind farm generates surplus electricity, the excess power can be directed to the electrolyzer. The electrolyzer converts the electrical energy into hydrogen gas by splitting water molecules into hydrogen and oxygen. This process enables the efficient storage of renewable energy in the form of hydrogen. The stored hydrogen offers various possibilities for enhancing offshore wind farm performance and providing ancillary services. Firstly, hydrogen can be utilized as a direct energy source during low wind or high electricity demand periods. The stored energy can be converted back into electricity using hydrogen fuel cells, providing a reliable and dispatchable power source. This capability ensures a steady and predictable power supply, contributing to grid stability and reliability.

The modeling and control approaches discussed in this thesis can be further improved to provide a higher level of adaptability in the operation of offshore wind farms with integrated energy storage. The control system can continuously monitor and analyze data to forecast energy production, storage capacity, and grid requirements. This information can be incorporated in the wind farm supervisory optimization problem discussed in Chapter 2 to enable better planning and decision-making, optimizing the overall performance and reliability of the system.

Furthermore, the discussed operational strategies in this thesis can play a beneficial role in optimizing the operation of the integrated system. The FCR control architecture introduced in Chapters 2 and 4 can be improved to assess the grid conditions, energy demand, and hydrogen storage capacity to determine the optimal allocation of energy between wind turbines, producing hydrogen, and meeting other energy demands. The data-driven MPC suggested in Chapter 3 can be adapted to optimize the operation of electrolyzers as well as wind turbine's power reference tracking to ensure efficient energy conversion and storage. The integration of electrolyzers and hydrogen production enhances the wind farm's participation in other ancillary service markets, such as frequency regulation, voltage control, and black start capabilities. The wind farm can quickly respond to grid demands by releasing stored hydrogen when needed, contributing to grid stability and power quality. This flexibility and ability to provide ancillary services can generate additional revenue streams for wind farm operators.

6.2.3 Advancing wind turbine health monitoring and ancillary services reliability

In wind turbine operations, achieving operational superiority involves addressing various aspects, including wind turbine health monitoring, system reliability, resilience, and the dependable provision of ancillary services, such as Frequency Control Reserve (FCR). Chapter 5 introduces a hybrid physics-based deep learning modeling approach, highlighting the critical need for continuous research and innovation in several key areas. The quality and quantity of data are central to the effectiveness of wind turbine health monitoring and FCR provision. Future research should prioritize expanding datasets, incorporating data from diverse wind turbines in various geographical settings and operating conditions. Furthermore, exploring advanced data augmentation techniques, such as synthetic data generation and missing data imputation, can address data limitations. A more comprehensive dataset not only strengthens anomaly detection but also enhances the precision of FCR predictions, ultimately bolstering the reliability of wind farm operations.

Moreover, future research should explore methods for fine-tuning models for multi-subsystem frameworks, i.e., wind farms with different manufactured wind turbines. This involves customizing the model to specific turbine configurations or exploring advanced transfer learning techniques. Adapting the model ensures optimized performance and resilience, enabling it to excel in varying operational scenarios. These systems should integrate with Supervisory Control and Data Acquisition (SCADA) systems, allowing for continuous model updates based on real-time data. This adaptability is essential for staying tuned to dynamic conditions and ensuring the model remains effective in practical wind farm environments.

Efforts should also focus on enhancing the model's interpretability for informed decision-making. Additional research should investigate the model's robustness against failures and data anomalies to ensure dependable performance. Developing collaborative systems that combine self-learned anomaly detection approaches with human expertise enables a comprehensive perspective on turbine maintenance and operational decision-making. This collaborative approach enhances wind energy systems' reliability and resilience, ensuring optimal and reliable ancillary service provision.

Finally, future research should integrate monitoring system information into maintenance strategies and ancillary service schedules, optimizing operations. Economic assessments are vital for assessing the cost-effectiveness of implementing monitoring systems. Additionally, ensuring compliance with industry standards and regulations is fundamental for the reliable provision of ancillary services, particularly FCR. In conclusion, these ongoing research directions have the potential to strengthen the reliability, resilience significantly, and overall sustainability of wind energy systems, contributing to a more environmentally friendly and efficient future.

6.2.4 Virtual Power Plants and Aggregation

Another research area for further investigation is Virtual Power Plants (VPPs) and aggregation techniques that can offer innovative approaches to improve offshore wind farm performance and grid integration. Aggregating multiple offshore wind farms into a single VPP can enhance their collective performance and grid integration. By combining the power output from various wind farms, the VPP can provide a more stable and predictable power supply to the grid. Aggregation allows for better management of fluctuations in wind power generation, as the combined output tends to be smoother and more controllable than individual wind farms. VPPs can also employ dynamic load management techniques to optimize wind energy utilization. By monitoring real-time grid conditions and electricity demand, the VPP can adjust the load profiles and effectively balance the power consumption with the offshore wind farm's generation capacity. This approach maximizes wind energy utilization, reduces curtailment, and improves grid stability.

Moreover, integrating energy storage systems with offshore wind farms within a VPP can enhance grid integration and improve performance. Energy storage technologies, such as large-scale batteries or compressed air energy storage, can store excess wind energy during periods of low demand or high wind output. The stored energy can be dispatched when demand is high or wind conditions are suboptimal, smoothing out fluctuations and increasing grid reliability. In parallel, VPPs can participate in demand response programs, where consumers voluntarily adjust their electricity usage based on grid conditions and price signals. By coordinating and aggregating the response of multiple consumers connected to the VPP, it can act as a flexible resource, balancing supply and demand. This approach helps to optimize the utilization of wind power and improve the integration of offshore wind farms into the grid.

Additionally, advanced forecasting techniques and predictive analytics discussed in this thesis can contribute to offshore wind farms' operational planning and scheduling within a VPP. Accurate wind power forecasts enable better prediction of the available generation capacity, which helps optimize the scheduling of maintenance activities, energy trading, and grid integration. VPPs can improve offshore wind farms' overall performance and reliability by reducing forecasting errors. The VPPs and aggregation techniques can contribute to optimizing offshore wind farm performance and enhancing their integration with the grid. Implementing these strategies requires advanced control and coordination systems and regulatory frameworks that enable VPPs to participate in energy markets and grid services.

6.3 Author bibliography

The following list gives a complete overview of all articles published in the frame of this PhD research.

1. **Kayedpour, N.**, De Kooning, J. D. M., Samani, A. E., Kayedpour, F., Vandevelde, L., and Crevecoeur, G. (2023). An Optimal Wind Farm Operation Strategy for the Provision of Frequency Containment Reserve Incorporating Active Wake Control. *IEEE Transactions on Sustainable Energy*, DOI: 10.1109/TSTE.2023.3288130.

2. **Kayedpour, N.**, Samani, A. E., De Kooning, J. D. M., Vandevelde, L., and Crevecoeur, G. (2021). Model Predictive Control with a Cascaded Hammerstein Neural Network of a Wind Turbine Providing Frequency Containment Reserve. *IEEE Transactions on Energy Conversion*, DOI: 10.1109/TEC.2021.3093010.

3. **Kayedpour, N.**, Samani, A. E., De Kooning, J. D. M., Vandevelde, L., and Crevecoeur, G. (2023). An Adaptive Operational Strategy for Enhanced Provision of Frequency Containment Reserve by Wind Turbines: data-driven based power reserve adjustment. *Electric Power Systems Research*,DOI: 10.1016/j.epsr.2023.109564.

4. **Kayedpour, N.**, Qing, J., Wauters, J., De Kooning, J. D. M., Couckuyt, I., and Crevecoeur, G. (2023). Wind Turbine Hybrid Physics-based Learning Model for a Health Monitoring Approach Considering Provision of Ancillary Servicest. *IEEE Transactions on Instrumentation and Measurment*, Revised Manuscript Submitted.

5. **Kayedpour, N.**, Samani, A. E., De Kooning, J. D. M., Vandevelde, L., and Crevecoeur, G. (2019, November). A data-driven approach using learning time series prediction for forecasting power system variables. In *2019 IEEE 2nd International Conference on Renewable Energy and Power Engineering (REPE)*, Toronto, Canada (Reviewed conference proceeding). DOI: 10.1109/REPE48501.2019.9025159.

6. **Kayedpour, N.**, Samani, A. E., De Kooning, J. D. M., Vandevelde, L., and Crevecoeur, G. (2019, October). Robust approximation models for predictive control of a variable pitch wind power drivetrain. In *8th Renewable Power Generation Conference (RPG 2019)*, Shanghai, China (Reviewed conference proceeding). DOI: 10.1049/cp.2019.0591.

7. **Kayedpour, N.**, Samani, A. E., Singh, N., De Kooning, J. D. M., Vandevelde, L., and Crevecoeur, G. (2020). An Optimal Control Strategy to

Maximize Power in an Offshore Wind Farm by Reducing Wake Interaction. In *16th EAWE PhD seminar*, Porto, Portugal (Reviewed conference proceeding).

8. **Kayedpour, N.**, Singh, N., De Kooning, J.D., Vandevelde, L. and Crevecoeur, G., (2022). An optimal wind farm control strategy for grid frequency support using particle swarm optimization. In *11th International Conference on Renewable Power Generation - Meeting net zero carbon (RPG 2022)*, London, United Kingdom (Reviewed conference proceeding). 10.1049/icp.2022.1675.

9. Samani, A. E., **Kayedpour, N.**, Kayedpour, F., De Kooning, J. D. M., Crevecoeur, G., and Vandevelde, L. (2023). An Optimal Operation Strategy for Collaborative Flexibility Provision of a Carbon Capture and Utilization Process with Wind Energy. *IEEE Transactions on Sustainable Energy*, DOI: 10.1109/TSTE.2023.3257044.

10. Asiaban, S., **Kayedpour, N.**, Samani, A. E., Bozalakov, D., De Kooning, J. D. M., Crevecoeur, G., and Vandevelde, L. (2021). Wind and Solar Intermittency and the Associated Integration Challenges: A Comprehensive Review Including the Status in the Belgian Power System. *Energies*, DOI: 10.3390/en14092630.

11. Samani, A. E., De Kooning, J. D. M., **Kayedpour, N.**, Singh, N., and Vandevelde, L. (2020). The Impact of Pitch-To-Stall and Pitch-To-Feather Control on the Structural Loads and the Pitch Mechanism of a Wind Turbine. *Energies*, DOI: 10.3390/en13174503.

12. Baetens, J., Van Eetvelde, G., Lemmens, G., **Kayedpour, N.**, De Kooning, J. D., and Vandevelde, L. (2019). Thermal performance evaluation of an induced draft evaporative cooling system through adaptive neuro-fuzzy interference system (anfis) model and mathematical model. *Energies*, DOI:10.1109/TSTE.2023.3257044.

13. Samani, A. E., **Kayedpour, N.**, De Kooning, J. D. M., and Vandevelde, L. (2019, November). Performance and Structural Load Analysis of Small and Medium Wind Turbines Operating with Active Speed Stall Control versus Pitch Control. In *2019 IEEE 2nd International Conference on Renewable Energy and Power Engineering (REPE)*, Toronto, Canada (Reviewed conference proceeding). DOI: 10.1109/REPE48501.2019.9025130.

14. Hosseini, S. A., Toubeau, J. F., Singh, N., De Kooning, J. D. M., **Kayedpour, N.**, Crevecoeur, G., ... and Vandevelde, L. (2021). Impact of fast

wind fluctuations on the profit of a wind power producer jointly trading in energy and reserve markets. In *The 9th Renewable Power Generation Conference (RPG Dublin)*, (Reviewed conference proceeding). DOI: 10.1049/icp.2021.1386.

15. Singh, N., Hosseini, S.A., **Kayedpour, N.**, De Kooning, J.D.M., De Greve, Z., Toubeau, J.F., Vallée, F., Crevecoeur, G. and Vandevelde, L. (2022, July). Prediction-based Wind Turbine Operation for Active Participation in the Day-Ahead and Reserve Markets. In *2022 IEEE Power and Energy Society General Meeting (PESGM)*, (Reviewed conference proceeding). DOI: 10.1109/PESGM48719.2022.9917213.

Offshore wind farms in the North Sea supporting decarbonized power system.